Studies on double fertilisation and early embryogenesis of *Arabidopsis thaliana* Heynh. and *Zea mays* L.

DISSERTATION ZUR ERLANGUNG DES DOKTORGRADES DER NATURWISSENSCHAFTEN (DR.RER.NAT.) DER FAKULTÄT FÜR VORKLINISCHE MEDIZIN UND BIOLOGIE DER UNIVERSITÄT REGENSBURG

vorgelegt von

Andreas Lausser

aus

Roding

im Jahre 2012

Das Promotionsgesuch wurde eingereicht am: 22.05.2012
Die Arbeit wurde angeleitet von: Prof. Dr. Thomas Dresselhaus

Unterschrift:_____
Andreas Lausser

Contents

Chapter 1 - General introduction: Sexual reproduction in plants

The following chapter is partly based on the review article Lausser and Dresselhaus 2010. The article was fully written by A. Lausser and edited by T. Dresselhaus. The topic of progamic pollen tube development was revisited by the review article Dresselhaus *et al.* 2011. The first two chapters on pollen capture, adhesion and hydration, germination at the stigmatic papillae, stigmata invasion and growth through the grass stigmata were fully written by A. Lausser and edited by T. Dresselhaus. The other chapters of Dresselhaus *et al.* 2011 were written by M.L. Márton and T. Dresselhaus.

1.1 Development and function of the female gametophyte in angiosperms

Sexual reproduction is a key process in biology. It is regarded as a basis of recombination and selection during evolution. Viridiplantae, a group of green photoautotrophic organisms, follow a live cycle of alternating haploid gametophytes and diploid sporophytes. The macroscopically visible plant bodies can be formed by the gametophyte, the sporophyte or both generations. In embryophytes, which comprise the spermatophytes (mosses, ferns, flowering plants) and some streptophyte green algae (for review see (Becker and Marin 2009) either gametophyte or sporophyte generations are dominant. In the case of the ferns and seed plants, the photosynthetic active plant body is formed by the sporophyte in contrast to mosses, which show a dominant gametophytic generation. The diploid sporophyte produces haploid meiospores which give rise to the gametophytes. The haploid gametophyte produces mitospores which give rise to a diploide sporophyte after a fertilization event (Valero *et al.* 1992). The seed plants, which are the ecological dominant and economical most important group of land plants, comprise gymnosperms and angiosperms. The gametophytic generation is strongly reduced in this group. Due to that reduction usually only six cell types form ten cells for both mature male and female gametophytes of angiosperms. These cell types have an almost exclusive role in double fertilisation. Therefore, development of gametophytic cell types and double fertilization will be discussed in parallel in the following.

In case of angiosperms, the female gametophyte (FG, Figure 1.1) is not released from the maternal sporophyte. The FG remains deeply embedded into the sporophytic tissue called

the ovule. The FG arises from the megaspore mother cell (MMC) which undergoes meiosis. In most angiosperms (around 70% species), including the model plants *Arabidopsis thaliana* and *Zea mays*, FG development follows the *Polygonum* type (Reiser and Fischer 1993). In this case, the FG arises from a single megaspore, namely the most chalazal spore of a linear tetrad originating from the MMC. This cell undergoes three mitotic divisions resulting in a seven-celled mature FG with six haploid cells (one egg cell, two synergids and three antipodals) and one di-haploid central cell (Reiser and Fischer 1993). In other types of FG-development, embryo sacs can consist of four to fourteen cells originating from one, two or all four megaspores (Huang and Russell 1992).

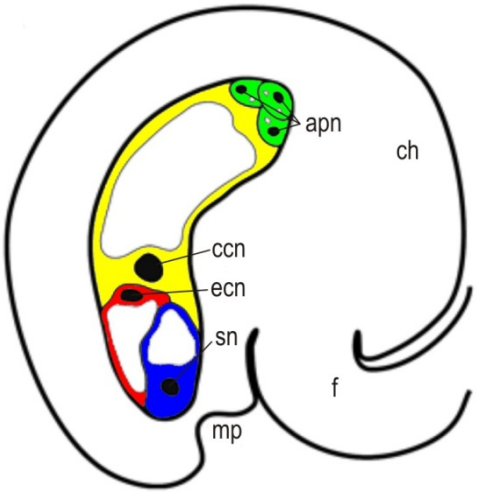

Figure 1.1 Cartoon of a chamylothrophic ovule with female gametophyte (FG) of the *Polygonum*-type. The egg cell (red) and the synerdis (blue) form the egg appartaturs. The large central cell (yellow) give rise to the endosperm after double fertilization. The antipodals (green) have variable fait in different species. In *Arabidospis*, antipodals degeneratate during FG maturation. In contrast to that, maize antipoals proliferate even after fertilization. Abbreviations: apn = antipodal nuclei, ccn = central cell nucleus, ch = chalaza, ecn = egg cell nucleus, f = funiculus, mp = micropyle, sn = synergid nucleus (Adapted from (Yadegari and Drews 2004)

A highly interesting field of plant development research is currently how the cell types of the gametophytes are specified and how they fulfil their roles (for review see Sprunck and Gross-Hardt 2011; Bedinger and Fowler 2009; Evans and Grossniklaus 2009). The egg cell is the most important cell of the FG (see also Figure 1.1), since it gives rise to the embryo after double fertilisation. Egg cell morphology differs from the synergids in terms of the position of vacuole and nucleus. The egg cell nucleus in many eudicot species including *Arabidopsis* faces towards the chalazal pole of the cell whereas the vacuole faces towards the micropylar pole (Christensen *et al.* 1997). A gene that is involved in egg cell

development is *RETINOBLASTOMA-RELATED 1* (*RBR1*). Mutant FGs of *rbr1*-plants show proliferation of egg cell nuclei ((Ebel *et al.* 2004; Ingouff *et al.* 2006; Ingouff *et al.* 2009). Similarly, the mutant *eostre* (Pagnussat *et al.* 2007) in which a homeodomain transcription factor is misexpressed show defective embryo sacs and supernumerary egg cells. Mutant embryo sacs of *lachesis* (*lis*, (Gross-Hardt *et al.* 2007; Voelz *et al.* 2012), *clotho* (*clo*, Moll *et al.* 2008) and *atropos* (*ato*, Moll, *et al.* 2008) show egg cell features in other FG cells. The mutant *multicopy suppressor of ira 1* (*msi1*) shows autonomous endosperm and embryo development (Guitton and Berger 2005). A phenomenon, which is still under investigation is the observation that double fertilisation requires a mechanism that distributes both sperm cells to the gametic cells of the FG. In contrast to the central cell, the egg cell seems to harbour a mechanism which blocks polyspermy (Scott *et al.* 2008). The nature of this polyspermy block is not yet known (Sprunck and Gross-Hardt 2011; Dresselhaus and Sprunck in press). Furthermore, the egg cell apparently controls sperm cell activation. This pathway includes five signalling peptides called AtEC1 (Sprunck *et al.* submitted).

The second cell, which is a direct target of double fertilization, is the central cell (CC). The CC gives rise to the triploid endosperm. Together with the egg cell, the CC is called a gametic cell (Sprunck and Gross-Hardt 2011). The haploid polar nuclei of the central cell fuse during embryo sac maturation as observed in *Arabidopsis* (Christensen *et al.* 1997) or shortly after fertilization in grasses including maize (Huang and Sheridan 1994). Together with the egg cell, the CC appears to be a master regulator of FG-cell fate. The splicing factor LIS, for example, seems to be required for lateral inhibition of synergids and antipodals which prevents the accessory cell form acquiring gametic cell fate (Gross-Hardt *et al.* 2007, Voelz *et al.* 2012). In maize, additional CCs appear to be formed in *indeterminate gametophyte1* (*IG1*) mutant ovules (Guo *et al.* 2004; Voelz, *et al.* 2012). IG1 encodes for a LATERAL ORGAN BOUNDARY-domain transcription factor (Evans 2007). Knock-down of the egg cell expressed gene coding for the putative signalling peptide *EGG APPARATUS1-LIKE 1* (*ZmEAL1*) leads to CC-like structures, which are likely derived from antipodal cells (Krohn *et al.* submitted); see ***Chapter 4***). For a general introduction into peptide signalling during development see 5.1.

In addition to the female gametes, the embryo sac contains accessory cells at both poles. An important cell type at the micropylar pole is the synergid cells. The two synergids and the egg cell are named as egg apparatus (Sprunck and Gross-Hardt 2011). The most important function of the synergid cells appears to be pollen tube (PT) guidance. For

Torenia fournieri, a plant species exhibiting a protruding embryo sac, it has been shown, that synergids are required and sufficient for species specific short range guidance of PTs (Higashiyama *et al.* 2001). These cells show features, which are associated with secretion and reception of compounds. This structure consists of finger like cell wall projections which extend into the lumen of the synergid cell and is called the filiform apparatus (Huang and Russell 1992). The *Arabidopsis* mutant *myb98* is defective in formation of the filiform apparatus and thus displays a lack in pollen tube attraction (Kasahara *et al.* 2005). A few synergid cell derived short-range guidance signals have been identified to date. In maize, the signalling peptide EGG APPARATUS 1 (ZmEA1) is shown (Dresselhaus *et al.* 2005; Márton *et al.* in press) to be responsible for micropylar guidance. For *Torenia*, so called LURE peptides have been identified as PT guidance signals in *T. fournieri* (Okuda *et al.* 2009) and *T. concolor*, (Kanaoka *et al.* 2011). Another important task of synergids is termed pollen tube reception. This process encloses disintegration of a PT and one (receptive) synergid cell. The sperm cells are released into the receptive synergid cell and can prepare for fusion with the two female gametes (Hamamura *et al.* 2011). In maize, it has been shown that ZmES4, a defensin like cysteine-rich peptide, is responsible for PT burst (Amien *et al.* 2010). The receptor kinase FERONIA (Escobar-Restrepo *et al.* 2007), the mildew resistance family o protein NORTIA (Kessler *et al.* 2010) and the GPI-anchored protein LORELEI (Capron *et al.* 2008), both from Arabidopsis, are also required for PT reception by the FG. It was further shown that functional peroxisomes are required for synergid function as indicated by the peroxisomal mutant in the gene *ABSTINENCE BY MUTUAL CONSENT* (Boisson-Dernier *et al.* 2008).

The accessory cells at the chalazal pole of the embryo sac comprise of the antipodal cells. Their function is still unclear. In *Arabidopsis* the antipodal cells degenerate shortly before fertilization and seem to be obsolete for fertilization and seed development (Sprunck and Groß-Hardt 2011). In grass species including maize, antipodal cells proliferate and undergo endoreduplication before and even after fertilization (Randolph 1936). Antipodal cell fate is probably regulated by the central cell. The recessive allele of a mitochondrially localised cysteinyl-tRNA-synthetase *syco-1* and disruption of mitchondria in the central cell by expression of an ATP/ADP-translocator (Kaegi *et al.* 2010) lead to prolonged life span of antipodals in *Arabidopsis* that supports this hypothesis.

1.2 Development and function of the male gametophyte in angiosperms

The development of the male gametophyte (MG) is macroscopically less complex than that of the FG. The MG consists only of three haploid cells, a vegetative tube cell and two sperm cells (for review on the Arabidopsis MG see (Wilson and Zhang 2009). Despite its rather simple architecture the MG has to fulfil the task of delivering the inmotile sperm cells to the FG for fertilization. This process is mainly governed by the pollinated sporophyte and only in terminal phases by the FG (Figure 1.2, Lausser *et al.* 2010); (Lausser and Dresselhaus 2010; Dresselhaus, Lausser et al. 2011; see also ***Chapter 3***). MG development is divided into three phases. The first is referred to as premeiotic development of microsporocytes, the second as microsporogenesis and microgametogenesis (for review on the maize MG see Bendinger and Fowler 2009). The last phase is called progamic development.

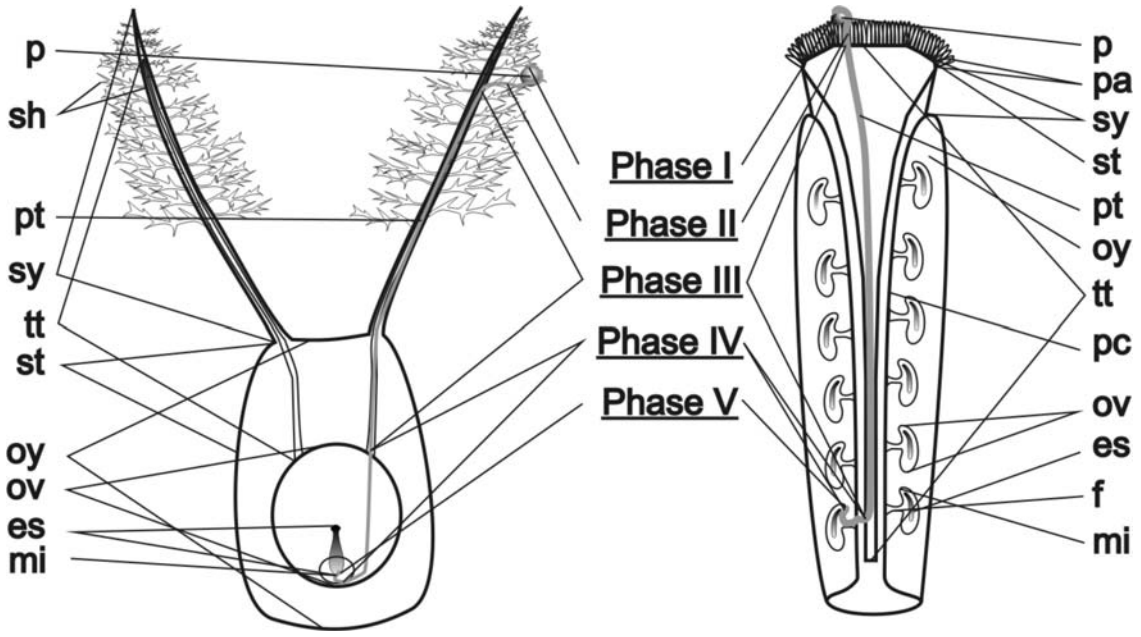

Figure 1.2 Scheme of progamic pollen tube development in grasses and eudicots The left-hand side of the scheme represents a typical grass pistil, whereas the right-hand side shows an *A. thaliana* pistil as a model of eudicots. The developmental phases are defined as (Phase I) pollen germination, (Phase II) stigma invasion, (Phase III) TT growth, (Phase IV) ovarial cavity growth in grasses and funicular growth/guidance in eudicots respectively, and finally (Phase V) gametophytic interactions that include micropylar growth and guidance as well as sperm release (taken from Lausser and Dresselhaus, 2010). Gametophytes are drawn in grey. Abbreviations: es, embryo sac; f, funiculus; mi, micropyle; ov, ovule; oy, ovary; p, pollen; pa, papillae; pc, placenta; sh, silk hair; st, stigma; sy, style; pt, pollen tube; tt, transmitting tract.

In the following, the first two phases will be briefly outlined. Premeiotic microsporocyte development occurs in the anther. The archesporial cells undergo mitotic divisions and differentiate into the sporogenous pollen mother cells (PMC) and four surrounding cell layers of the anther wall, of which the outermost forms an epidermis. Towards the centre of the anther the layers are called endothecium, middle layer and the innermost tapetum. Many components of the pollen coat originate from the tapetum, which undergoes programmed cell death in course of premeiotic microsporocyte development in maize (Bendinger and Fowler 2009). Within the anther, PMC undergo meiosis leading to tetrads of haploid microspores. This phase equals microsporogenesis and is followed by microgametogenesis (Bendinger and Fowler 2009). The MG is strongly reduced and development encloses only two mitotic divisions. The first asymmetric division results in a vegetative cell and a generative cell which undergoes a second division forming the two sperm cells. The mature pollen is finally released from the anther during anthesis (Bendinger and Fowler 2009). After it arrived on a compatible stigma the progamic phase starts (Figure 1.2). It involves all events after pollination and is described in more detail in ***Chapter 2***.

1.3 Genetic and hormonal control of embryo development in maize

After fertilisation a new sporophytic generation begins. The early phases of embryo development occur in a more or less stereotypic species-specific manner. Embryo development in the model plant *Arabidopsis thaliana* has been intensively studied for many decades (for review (De Smet *et al.* 2010). The same was done for the important crop plant and genetic model *Zea mays* (for review see Nardmann and Werr 2009). In the following the focus will be on embryo development of maize.

The morphological development of the embryo is described in different stages (Abbe and Stein 1954; Figure 1.3). In contrast to the rather stereotypic cell division pattern in *Arabidopsis*, only the first cell divisions in maize embryo development follow predictable cell division planes. The zygote divides asymmetrically into the small apical cell facing towards the chalazal pole of the ovule and a bigger basal cell facing towards the micropyle. The apical cell gives rise to the embryo proper, whereas the basal cell gives rise to the suspensor (Randolph 1936). The small apical cell divides first in a longitudinal manner and both structures grow until the transition stage. At this time point the embryo has the shape

of a club and besides the differentiation between the small embryo proper cells and the large vacuolated suspensor cells no further macroscopically visible structures are formed (Nardmann and Werr 2009).

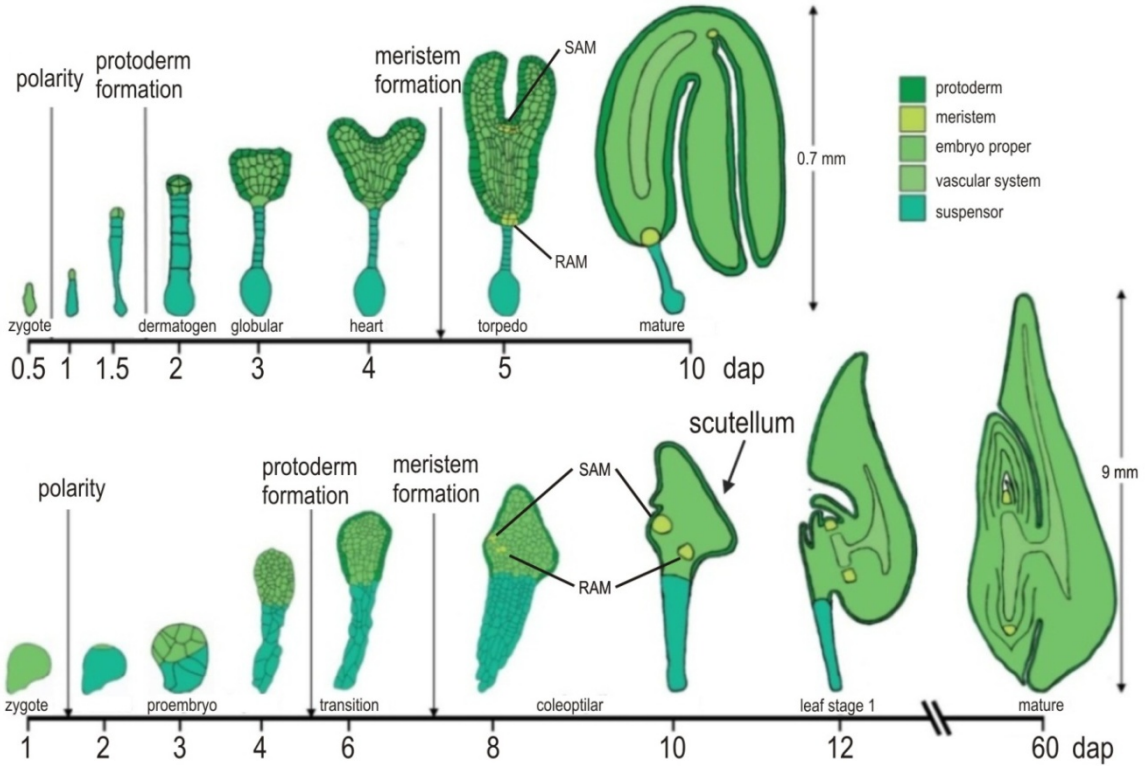

Figure 1.3 Scheme of embryo development in *Arabidopsis thaliana* and *Zea mays*. Embryo development of maize (lower row) differs from *Arabidopsis* (upper row) in many aspects. Whereas *Arabidopsis* embryos develop their cotyledons and all embryonic cell types including the stem cell niches already at heart stage, maize embryos develop no such distinct structures at the comparable transition stage. Some authors revere to maize embryos like drawn here for 8 dap as late transition stage. This work classifies these embryos as coleoptylare stage like depicted above (adapted from Vernoud *et al.* 2005). Abbreviations: dap = days after pollination, SAM = shoot apical meristem, RAM = root apical meristem.

However, during early embryogenesis several decisions have to be made and structures have to be determined such as the apical-basal axis and the radial axis. Furthermore, the bilateral symmetry needs to be established and the stem cell pools for root and shoot meristems need to be specified (de Smet *et al.* 2010). In the initial phases of embryogenesis in maize, no distinct structures are histologically detectable. The first obvious tissue is the protoderm, a single cell L1 layer surrounding the embryo proper starting at late proembryo/transition stage (Randolph 1936). A marker gene expressed in the maize protoderm is the *LIPID TRANSFER PROTEIN 2* (*LTP2*, (Sossountzov *et al.*

1991). At the position where the SAM will arise, *LTP2* expression is absent. At this adaxial position the *WUSCHEL RELATED HOMEOBOX 2a* (*WOX2a*) transcription factor is expressed (Bommert and Werr 2001). *WOX2a* is already expressed in the apical cell after zygote division (Nardmann *et al.* 2007). Another group of transcription factors, called *OUTER CELL LAYER* (*OCL*) is expressed in the protoderm. Interestingly, *OCL4* expression is predominate at the adaxial side whereas *OCL5* is expressed at the abaxial side of the proembryo (Ingram *et al.* 2000). This indicates that the proembryo is already unequally organized at the adaxial and the abaxial side although morphological differences are not visible (Nardmann and Werr 2009). Below the adaxial protoderm the SAM is initiated. This cell population is marked by expression of *KNOTTED 1* (*KN1*, Smith *et al.* 1995), the maize homologue of *SHOOT MERISTEMLESS* (*STM*) of *Arabidopsis* (Long *et al.* 1996). The protodermal L1-layer, where *KN1* is absent, is an expression domain of *NO APICAL MERISTEM* (*NAM*), a homologue of *CUP SHAPED COTYLEDON 2* (*CUC2*) from *Petunia hybrida* (Zimmermann and Werr 2005).

The distribution of auxin and the expression pattern of the auxin efflux carrier *PINFORMED 1a-c* (*ZmPIN1a-c*) during maize embryogenesis has been studied recently by immunolocalisation and *in situ* hybridisation (Forestan *et al.* 2010). All three *PIN1* genes are expressed in a more or less equal expression pattern during kernel development from the unpollinated kernel stage onwards. The endosperm exhibits *PIN1* expression already before cellularisation. When the embryo reaches the transition stage, *PIN1* expression is found in the basal endosperm transfer layer (BETL) and the embryo surrounding region (ESR). In transition stage embryos *PIN1* transcript and protein is most strongly present in the protoderm. Later on *PIN1* expression is most abundant at the adaxial surface of the embryo proper and at the tip of the evolving scutellum. Localisation of auxin in the endosperm is found in the BETL, ESR and aleurone. It largely overlaps with *PIN1* expression. In the embryo auxin is detectable at the top of the proembryo. At transition stage auxin accumulates in the developing protoderm. At coleoptylare stage, high auxin signals is localised in the tip of the scutellum, the protoderm, the adaxial side of the embryo proper, the tip of the developing coleoptile and in the embryonic root. These patterns are disturbed by the auxin export inhibitor *N*-1-naphthylphthalamic acid (Forestan et al. 2010).

A second important phytohormone of which the distribution and accumulation has been studied in the developing maize caryopse is cytokinin. High levels of cytokinins can be found in transition stage embryos and in the ESR. The signal in the transition stage embryo

appears to be the strongest at the adaxial side of the embryo proper. At the coleoptylar stage, strongest cytokinin concentrations are found at the positions of the arising SAM and RAM. The endosperm shows the strongest cytokinin concentrations at the BETL (Rijavec and Dermastia 2010). A link between cytokinin signalling and SAM development during early embryogenesis is indicated by the expression of the A-type response regulator *ABERRANT PHYLLOTAXY 1* (*ABPHYL1*). The transcript of *ABPHYL1* is found in the SAM starting in transition stage embryos. The gene is cytokinin inducible in shoots and at its expression domain in the SAM but not in leaves. The corresponding mutant shows changes in SAM size. Its name was given due to decussate instead of alternating phyllotaxy (Giulini *et al.* 2004).

1.4 Aims of the work

The aim of the following work was to address various questions related to sexual reproduction in plants. The first investigations should provide answers to the question to which extent the pollinated sporophyte and the FG regulate pollen tube (PT) growth and guidance towards the female gametophyte in maize. Of special interest was the range of influence of the FG compared to the model system *Arabidopsis thaliana*. The results of these experiments are discussed in ***Chapter 2*** and have been published recently (Lausser et al. 2010). Another aspect of double fertilisation studied in this work are signalling events. *Arabidopsis thaliana* marker lines have been generated in order to address the question about calcium signalling during double fertilisation. For detailed introduction into calcium signalling in general and in context of double fertilisation see ***Chapter 3***. The lines generated express a recombinant calcium sensor (CerTN-L15; Heim and Griesbeck 2003) under constitutive and gametophytic cell specific promoters. Results about the various calcium sensor lines are discussed in this chapter. Questions on FG development and cell identity in maize are addressed in ***Chapter 4***. *ZmIG1* was identified in the course of this thesis as potential downstream target of egg cell signalling the secreted peptide EAL1. Auxin dependent gene expression of *EAL1* was tested in BMS suspension cells. A manuscript enclosing these findings together with data on the role of EAL1 in embryo sac development has been resubmitted with minor revision (Krohn et al. submitted). Furthermore, the influence of EAL1 on early embryo development in maize was investigated and represents the major achievement in this thesis. The results include the characterisation of EAL1 interaction candidates isolated from a yeast-2-hybrid screen, the

analysis of *eal1*-RNAi-lines constructed by N. Krohn (see above) during embryogenesis, identification of downstream targets by microarray analysis and pattern formation in early embryo development using publicly available marker lines. These results are shown and discussed in ***Chapter 5***. Finally, a comprehensive discussion and outlook is presented as ***Chapter 6***.

Chapter 2 - Sporophytic control of pollen tube growth and guidance in maize

The following experimental chapter is based on the publication by Lausser et al. 2010 (see below): The manuscript was fully written by A. Lausser and edited by T. Dresselhaus. The *fg*-RNAi-plant line used in this study and the confocal microscopy images (Figure 2.5A and B) were generated by K.o. Srilunchang. All other experiments were conducted by A. Lausser except the studies on transmitting tract targeting (Figure 2.4), which were carried out by I. Kliwer. Data on pollen tube germination and reach were already acquired for the diploma thesis of A. Lausser (Figures 2.1-2.3 and Table 2.1; Lausser 2007).

2.1 Introduction

Wide hybridization between different taxonomical plant species is very common in nature. In some genera like *Quercus*, hybrids can be more abundant in the landscape of an area than the pure parental species and form stable hybrid swarms (Whittemore and Schaal 1991). Moreover, hybridization barriers between plants of the same or related species is thought to be one of the driving forces of speciation and therefore represents an important process in flowering plant evolution (Rieseberg and Willis 2007). For plant breeders, hybridization of crop plants with closely related wild species is an important way of introducing new traits, such as biotic and abiotic resistance, into economically important species. Unfortunately, hybridization often has drawbacks in terms of reduced seed set and fertility of the F1 generation. Understanding the mechanism of pre- and post-zygotic inter- and intra-specific crossing barriers in crop plants are therefore of great interest for reproductive and evolutionary plant biology as well as for plant breeding. In particular, the long studied prezygotic barriers related to pollen tube (PT) germination, growth, and guidance represent the major hybridization controls in nature (Arnold and Hodges 1995); (Widmer *et al.* 2009). Various stages of progamic PT development and growth from pollen–stigma contact to sperm cell discharge offers many possibilities to reject alien pollen and to prevent unfavourable fertilization by alien pollen. In the model plant system *Arabidopsis thaliana* Heynh., for example, progamic male gametophyte development has been divided into five distinct phases (Johnson and Preuss 2002; Swanson *et al.* 2004). Phases I–III, from capture of the pollen grain at the stigma surface, tube growth initiation,

and navigation between the stigma cells towards and inside the transmitting tract (TT), are mainly governed by anatomical aspects of the stigma and style as well as species-specific pollen–stigma interaction and signalling. In Phase IV, during growth along the ovule surface, PTs are thought to depend on signals from both the haploid female generation and the diploid maternal tissue of the ovule. In Phase V, the micropyle is targeted and the sperm cells are released inside the egg apparatus. This final phase is thought to be under gametophytic control (Shimizu and Okada 2000; Johnson and Preuss, 2002; Higashiyama and Hamamura 2008). Similar determinations of PT growth phases have been made for other eudicots such as cotton (*Gossypium barbadense* L.; Ram *et al.* 2008) and *Torenia fournieri* Lind. (Kikuchi *et al.* 2007). Due to anatomical differences related to a single ovule inside the ovary, the progamic male gametophyte development in grasses (Poaceae) has been classified in a slightly different way (Heslop-Harrison 1982). Phases I–III in maize (*Zea mays* L.), for example, can be regarded as homologous to those described in A. thaliana. However, during Phase IV, the TT in the upper ovary wall (upper style) plays an important role in PT number reduction and is the last location where the PTs are growing between sporophytic cell layers. At the end of the TT, PTs leave the sporophytic tissue to enter the ovarial cavity and to grow at the surface of the inner integument towards the micropylar region (Heslop-Harrison *et al.* 1985). The ovarial cavity and the micropyle are thought to contain chemotropic signals to guide the growing PT (Heslop-Harrison, 1982; Márton et al., 2005; Higashiyama and Hamamura, 2008; Okuda et al., 2009). In the last decade, many small proteins and other general compounds like calcium, c-amino butyric acid, or nitric oxide have been discussed to be involved in progamic PT germination, adhesion, growth, and guidance. Most advances have been made in the Brassicaceae and Solanaceae families including their well understood self-incompatibility (SI) systems (for reviews see (Hiscock and McInnis 2003; Swanson et al., 2004; McClure and Franklin-Tong 2006). SI is a first distinct obstacle for the male gametophyte, preventing not only self but also hetero-pollination by alien species if severe physiological and anatomical disharmony between pollen and female organs is neglected. Hybridization between closely related self-compatible and self-incompatible plant species regularly fail, if the self-incompatible species is pollinated with pollen from the self-compatible one. However, hybridization can be successful if pollination is carried out vice versa (Lewis and Crowe 1958). In contrast to the Brassicaceae and Solanaceae families, much less is known about SI in the Gramineae. Grasses are known to have two loci (S and Z) based on a gametophytic SI-system. Although the grass SI-system is genetically gametophytic, the

appearance is sometimes more similar to the sporophytic SI system of the Brassicaceae. Pollen can be rejected at the level of pollen hydration and germination but also during growth through the style and even at the ovule surface or via postfertilization events (Yang *et al.* 2008). In the important crop plant *Z. mays*, which is generally self-compatible, several loci are known to lead to incompatible pollination or to influence progamic male gametophyte development. Among these, the gametophte factors (*ga*) are best described. When silks, homozygous for the dominant *Ga1* allele, for example, are pollinated with a mixture of *Ga1* and *ga1* pollen, those carrying the recessive allele are rarely involved in fertilization (Nelson 1994). The strongest phenotype is observed in the pollination of *Ga1s*/*Ga1s*-silks with ga1-pollen. This combination leads to a complete lack of seed set due to a slowed and finally interrupted growth of PTs in the silks (House and Nelson 1958; Bedinger and Fowler, 2009). Another genetically linked, but distinct crossing barrier is based on the *teosinte crossing barrier 1* (*tcb1*) locus mediating unilateral crossing barrier between maize and its closely related subspecies teosinte. Maize pollen, usually carrying the recessive *tcb1* allele, is unable to fertilize teosinte (generally homozygous for the *Tcb1s* allele). Both barriers act independently and through incongruity rather than active rejection. In both cases, *ga1* and *tcb1*, the genotype affects the male gametophyte and sporophytic maternal tissues. The recessive alleles are thought to be null alleles (Kermicle and Evans 2005). Hitherto, the molecular basis of both phenomenons remained unknown. Other maize mutants like *white pollen1* (*whp1*) and *colorless2* (*c2*), both defective in chalcone synthase and thus flavonol biosynthesis, are also hampered in PT growth in the style (Pollak *et al.* 1995). A member of a sister genus of *Zea*, namely *T. dactyloides*, has been shown to be able to hybridize with maize at unnatural conditions. Whereas pollination of *Tripsacum* with maize is regularly successful, *T. dactyloides* pollen in general is only able to fertilize maize if silks are cut back to a length of less than 2.5 cm (Mangelsdorf and Reeves 1931). Finally, in analogy to Phase V of progamic male gametophyte development in *A. thaliana* and other dicotyledonous species, species-specific signals or barriers by the female gametophyte (embryo sac) are postulated also to exist in grasses controlling PT growth and guidance around the micropyle. A small secreted protein, ZmEA1, expressed in the egg apparatus, is the first candidate for a micropylar guidance signal in maize (Márton et al., 2005), and recently defensin-like proteins secreted by the synergids have been shown to guide the PT towards the egg apparatus in the micropylar region of *T. fournieri* in a species-specific manner (Okuda et al., 2009).

In order to gain more insights into crossing barriers and progamic PT development in maize at the cellular level, cross-pollination experiments were performed among and between maize and *T. dactyloides*, and in addition PT behaviour of other plant species on maize and *T. dactyloides* silks was analysed. Pollen germination efficiencies and tube growth in silks as well as in the ovarial cavity were investigated and compared, including also the genetic gametophyte factor *Ga1s*/*ga1*-system. To determine the role of the female gametophyte for PT attraction during progamic Phases IV and V, a novel mutant line was applied, displaying fully differentiated maternal ovary tissues but completely disintegrated embryo sacs.

2.2 Experimental procedures

2.2.1 Plant material, pollination and sample preparation

2.2.1.1 Plant growth

In addition to wild type maize inbred lines A188 and K55, near isogenic lines *Ga1s/Ga1s*, *Ga1s/ga1* and *ga1/ga1*, all based on the genetic background of K55, and the respective backcrosses were used. Tetraploid and hexaploid accessions of *T. dactyloides* were applied for various experiments. Rice (*Oryza sativa* L. ssp. *japonica*) pollen was collected from the commercial inbred line M 202, and from greenhouse grown grasses *Poa nemoralis* L. and *Lolium multiflorum* Lam. All Poaceae were kept in the greenhouse under long-day conditions (16 h of light). The temperature was kept at 25 °C during the light period and at 18 °C in the dark. Flowering of rice was induced by short-day treatment (9 h of light) for two weeks. *A. thaliana* (ecotype Columbia-O) was raised under short day conditions and shifted to long day conditions after four weeks. Long and short day chambers were kept at 20-22 °C and 70% humidity. Lily (*Lilium longiflorum* Thunb.) flowers were obtained as cut material from local flower shops. Pollen from all plants except maize and *T. dactyloides* was obtained by harvesting anthers one day before or at anthesis. Maize and *T. dactyloides* pollen was obtained by shaking fresh pollen into a paper bag between 9:30 and 10:00 a.m. Older pollen was removed from tassels by vigorous shaking the evening before pollen harvest.

2.2.1.2 Pollination and sample preparation

Pollinations were carried out either *in vitro* or in the greenhouse using whole plants. For *in vitro* pollination, emasculated flowers were placed into a humid chamber and pollen was applied by shedding or usage of a fine brush. In order to prevent unintended pollination of distal parts of silks, they were covered with a piece of paper. After incubation, silks were fixed for aniline blue staining as described below. For cross-sections, fixed and stained silks of maize and *T. dactyloides* were imbedded in 5% low melting agarose. Slices of 80 µm were cut using a vibratome (Leica VT 1000S) and observed under an inverted microscope (Nikon Eclipse 1500). *In vitro* pollinated silks were incubated in a humid chamber for 3 to 24 hours at 21 °C in the dark. Seed set after pollination of plants was monitored after two weeks.

2.2.2 Aniline blue staining (modified after Martin 1959) and microscopy

Silk tissue and ovules were fixed over night in 9:1 ethanol:acetic acid at 4 °C. Fixed samples were rehydrated by an ethanol series (70%, 50% and 30%) each for 5 min and washed with 0.1 M potassium phosphate buffer pH 8.0. Subsequently samples were incubated for 5 minutes in 10% chloral hydrate and afterwards for 10 minutes in 5 M sodium hydroxide solutions each at 65 °C. After each step, samples were washed with potassium phosphate buffer. The thereby cleared and smoothened tissue was stained for 15 minutes at 21 °C or up to several days at 4 °C with 0.1% aniline blue solution (water blue, Fluka) prepared with potassium phosphate buffer (see above). Specimen were mounted with fresh staining solution on a slide with cover slip and analysed at an inverted microscope (Nikon Eclipse 1500) with near UV excitation.

2.2.3. Histological studies of fixed and cleared ovules

Whole cobs were treated according to a fixing/clearing method using Kasten's fluorescent periodic acid-Schiff's reagent described by (Vollbrecht and Hake 1995). The phases for hydration and dehydration of ears were prolonged from 20 to 30 minutes in each step and ears were dissected after after clearing with methyl salicylate (Young *et al.* 1979). Samples were mounted in methyl salicylate on glass slides under a cover slip and analysed with a

LSM510-META confocal laser scanning microscop (Zeiss) with 488 nm excitation and a LP 505 filter.

2.3 Results

2.3.1 Pollen germination efficiency

In an initial experiment, we determined the ability of pollen from different plant species to germinate on silks of maize and *Tripsacum dactyloides*, respectively. In order to rule out bias of germination rates by inadequate temperature and air humidity conditions, silks or stigmas of donor plants were always *in vitro* pollinated in the same growth chamber. Subsequently, pollinated silks were stained with aniline blue to determine the ability of PTs to penetrate the stylar tissue (Figure 2.1A-H). Almost all other PTs studied were able to germinate, but either failed to invade or stopped growth within the silk hairs. Germinated pollen of *A. thaliana* is shown as an example in Figures 1D and H. Only the large PTs of maize (Figure 2.1A, B, and G) and *T. dactyloides* (Figure 2.1C, E and F) were able to grow completely through the silk hairs and reach the stylar tissue. Due to this finding, further detailed *in vitro* experiments were carried out only with pollen of these two plant species. To normalize obtained germination rates, we determined the average of germinated pollen on maize or *T. dactyloides* silks in relation to the average of germination rates observed after self-pollination (detailed numbers are given in Table 2.1).

Table 2.1. Pollen germination in silks/stigma after 4 h *in vitro* incubation at room temperature.

Silk	Pollen	Pollen total	Pollen germinated	Germination index	Normalized index	Standard deviation
A. thaliana	*A. thaliana*	317	289	90.81%	100.00%	4.31%
T. dactyloides	*A. thaliana*	322	109	34.25%	37.71%	4.63%
Z. mays	*A. thaliana*	316	67	21.32%	23.47%	0.88%
L. longiflorum	*L. longiflorum*	327	177	54.31%	100.00%	2.93%
T. dactyloides	*L. longiflorum*	375	4	1.18%	2.18%	1.10%
Z. mays	*L. longiflorum*	325	0	0.00%	0.00%	0.00%
L. multiflorum	*L. multiflorum*	259	82	30.99%	100.00%	6.18%
T. dactyloides	*L. multiflorum*	284	31	10.74%	34.66%	2.80%
Z. mays	*L. multiflorum*	291	36	11.63%	37.52%	3.02%
O. sativa	*O. sativa*	247	74	30.31%	100.00%	2.73%
T. dactyloides	*O. sativa*	453	52	11.61%	38.31%	0.84%
Z. mays	*O. sativa*	501	46	10.09%	33.30%	8.85%
P. nemoralis	*P. nemoralis*	176	67	36.06%	100.00%	4.83%
T. dactyloides	*P. nemoralis*	270	41	15.39%	42.68%	0.43%
Z. mays	*P. nemoralis*	242	55	23.69%	65.69%	2.99%
T. dactyloides	*T. dactyloides*	359	263	72.20%	100.00%	20.43%
Z. mays	*T. dactyloides*	315	231	73.14%	101.31%	9.83%
T. dactyloides	*Z. mays*	288	99	35.04%	54.74%	18.97%
Z. mays	*Z. mays*	413	269	64.01%	100.00%	15.92%

These percentages are shown in Figure 2.1I for maize silks and in Figure 2.1J for *T. dactyloides* silks. Notably, *T. dactyloides* pollen show high relative germination efficiencies on both, self and alien species, whereas germination efficiency of maize pollen is reduced to 50% on *T. dactyloides* silks. Pollen of other, distant related Poaceae showed relative germination efficiencies of 30-60% on silks of both, maize and *T. dactyloides*, respectively. Interestingly, the dicotyledonous plant *A. thaliana* shows germination efficiencies in the range of distant related Poaceae, while pollen of the monocot *Lilium longiflorum* did not germinate on grass silks.

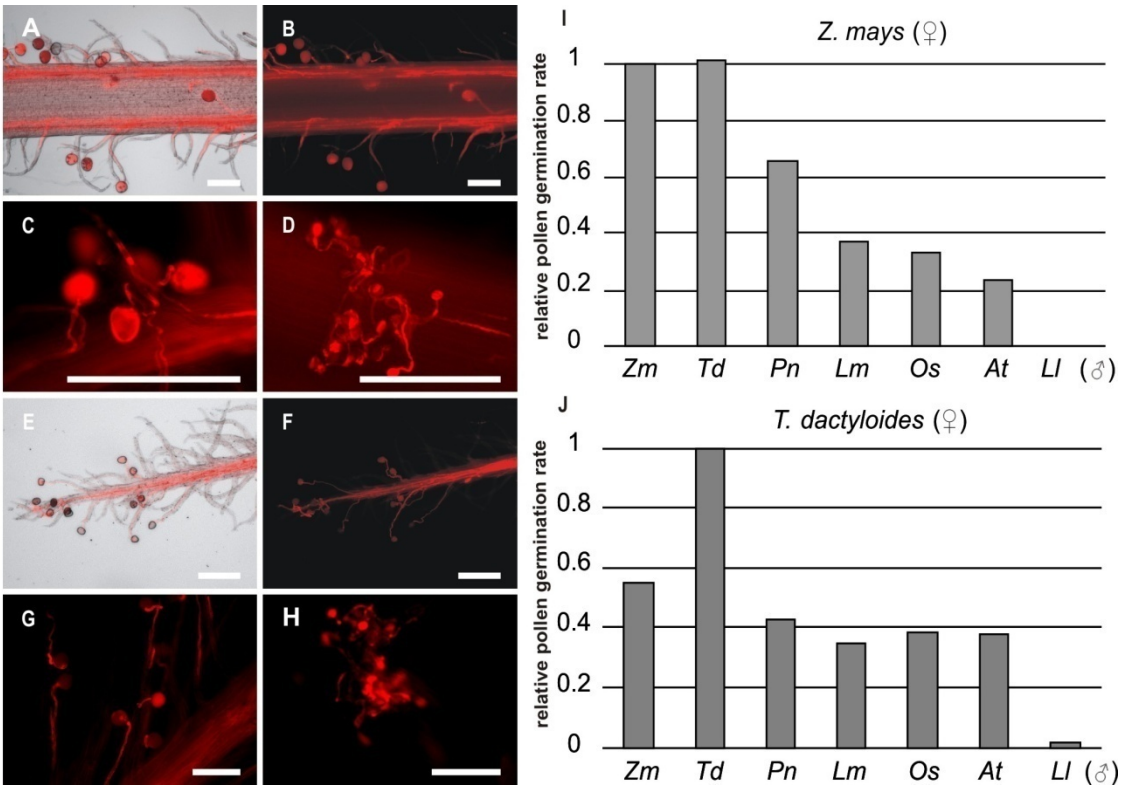

Figure 2.1 Germination rates of pollen from various monocot and dicot species on silks of maize and *Tripsacum dactyloides*, respectively. Silks of maize (A - D) and *Tripsacum dactyloides* (E - H) were pollinated with pollen from different species in a humid chamber at room temperature. All specimen were stained with aniline blue and false red color animated for better contrast. Most of the pollen grains germinated silks of both, maize and *T. dactyloides* (maize pollen shown in A, B and G; *T. dactyloides* pollen shown in C, E and F; *Arabidopsis thaliana* pollen shown in D and H) To determine the relative pollen germination efficiency (I and J), germination was evaluated after 3 to 7 hours without staining and each value related to the germination rate after self pollination. See Table 2.1. Abbreviations: *Zm = Zea mays, Td = Tripsacum dactyloides, Pn = Poa nemoralis, Lm = Lolium multiflorum, Os = Oryza sativa, At = Arabidopsis thaliana, Ll = Lilium longiflorum.* Scale bars: 200 µm.

2.3.2 Pollen tube growth range in maize and *Tripsacum dactyloides* silks

PT growth length is known to be the critical factor in the unilateral incompatibility phenomenon between *ga1*-pollen and *Ga1s*/*Ga1s*-silks (House and Nelson 1958). The ability of *T. dactyloides* pollen to fertilize maize when silks are cut back suggests that this might also be the case for the natural maize-*Tripsacum*-crossing barrier (Mangelsdorf and Reeves 1931). In order to compare both hybridization barriers and tube growth range, silks of the maize inbred lines A188 and K55 as well as the near isogenic line *Ga1s*/*Ga1s* and its backcross progenies with K55 were analysed over a length of at least 10 cm. Cob segments

were placed in a humid chamber, pollinated and analysed as shown in Figure 2.2A. The presence of PTs in the various silk segments was monitored by aniline blue staining (Figures 2.2B-G). After pollination of silks from A188 with hexaploid and tetraploid *T. dactyloides* pollen, PTs were frequently found in the segments 0 to 4 cm distal to the pollination area. In rare cases, PTs were found in segments 4 to 8 cm distal but never in the proximal (>8 cm distal) part of the silk (Figure 2.2H). Many *T. dactyloides* PTs grew outside the transmitting tract (Figure 2.2F). With few exceptions, when maize PTs outside the transmitting tract stopped growth after a few cm (Figure 2.2G), close to 100% of maize PTs from inbred line A188 grew straight inside the transmitting tract (Figures 2.2D and E) and further all the way through the silk tissues.

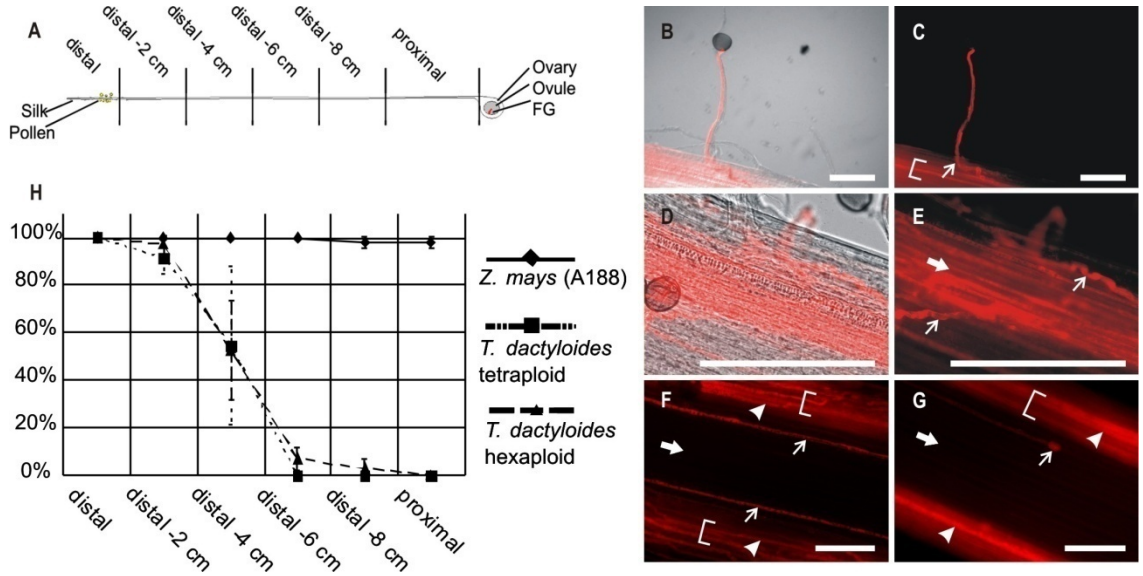

Figure 2.2 Pollen tube growth range in silks of maize inbreed line A188. (A) Cob segments have been placed in a humid chamber and were pollinated with pollen from maize as well as tetraploid and hexaploid *Tripsacum dactyloides*, respectively. 16h after incubation at room temperature, silks were cut in 2 cm pieces with proximal ends varying in length. Specimens were fixed, analyzed after anilin blue staining and false red color animated for better contrast (B - G). (B and C) Maize PTs outside and inside the silk tissue (arrow in C) within the transmitting tract (bracket). (D and E) PTs of both species, maize and *T. dactyloides* grow towards transmitting tracts surrounding parechymal cells (arrow in E). (F) Some *T. dactyloides*-PTs grew outside the transmitting tract (arrows) and (G) arrested after shorter growth than those inside transmitting tracts (brakets; PTs marked with arrowheads). *T. dactyloides* PT (arrow) growth arrest was observed in silk segments at 2 to 8 cm distance to the area of pollination. PTs inside transmitting tracts (brackets; PTs marked with arrowheads) continue growth. (H) Silk segments containing PTs were counted and set in relation to the total number of silks investigated. Brakets indicate transmitting tracts. Bold arrows indicate PT growth direction towards the ovary. Scale bars: 200 µm.

Pollination of *Ga1s*/*Ga1s*-silks with pollen from different maize genotypes and *T. dactyloides* revealed that in the incompatible *Ga1s*/*Ga1s*×*ga1*/*ga1* cross pollination, PTs display similar growth behaviour like in maize×*T. dactyloides* pollination experiments (Figure 2.3A). *ga1*-PTs stop their growth even more frequently after a shorter distance than *T. dactyloides* PTs. *T. dactyloides* and *ga1* PTs reach the proximal part of *Ga1s*/*Ga1s* silks in very rare cases. In this experiment, no striking difference was found between PTs originated from *Ga1s*/*Ga1s*- and *Ga1s*/*ga1*-plants, respectively. Silks of heterozygous *Ga1s*/*ga1*-plants show intermediate PT growth length behaviour when pollinated with *ga1*-pollen but not when pollinated with *T. dactyloides* (Figure 2.3B). On silks of the inbred line K55, PT growth of all maize genotypes and *T. dactyloides* show the same behaviour like on silks of the inbred line A188 (Figure 2.3C).

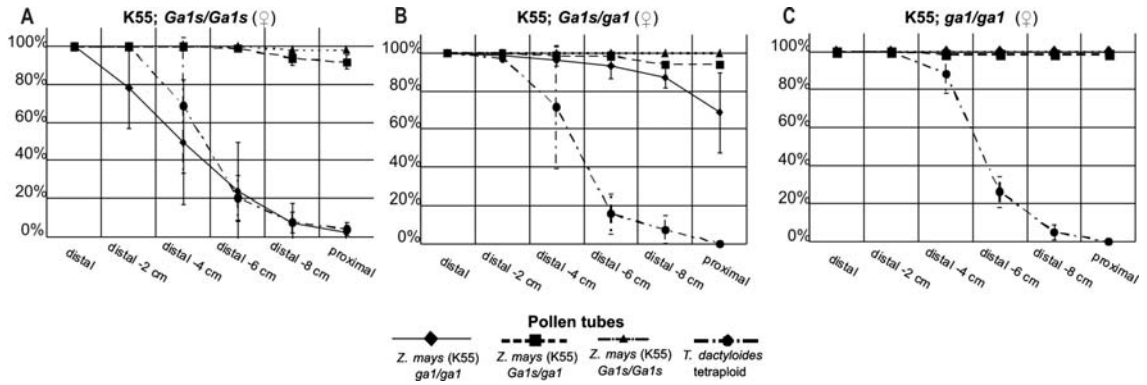

Figure 2.3 Pollen tubes growth range in silks of maize inbreed line K55 harboring different allele combinations of *Ga1s*. Cob segments were placed in a humid chamber and were pollinated as indicated. After 16h incubation at room temperature, silks were cut, stained and PTs counted as described before. (A) Silks dominant for *Ga1s*. (B) Silks heterozygous for *Ga1s*. (C) Silks recessive for *Ga1s* (*ga1/ga1*).

In order to address the question of the physiological and cellular basis of reduced PT growth length, we investigated cross sections of maize silks 2 and 6cm distal of the area of pollination in order to study the location of PTs inside the style. Firstly, the position of the vascular tissue was determined by safranin and astra blue or phloroglucin/HCl staining in unpollinated silks (data not shown) or after aniline blue staining (Figure 2.4A). Notably, tracheae vessels of maize stained both for safranin/phloroglucin (cellulose) and aniline blue (callose). The latter was used as a marker to visualize tracheae vessels in pollinated silks. In control pollinations of maize (Figure 2.4B) and *T. dactyloides* (Figure 2.4G) silks with self-pollen, it was shown that PTs were detected almost exclusively in the intercellular spaces between transmitting tract cells, which are in close association with the

vascular bundles (Figures 2.4A and 2.4F). In the incompatible pollination of silks of the genotype *Ga1s*/*Ga1s* with recessive pollen (*ga1*), most of the PTs were found inside the transmitting tracts. Few PTs failed to target the transmitting tract and grew below the epidermal cell layer towards the ovule (Figure 2.4C). These PTs showed shorter growth length than those growing inside the transmitting tract. When *T. dactyloides* pollen was applied on maize silks, many PTs failed to enter the transmitting tract (Figure 2.4D) and instead displayed a rather homogenous distribution throughout the silk tissue. Those *T. dactyloides* PTs that found their way inside the transmitting tract achieved a longer growth length, but finally growth was arrested (Figure 2.4E). Cross sections of *T. dactyloides* silks (Figures 2.4F-H) revealed that all PTs of both *T. dactyloides* (Figures 2.4G) and maize (Figure 2.4H) quickly reach the transmitting tracts and make their way towards the ovule.

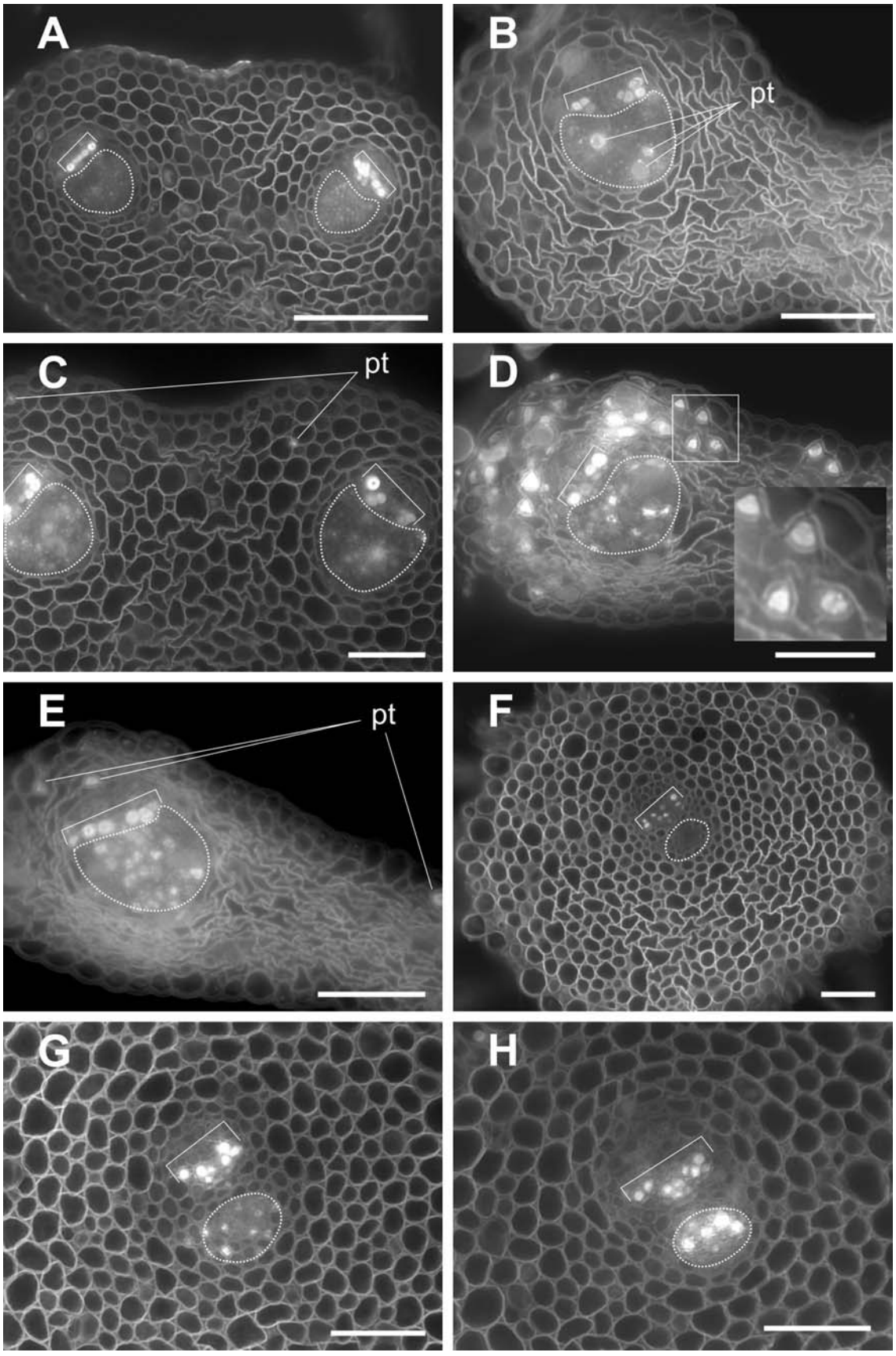
A
B
pt
C
pt
D
E
pt
F
G
H

Figure 2.4 Cross sections of maize and *T. dactyloides* silks stained with aniline blue. (A) In an unpollinated maize silk, xylem elements (brackets) of the vascular bundle show strong aniline blue staining whereas other cell walls lead to a light background signal. The transmitting tract (encircled) is composed of small longitudinal cells in close proximity to the xylem elements. (B) 24h after pollination with wild type maize pollen, PTs appear as large, round and brightly stained structures growing in the intercellular space between tt cells. (C) After pollination of *Ga1s*/*Ga1s* silks with recessive pollen (*ga1)*, some PTs (pt) grow outside of the tt towards the ovule. (D) The same phenomenon can be seen regularly in maize silks pollinated with *T. dactyloides* pollen. If pollinated silks are cut at the site of pollination, several PTs grow outside the tt right below the epidermis (four PTs between parechymal cells are visible in the onset). (E) These PTs stop their growth earlier and are therefore less abundant in more distal parts of the silk. (F) Compared to maize, *T. dactyloides* transmitting tracrs are more deeply embedded into the silk tissue and contain only one vascular bundle (bracket) with associated tt (encircled). Cross section of pollinated silks show PT growth only in tt in *T. dactyloides* silks pollinated with *T. dactyloides* (G) and maize (H) pollen. Scale bars: 50 µm.

2.3.4 PT guidance towards the ovular cavity and micropyle

PT guidance in the ovular cavity is thought to be controlled by specific chemotropic signals secreted by the female gametophyte. In maize plants, where the *ZmEA1* is down regulated by RNAi, PTs grew in close proximity to the micropyle, but failed to enter it for successful fertilization (Márton et al. 2005). In order to study the role of the female gametophyte for ovular and micropylar guidance in maize, we used novel RNAi-lines lacking embryo sacs (Srilunchang *et al.* 2010). Mature ovules of these mutants contain fully differentiated sporophytic ovule tissues, but completely disintegrated embryo sacs (Figure 2.5B). These RNAi-lines enabled us to investigate the role of the female gametophyte for PT guidance. Using wild type ovules, PTs grew inside the ovular cavity after leaving the two transmitting tracts towards the micropyle and one PT penetrates the micropylar nucellus cells to achieve double fertilization (Figures 2.5C and D). In contrast, PTs grew at the surface of mutant ovules towards the micropyle until an area of approximately 100 µm apart from the centre of the micropylar cone (Figures 2.5E and F). Arriving PTs of maize or *T. dactyloides* showed the same behaviour and seem either not to be attracted or repelled the micropyle no matter if they originated from. Interestingly, late coming PTs are also excluded from an area of approximately the same diameter on wild type ovules (Figures 2.5C and D). These experiments indicate that with the exception of

micropylar short range guidance, PT guidance in maize is completely controlled by the tissues of the sporophyte.

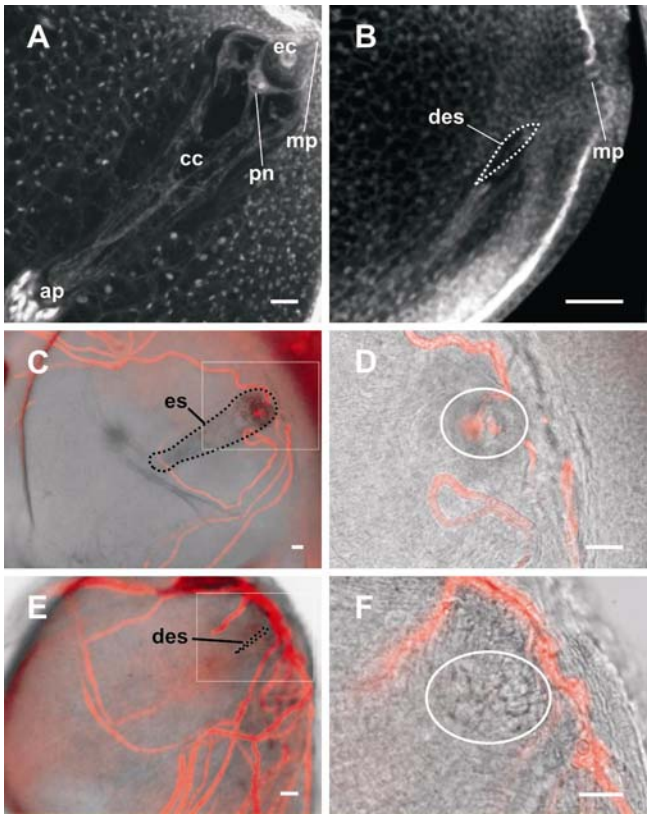

Figure 2.5. Pollen tube growth and attraction in the micropylar region of the ovule. (A) CLSM longitudinal section through a WT ovule displaying a mature female gametophyte. (FG). (B) *fg*-RNAi mutant ovule lacking a functional FG that is completely disintegrated after stage FG5 (Srilunchang *et al.* 2010). (C) WT ovule 24h after pollination and anilin blue staining (false colour red staining was used for better visuality of PTs). Several PTs arrived at the ovule surface and grew towards the micropylar region. One PT grew inside the micropyle and the tip is enlarged inside the synergid. The box indicates the enlarged region shown in (D). (D) Enlargement of the region indicated in (C). Only one PT succeeded in entering the micropyle (circle). Additional PTs are no longer attracted by the micropylar region. (E and F) Ovules of the *fg*-RNAi mutant line. The FG is disintegrated (encircled) and PTs (arrowheads) grew in 50 to 100 µm proximity of the center of the micropylar cone (circle), but did not enter. Abbreviations: ap = antipodal cells, cc = central cell, des = degenerated embryo sac, ec = egg cell, es = embryo sac mp = micropyle, pn = polar nuclei. Scale bars: 50 µm.

In order to address the question, if in incompatible pollinations some PTs are still able to reach and fertilize the embryo sac, we carried out mass pollinations at maize and *Tripsacum* plants with pollen of various grasses (Table 2.2). First, we could confirm the findings of incompatibility reactions after pollinating maize plants with full length silks.

Table 2.2. Seed set of maize and *Tripsacum* two weeks after pollination with different grass pollen. Ovules, which appeared to initiate seed development, have been counted. For pollination of maize plants with shortened silks (< 5cm), the husks around the cob have been peeled of and silks were cut with scissors. Inflorescences of *Tripsacum* have been emasculated before anthesis.

Female	Male	Sum silks	Seed set	Efficency
***Z. mays* silks >10 cm**	***Z. mays***	1768	690	37%
	***T. dactyloides* 4n**	461	0	0%
	L. multiflorum	344	0	0%
	O. sativa	289	0	0%
	P. nemoralis	319	0	0%
***Z. mays* silks < 5 cm**	***Z. mays***	894	289	32%
	***T. dactyloides* 4n**	742	274	36%
	O. sativa	217	0	0%
***T. dactyloides* 4n**	***T. dactyloides* 4n**	96	48	50%
	Z. mays	36	8	22%
	L. multiflorum	24	3	13%
	O. sativa	21	4	19%
	P. nemoralis	20	2	10%
	no pollen	27	0	0%

Silks of each cob were separated into two populations and pollinated either at one side always with pollen from A188 or on the other side with alien or incompatible pollen (Figure 2.6A). We found that the existing barriers in the maize×*T. dactyloides* and the *Ga1s*/*Ga1s*×*ga1*/*ga1* crossings can be overcome by shortening maize silks to a length of less than 5 cm and by applying pollen directly to the huskless cob (Figure 2.6B). Embryo development and seed set was only observed after silk shortening. Pollination of tetraploid *T. dactyloides* with pollen of various Poaceae species led to a significant number of developed seeds (Table 2.2). Besides undeveloped (10-40%) and fully developed seeds (10-50%), we obtained a number of seeds (10-40%) which were aborted (Figure 2.6C).

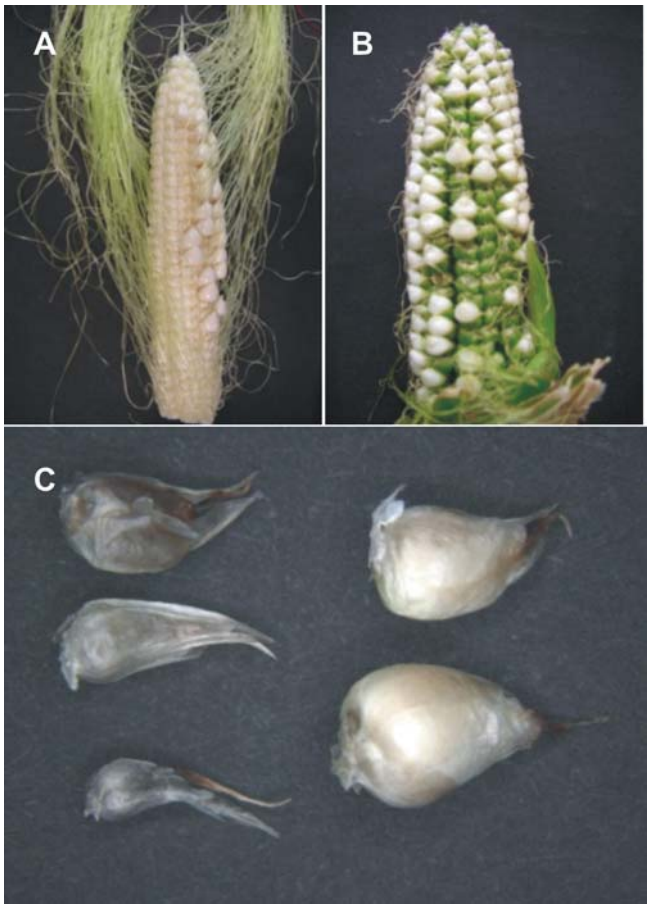

Figure 2.6 Seed set of maize and *Tripsacum dactyloides* two weeks after pollination with pollen from different grass species. (A) Silks have been separated in two populations (left and right). One half has been covered while the other one was pollinated. The picture shows a cob, pollinated in this case with *T. dactyloides* pollen (left side) and maize (right side) as a control. (B) Seed set after pollination of shortened maize silks. Husks were peeled of a mature cob and silks cut with scissors to a length of max. 5 cm. Cobs were pollinated with pollen from maize (left) and *T. dactyloides* (right), respectively. (C) Five *T. dactyloides* seeds are shown after pollination with self pollen. Husks were removed. The seeds had to be isolated to determine the developmental stage. The two seeds on the top left side are aborted and the one at the bottom left side was not developed at all. Two seeds on the right side are fully developed.

2.3 Discussion

Maize is generally considered as a self-compatible species (Yang et al. 2008), but many popcorn strains cannot be fertilized by pollen of dent, sweet and flints strains, although the reciprocal crosses are successful (House and Nelson 1958; Kermicle and Evans 2005). Especially the dominant gametophytic factor *Ga1-s* present in many varieties of popcorn is involved in the prevention of fertilization (Nelson 1952). The molecular nature of Ga1-s is not known to date. After applying alien pollen on maize and *T. dactyloides* silks, our investigations revealed the occurrence of inter-specific crossing barrier at various levels in maize. With the exception of lily, pollen capture, hydration and germination do not seem to represent essential crossing barriers. In general, a striking physiological difference between the plant species analysed is the separation of plants into “dry”- and “wet”-stigma types. Among the plant species used in this study, only lily is of the “wet” stigma type, while grasses and *Arabidopsis thaliana* belong to the “dry”-stigma type (Heslop-Harrison and Shivanna 1977; Swanson et al., 2004) explaining the incompatibility of lily pollen to germinate neither on maize nor on *T. dactyloides* silks. Pollen adhesion at the silks is also known as a critical factor for a successful pollination (Bendinger and Fowler, 2009). Our observations indicate that lack of adhesion does not represent a hurdle in maize and *T. dactyloides*, but most PTs were unable to enter the silk hairs, which thus represents a first hybridization barrier of pollen from most plant species in maize and *T. dactyloides*. This finding further supports the assumption that specific factors from the pollen tube and silk hair, like the xylanase XYN1 or other hydrolases, might enable the PT to invade the silk hairs (Bendiger and Fowler 2009). A bias in these interactions prevents pollination of maize and *T. dactyloides* by distantly related plant species, but not by pollen from the sister genus. This barrier can thus be classified as an “early growth arrest” of PT.

Further obstacles are connected to the transmitting tract (TT) and lead to reduced PT growth length. PT growth length reduction in maize was first described as a unilateral crossing barrier caused by the *Ga1s*-allele (Nelson 1952; House and Nelson 1958). Although not studied at the cellular level, it has been reported that pollen tube growth length is crucial to overcome crossing barriers existing between teosinte and maize (Evans and Kermicle 2005) as well as teosinte and *T. dactyloides* (Mangelsdorf and Reeves 1931). In our experiments, we found that PT growth length in the incompatible *Ga1s*/*ga1* system is comparable to that of the growth length of *T. dactyloides* PT in maize silks. House and Nelson (1958) reported a growth arrest of *ga1*-pollen after 2-3 cm, while compatible pollen

displayed a linear growth of about 12 mm/h. Calculations indicated that maize pollen grains could support around 2 cm of tube growth using exclusively endogenous reserves (Heslop-Harrison 1982; Heslop-Harrison *et al.* 1984). This finding suggests that lack of further growth support by the sporophytic tissues might represent the major cause of tube arrest described above. In both cases we found that PTs are less precisely targeted to the TT. The majority of mistargeted PTs were observed in the silk tissue right below the epidermal cell layer. However, even PTs growing inside the TT tissue stopped growth after an additional 1-2 cm compared with the PTs growing outside the TT. The observation that the smaller *T. dactyloides* pollen can form tubes longer than 2 cm, especially inside the TT, indicates that its PTs are principally capable to take up nutrients from the alien host silk. Under natural conditions, targeting to the TT is a prerequisite of PTs to completely grow through maize silks. Our data thus supports an old hypothesis from (Heslop-Harrison, Heslop-Harrison et al. 1985) that TT cells attract PTs by secretion of chemotropic signals. This process is hampered in the *Ga1s*/*ga1*- and in the maize-*Trispsacum* barriers suggesting that the involved signalling molecules might be species-specific. PT mistargeting of the transmitting tract occurs less frequently in an incompatible *Ga1s*/*ga1*-crossing compared with maize-*Tripsacum* crossings, which indicates that both barriers might be based on the same physiological process, but are impaired to a different extend. Both barriers don't appear in the reciprocal crossing were no growth-defect or TT-mistargeting was found. Nutrition problems similar to *colourless2* (*c2*) or *white pollen1* (*whp1*) mutants could explain our findings concerning *T. dactyloides* pollen tube growth arrest in maize silks. Both mutants are self-incompatible but can be rescued either by shortening silks (Pollak, Hansen et al. 1995) or by mixing pollen with flavonols (Mo *et al.* 1992) If flavonols were not supplemented, PTs grew to a length of only 2.5 to 4 cm (Pollak et al. 1995).

When PTs leave the TT of maize and enter the ovary cavity, almost the whole pollen tube pathway is accomplished. The last remaining task for the tube is to reach the micropyle, enter the micropylar nucellus region and discharge the two sperm cells in the receptive synergid cell for double fertilization. It was found that, with the exception of micropylar short range guidance, PT guidance signals in the ovary cavity are exclusively controlled by the maternal sporophytic tissues of the ovule. In addition, we found that repelling of late coming PTs from the micropylar area, which don't enter this area, is also sporophytically controlled and we thus suggest that this is the default status for this area. From the above data, we draw an up-date model of the PT pathway of maize in analogy to the pathway in

A. thaliana (Johnson and Preuss 2002) and based on the classification of Heslop-Harrison (1982) taking detailed anatomical surveys into account. As shown in Figure 2.7, PT growth was divided in five phases. Phase I includes pollen grain capture, adhesion, hydration and germination. This phase is mainly governed by general physiological parameters. In contrast to the SI-systems in the Brassicaceae and Solanaceae (Swanson *et al.* 2004) species-specificity plays a minor role in maize and *T. dactyloides*, and this does not represent a major hybridization barrier. We have further defined Phase II by the entry of the PT into the sporophytic tissue until it has reached the TT. This phase shows higher specificity and requires species-specific interactions between the male gametophytic and sporophytic cells. The TT cells likely generate species-preferential chemotropic guidance signals guiding the PT inside its intercellular spaces, preformed by the anatomy of silks and silk hairs. Phase III, stylar PT growth, begins when PTs enter the TT and ends when they are leaving it towards the ovular cavity. Although this phase is believed to be regulated by tract geometry (Heslop-Harrison 1982), we found that stylar pollen tube growth depends on support and nutrients provided and controlled by the sporophytic tissues thus representing another hybridization barrier. During growth through the TT, pollen tube-silk-interactions cause degeneration of the abscission zone (AZ) proximal to the ovule once it was passed by the first 5-10 tubes (Heslop-Harrison *et al*. 1985). This barrier to the entry of supernumerary tubes thus represents one of the components to avoid polyspermy. While the AZ degenerates, vascular bundles and presumably TTs are quickly interrupted. Injured TTs also lead to an inability of the pollen tube to pass its destroyed tissue (Booy *et al.* 1992). At the end of the transmitting tract, PTs enter the ovular cavity in Phase IV. With the process of leaving the transmitting tract, anatomical and physiological aspects between *A. thaliana* and maize are different: in *A. thaliana*, PTs are directed from various positions of the TT towards the placental surface along the septum tissue. In grasses in general, and in maize in particular, TTs end blindly close to the upper ovary and PTs enter the ovary cavity by breaking through the inner epidermis of the ovary wall (Heslop-Harrison *et al.* 1985). An additional difference between both model systems is that PTs of *A. thaliana* grow on the septum surface in an air-filled environment, whereas grass PTs remains constantly surrounded in the ovary cavity by the ovary and the inner integument cell walls. Here, the elongated cells of the inner integument are aligned towards the micropylar region providing an anatomical growth direction clue (Figure 2.5F). Finally, in Phase V, *A. thaliana* PTs have to find and pass structures such as the

funiculus, whereas grass PTs are immediately directed towards the micropylar cone after leaving the TT.

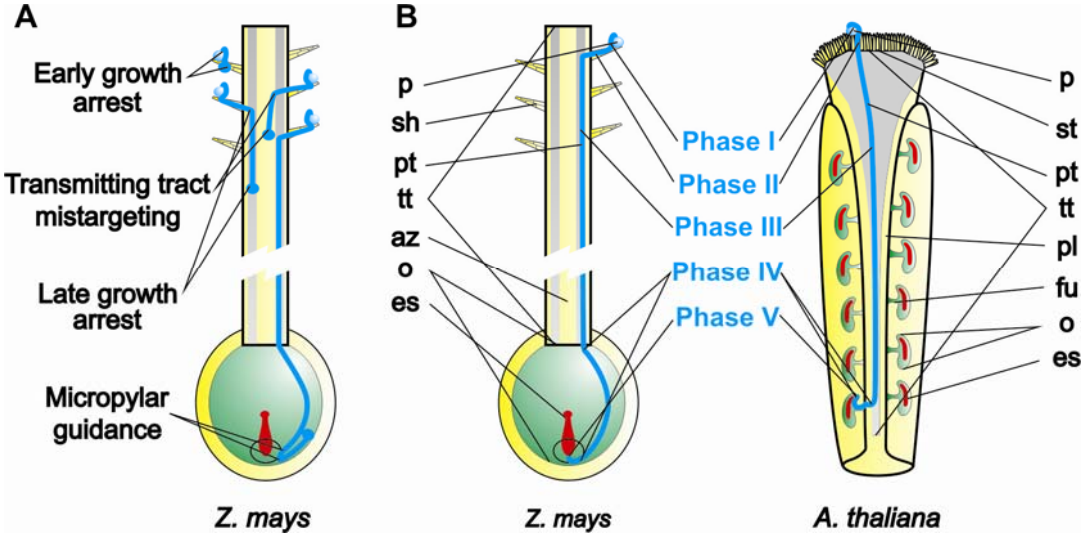

Figure 2.7 Summary of comparative progamic pollen germination and growth in maize and *Arabidopsis*. Although anatomical structures are named differently, Phase I to III can be widely homologized between maize and *Arabidopsis*. (A) Scheme showing progamic pollen tube growth failures observed in this survey. Early growth arrest was observed with pollen of rice, *Poa, Lolium* and *Arabidopsis*. Lily pollen did not germinate or stopped growth before leaving the silk hair. (B) PTs of these species arrested in Phase I (lily) or Phase II (most grasses and *Arabidopsis*). *Tripsacum* and incompatible maize PTs show two linked phenomena. Many PTs are mistargeted and grow outside the transmitting tract. Those PTs which find their way into the transmitting tract stop growth after few centimeters (Phase III). After passing the abzission zone in maize, PTs reach the end of the transmitting tract and enter the ovarial cavity. Growth in the ovarial cavity of grasses and accordingly growth on the septum surface, funiculus and ovule surface of *Arabidopsis* represent Phase IV. Whereas female gametophytes of *Arabidopsis* contribute to funicular and micropylar guidance, maize embryo sacs only provide micropylar guidance cues (Phase V). As a sporophytic default status, maize PTs are guided towards the micropyle, but do not enter an area about 100 µm in diameter around the micropylar cone. Ovules are shown in green, transmitting tracts in grey, embryo sacs in red and male gametophytes in blue. Abbreviations: az = abzission zone, es = embryo sac, fu = funiculus, o = ovule, p = pollen, pl = placenta, pt = pollen tube, sh = silk hair, st = stigma, tt = transmitting tract

PTs of *A. thaliana* thus need more distinct signals including funicular and micropylar guidance in order to accomplish fertilization (Hamamura and Higashiyama 2008). Both processes are thought to depend on signalling governed by the female gametophyte. In contrast, grass PTs only need to be guided to the micropyle towards the egg apparatus. The possibility that the egg apparatus itself and especially the synergids produce the respective

chemotropic factors has been discussed already since many years (Van Der Pluijm 1964). Until now only one candidate short range guidance molecule has been discovered in maize (Márton *et al*., 2005). ZmEA1 is secreted from the egg apparatus towards the cell walls of the micropylar nucellar cells. PTs in RNAi *ZmEA1*-knock down plants reach the micropylar cone up to a distance of about 100 µm, thus the same distance that we have described here for ovules lacking female gametophytes. In conclusion, progamic PT development is largely governed by interactions and communication between the male gametophyte and the surrounding sporophytic tissues. Pollen germination is relatively unspecific and seems to depend mainly on the environmental conditions at the silk surface. Initial growth of PTs in the silks hairs appears to be a more specific and thus represent a first hybridization barrier. Pollen of more distant related grass species arrest their growth in the silk hairs (second hybridization barrier), whereas PTs of maize and *T. dactyloides* are capable to grow further towards the transmitting tract. In incompatible cross pollinations between maize and *T. dactyloides*, and in maize itself, PTs frequently fail to target the transmitting tract and arrest growth after 4-6 cm pointing to a third hybridization barrier. This indicates a bias of species-specific recognition, nutrition and guidance signalling between male gametophyte and sporophytic silk tissues. In maize, guidance by the female gametophyte is restricted to small area around the micropyle and probably represents a fourth hybridization barrier in analogy with findings in *Torenia fournieri* where, similar to polymorphic ZmEA1 protein (Márton *et al*., 2005), polymorphic defensin-like proteins LURE1 and LURE2 control micropylar PT guidance in a species-specific manner (Okuda et al., 2009). Our findings thus support the idea that prezygotic barriers to genetic exchange are stronger than postzygotic barriers (Rieseberg 2007, Widmer et al. 2009) and thus also represent a major driving force for speciation in the grasses.

2.5 Summary

Pollen tube germination, growth, and guidance (progamic phase) culminating in sperm discharge is a multi-stage process including complex interactions between the male gametophyte as well as sporophytic tissues and the female gametophyte (embryo sac), respectively. Inter- and intra-specific crossing barriers in maize and *Tripsacum* have been studied and a precise description of progamic pollen tube development in maize is reported here. It was found that pollen germination and initial tube growth are rather unspecific, but an early, first crossing barrier was detected before arrival at the transmitting tract. Pollination of maize silks with *Tripsacum* pollen and incompatible pollination of *Ga1s*/*Ga1s*-maize silks with *ga1*-maize pollen revealed another two incompatibility barriers, namely transmitting tract mistargeting and insufficient growth support. Attraction and growth support by the transmitting tract seem to play key roles for progamic pollen tube growth. After leaving transmitting tracts, pollen tubes have to navigate across the ovule in the ovular cavity. Pollination of an embryo sac-less maize RNAi-line allowed the role of the female gametophyte for pollen tube guidance to be determined in maize. It was found that female gametophyte controlled guidance is restricted to a small region around the micropyle, approximately 50–100 mm in diameter. This area is comparable to the area of influence of previously described ZmEA1-based short-range female gametophyte signalling. In conclusion, the progamic phase is almost completely under sporophytic control in maize.

Chapter 3 - Calcium signalling during double fertilisation in *Arabidopsis thaliana* ovules

3.1 Introduction

For plants calcium is a macronutrient (for review see White and Broadley 2003). This bivalent cation occurs in milli-molar amounts in fresh plant tissue and has diverse cellular functions. Because phosphates have a strong tendency to precipitate in the presence of calcium, every living cell is urged to keep cytosolic calcium concentration low in order to preserve its energy household. This leads to the need for effective export of calcium from the cytosol into membrane enclosed compartments or the extracellular space. Calcium signalling (for review see Clapham 2007; Dodd *et al.* 2010) takes advantage of the steep gradient over membranes between the cytosol and extra-cytosolic stores like vacuole, ER, plastids, mitochondria or the apoplast (Stael *et al.* 2012). The signalling function is conserved over the entire domain of eukaryotes. Considering this physiological background three elementary questions on cellular calcium signalling arise. First, what is the nature of calcium signals regarding their temporal and spatial properties? Second, what are the key players in generation, regulation and translation of these signals? And finally, which biological processes depend on calcium signalling? Although some questions have already been answered for other biological systems, the following paragraphs will focus on the current knowledge about the situation in plants. It is emphasised that in this context the term "plant" will be used only for embryophytes (for taxonomic relations see also 1.1) which includes mosses, ferns, seed plants and some green algae (Wheeler and Brownlee 2008).

3.1.1 Calcium signals

Since calcium diffusion within the cytoplasm is slow (Clapham 1995) and buffering of calcium is high (Malho *et al.* 1998, Trewavas 1999) elevated calcium levels at open pores are a very local event. The entire concentration gradient of five orders of magnitude manifests in few hundred Å in the cytosol next to an open pore (Figure 3.1). This local event can result in a calcium "wave" spreading across a cell and even cell-to-cell across a tissue. A well studied example for these waves, called CICR (calcium-induced calcium

release), occurs in skeleton and heart muscle cells (for review see Endo 2009). Calcium channels, the so-called ryanodine receptor protein (RyR), are organised in clusters located in the membrane of the sarcoplasmatic reticulum (SR). Because calcium itself can trigger the activation of such a cluster, a wave of calcium signalling can spread over the muscle cell ((Niggli 1999; Thomas *et al.* 2000). Since no homologue for RyR exists in plants (Verret *et al.* 2010) a homologous mechanism of spatial calcium signal propagation cannot be expected to be found. Nevertheless, calcium waves have been observed in response to salt stress (Drobak and Watkins 2000) and in several fertilisation related processes (see below). Spatial propagation of elevated intracellular calcium levels is also observed in guard cells in response to abscisic acid (McAinsh *et al.* 1992).

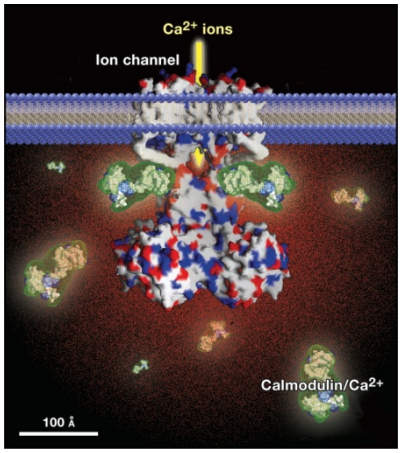

Figure 3.1 Model of calcium distribution in the surrounding of the open pore of a calcium channel. The cartoon illustrates how the nature of cytosolic calcium concentration is altered at the open pore of a hypothetical calcium channel. The red dots indicate cytosolic calcium which forms a steep gradient over a few hundred Å. The plasma membrane/lipid bilayer is indicated in blue. (Figure taken from Clapman 2007)

3.1.2 Proteins involved in calcium signalling

After a short glimpse at the nature of calcium signals in plants one has to ask, which players are required for such phenomena? The already mentioned steep gradient of calcium across membranes requires on the one hand an effective export mechanism. On the other hand, more or less selective channels in the membrane are needed for a controlled influx of calcium along the concentration gradient into the cytosol where the signalling occurs (White and Broadley 2003). Calcium transport in plants is driven by either ATP-hydrolysis or a proton-gradient. The first is called a primary, the latter a secondary active transport

(Poole 1978). The primary active pathway is represented by two protein groups in plants. The first group comprises the ER-type Calcium-ATPases (ECA), the second one the Calcium/calmodulin dependent autoinhibited Calcium-ATPases (ACA) (Dodd *et al.* 2010). Currently, the members of ECA-family are not believed to be directly involved in calcium signalling (Dodd *et al.* 2010). ACA pumps have been shown to be necessary for male fertility (*ACA9*, Schiott *et al.* 2004) and inflorescence development (*ACA10*, George *et al.* 2008) in *Arabidopsis*. Hitherto it is assumed that ACA activity is required for calcium signalling in plants (Dodd *et al.* 2010). Also genes encoding secondary active transport proteins can be identified in plant genomes. In the case of *Arabidopsis* six members of the so called cation-exchanger gene family (CAX) have been found (Shigaki and Hirschi 2006). Up to now there is no definitive proof that the CAX proteins play a role in calcium signalling (Dodd *et al.* 2010), which would be comparable to the one of Na^+/Ca^{2+}-antiporters in excitable cells of metazoe (for review see Berridge *et al.* 2003). Another important component of calcium signalling at membranes are channels. Whereas animals and algae express a numerous ion-channels families with calcium conductivity, the repertoire of plants is limited (for review see Verrer *et al.* 2010). The best characterised calcium channel in plants is the voltage-gated two-pore-channel-family protein AtTPC1. It is localized in the vacuolar membrane and is involved in calcium induced stomatal movement and ABA mediated seed dormancy. It is permeable for monovalent ions (Peiter *et al.* 2005). AtTPC1 is probably responsible for maintenance of vacuolar membrane potential and potassium homeostasis rather than being involved in generation of calcium signals (Beyhl *et al.* 2009). Besides these voltage-gated channels also genes for ligand-gated channels can be found in plant genomes (Verret *et al.* 2010). The best-studied ones are those encoded by the so-called *glutamate receptor-like* genes (*GLR*). Like TPCs, GLRs are not strictly selective for calcium (Roy *et al.* 2008; Tapken and Hollmann 2008). Nevertheless, some data indicate that GLRs might be channel proteins involved in calcium signalling. Putative agonists like glutamate and glycine can induce elevation of cytosolic calcium and AtGLR3.4 is reported to be sensitive to touch and cold (Meyerhoff *et al.* 2005). Recently, *AtGLR1.2* was shown to have an impact on PT growth and cytosolic calcium oscillations in the PT tip (Michard *et al.* 2011). The other class of ligand-gated channels present in plants is called cyclic nucleotide-gated channels (CNGCs). *AtCNGC18* has been shown to be required for PT growth (Frietsch *et al.* 2007). *AtCNGC2* is known to be involved in cAMP-gated Calcium-fluxes at the plasma membrane in response to bacterial elicitors (Ali *et al.* 2007). The two remaining groups of putative ion channels in

plants, the annexins and the mechanosensitive ion channels (MscS) are less intensively studied. In maize, annexins have been shown to confer calcium conductivity *in vitro* (Laohavisit *et al.* 2009). MscS activity can be found in root cells of *Arabidopsis thaliana*, but may not contribute directly to calcium signals (Haswell *et al.* 2008). One of the deepest gap in the understanding of calcium signalling nowadays is the missing link between second messengers like inositol-1,4,5,-trisphosphate ($InsP_3$), cyclic adenine dinucleotide phosphate ribose (cADPR) and NAADP, which are known to release calcium from intracellular stores. Until now, no putative plant calcium channel has been functionally hooked up to a known second messenger (Dodd *et al.* 2010).

In order to serve as a signal, increases in cytosolic calcium concentrations must be sensed and translated into a cellular response. The first role required in this process is the one of a calcium sensor. Such a sensor needs a domain to bind the upstream factor calcium and downstream factors to transmit the calcium information. A widespread calcium binding motive is the so called EF-hand after the E- and F-domain of parvalbumin ((Nakayama and Kretsinger 1994). Upon calcium binding calmodulin (Calcium/CaM) undergoes a conformational change, which mediates dimerisation with target proteins. A protein similar to CaM, called Troponin C, is an important player in muscle contraction (for review see Parmacek and Leiden 1991). Troponin C from chicken muscle is employed in the recombinant calcium probe (Figure 3.2) used in course of this work (Heim and Griesbeck 2003). CaMs of plants have been linked with numerous cellular and developmental processes and responses (White and Broadley 2003). CAMTA transcription factors bind to CaM and their function is calcium-dependent (Finkler *et al.* 2007). In *Arabidopsis* this transcription factors are probably involved in stress and hormone responses (Yang and Poovaiah 2002).

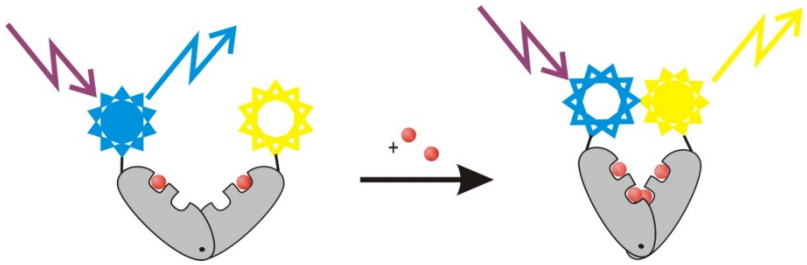

Figure 3.2 Scheme of recombinat Foerster resonance energy transfer (FRET)-based calcium probe. In the absence of free calcium the TroponinC-linker (grey) has two calcium ions (red balls) bound. Exitation (purple arrow) of CFP (blue star) results in CFP-fluorescence (blue arrow). If two additional calcium ions are bound to TroponinC undergoes a conformational change enabling FRET from CFP to YFP (yellow star). Since this results in YFP-flourescence (yellow arrow), calcium concentrations can be measured be calculation of the CFP/YFP-flourscence intensity rations in such a sample.

Another class of calcium sensor proteins are calcineurin B-like proteins (CBL), showing similarity to the neuronal calcium sensor calcineurin (Kudla *et al.* 1999). CBLs contain four EF-hand domains, are probably myristoylated (Luan *et al.* 2002) and interact with CBL-interacting protein kinases (CIPKs). CIPKs are targeted to their subcellular compartment by the interaction with CBL (Batistic *et al.* 2008). CBL/CIPKs are involved in regulation of sodium (Cheong *et al.* 2007) and potassium (Kim *et al.* 2007) homeostasis, stress ((Cheong *et al.* 2003) and ABA (Pandey *et al.* 2004) responses. Another EF-domain-containing Calcium-signalling protein is called calcium dependent protein kinases (CDPKs). This protein family has 34 members in *Arabidopsis* (Hrabak *et al.* 2003). CDPKs are involved in ABA signalling by modulating S-type anion channels (Mori *et al.* 2006) and phosphorylate ABA-responsive transcription factors (Zhu *et al.* 2007) in *Arabidopsis thaliana*. As already mentioned, not all calcium binding proteins utilise EF-hand-domains. Phospholipase D (PLD) binds Calcium via a C2-domain (Wang 2001). PLDs are involved in many processes like stomatal closure, responses to ethylene, pathogens, ABA, leaf senescence and drought tolerance ((Ritchie *et al.* 2002).

3.1.3 Calcium signalling in plant life

In general the role of calcium signalling in guard cells and stress responses is also well studied (White and Broadley 2003). Furthermore, a distinct role of calcium in signalling processes during fertilisation can be deduced from several recent or long standing findings (for review see Dumas and Gaude 2006 and Ge *et al.* 2007). A prominent example for

calcium signals in fertilisation processes is egg activation. For this event a cytosolic calcium wave is required in animal systems (Jaffe 1983). An essential role for calcium in egg cell activation is also evident in the brown algae *Fucus serratus* (Roberts *et al.* 1994). *In vitro*, extracellular calcium is required for gamete fusion in plants with (Kranz *et al.* 1991), (Antoine *et al.* 2001). Furthermore, it is known that calcium fluxes occur at the egg cell membrane (Digonnet *et al.* 1997) and cytosolic calcium waves can be detected (Antoine *et al.* 2001). On the transcriptional level it has been shown, that the calcium sensor calreticulin is expressed in zygotes generated *in vitro* (Dresselhaus *et al.* 1996). Hitherto, neither there is direct evidence for the role of calcium in egg activation *in planta* (Ge *et al* 2007). For other cell types of the female gametophyte (FG) there is even less known about possible calcium dependent signals. The synergid cells have been known for many decades to be calcium rich (Jensen 1965). Free calcium concentrations in synergids change before degeneration of the receptive synergid (Tian and Russell 1997). The central cell also contains high amounts of free calcium (Tian and Russel, 1997). Recently it has been shown by *in vitro* experiments that central cells of tobacco do not show an increase in cytosolic calcium concentration after gamete fusion (Peng *et al.* 2009). Up to now, *in invo* data for calcium signalling in synergids or central cells are not available. In contrast to the FG the MG is much better understood in terms of calcium-dependent phenomena. The relevance of exogenous calcium for PT growth is extensively studied (Ge *et al.* 2007). The first proof for intracellular tip focused calcium oscillations was found in *Lilium longiflorum* with the help of a calcium sensitive dye (Nobiling and Reiss 1987). In the early phase of fertilisation, elevated calcium levels are detected in pollen grains at the site where the tube emerges and in papilla cells after pollen hydration, pollen protrusion and during penetration of the papilla cell wall by the PT (Iwano *et al.* 2004). Recently, these oscillations and calcium fluxes at PT membranes of *Arabidopsis* and tobacco have been shown to be influenced by GLR-specific drugs, D-serine and being altered in *glr1.2*-mutant in *A. thaliana* (Michard *et al.* 2011). About PTs of the self-incompatible poppy species *Papaver rhoeas* it is known that incompatible reaction includes a transient cytosolic calcium increase in the shank of the PT (Franklin-Tong *et al.* 2002). Taken together, these findings highlight the important role of calcium as signalling molecule for PT growth *in planta*.

3.1.4 Aim of this work

This study tries to shed more light on physiological details of calcium signalling during double fertilisation. A plasma membrane marker line should be generated with the goal to mark the cell boundaries of the growing PT and the FG. For this purpose, the polyol transporter protein *AtPLT5* (Klepek *et al.* 2005) was translationally fused with eGFP at it's carboxy-terminus and expressed under the constitutive promoter of *ACTIN 11* (*ACT11*,Huang *et al.* 1997) In contrast to the constitutive viral promoters 35S (Guilley *et al.* 1982) *ACT11* is supposed to be active in gametophytic cell types. The resulting plasma membrane marker line should be analysed for transgene expression by means of confocal laser scanning microscopy (CLSM) and conventional fluorescence microscopy.

In order to investigate calcium signalling *in vivo* plant lines expressing the recombinant calcium sensor CerTN-L15 (Heim and Griesbeck, 2003) in vegetative and various reproductive cell types should be generated. For expression in vegetative tissues the 35S promoter was used. For gametophyte specific expression three different promoters were applied. Expression in the egg cell was achieved by use of the *EC1.1* promoter *(Ingouff et al.* 2009). For synergid specific expression the promoter of *MYB98 (Kasahara, Portereiko et al. 2005)* was applied. For pollen specific expression of the calcium probe the promoter of *ARO1* (Gebert *et al.* 2008) was used. Transgene expression should be assayed by fluorescence microscopy and western blot analysis. The functionality of the calcium probe should be tested in *pARO1::CerTN-L15* lines during *in vitro* PT growth by CLSM.

3.2 Experimental procedures

3.2.1 *Arabidopsis thaliana* material and growth conditions

3.2.1.1 Plant growth

Arabidopsis thaliana wild type and transgenic plants were grown on agarose plates or soil in climate chambers. After sowing, *A. thaliana* seed received a stratification treatment for 2 days at 4 °C in the dark. Plantlets were raised on soil under short day conditions (9 h light, 20-22 °C, 70% humidity) for 4 weeks, subsequently shifted to long day conditions (16 h light, 20-22 °C, 70% humidity) and grown to maturity. For plant growth on agarose plates seeds were surface sterilised. Sterilisation was carried out in a sterile 1.5 ml reaction tube under a laminar flow hood. Seeds were treated with 70% ethanol for 3 min and mixed several times. After every treatment seeds were collected by short centrifugation (10,000 rcf for 15 sec) and the solutions were replaced by pipetting. After ethanol treatment plants were incubated in 1% NaOCl/0.1% Mucasol-solution for 2 min as described above. Afterwards seeds were washed 5 times with sterile water. Finally, seeds were plated on 0.5x MS-medium (Duchefa Cat.# M0254) plates with 0.7% Phytoagar with a sterile pasteur-pipette. Plates were sealed with surgical tape. Plates were put to stratification and grown under short day conditions as described above. The ecotype Columbia-0 (Col-0) served as a wild type control. Transgenic *Arabidopsis* lines used in this work are listed in Table 3.1.

Table 3.1 Stable transgenic *A. thaliana*-lines used and generated during the course of the thesis.

Line	Back-ground	Gene of interest	Selection marker	Reference
HTR10	Unknown	*Histone3.3::Histone3.3-mRFP*	Kanamycin	(Ingouff *et al.* 2007)
AcPMG	Col-0	*AtACT11::AtPLT5-GFP*	Hygromycin	This work
ARC	Col-0	*AtARO1::CerTN-L15*	Glufosinate	This work
MYC	Col-0	*AtMCB98::CerTN-L15*	Glufosinate	This work
ECC	Col-0	*AtEC1::CerTN-L15*	Glufosinate	This work
35C	Col-0	*35S::CerTN-L15*	Glufosinate	This work

3.2.1.2 Stable transformation of *A. thaliana*

Stable transformation of *A. thaliana* was carried out according to the "floral-dip"-protocol (Clough and Bent 1998). Agrobacteria of the strain GV3101 (Table 3.2) were grown to a dense culture of 500 ml in YEP-medium (for recipe see 3.2.3) containing antibiotics selecting for the helper plasmid and the binary plasmid, respectively. Cultures were supplemented with 15 g sucrose and 250 µl Silwet77. *Arabidopsis* plants with many young flower buds were dipped into the bacterial suspension for 1 min. Three pots per construct, five plants each, were transformed. Excess of suspension was removed with a clean paper towel and plants were kept 2 days under a plastic bag under long day conditions. Selection for transgenic plants was carried out by selection on glufosinate-resistance, hygromycin-resistance or verification of transgene expression under the fluorescent microscope in following generations. Selection on glufosinate-resistance was done on soil. Plantlets one week after sowing were sprayed intensively with a solution of 200 mg/L glufosinate and 0.1% Tween20 three times within one week. Selection on hygromycin-resistance was carried out on plates. Sterilized seeds were plated on 0.5x MS-medium containing 25 mg/L Hygromycin B (Duchefa). Seeds were stratified and grown for one week under short day condition. Plantlets that developed more leaves than the two cotyledons after 10-14 days were transferred to MS-plates without selection until they developed roots and finally transferred on soil and grown under long day conditions until maturity.

3.2.1.3 Assay of transgene expression

Transgene expression was assayed in leaves, roots and reproductive organs. If root material was desired, plants were grown on agarose plates which were put upright in order to enhance root development. Roots were monitored directly on plates for GFP or YFP expression, respectively (see 3.2.5 for microscopy). Leaves were removed from plantlets grown on soil and mounted on an object slide in tap water. Stamen and ovules were prepared from closed flower buds (Flower development stage 12 according to Smyth *et al.* 1990) and mounted on an object slide in 50 mM sodium-phosphate-buffer pH 7.5.

3.2.1.4 Genomic DNA isolation

Genomic DNA form *Arabidopsis thaliana* was prepared from rosette leaves. A small piece of leaf material was mashed in 1.5 ml reaction tube for 15 sec. 400 µl of At-gDNA-extraction buffer (200 mM Tris/HCl pH 7.5; 250 mM NaCl; 25 mM EDTA; 0.5% SDS) was added and the reaction was mixed for 5 sec. Cell debris was removed by centrifugation for 1 min at 20.800 rcf. 300 µl of the supernatant were transferred to a fresh tube. 300 µl of isopropanol was added, the reaction was mixed by inverting and incubated at ambient temperature for 2 min. The precipitate was collected by centrifugation for 5 min at 20.800 rcf. The supernatant was discarded and the pellet was dried. Finally, the pellet was dissolved in 100 µl TE-buffer and stored at 4 °C until later use.

3.2.2 Tobacco growth conditions and transient transgene expression

Nicotiana benthamiana Domin. was grown under green house conditions as described for maize (2.2.1). Plants were used for transient protein expression 4-8 weeks after sowing. Transformed plants were kept at ambient under natural light conditions. Leaf material for microscopy was sampled by cutting leaves along the surface of the abaxial leaf side with a razor blade. Leaf material was mounted in tap water and analysed at an inverted fluorescence microscope 2 dai (3.2.5). Transient protein expression in *N. benthamiana* was achieved by infiltration of *A. tumefaciens* suspension into the leaf using a syringe (see below). A single bacterial colony was inoculated and grown for 24 h as described (3.2.3). This culture was re-inoculated 1:10 with fresh YEP containing 20 µM acetosyringone (1 M stock in DMSO) and antibiotics. The culture was grown to an OD_{600} = 1. Bacteria were harvested by centrifugation (20 min, 4000 rcf) and the pellet was each resuspended in an equal volume of Infiltration-Buffer (10 mM MES/KOH pH 5.7; 10 mM $MgCl_2$; 100 µM acetosyringone). The buffered suspension was used immediately or stored at room temperature for up to 24 h. Infiltration of tobacco leaves was done with a 10 ml one-way syringe (Braun) without needle. The syringe was pressed softly against the abaxial side of the leave and the suspension was slowly infiltrated (Sparkes *et al.* 2006).

3.2.3 Bacterial material, transformation and growth conditions

Bacteria were grown in sterile containers in liquid medium or on agar-plates, respectively. Stock cultures were prepared by supplementing 800 ml stationary culture with 200 µl sterile 87% glycerol. The glycerol culture was mixed thoroughly, frozen on liquid nitrogen and stored at –80 °C. For cloning purposes of promoters into the Gateway®-vector pB2GW7 (Karimi *et al.* 2007) the *Escherichia coli* strain DB3.1 was used. For Gateway®- and TOPO®-cloning the strain DB5α was applied. Expression clones were transformed into the *Agrobacterium tumefaciens* strain GV3101. The genotypes of the above mentioned strains are given in Table 3.2.

Table 3.2 Bacterial strains.

Species	Strain	Genotype	Reference
E. coli	DH5α	*F⁻ endA1 glnV44 thi-1 recA1 relA1 gyrA96 deoR nupG Φ80dlacZΔM15 Δ(lacZYA-argF)U169, hsdR17(r_K^- m_K^+), λ–*	Invitrogen
E. coli	DB3.1	*F- gyrA462 endA1 glnV44 Δ(sr1-recA) mcrB mrr hsdS20(r_B^-, m_B^-) ara14 galK2 lacY1 proA2 rpsL20(Sm^r) xyl5 Δleu mtl1*	Invitrogen
A. tumefaciens	GV3101[1]	No information available	(Hamilton and Fall 1971)

[1]Strain harbours pMK90-helper plasmid (Ref.) conferring gentamycin-resistance.

LB-medium (5 g/L yeast extract; 10 g/L tryptone; 10 g/L NaCl; Bertani 1951) was used as standard growth medium for *E. coli*. Bacterial cells were grown either in suspension or on plates containing 2% Agar-Agar and appropriate antibiotics (Supplement Table 1.1). *E. coli* suspension cultures were cultivated in sterile containers under continuous shacking (200 rpm) at 37 °C. Transformation of chemically competent *E. coli* was performed according to a "heat-shock"-protocol (Inoue *et al.* 1990). Clones were analysed by test digestion or PCR and sequencing. Sequencing reactions were purchased from the companies Starseq, Seqlab and GATC. Sequence data were analysed using the software FinchTV, DNAStar and VectorNTI (Invitrogen).

Agrobacterium tumefaciens was handled under steril conditions as described above. Bacteria were grown at 28 °C with appropriate antibiotics (Supplementary Table 1.1) in liquid YEP-medium (10 g/L yeast extract; 10 g/L peptone; 5 g/L NaCl; pH 7.0) at continuous shaking (200 rpm) or onto solid YEP-plates containing 2% agar-agar, respectively. Transformation of *Agrobacteria* was done according to the "freeze-thaw"-

protocol (Chen *et al.* 1994). Clones were analysed by test digestion, PCR or transgene expression in *N. benthamiana*. Clones used for stable transformation of *A. thaliana* were always analysed by test digestion along with the *E. coli* clone. If insufficient plasmid for test digestion was obtained from the *Agrobacteria*-cultures, plasmids were retransformed to *E. coli* and further analysed. Plasmid DNA from *E. coli* and *A. tumefaciens* was prepared using the Plasmid Mini-Kit (Avegene) according to the manufactures protocol.

3.2.4 PCR and molecular cloning

3.2.4.1 PCR and DNA-modifying reactions

Standard PCR reactions were performed in sterile plastic cups (Sarstedt) in non-gradient or gradient thermo cyclers (Biometra). The standard *Taq*-DNA-polymerase was purchased from MBI-Fermentas. Standard PCR-reaction and -programme were used according to manufactures intructions. Annealing temperature was used as suggested by the software Clone Manager 6 (version 6.00), Primer Designer 4 (version 4.10) and Align Plus 4 (version 4.20) (all scientific and educational software) or determined empirically by gradient PCR. Elongation time was calculated for each template for a synthesis speed of 1 kb/min (*Taq*) or 2 kb/min (proof-reading enzymes), respectively. For PCR-based cloning and subcloning DNA-polymerases with proof-reading activity were used. The proof-reading polymerases Phusion® and Kapa® were purchased from Finnzymes and Peqlab, respectively. Detailed information about primer used in this work are given in Supplement Table 1.3.

All cloning and subcloning steps were done according to (Sambrook and Russell 2001) or as suggested by the supplier of the cloning kits employed. Cloning strategies are described below. Vector maps and can be found in Supplementary information. Maps have been drawn using Vector NTI Advanced 9 (Invitrogen). Sequences were taken from the *Arabidopsis* genome database TAIR (www.arabidopsis.org).

3.2.4.2 Cloning strategies

The recombinant calcium sensor CerTN-L15 (Heim and Griesbeck 2003) was provided by O. Griesbeck in a pcDNA3-cloning vector (Invitrogen). The coding sequence was PCR-amplified as follows in two parts preparing the fragment for BP Clonase subcloning: CerTN-CFP was amplified from the pcDNA3-cloning vector with the primer pair P12/P25 (Supplement Table 1.3). CerTN-YFP was amplified from the pcDNA3-cloning vector with the primer pair P16/P26 (Supplement Table 1.3). The PCR-fragment of the correct length was purified from an agarose gel. Both fragments contain an *Eco*52I-site which is unique in the coding sequence of CerTN-L15. Both fragments were digested with *Eco*52I (MBI-Fermentas) and ligated. To eliminate undesired side products, the ligation reaction was separated on a gel and the area of approx. 2 kb was purified (QIAquick Gel extraction) from the gel. 5 µl of the eluate were used to reamplify the complete coding sequence of CerTN-L15 extended for the attB1 and attB2 sites with the primer pair P12/P16 (Supplement Table 1.3). All PCR reactions were carried out with Phusion® (Finnzymes) using HF-Buffer and the standard reaction and program given by the manufacturer. 5 µl of the PCR-reaction were used in BP-reaction (BP-clonase II; Invitrogen) with the donor-vector pDONR207 (Invitrogen) according to the manufacturer's protocol. The reaction was transformed into *E. coli* DH5α and analysed by sequencing. The coding sequence without stop codon of the polyol transporter *AtPlt5* (At3g18830, Klepek et al. 2005) was provided in a vector for transient expression by N. Sauer. The sequence was amplified from the vector using the primer pair P53/P54 (Supplement Table 1.3). The PCR-reaction was purified (QIAquick PCR Purification Kit, Quiagen) and used with the pENTR/D/TOPO-Kit (Invitrogen) according to the manufactures protocol. The reaction was transformed in *E. coli* DH5α and the clones were analysed by sequencing. The sequences of the promoters of the genes *AtEC1.1* (454bp upstream of the start codon ATG of At1g76750;(Ingouff *et al.* 2009), *AtARO1* (701bp upstream of the start codon ATG of At4g34940; Gebert *et al*., 2008) and *AtMyb98* (1494bp upstream of the start codon ATG of At4g18770; Kashara et al. 2005) were subcloned into the destination vector pB2GW7 (Karimi, Depicker et al. 2007), *pARO1* was amplified with the primer pair P30/P31 (Supplement Table 1.3) from the vector pMG2000-Aro1-GUS (Gebert *et al. 2*008). *pEC1* was amplified using the primer pair P9/P10 (Supplement Table 1.3) from the vector EC1-GUS (Ingouff *et al.* 2009). *pMyb98* was amplified with the primer pair P7/P8 (Supplement Table 1.3) using the plasmid pN7-Myb-EC1 (S. Sprunck, unpublished) as template. The sequence of the

promoters of the gene *AtACT11* (847bp upstream of the start codon ATG of At3g12110; (Huang, An et al. 1997)) was cloned from gDNA of the *A. thaliana* ecotype Col-0 into the destination vector pH7FWG2 (Karimi *et al.* 2007) using the primer pair P51/P52 (Supplement Table 1.3). The PCR reactions were carried out with Phusion®-DNA-Polymerase (Finnzymes) using HF-Buffer, 30 cycles and otherwise manufacturers' protocol and programs. All PCR-products contain a *Sac*I-site at the 5' and *Bcu*I-site at the 3'-end of the promoter sequence. Both sites were used to clone the promoters *pARO1*, *pEC1* and *pMyb98* into the pB2GW7-vector replacing the 35S-promoter. *pACT11* was cloned into pH7FWG2 in the same way. Ligations were transformed into DB3.1 and analysed by DNA sequencing.

The recombinant calcium sensor CerTN-L15 was subcloned into the four destination vectors pB2GW7, pB2GW7-pEC1, pB2GW7-pMyb98 and pB2GW7-pARO1 using the pDONR207-CerTN-L15 vector constructed as described above. The recombination reaction was performed using the LR Clonase II-Kit (Invitrogen) according to the manufacturer's protocol. The coding sequence of the membrane protein *AtPLT5* was recombinated into the destination vector pH7FWG2-pACT11 as described above. The reactions were transformed into DH5α. Clones were analysed by test digestion and transformed into GV3101. Clones were analysed by test digestion after retransformation into DH5α. The expression clone pH7FWG2-pACT11-PLT5 was tested by transient expression in *N. benthamiana*.

3.2.5 Fluorescence microscopy

Detection of fluorescent proteins was carried out at an inverted fluorescence microscope (Nikon Eclipse 1500). Fluorescent proteins were exited with a mercury bulb. Filter cubes containing band pass emission filters suitable for GFP or YFP detection were used. Emission was detected using a CCD-camera (Zeiss). Image processing was carried out using Axiovision 3.6 software (Zeiss).

3.2.6 Confocal microscopy, FRET-assay and data processing

The functionality of the recombinant calcium sensor CerTN-L15 was tested *in planta* as follows: *Arabidopsis* pollen was *in vitro* germinated according to Li *et al.* 1999. Pollen germination medium PGM (18% Sucrose, 0.01% boric acid, 1 mM $MgSO_4$, 1 mM $CaCl_2$, 1 mM $Ca(NO_3)_2$, 0.5% agar-agar) was prepared freshly before each experiment. After pouring plates were allowed to dry for 1 h in a laminar flow hood. Pollen was applied by to the surface of plates by dipping newly opened flowers gently on the plate. Plates were sealed with Parafilm® (Pechiney plastic packaging) and incubated at 22 °C for 3-5 h. Pollen tubes were checked for transgene expression at an inverted fluorescence microscope (Eclipse TE1500, Nikkon) or at the CLSM LSM510 (Zeiss), respectively, as described below.

CFP and YFP fluorescence at a LSM510: excitation was performed with 458 nm. CFP and YFP-emission were detected simultaneously. For CFP-emission a 475-525 nm band pass filter and for YFP-emission a 530 nm long pass filter was applied. The ratio of CFP and YFP intensities was calculated using the ratio-tool embedded in the software LSM510 (Zeiss).

For detection of GFP-fluorescence excitation was done at 488 nm. Emission passed through a 505 nm long pass filter.

3.3 Results

In order to study calcium signalling during double fertilization in *Arabidopsis*, several marker lines had to be constructed. First, a marker line which was supposed to lable the boundaries of the gametophytic cell was made. Additionally, lines were constructed which expessed the recombinat calcium probe CerTN-L15 (Heim and Griesbeck 2003) in vegetative tissues, egg cells, synergids and pollen. The later line was used to test the probe for functionallty in *in vitro* grown pollen tubes.

3.3.1 Expression of the plasma membrane marker AcPMG in tobacco and *Arabidopsis thaliana*

For visualisation of cell boundaries in reproductive tissues, the polyol transporter AtPLT5 (Klepek *et al.* 2005) was translationally fused with eGFP at the carboxy-terminus of the membrane protein. The fusion construct was transiently expressed in *Nicotiana benthamiana* under the control of the constitutive viral 35S promoter (Guilley *et al. 1982)* in order to test its suitability prior to stable transformation. The expression in the tobacco epidermis cell resulted in a detectable labelling of the cell boundaries. The intracellular background is homogenous with few small dots. No distinct cellular compartments are labelled. When two adjacent cells expressed the construct, two parallel lines were detected reflecting plasma membrane localization (Figure 3.3).

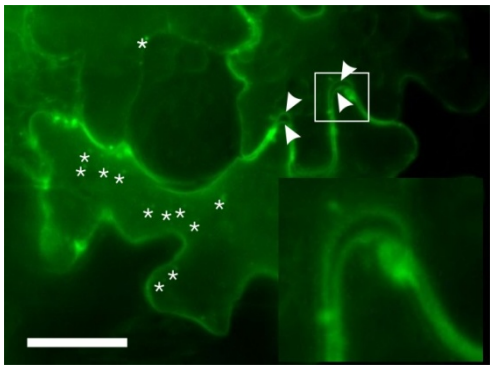

Figure 3.3 Transient expression of the plasma membrane marker *PLT5-eGFP* in leaves of *N. benthamiana*. The GFP-construct labels the cell boundaries. The intracellular background is homogenous with few dots (asterisks). When two adjacent cells expressed the construct, two parallel lines (arrowheads) were detected, likely reflecting the plasma membrane. The white rectangle marks the area shown in the inset. Scale bar = 50 µm.

After stable transformation of *A. thaliana*, expression of the PLT5-eGFP-fusion under control of the "constitutive" *AtACT11* promoter (Huang *et al,* 1997) was monitored in reproductive tissues. High expression levels were found in pollen (Figure 3.4A). Expression was not detectable in sporophytic tissues of the anther. The fusion protein did not label distinct structures inside the pollen grain (Figure 3.4A). The expression level in ovules and the female gametophyte was low compared with pollen grains (Figure 3.4). Furthermore, the fusion protein was detectable in sporophytic cells of the ovule. The synergids and the central cell membranes were labeled (Figure 3.4B and C). Other cell types of the gametophyte, namely the egg cell and the antipodal cell did not show significant GFP fluorescence (Figure 3.4B and C). These expression patterns were found in six independent AcPMG lines after selection for hygromycin resistance. The subcellular localisation in the pollen tube shows a predominant occurrence of the fusion protein at the boundary of the emerging pollen tube. The highlighting of this outer cell border is most distinct close to the pollen grain and becomes more and more diffuse towards the tip. Inhomogeneous GFP signals and distinct spots can be found additionally inside the growing pollen tube (Figure 3.4D).

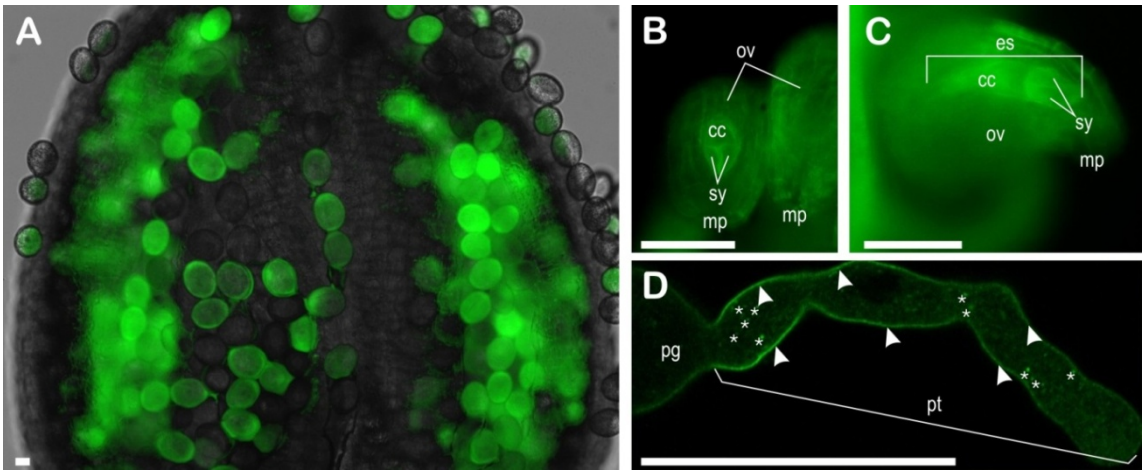

Figure 3.4 Stable expression of the plasma-membrane marker *PLT5-eGFP* in *A. thaliana* under control of the *AtActin11* promoter. A heterozygous line is shown. (A) Transgenic (green) and non-transgenic (colourless) pollen grains in an immature anther of a T1-generation plant. Transgenic pollen grains show high expression levels of GFP without highlighting distinct structures inside the grain. The picture is a merge of a DIC and a fluorescence channel depicted in false colour green. (B) Fluorescence false colour image of T1-plant ovules, focussing at their micropylar sides. The ovule on the left side exhibits expression of the marker construct in the synergids and the central cell of the female gametophyte. Expression in sporophytic cells, forming the surface of the ovules is found in both ovules shown. (C) Lateral fluorescence false colour image view of a T1-plant ovule. The synergids and the central cells can clearly be discriminated form signals originating from sporophytic expression and background fluorescence. Neither the egg cell nor the antipodal cells can be visualised in transgenic embryo sacs of transgenic lines. (D) Confocal false colour image of *in vitro* germinated transgenic pollen. The fusion protein can be found at the boundary of the growing pollen tube, labelling most likely the plasma membrane (arrowheads). Close to the pollen grain the labelling of the membrane is very distinct. This labelling becomes more and more diffuse the more it is approaching the pollen tube tip. The fusion protein appears as well inside the growing pollen tube and in distinct dots (asterisks). Abbreviations: cc = central cell, es = embryo sac, mp = micropyle, ov = ovule, pg = pollen grain, pt = pollen tube, sy = synergid. Scale bars = 50 µm.

3.3.2 Expression of the recombinant calcium sensor CerTN-L15 in vegetative and gametophytic cell types of *Arabidopsis thaliana*

Stable transgenic *A. thalina* lines have then been constructed expressing the recombinant calcium sensor CerTN-L15 (Heim and Griesbeck 2003) in vegetative and reproductive tissues. These lines are tools for studying calcium signalling in vegetative tissues and during double fertilisation. Expression was tested by detecting YFP-fluorescence in tissues of interest. For expression in vegetative tissues, the viral 35S-promoter (Guilley *et al.*

1982) was chosen to drive the calcium-sensor-construct (35C). Plantlets were tested for transgene expression in leaves and roots. Three independent 35C lines have been analysed and propagated. All lines showed expression in leaves (Figure 3.5A) and roots (Figures 3.5B and C). In roots, an intensive signal is detectable in the vascular cylinder and the root cap. Parenchyma cells show weaker expression (Figure 3.5B and C). Expression in ovules of the lines harbouring the *MYB98*-(Kasahara *et al.* 2005) or the *EC1*-promoter (Ingouff *et al. 2009)*constructs was tested detecting YFP-fluorescence in ovules prepared one day after emasculation. The position in the FG (Figure 3.5H) can be estimated from DIC microscopy image (Figure 3.5D and F), which allows identifying the large vacuolated central cell. Egg cell and synergids can be discriminated by the position of the vacuole, indicated by weaker fluorescence along the longitudinal (micropyle-chalaza) axis of the cells. The *CerTN-L15* construct, driven by the *MYB98* promoter showed strong and exclusive expression in two cells adjacent to the central cell of the FG in ten independent MYC lines. The cells exhibited polarity along the longitudinal axis of the FG with an intense signal at the micropylar and a weaker signal at the chalazal pole of the cell (Figures 3.5D and E). The position at micropylar pole with the vacuole facing towards the chalazal pole of the FG is an expected feature of synergid cells. Under control of the *EC1* promoter, YFP-expression was found exclusively in the egg cell at high levels (Figure 3.5F and G). Expression of the recombinant calcium probe in pollen was tested by detection of YFP-fluorescence in anthers. The stamens were collected when the theka was still closed in order to ease identification of hetero- or homozygous plants (flower development stage 12 according to (Smyth *et al.* 1990). The construct driven by the *ARO1* promoter (Gebert *et al.* 2008) was transformed into Columbia-0 wildtype plants carrying the sperm cell-specific histone marker line HTR10 (Ingouff *et al.* 2007). Plants from both lines were selected on glufosinate-resistance. The HTR10-lines were additionally analysed for *Histone3.3::Histone3.3-mRFP* expression by means of fluorescence microscopy. At the given floral stage, ten independent lines in each background (ARC or ARC/HTR10, respectively) were found to express YFP in pollen grains (Figure 3.5I and J). None of the lines tested was found to express YFP in the egg cell (data not shown) as predicted from ARO1-promoter activity published elsewhere (Gebert *et al.* 2008).

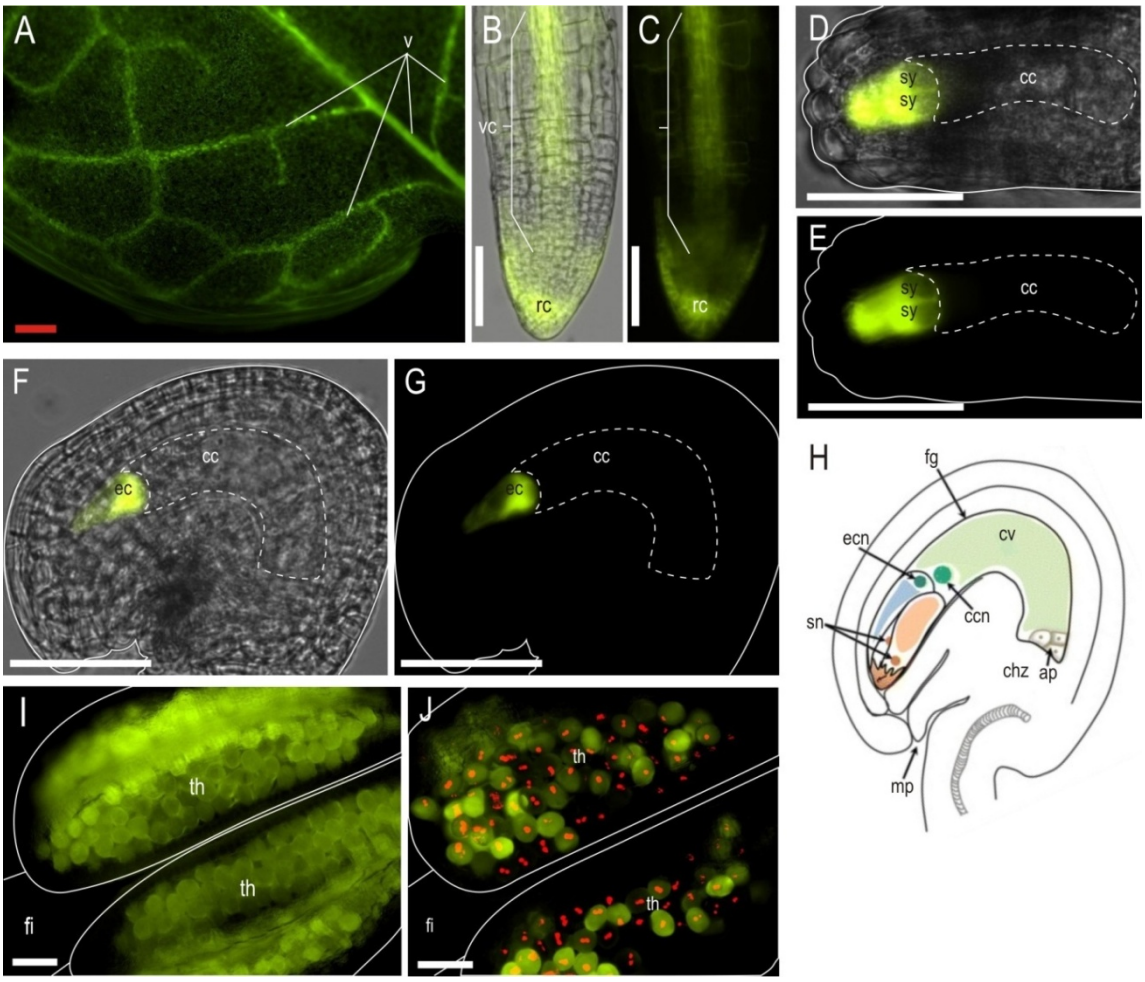

Figure 3.5 Expression of the recombinant calcium-sensor *CerTN-L15* in vegetative tissues and gametophytic cell types of *Arabidopsis thaliana*. A-C Expression of *CerTN-L15* driven by the 35S promoter. (A) The leaf-veins of a cotyledone are highlighted as expected for ubiquitous expression of a cytosolic protein due to the different cell architecture in the tissues of this organ. (B and C) The brightest signals can be detected in the root cap and the vascular cylinder. In more proximal parenchyma cell, weaker expression levels of *CerTN-L15* can be detected. (D and E) Expression of *CerTN-L15* under control of the *MYB98* promoter. The ovule (boundaries as solid line) is depicted in a top view with the micropylar end facing towards the left and the chalazal end facing to the right. The large central cell can be identified in the merged image (D). The *YFP*-expressing cells are found adjacent to its boundaries (dashed line). With the cytosol-rich pole facing towards the micropyle (brighter signal) and the vacuolated pole facing towards the chalaza (weaker signal) the cells can be identified as synergid cells. (F and G) Expression of *CerTN-L15* under control of the *EC1* promoter. The ovule (boundaries as solid line) is depicted in a longitudinal view with the micropylar end facing to the left and the chalazal end facing to the right. The large central cell can be identified in the merged image (F). The *YFP*-expressing cell is found adjacent to its boundaries (dashed line). With the cytosol-rich pole facing towards the chalazal end (brighter signal) and the vacuolated pole facing towards the micopylar end (weaker signal) the cell can be identified as the egg cell. (H) Cartoon of a mature ovule showing the position of nuclei and

vacuoles of female gametophytic cells (addapted from Sprunck and Groß-Hardt 2011). (I and J) Expression of CerTN-L15 under control of the *Aro1* promoter in Col-0 (I) and HTR10 (J) background, respectively. Stamens were collected at floral development stage 12 (Smyth *et al* 1990). The pollen containing theca at the end of the filament are still closed. Homozygous plants can be rapidly identified by their expression of *YFP* in all pollen grains (I). Heterozygous plants produce fluorescent and non-fluorescent pollen (J). In the homozygous *HTR10*-background, all pollen grains show additional red staining of the two sperm cell nuclei (J). The YFP-channel is depicted in false colour yellow, the RFP-channel in false colour red. Abbreviations: ap = antipodals, cc = central cell, ccn = central cell nucleus, chz = chalaza, cv = central cell vacuol, ec = egg cell, ecn = egg cell nucleus, fg = female gametophyte, fi = filament, mp = micropyle, rc = root cap, sn = synergid nucleus, sy = synergids, th = theca, v = veins, vc = vascular cylinder. Red scale bar = 200 µm; white scale bar = 50 µm.

3.3.3 *In vitro* growth of CerTN-pollen tubes and FRET-measurement

In order to test the functionality of the CerTN-L15 sensor protein *in planta* it was tried to verify transient elevations of intracellular calcium concentrations in growing *A. thaliana* pollen tube tips. Pollen tubes were grown *in vitro* and the CFP and YFP emission after excitation at 458 nm was detected using a LSM510 Meta CLSM (Zeiss). During pollen tube growth, no elevated tip-localised calcium concentrations were detected (Figure 3.6). It was therefore decided to continue experiments in collaboration with the lab of Prof. W. Frommer (Stanford University, USA) that is very experienced with the development and study of molecular sensors and which possesses the necessary microscopical setup.

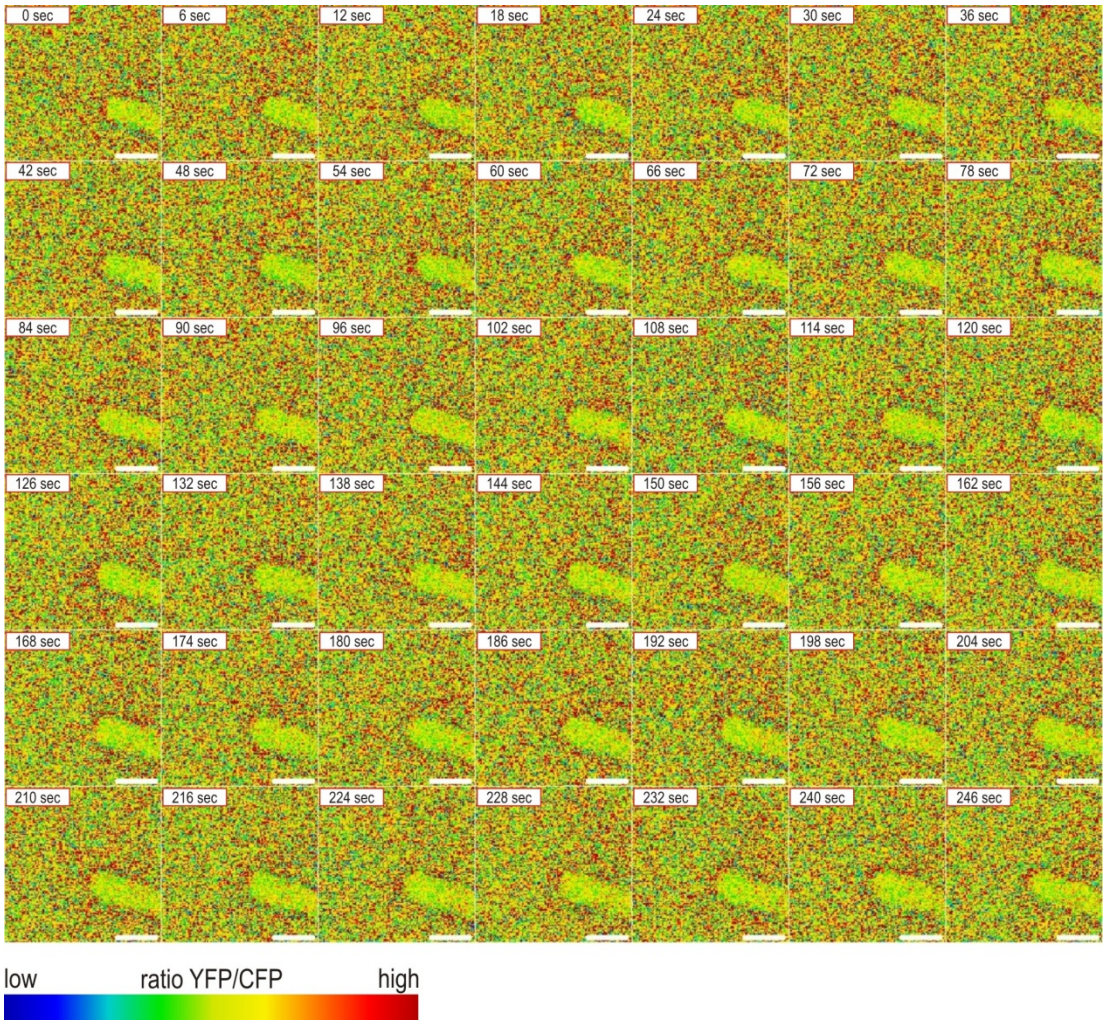

Figure 3.6 Ratio images of CFP and YFP in growing pollen tubes. Excitation was performed at 458 nm. During pollen tube growth over a time period of 246 sec a tip-localised elevation of intracellular calcium concentration could not be detected. Scale bar 10 µm.

3.4 Discussion

The previously described plasma membrane marker construct *AtPLT5-eGFP* (Klepek *et al.* 2005) under control of the *ACT11* promoter (Huang, An et al. 1997)localises the encoded fusion protein to the plasma membrane of growing pollen tube. The construct alone or co-expressed with other pollen tube cytosolic and sperm cell fluorescent fusions proteins could be used for *in vivo* studies of double fertilisation. However, although the GFP-fusion protein is predominantly located in the plasma membrane the construct generates a not negligible background in the cell. In the transient assay, this background was more pronounced probably due to residual construct in the ER. Punctate aggregation with high GFP-intensity was found in both, transient and stable expression. These phenomena are likely to be a result of overexpression from the *35S*-promoter (Guilley *et al.* 1982)in the transient study or the *AtACT11*-promoter in stable AcPMG plants. Insufficient secretion would result in detection of the fusion construct in the ER. Moreover this marker line is hampered by expression in sporophytic cells of the ovule. Taken together AcPMG is of limited use for marking the boundaries of FG cells but expression in pollen tube nicely labels its plasma membrane and could be of further use.

The constitutive expression of the calcium probe CerTN-L15 (Heim and Griesbeck 2003) under the 35S-promoter (35C) and the cell specific expression in the synergid (MYC), egg cell (ECC) and pollen (ARC and ARC/HTR10) was successful and resulted in the generation of lines showing high sensor protein levels in several independent lines per construct. Yet, it was not possible to prove that the above mentioned lines contain a functional calcium sensor. Expression of YFP is easy to detect at high levels in the fluorescence microscope. Since YFP is the most C-terminal domain of the recombinant calcium probe, this indicates transcription of the full-length CerTN-L15 protein. Western blot analysis revealed, however, that the 35C line contains a protein of 62 kDa, which is about 10% smaller than the predicted size of 70 kDa (data not shown). Detection of signals in the CFP- and YFP-channels of the CLSM indicates expression of full-length CerTN-L15. Finally, this work could not clarify whether the construct is fully functional in plants. Although initial attempts to reproduce published calcium elevations in PTs (Iwano *et al.* 2004) in the ARC-lines failed, the plant lines might still be a very valuable tool for further studies after functional validation of CerTN-L15 in plants.

Recently, the group of W. Frommer utilised the 35C-line to show calcium signalling in roots under salt stress and the MYC-line was used to identify calcium spikes in the synergid cells upon pollen tube arrival (P. Denninger and G. Grossmann, personal communication). The latter finding was observed independently by the group of M. Iwano (personal communication). Additionally, these results indicate that the lines ECC and ARC likely express a functional calcium sensor as well.

Combination of the generated calcium sensor lines and expression data of the gametophyte cells in *A. thaliana* (L. Šolijć and S. Sprunck, unpublished) now pave the way to study the nature of calcium signalling during double fertilization *in planta*. It would be strait forward to characterise mutants of known players in calcium signalling in the course of double fertilisation starting form candidates for calcium channels, pumps, calmodulins or others downstream targets. Besides phenotypic analyses in respect to double fertilisation, knock-out-lines of these genes can be crossed or transformed with the given calcium probe construct and characterised at the physiological level of calcium signalling. In addition to that it could be fruitful to study calcium signalling in mutant lines impaired in double fertilisation. A good candidate for calcium signalling in the synergid cells would be, for example, *feronia* (Escobar-Restrepo *et al.* 2007). Assuming that *FERONIA* is involved in pollen tube recognition the MYC-line now allows to study if Ca^{2+}-spiking in the synergid is an element of the *FERONIA*-pathway of PT recognition. The same strategy could be applied for all mutants defective in double fertilization. In the long run the tools created in this work could allow unravelling the role of calcium in double fertilisation of the model plant *A. thaliana*.

3.5 Summary

For studying calcium signalling during double fertilization *in vivo*, one membrane marker construct and three calcium probe constructs were transformed into *Arabidopsis thaliana*. The aim of the membrane marker line was to label the boundaries of the gametophytic cells. In order to achieve this, GFP was fused to the polyol transporter *AtPLT5* at its carboxy terminus (AcPMG). The construct led to intracellular background signals and diffuse signal at the tip of the growing pollen tube. Expression in cells of the female gametophyte was achieved in synergids and central cells but not in egg cells. Taken together, the membrane marker line didn't fulfil the demands of distinct background free membrane labelling of all gametophytic cells. The use of AcPMG for cell identification during double fertilisation in experiments together with lines expressing the recombinant calcium probe CerTN-L15 (see below) in gametophytic cells is thus limited. Therefore, the line AcPMG was not applied in other experiments of this study but might be useful as green plasma membrane marker for growing pollen tubes during other studies.

Five calcium sensor lines have been constructed. Two of which have been shown to generate a functional CerTN-L15-sensor (experiments perfomed by P. Denninger in the group of Prof. W. Frommer in Stanford/USA). The line 35C expresses the sensor under the viral *35S*-promoter and allows measuring elevated calcium levels during salt stress (P. Denninger and G. Grossmann, personal communication). A synergid-line (MYC) was used to detect calcium spiking upon pollen tube arrival (P. Denninger and G. Grossmann, personal communication). Additional lines expressing the calcium sensor in the egg cell (ECC) and the pollen tube (ARC and ARC/HTR10) were made. The pollen specific construct was transformed into wild type (ARC) and sperm cell marker lines (ARC/HTR10), respectively. Since the lines ECC, ARC and ARC/HTR10 were generated with the same functional sensor construct, they might also be useful for further investigations. For the ARC-lines, expression of full length constructs could be confirmed, but successful FRET-experiment could not be conducted in the frame of this study due to the limitations in microscope equipment. In summary, the calcium sensor lines ECC (egg cell), MYC (synergid), ARC (pollen), ARC/HTR10 (pollen) and 35C (vegetative) have been generated and can now be used as a valuable tool for studying calcium signalling in gametophytic cells and sporophytic tissues during double fertilization.

Chapter 4 - Egg cell signaling by ZmEAL1 controls antipodal cell fate

The following chapter is based on the publication (Krohn, Lausser et al. submitted). A. Lausser contributed the qRT-PCR-experiments (Figure 1J and Figure 5G) and wrote the corresponding paragraphs in the section on experimental procedures (4.2.9).

4.1 Introduction

The female germ lineage of flowering plants is initiated with the differentiation of a hypodermal cell at the tip of ovule primordia into a primordial germ cell (PGC), or archesporial cell (Grossniklaus 2011; Yang *et al.* 2011). The PGC differentiates into the polar megasporocyte and undergoes meiosis forming a linear tetrad of four haploid megaspores in most angiosperm families. The three most micropylar megaspores degenerate and the nucleus of the functional megaspore undergoes three rounds of stereotypic mitotic divisions forming an eight-nucleated syncytic cell (Ma and Sundaresan 2010; Sprunck and Gross-Hardt 2011). This large cell, the immature female gametophyte or embryo sac, is partitioned into seven cells, namely the two female gametes, egg and central cell, as well as two accessory cells at the micropylar pole (synergid cells) and three accessory cells (antipodal cells) at the chalazal pole. The antipodal cells start to proliferate in grasses, forming a cluster of up to 40 polyploid cells (Diboll and Larson 1966; Kapil and Bhatnagar 1981). Antipodal cells in other plant families including the model plant Arabidopsis degenerate during embryo sac maturation and are dispensable for fertilization and seed development (Yang, Shi et al. 2011; Sprunck and Gross-Hardt 2011).

The molecular mechanisms governing cell specification in the eight-nucleated syncytic embryo sac are largely unknown. In Arabidopsis, it was reported that auxin-concentration dependent cell-type specification occurs in the immature embryo sac and depends on an intrinsic positional information gradient, with the highest auxin accumulation occurring at the micropylar pole. It was further proposed that the intrinsic auxin gradient is established by localized auxin biosynthesis at the micropylar pole of the uncellularized embryo sac (Pagnussat *et al.* 2009). Other reports in Arabidopsis and maize support the hypothesis that cell-specification occurs according to nuclear positions in the syncytical embryo sac. Overproliferation of nuclei in the Arabidopsis cell cycle mutant *rbr1* (*retinoblastoma-*

related 1) and in the maize mutant *ig1* (*indeterminate gametophyte1*), for example, leads to extra synergid, egg and central cells individually specified according to their position (Ebel *et al.* 2004; Guo *et al.* 2004). Moreover, a lateral inhibition mechanism was postulated, such that after initial specification of gametic cells, and especially of the egg cell, it may be necessary to maintain cell fates and to prevent accessory cells from differentiating into germ cells, since all cells of the embryo sac seem to be competent to differentiate into each other (Gross-Hardt, Kaegi et al. 2007; Sprunck and Gross-Hardt 2011). Based on recent genetic studies this model was further developed indicating that differentiation of embryo sac cells depends on egg cell signaling (Voelz *et al.* 2012).

We have used maize as a grass model to study specification of the female germ lineage and report here on an egg cell secreted peptide whose gene is expressed in the micropylar pole of the immature embryo sac. We show that *Zea mays EA1-like 1* (*ZmEAL1*), an EA1-box (Márton *et al.* 2005) encoding peptide gene, is auxin insensitive in cell culture and encodes a secreted, non-cell autonomous peptide factor that functions to prevent antipodal cells from adopting central cell fate. Moreover, we report here that ZmEAL1 activity is required to regulate the LOB domain transcription factor gene *IG1* that is predominately expressed in the chalazal pole of the embryo sac.

4.2. Experimental procedures

4.2.1 Plant material

Maize inbred lines A188 and H99 as well as transgenic lines were grown under standard greenhouse conditions as described 2.2.1.

4.2.2 Histological studies, immunostaining and eGFP imaging

Transgenic plants with glufosinate ammonium resistance lacking integration of the RNAi construct were used as a wild type control for phenotypical analysis of *ZmEAL1*-RNAi embryo sacs. Immature and mature cobs were harvested from greenhouse grown maize plants. After removal of leaves whole cobs were treated according to the procedure described by (Srilunchang, Krohn et al. 2010). For microscopic analyses, only ovaries from the middle cob regions were manually dissected after clearing with two longitudinal sections to the silk axis after they were cleared, mounted in methyl salicylate on glass slides under a cover slip and analyzed with a LSM 510-META confocal laser scanning microscopy (CLSM, Zeiss) with 488 nm excitation and a LP 505 filter. For immunocytochemistry, mature cobs were freshly harvested from greenhouse grown plants and ovaries were longitudinally hand-sectioned using a razor blade. Sections were fixed for 2 h [4% paraformaldehyde in PHEMS buffer (60 mM Pipes, 25 mM HEPES, 10mM EGTA, 2 mM $MgCl_2$ and 0,32 M sorbitol pH 7.2)], washed few times in PHEMS buffer and then embedded in polyacrylamide following the protocol of (Bass *et al.* 1997). Immunostaining was performed as described (Singh *et al.* 2010)with minor modifications described in Supplementary Experimental Procedures. For the analyses of eGFP expressing embryo sacs, ovaries were dissected with two longitudinal sections to the silk axis to remove nucellar tissue. eGFP fluorescence from embryo sacs as well as from transiently transformed BMS suspension cells were monitored by CLSM with 488 nm excitation and a BP 505-550 filter for selective EGFP visualization. Image capture and processing were done using the Zeiss LSM 510 META software and the Zeiss LSM image browser version 3.5.0.359.

4.2.3 Isolation of male and female gametophytic cells from maize

Cells of unfertilized female and male gametophytes were isolated as described (Kranz, Bautor et al. 1991)). Zygotes were isolated 24 h after *in vivo* pollination. The *in vivo* pollination procedure was performed using cobs with fully developed embryo sacs. Silks of cobs were shortened in a way that 2 cm in length were left between the cutting side and the top of the last ovary row. Zygotes were isolated from ovules dissected from the central part of the cob using the procedure described to microdissect egg cells (Kranz, Bautor et al. 1991). Single cells of the female gametophyte and single zygotes were washed twice in droplets of mannitol solution (570 mosmol/kg H_2O) and transferred to plastic microtubes each with about 15 nl osmotic solution. 50 sperm cells were collected for each experiment after osmotic burst of pollen grains and transferred to plastic microtubes containing 50 nl mannitol solution (550 mosmol/kg H_2O). Cells were frozen in liquid nitrogen and stored at -80 °C until usage.

4.2.4 Plasmolysis and PCIB treatment

To study plasmolysis of BMS cells, osmolarity of the MS medium was measured (usually at 550 mosmol·kg^{-1}). Hepes buffer (10 mM) pH 7.2 was prepared and mannitol was added as osmotic agent to adjust the osmolarity to 950 mosmol·kg^{-1}. BMS suspension cells were transformed with P_{ZmEAL1}*:ZmEAL1-eGFP*, P_{ZmEAL1}*:eGFP* and *PMON30049* (Pang *et al.* 1996); used as a positive control) and cultivated. Before microscopic observations, medium was sucked up from the suspension cells and 1 ml of Hepes buffer with osmotic agent was added to suspension cells followed by incubation at room temperature for 30 min and shaking at 110 rpm. To study auxin responses in BMS cells, PCIB (Oono *et al.* 2003), purchased from Sigma, dissolved in DMSO) was added to 5 ml aliquots of the above mention cell culture to a final concentration of 100 µM and incubated as described. Control cells were treated only with DMSO for the same period of time and gene expression was assayed with semi-quantitative PCR (data not shown). After incubation, cell were collected by filtration and frozen immediately in liquid nitrogen for later gene expression studies. The expression of *ZmEAL1* and *ZmSAUR1* were evaluated through quantitative real-time PCR (described in Suppl. Experimental Procedures) using *GAPDH* and *Ubiquitin* as control for housekeeping genes).

4.2.5 Generation of constructs and stable maize transformation

ZmEAL1-RNAi construct (*P_{UBI}:ZmEAL1-AS:iF2intron:ZmEAL1:OCSt*): the RNAi construct directed against *ZmEAL1* under the control of the maize ubiquitin promoter (*Ubi1*) was constructed by DNA Cloning Service (Hamburg) using the plasmid P_{UBI}-*iF2* (DNA Cloning Service). In a first step, a 368 bp fragment starting at 20 bp upstream of the predicted start codon to 125 bp downstream of the stop codon of the *ZmEAL1* gene was amplified from gDNA using the primers 222-BSR and 222-Mlu introducing *BsrGI* and *MluI* restriction sites allowing the cloning of the *ZmEAL1* fragment in sense orientation into the P_{Ubi}-*iF2-222* vector. Further, the *ZmEAL1* fragment was PCR amplified from vector P_{Ubi}-*iF2-222* using primers 222-Eco and 222-Bam and cloned in anti-sense orientation into the *Bam*HI and *Eco*RI restriction sites of the vector P_{Ubi}-*iF2-222* vector generating the *ZmEAL1*-RNAi construct.

P_{ZmEAL1}*:eGFP:NOSt*: the *pLNU-eGFP* vector (DNA Cloning Service-Hamburg) was digested with *Not*I and *Bam*HI to cut out the *Ubi* promoter with a final purification step of the fragment of interest. The promoter of *ZmEAL1* was amplified from gDNA using the primers A188-EC222-GFP-fwd and EC222-GFP-control-rev introducing *Not*I and *Bam*HI restriction sites to clone the *ZmEAL1* promoter into the *pLNU-eGFP* vector generating the P_{ZmEAL1}*:eGFP* vector.

P_{ZmEAL1}*:ZmEAL1-eGFP:NOSt:* for expressing ZmEAL1-eGFP-fusion protein under control of the *ZmEAL1* promoter, e*GFP* was C-terminally fused to the coding sequences of *ZmEAL1*. The *pLNU-eGFP* vector (see above) was used and digested with *Not*I and *Spe*I with a final purification step of the fragment of interest. The *ZmEAL1* gene (promoter, 5'UTR and ORF) was amplified from gDNA using the primers B73-EC222-GFP-fwd and B73-EC222-GFP-rev introducing the *Not*I and *Spe*I restriction sites to clone the *ZmEAL1* gene into the *pLNU-eGFP* vector generating the P_{ZmEAL1}*:ZmEAL1-eGFP* vector.

Immature hybrid embryos of the maize inbred lines A188 and H99 were isolated 11 to 13 days after pollination for subsequent stable transformation using biolistic particle bombardment with the PDS-1000/He system (BioRad). The constructs *ZmEAL1*-RNAi, P_{ZmEAL1}*:eGFP* and P_{ZmEAL1}*:ZmEAL1-eGFP* were each co-transformed with the vector P_{35S}*:PAT* carrying the selectable marker PAT for glufosinate ammonium resistance (Becker *et al.* 1994). Particle bombardment, tissue culture and selection of transgenic maize plants were performed using modified N_6 medium (Dhalluin *et al.* 1992) according to (Brettschneider *et al.* 1997).

4.2.6 Semi-quantitative Single Cell RT-PCR (SC RT-PCR)

SC RT-PCR was performed as described (Richert et al., 1996) with minor modifications. First-strand cDNA synthesis was performed using 100 units of RevertAid™ H Minus Reverse Transcriptase (MBI Fermentas) with addition of buffer supplied with 20 units of RiboLock™ RNase Inhibitor (MBI Fermentas), 2,5 μM primers ZmGap2 and ZmEC222-500-rev (see primer sequences in Suppl. Experimental Procedures). The RT reaction was performed at 50 °C for 70 min and the enzyme was subsequently inactivated at 70 °C for 10 min. After RT, each reaction was equally split into two reaction tubes and PCR reactions were carried out as follows: the first reaction was performed with primers ZmGap1 and ZmGap2 primer pairs as a control to visualize gDNA contaminations. For the second reaction the primer pair ZmEC222-RT-fwdand ZmEC222-500-rev was used. Both PCR reactions were conducted with 40 cycles and PCR products were separated onto agarose gels, blotted on membranes hybridized with probes labeled with ^{32}P-α-dCTP (as described in Suppl. Experimental Procedures). After hybridization, membranes were exposed and scanned for quantification using the Cyclone™ Storage Phosphor System (PerkinElmer). Signal quantification was performed by using the OptiQuant™ Image Analysis Software (PerkinElmer). Expression levels of *ZmEAL1* were normalized with *GAPDH* signals.

4.2.7 DNA and RNA extraction, Southern blot analysis and RT-PCR

Genomic DNA (gDNA) extraction from leaves was performed according to (Pallotta *et al.* 2000). For Southern blot analysis restriction endonuclease digestion of gDNA of P_{ZmEAL1}*:eGFP* and P_{ZmEAL1}*:ZmEAL1-eGFP* plants was performed with *Bgl*II and *Swa*I and of *ZmEAL1*-RNAi plants with *Not*I and *Afl*I, respectively. These enzyme combinations cut out the whole cassette from the various vectors. 30 μg restricted gDNA was separated on 0,8% agarose gels. Agarose gels were treated with denaturating and neutralizing solution with posterior transfer of gDNA onto Hybond-XL membranes (GE Healthcare) by capillary transfer with 20xSSC. gDNA was fixed to the membrane by using UV crosslinking (UV Stratalinker TM 1800; Stratagene, USA) procedure, with 70,000 μjoules/cm^2. Gel treatment, blotting, pre-hybridization, hybridization and washing procedures were performed according the Hybond-XL membrane descriptions. Pre-hybridization and hybridization were performed in Church buffer (Dresselhaus, Amien et

al. 2005). Specific probes for hybridizations were generated by PCR, purified and labelled with ^{32}P-α-dCTP according to specifications of the Primer-it II Random Primer Labeling Kit (Stratagene). After washing membranes were exposed onto X-ray films at -80 °C with posterior development.

For the expression analysis of a *ZmEAL1*-RNAi construct in transgenic maize lines total RNA was isolated with TRIzol® (PEQLab). 1 µg of total RNA was each used for first-strand cDNA synthesis using Oligo $(dT)_{18}$ (MBI Fermentas) and Reverse Transcriptase (RevertAid™ MMuLV Reverse Transcriptase, MBI Fermentas) following the manufacturer's protocol. The quality of generated cDNAs was analyzed by PCR using maize *GAPDH* (Glyceraldehyde 3-phosphate dehydrogenase)-specific primers ZmGap1 and ZmGap2. To verify the expression of the *ZmEAL1*-RNAi construct PCRs were performed with the primer pair UbiD-fwd and ZmEC222-1-fwd.

4.2.8 Transient transformation of maize BMS cells

BMS cells growing on solid MS medium (30 g/l of sucrose, 4.4 g/l of MS-salts from Duchefa, 2 mg/l of 2,4-Dichlorophenoxyacetic acid, pH 5.8) were first sterile filtrated through a 500 µm metal net, passed through a 100 µm pore sized nylon mesh, transferred to liquid MS medium and cultivated for one week at 26 °C in a dark chamber shaking at 110 rpm. After growing for one week 25 ml of cell culture was transferred to a clean and sterile flask and 35 ml fresh MS medium was added. Cultures were cultivated again for one week. Before biolistic transformation, a small volume of the cell culture was uniformly distributed in a thin layer of cells on solid MS medium. Cells were incubated at 26 °C for 2 h. BMS cells were bombarded with gold particles (0.6 µm) coated with plasmid DNA. 10 µg of plasmid DNA (2 $\mu g \cdot \mu l^{-1}$) was precipitated on 2 mg of gold particles (dissolved in 50 µl of absolute ethanol) using 50 µl of $CaCl_2$ (2.5 M) and 20 µl of spermidine (0.1 M). After DNA precipitating and washing procedures with absolute ethanol, coated gold particles were resuspended with 150 µl of ethanol. 7.5 µl of the solution containing coated gold particles was applied on macrocarriers. Each plate, with BMS cells on the surface, was bombarded three times using the particle delivery system PDS1000/He (BioRad) with 1,100-psi rupture discs, a partial vacuum of 28 inch Hg and a 6 cm target distance. After transformation, plates were incubated overnight in the dark at 26 °C. Cells were transferred

to fresh liquid medium and cultivated in darkness using a shaker at 110 rpm for at least 4 h before microscopic observations

4.2.9 Quantitative Real-Time PCR (qRT-PCR)

For qRT-PCR studies, BMS cell samples were first ground to powder in liquid nitrogen. Approximately 100 mg BMS cell suspension powder was used for total-RNA extraction using TriFast reagent (PEQLab) according to the manufactures protocol. DNA-contaminations were removed with DNAseI (Fermentas) digestion. cDNA was generated using MMuLV-reverse transcriptase with oligo dT-Primers (both Fermentas) according to manufactures protocols. RT-reaction was used as template in PCR reactions (approximately 11 ng total RNA was used per PCR reaction).

QRT-PCR reactions were performed in a cycler (Realplex 2, Eppendorf) suitable for SYBR-Green detection. The SYBR-Green mix (QuantiTect SYBR-Green) was purchased from Qiagen. PCR efficiency was estimated by a standard series of pooled cDNA-samples and diluted 1:3 with 50 ng/µl λ-DNA as carrier solution (Fermentas) for each primer pair. The carrier solution was used as template in non-template controls. All reactions were performed with 30 seconds elongation step at 72 °C. Annealing was done for 30 seconds at 60 °C for *Ubiquitin*, *GAPDH* and *ZmEAL1* or at 67.5 °C for *ZmSAUR1*, respectively. All biological replicates were pipetted as technical triplicates and standard reactions as technical duplicates.

Statistical processing of the raw qRT-PCR data was carried out as described in the manual for the GeNorm-Software (Vandesompele *et al.* 2002). First, Ct-values were transformed into $2^{\Delta Ct}$-values with lowest Ct-values of each gene as calibrator. A normalization factor was calculated as geometric mean of the $2^{\Delta Ct}$-values of *GAPDH* and *Ubiquitin*. This normalization factor was used to normalize the $2^{\Delta Ct}$-values of every gene by division of the $2^{\Delta Ct}$-values through the normalization factor. Fold changes were calculated by dividing the normalized expression values for every gene and time point through the corresponding value at time point zero. This was done independently for every biological replicate. All deviations were calculated as the 1.96-times standard error.

For determining expression levels of *ZmIG1* in embryo sac of RNAi and wt plants total RNA was extracted from ~100 mg of nucellus tissue (equals ~90 nucelli). RNA-extraction and DNAaseI-treatment was carried out as described above. Superscript III-reverse transcriptase (Invitrogen) along with the gene-specific primers P189 and P134 was used to

produce cDNA according to suppliers protocols. Expression levels were investigated by qRT-PCR using the KAPA™ SYBR® Fast Universal qPCR-mix (Peqlab) according to manufactures instructions. Foldchanges of steady-state-mRNA-levels of *ZmIG1* were normalised against the housekeeping gene *GAPDH* by applying the $2^{-\Delta\Delta Ct}$-equation (according to PE Applied Biosystems; Perkin Elmer). ΔΔCt represents the difference of the Ct-values of the houesekeeping gene (*GAPDH*) and the gene of interest (*IG1*) in the RNAi-sample subtracted from the same difference in the wild-type-samples. The $2^{-\Delta\Delta Ct}$-value was calculated separately for three individuals per line. In the diagram the mean $2^{-\Delta\Delta Ct}$-value of the three individuals is blotted. The error is calculated as mean deviation of the $2^{-\Delta\Delta Ct}$-values of each line.

For PCR housekeeping gene-specific primers P133 and P134 were used for *GAPDH* and P141 and P142 (Muehlbauer *et al.* 1999) for *Ubiquitin*. For the auxin-regulated gene *ZmSAUR1* (Yang and Poovaiah 2002) the following primer pair P97 and P98 was used. The primer pair P123 and P124 was applied for determining the mRNA levels of *ZmEAL1*. For amplification fo a fragment from *ZmIG1* the primer pair P188 and P189 was used. All primers were used at final concentration of 50 nM.

4.2.10 Immunocytochemistry

Immunocytochemistry was basically performed as described by Singh *et al.* 2010 with minor modifications: samples were digested in an enzymatic solution [1% driselase (Sigma-Aldrich), 0.5% cellulase "Onozuka R10" (Serva), 1% pectolyase Y23 (Karlan) and proteinase inhibitor cocktail cOmplete, Mini, EDTA-free (Roche) in PHEMS buffer, pH 5.3] for 20-30 min at 37 ºC. Samples were incubated overnight in a humid chamber at 4 ºC with a 1:1000 dilution of an anti-eGFP antibody (Roche). After washing several times in 1xPBS and 0.1% Triton X-100 for 8 h, samples were incubated in a Cy3-conjugated goat anti-mouse antibody (Jackson ImmunoResearch) at a dilution of 1:400 in 1xPBS overnight. The same washing procedure was perfomed the following day. Ovule sections were mounted in self-made antifading solution (Jackson ImmunoResearch recipe) and sealed with a coverslip. Three-dimensional images of embryo sacs were captured on a LSM 510-META laser scanning confocal microscope (Zeiss) using 543 nm excitation and a LP 560 filter. Image J software (http://rsbweb.nih.gov/ij/) was used to create two-dimensional images as a maximum intensity projection of selected optical sections.

4.3 Results

4.3.1 Activation of *ZmEAL1* at the micropylar pole of the syncytic embryo sac occurs independent from auxin

With the goal to study egg cell signaling, we have analyzed an egg cell cDNA library of maize (Dresselhaus *et al.* 1994) for the presence of transcripts encoding small secreted proteins or peptides. Detailed studies of first candidates led to the identification of ZmEA1 and ZmES4, which are secreted from the micropylar pole of the egg apparatus (egg and synergis cells) to attract pollen tubes (Márton *et al.* 2005) and to mediate the release of sperm cells (Amien *et al*. 2010), respectively. Here we report on the analysis of *ZmEAL1* (*Zea mays EA1-like 1*), which is exclusively expressed in the egg cell of mature ovaries. In order to study the time course of *ZmEAL1* expression during germline development, we have used 700 bp upstream of the predicted open reading frame (ORF) as *ZmEAL1* promoter to drive eGFP expression. Seven independent transgenic lines were generated containing full-length integrations of the promoter-marker construct. The three lines showing detectable eGFP fluorescence in mature ovules were analyzed in more detail. Additionally, an eGFP expressing line containing 2 kbp upstream of the ORF was analyzed. Three to four T1 plants of all lines were investigated from the formation of PGCs towards the maturation of embryo sacs at stage FG7. We found that both *ZmEAL1* (*Zea mays EA1-like 1*) promoter fragments are activated exclusively at the micropylar pole at the syncytical eight-nucleate stage (stage FG5), and are inactive at the chalazal pole (Figure 4.1A and B). After cellularization (stage FG6), *ZmEAL1* promoter activity becomes restricted to gametic cells (major signals in the egg cell and weaker signals in the central cell) and is exclusively active in the egg cell of mature gametophytes (Figure 4.1C-E). After fertilization, eGFP signals obtained from *ZmEAL1* promoter activity decrease but are stronger in the apical rather than basal cell after asymmetric zygote division (Figure 4.1F and G). Single cell RT-PCR was used to quantify and verify *ZmEAL1* transcript levels in mature embryo sac cells. We found that *ZmEAL1* is highly expressed in egg cells and not in the other cells of the embryo sac, with decreasing transcript amounts after fertilization (Figure 4.1H). Sperm cells show a very weak signal. Furthermore, we observed *ZmEAL1* promoter activity in maize BMS (black mexican sweet) suspension cells (Figure 4.1I) and took advantage of this observation to study the regulation of *ZmEAL1* by auxin. We established a method to down-regulate auxin responsive genes such as

ZmSAUR1 (Yang and Poovaiah 2002) using the auxin response inhibitor p-Chlorophenoxyisobutyric acid (PCIB; Oono *et al.* 2003). As shown in Figure 4.1J *ZmSAUR1* is strongly down-regulated at 90 and 420 min after PCIB treatment, while control transcripts of *GAPDH* and *Ubiquitin* remain unchanged. *ZmEAL1* transcript levels are neither significantly altered after PCIB treatment nor after 10-fold increase of auxin concentration in the medium (data not shown). In summary we conclude that *ZmEAL1* expression at the micropylar pole of the syncytic embryo sac is not significantly regulated by auxin.

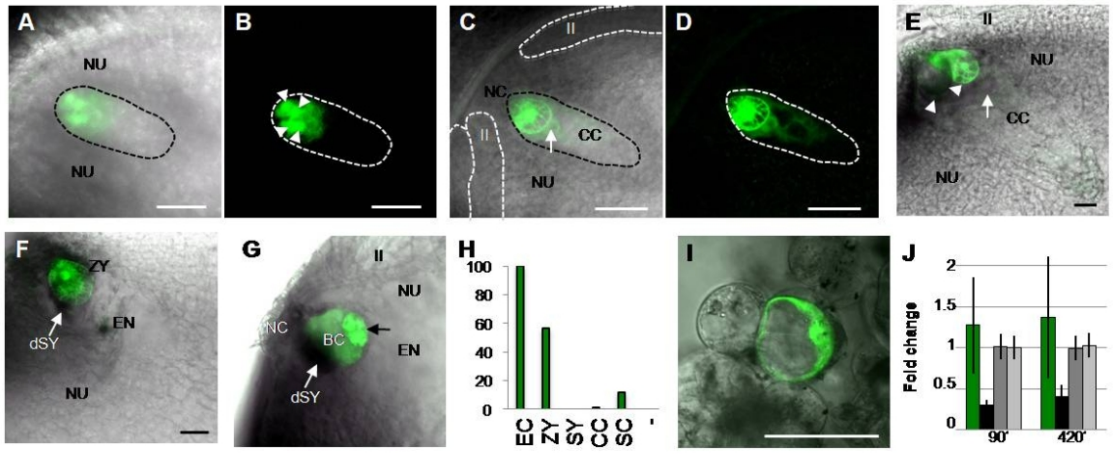

Figure 4.1 Expression of *ZmEAL1* during female germ cell differentiation in maize. *ZmEAL1* promoter activity drives expression of the eGFP marker protein. (**A**) Promoter activity is first visible at stage FG5 at the micropylar pole of the eight-nucleate immature embryo sac or female gametophyte (encircled). (**B**) Enhanced fluorescence image of (A). The four micropylar nuclei are indicated by arrowheads. (**C**) After cellularization eGFP signals are visible in the cytoplasm and nucleus of the immature egg cell at stage FG6. Polar nuclei of the central cell are indicated (arrow). Integuments are marked by white interrupted lines and the embryo sac with a black dashed line. (**D**) Enhanced fluorescence image of (C). The embryo sac is indicated by a black dashed line. (**E**) eGFP signals in the mature embryo sac at stage FG7 are restricted to the pear shaped egg cell. Synergid cells (arrowheads) and central cell (arrow points towards the polar nuclei) are indicated. (**F**) 24 h after pollination. Note that the zygote rounded up and its nucleus migrated slightly towards the micropylar pole. (**G**) 48 h after pollination. The apical cell divides longitudinally (black arrow), while division of the large basal cell is delayed. (**H**) Single cell semi-quantitative RT-PCR with isolated cells of the mature embryo sac. Relative values (%) are shown. Note that 50 sperm cells have been used in each experiment compared with single embryo sac cells. (**I**) Bombardment of maize BMS suspension cells with the *ZmEAL1* promoter driving the expression of eGFP marker protein. (**J**) Quantitative RT-PCR of *ZmEAL1* expression in BMS suspension cultures after treatment with the auxin response inhibitor PCIB. The auxin-regulated gene *ZmSAUR1* (black bars) is used as a positive control and *Ubiquitin* (dark grey bars) as well as *GAPDH* (light grey bars) as

negative controls. *ZmEAL1* is shown by green bars. Abbreviations: AP: antipodal cells, BC: basal cell, CC: central cell, dSY: degenerated synergid cell, EC: egg cell, EN: endosperm, II: inner integument, NC: nucellar cap, NU: nucellus, OI: outer integument, SC: sperm cells, SY: synergid cell, ZY: zygote, -: water control. Scale bars: 50 µm.

4.3.2 Z*mEAL1* encodes an egg cell secreted EA1-box peptide

To study the role of *ZmEAL1* during embryo sac maturation and cell differentiation, we first studied the localization of the encoded protein fused to eGFP and its secretion to the cell wall. *ZmEAL1* encodes a member of the highly conserved EA1-box peptides, containing an alanine-rich motif at the very C-terminus (Figure 4.2A). Its N-terminal signal peptide is predicted to be cleaved after the P-box, releasing a mature hydrophobic peptide of 48 amino acids (Figure 4.3A). Positively charged amino acids, such as arginine and lysine, as well as possible phosphorylation sites (serine and threonine) occur at highly conserved positions, indicating a possible function of these sites. Structure predictions indicate that mature ZmEAL1 peptide contains a α-helix flanked by conserved proline residues acting as helix breakers as well as three short ß-sheets (Figure 4.2B). ZmEAL1 contains one cysteine that may allow the protein to form a dimer, while most EA1-box peptides do not contain cysteine residues indicating that they may act as monomers. All Gramineae species investigated contain genes for EA1-box peptides, however, based solely on sequence analysis, we cannot predict which of the genes are *ZmEAL1* orthologs (Figure 4.3).

Due to the N-terminal signal peptide, eGFP was fused to the C-terminus of ZmEAL1 to study its (subcellular) localization during cell differentiation in the embryo sac. 2 kbp upstream of the predicted ORF of *ZmEAL1* was used to drive ZmEAL1-eGFP fusion protein expression. Two out of three independent full-length integrations lines showed eGFP signals in egg cells. Three to four T1 plants of both lines were studied in detail. In contrast to its promoter activity, ZmEAL1-eGFP fusion protein is not detectable before cellularization, which occurs at stage FG5; Figure 4.2C). The fusion protein first accumulates in the endoplasmic reticulum (ER) surrounding the nucleus of the immature egg cell (stage FG6; Figure 4.2D and E). In the mature embryo sac (stage FG7), ZmEAL1-eGFP fusion protein is localized in the ER surrounding the egg nucleus as well as in numerous small vesicles moving towards the surface of the cell (Figure 4.2F and G). After fertilization, ZmEAL1-eGFP levels strongly decrease (Figure 4.2H). Due to the pH

dependence of eGFP (Ward *et al.* 1982) and the acidification of vesicles in the secretory pathway from around 7.2 in the ER to 5.7 or even 5.2 in secretory granules (Paroutis *et al.* 2004), we have investigated true cellular fusion protein accumulation via immunohistochemistry using a monoclonal eGFP antibody. As shown in Figure 4.2I-K, ZmEAL1-eGFP mainly accumulates in granules directed towards the chalazal pole of the egg cell and appears weaker in the ER around the egg nucleus compared with eGFP fluorescence. Overexposure displays weak signals in antipodal cells, but signals around the central cell could not be detected (Figure 4.4). Control experiments using antibodies on wild type plants do not show any signal (Figure 4.4C). The egg cell does not contain cell wall material at its chalazal pole. It was therefore not possible to visualize secreted fusion protein in the extracellular space between egg and central cell. We have therefore exploited the observation that the *ZmEAL1* promoter is active in BMS suspension cells and studied the fusion protein in these cells. Similar to egg cells, fluorescence signals are visible in the ER around the nucleus, as well as in small vesicles within cytoplasmic strands (Figure 4.4D and E). After plasmolysis, fusion protein is additionally detectable in the cell wall (Figure 4.4F and G), which was never observed in controls using free eGFP (Figure 4.4H-K). Based on the data described above, we conclude that ZmEAL1 is secreted from egg cells and likely functions before fertilization.

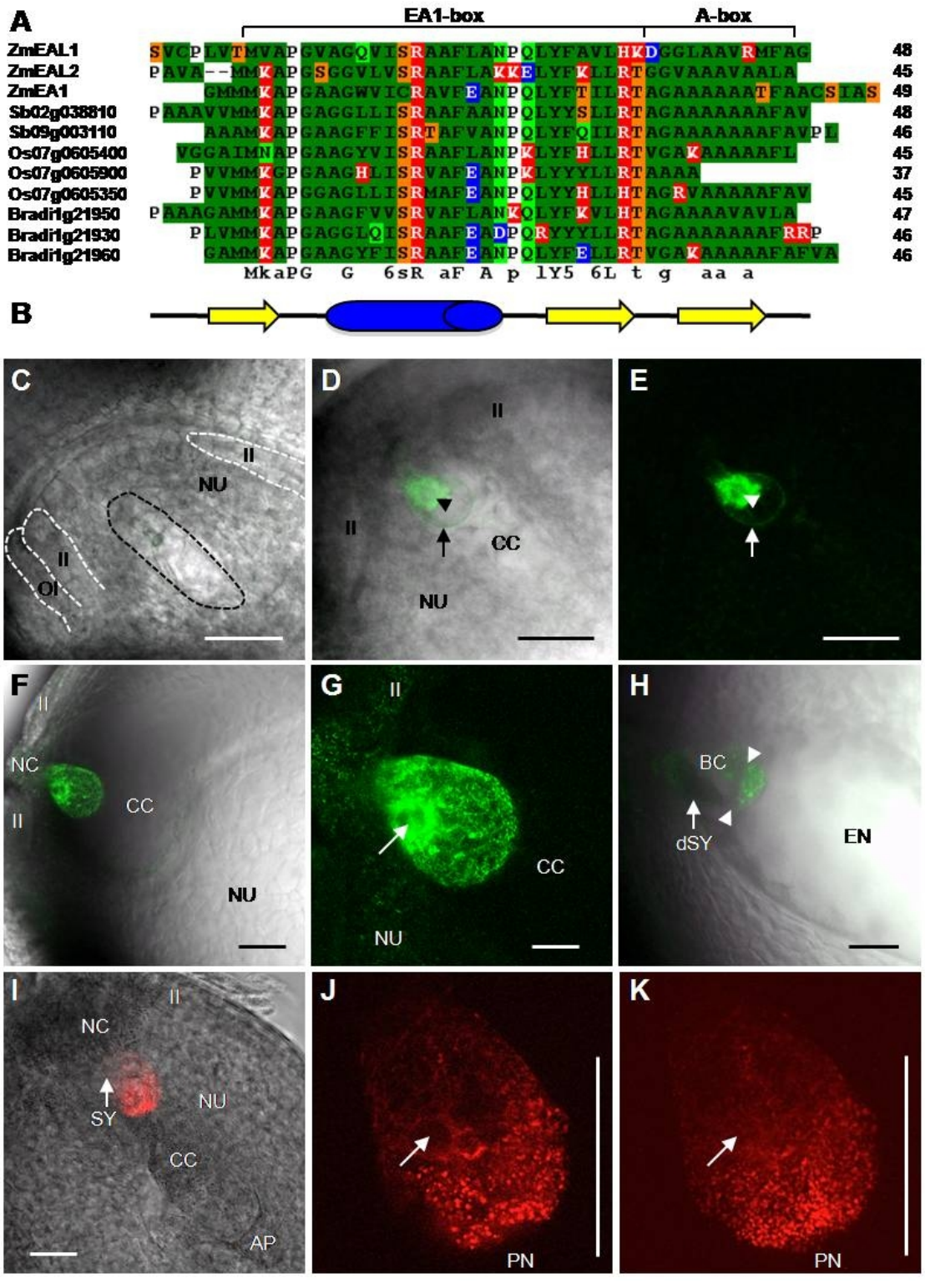
A
EA1-box
A-box
ZmEAL1
ZmEAL2
ZmEA1
Sb02g038810
Sb09g003110
Os07g0605400
Os07g0605900
Os07g0605350
Bradi1g21950
Bradi1g21930
Bradi1g21960
48
45
49
48
46
45
37
45
47
46
46
MkaPG G 6sR aF A p lY5 6L t g aa a
B
C
II
NU
II
OI
D
II
II
CC
NU
E
F
II
NC
CC
II
NU
G
II
CC
NU
H
BC
dSY
EN
I
II
NC
SY
NU
CC
AP
J
PN
K
PN

Figure 4.2 *ZmEAL1* encodes an EA1-box protein accumulating in secretory vesicles at the chalazal pole of the egg cell. (A) Properties of predicted mature EAL-proteins. Basic amino acids are shaded in red and acidic amino acids in blue. Putative phosphorylation sites at serine or threonine residues are indicated in orange, neutral amino acids and predominantly hydrophobic amino acids are shaded in light green and dark green, respectively. The consensus sequence is shown below the alignment and the size of the predicted mature proteins (kD) is indicated at the right. All proteins share the conserved EA1-box and an alanine-rich C-terminal tail (A-box). (B) Predicted secondary structure of mature EAL-proteins generated using the YASPIN program. (C-H) Localization of ZmEAL1-eGFP fusion protein during cell differentiation in the maturating embryo sac. (C) Stage FG5. Integuments and embryo sac are indicated by white and black dashed lines, respectively. (D) Stage FG6. Arrow points towards the nucleus of the immature egg cell. Arrowhead points towards one of the two synergid cells. (E) Enhanced fluorescence image of (D). (F) Mature stage FG7. (G) Enhanced fluorescence image of (F). The arrow points towards the egg cell nucleus. (H) 48 h after pollination. Asymmetric zygote division is indicated (arrowheads). (I) Immunostaining of a mature ZmEAL1-eGFP ovule using a monoclonal GFP antibody. (J) Optical section through the egg cell nucleus of a similar ovule as shown in (I). (K) Projection of all optical sections for the same egg cell as in (J). Abbreviations: BC: basal cell, CC: central cell, dSY: degenerated synergid cell, EN: endosperm, II: inner integument, NU: nucellus, OI: outer integument; PN: polar nuclei. Scale bars: 50 µm.

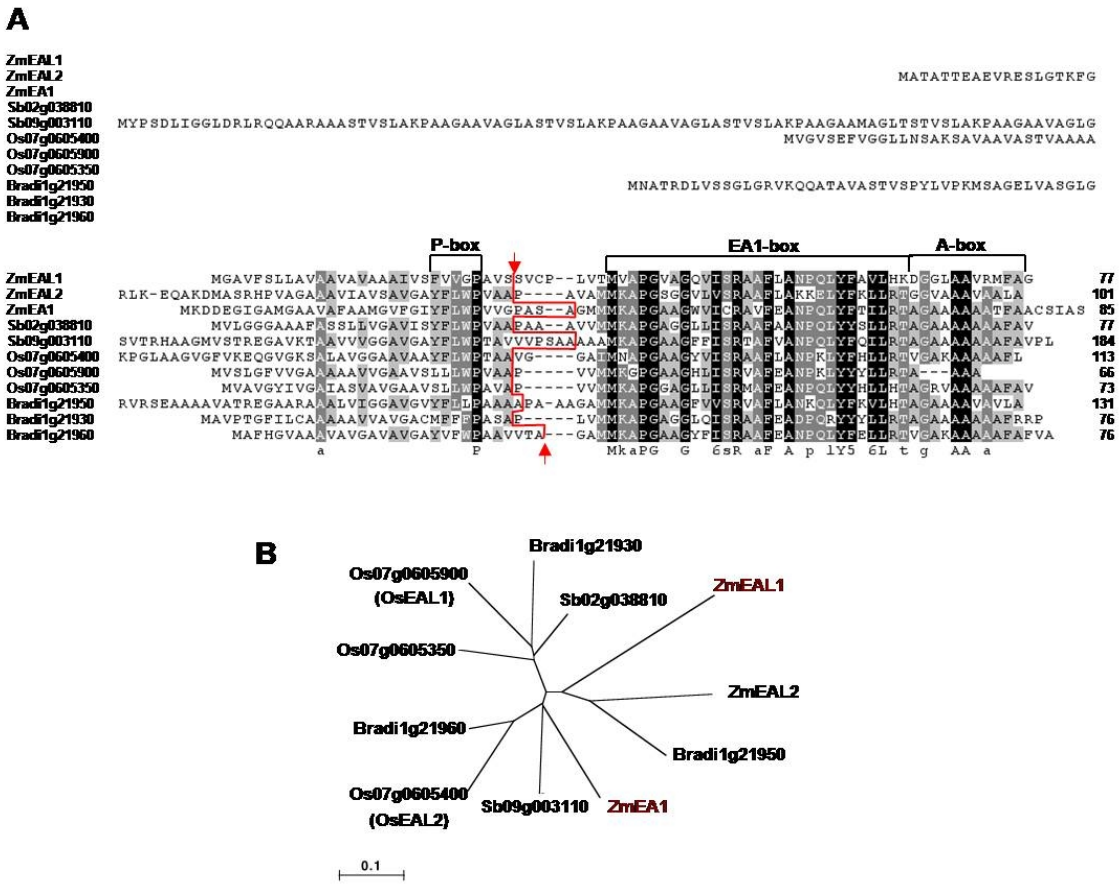

Figure 4.3 Alignment and phylogenetic tree of ZmEAL1 (ZmEA1-like1) precursor protein and its closest homologs from the grass species *Zea mays* (Zm, B73 cultivar), *Sorghum bicolour* (Sb), *Oryza sativa* (Os) and *Brachipodium distachyon* (Bradi), respectively. Note that genes encoding homologous proteins are not detectable in model dicotyledonous plants. (A) The alignment shows that EAL proteins are conserved in their predicted mature C-termini, but display little homology among their hydrophobic N-termini. EAL proteins are predicted to be cleaved after the P-box (often between an alanine and a proline residue; indicated by a red line) to generate mature proteins consisting of the highly conserved EA1-box and a variable alanine-rich A-box. The consensus sequence is indicated below the alignment. The alignment was performed using ClustalW2 and was drawn with GeneDoc. The figure was modified after (Dresselhaus, Lausser et al. 2011). Note that the EA1-box was elongated by one amino acid to include the conserved threonine at the C-terminus. (B) Unrooted phylogenetic tree of predicted mature EAL protein sequences drawn using NJPlot. The dendogram file used to generate the tree was obtained after ClustalW using the predicted mature protein sequences shown in Figure 2A. Branch lengths are proportional to phylogenetic distances and scale bar represents 10% substitutions per site. Short branch lengths indicate high conservation among EAL proteins. OsEAL proteins were previously classified by (Márton *et al.* 2005).

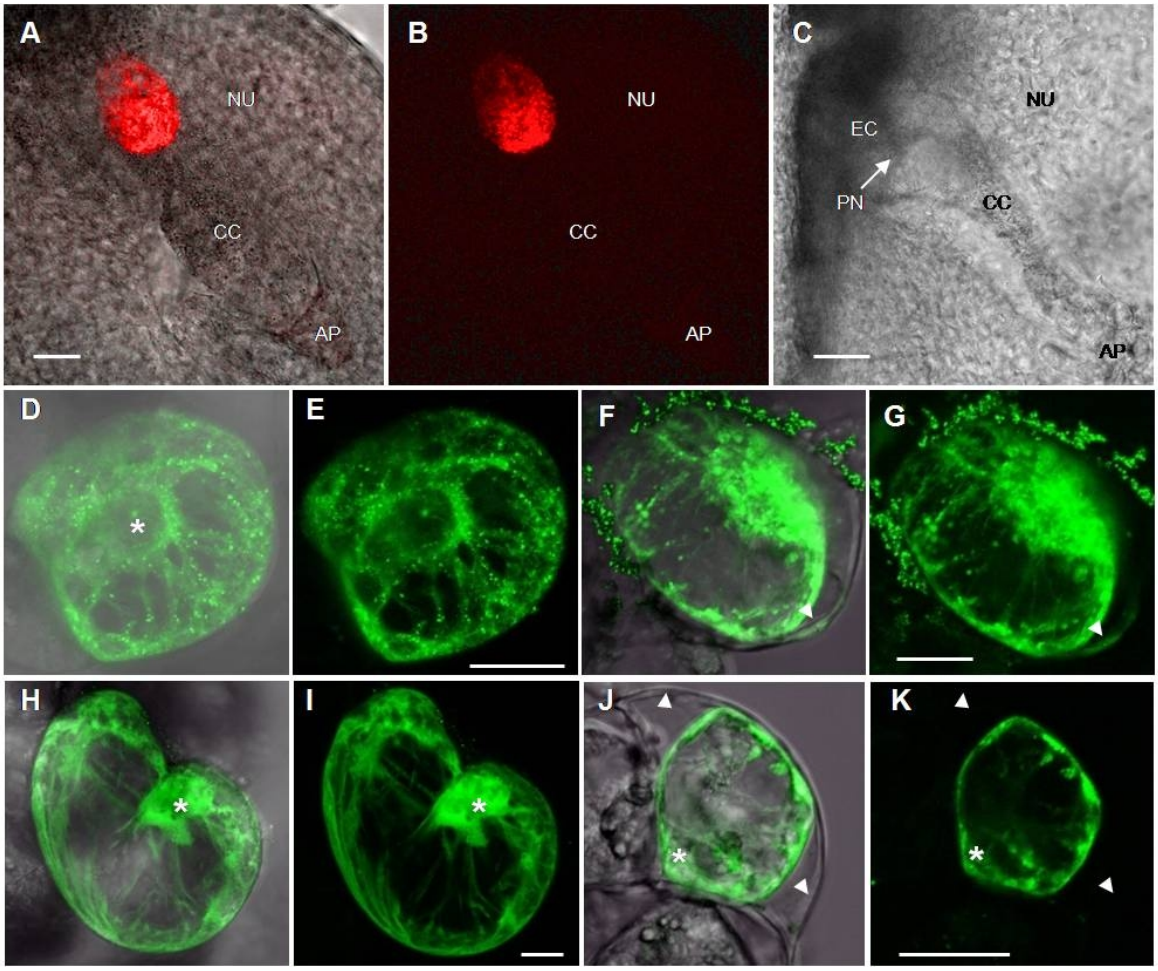

Figure 4.4 ZmEAL1 is localized to granules directed towards the central cell and is secreted to the cell wall of transiently transformed maize BMS suspension cells. (A-C) Immunostaining of maize ovules with a monoclonal GFP antibody. (A) Merged bright field and UV image of *pZmEAL1:ZmEAL1-eGFP* ovules show fluorescence from antibody staining specifically in egg cell vesicles directed towards the central cell. (B) Overexposed UV image to show that fusion protein is not detectable moving around the central cell. Note that faint signals are visible in antipodal cells. (C) Signals were not detectable in mature wild type ovules. (D-K) The endogenous *ZmEAL1* promoter was used to drive expression of GFP proteins in transiently transformed BMS cells. (D and E) ZmEAL1-GFP fusion protein is visible in small vesicles in cytoplasmic strands and around the nucleus, but is excluded from the nucleus (asterisk) before plasmolysis. (F and G) After plasmolysis weak ZmEAL1-GFP signals are additionally visible in the cell wall (arrowheads). (H-K) As a control free GFP is localized in the cytoplasm and nucleus (asterisk) before (H and I) and after plasmolysis (J and K). Arrowheads indicate cell walls of a plasmolysed cell lacking fluorescence. (A, C, D, F, H and J) Merged bright field and fluorescence images. (B, E, G, I and K) Corresponding fluorescence images. Each image represents a stack of 5-13 CLSM sections to display between 600-1,000 µm of the cells shown. Abbreviations: NU=nucellus, CC=central cell, AP=antipodal cells, EC=egg cell, PN=polar nuclei. Scale bars in (A-C)=50 µm and in (D-K)=20 µm.

4.3.3 ZmEAL1 activity is required to prevent antipodal cells from adopting central cell fate

Due to the lack of insertional mutant lines, an RNAi approach was chosen to investigate the function of *ZmEAL1*. Gene activity was down regulated by expressing a *ZmEAL1* hairpin construct using the constitutively expressing *ubiquitin* promoter of maize that is active in all cells of the embryo sac including the egg cell (Srilunchang, Krohn et al. 2010). T2 progeny plants of three independent lines (14-3, 14-7 and 14-9; see also Table 4.1) showing strong expression of the RNAi transcript in vegetative tissues (data not shown) were investigated in more detail. 27 RNAi plants (9 of each line) were studied in detail and their development compared with that of 13 wild type plants. Vegetative and reproductive organs of transgenic and wild type (wt) plants developed normally until maturation of embryo sacs occurred (stage FG6; Figure 4.5A). In contrast to 455 analyzed wt ovules, we detected additional central cells (Figure 4.5B-F and Figure 4.6) in 50 of 2095 ovules dissected of all RNAi lines (ranging from 0 to 10% among cobs of the 27 plants analyzed with an average of 2.33%; Table 4.1). Cell identity was unequivocal as the extra or secondary central cells (see enlarged central cells in Figure 4.6B) always contained polar nuclei, a typical characteristic of grass central cells which does not occur in any other cell type. Up to three secondary central cells were observed originating from the antipodal cell cluster (Figure 4.5C) as indicated by a number of antipodal cells spacing these cells from the primary central cell. Some secondary central cells contained a polar nuclei cluster consisting of up to ten nuclei (Figure 4.5D). In one line (14-3), we observed four ovules (0.8% analyzed ovules) in cobs of two plants showing precocious proliferation of the secondary central cells into endosperm tissue (Figure 4.5E and Figure 4.6; Table 4.1). Despite the altered cell fates, fertilization of mutant ovules was not significantly affected. As shown in Figure 4.5F and Figure 4.6D and E) the egg apparatus (egg cell and synergid cells) as well as the primary central cell was functional: double fertilization occurred and embryo as well as endosperm development was initiated. Secondary central cells remained unfertilized. Although the phenotypes described above were rare (in about 2.33% of the ovules in all three transgenic lines), they are significant according to a *t*-test and have not been observed in any of the 13 analyzed wt cobs (Table 4.1). In addition to the presence of extra central cells, two of the lines showed a higher number of degenerated embryo sacs (line 14-7: 7.9% and line 14-9: 21.9%, respectively) compared with WT ovules (4.9%) at full ovule maturity (late stage FG7). Degenerated embryos sacs were not observed in any of the RNAi lines at earlier stages (FG2 to FG6/early FG7; 50 ovules from three different

RNAi plants for each line were analyzed). These lines also showed a stronger reduction of the transcript encoding the LOB domain protein IG1 (see below) indicating that the RNAi effect might be stronger in these lines. A detailed quantitative analysis of ovules at late stage FG6/early stage FG7 may provide a clue whether mis-organized embryo sacs degenerate and whether the occurrence of multiple central cells was higher in these lines before embryo sac degeneration.

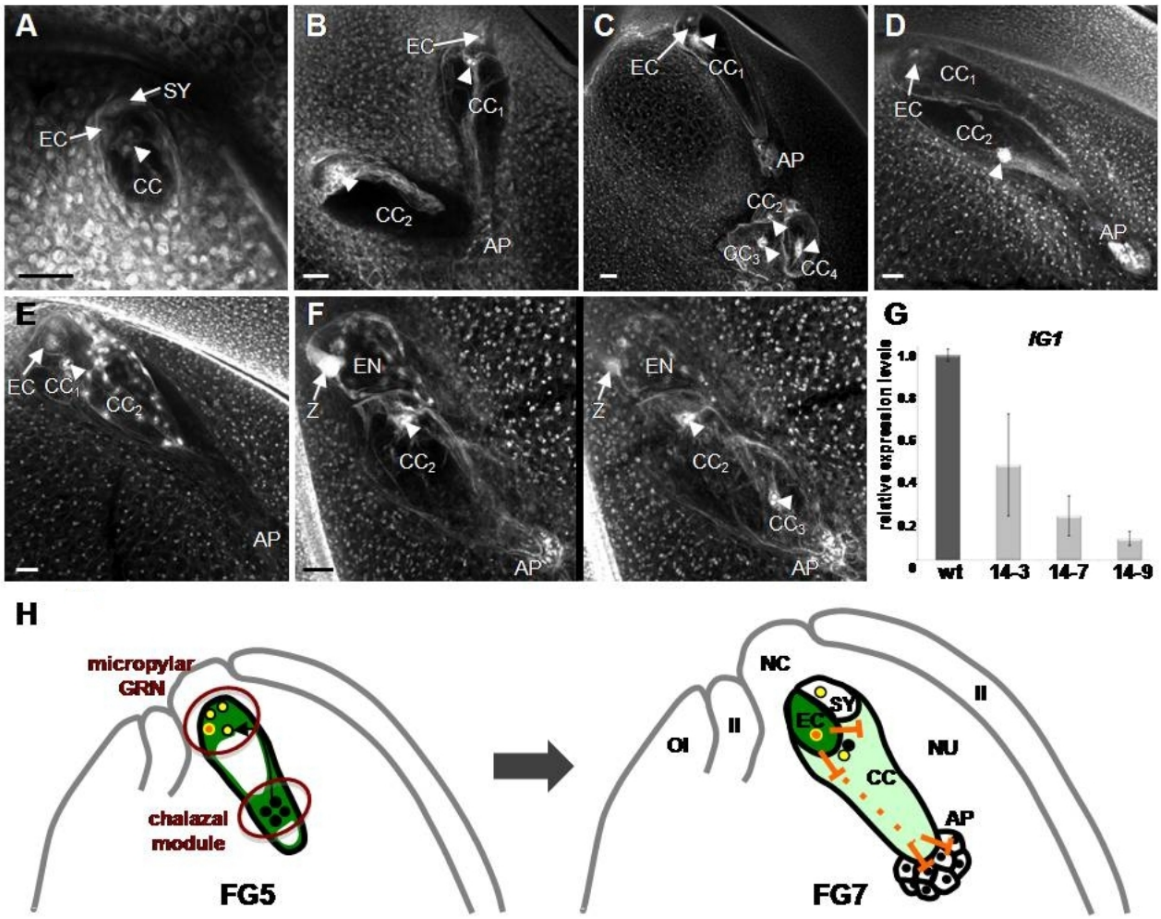

Figure 4.5 RNAi lines of *ZmEAL1* form multiple central cells in the position of antipodal cells and contain reduced *IG1* transcript levels. Manually dissected ovule pieces containing mature embryo sacs were scanned by CLSM. Stacks of four to seven sections are shown in each image. Polar nuclei are indicated in all images by arrowheads. The original or primary central cell is named as CC_1 and additional or secondary central cells as $CC_{2\text{-}4}$. (A) Until stage FG6 embryo sacs of RNAi lines are indistinguishable from wild type ovules. (B) Example showing a secondary central cell at stage FG7 expanding from the area of antipodal cells deep into ovular tissue. (C) Separated by a cluster of antipodal cells from the primary central cell, three secondary central cells have formed each containing central cell-specific polar nuclei. (D) A secondary central cell formed laterally to the primary central cell. Note that in this example the polar nuclei overproliferated consisting of eight nuclei. (E) Example showing endosperm-like proliferation of secondary central cell nuclei. The egg cell and primary central cell are unaffected. (F) Examples showing that the egg

cell and primary central cell can be fertilized. At 48 hap, a zygote and proliferating endosperm containing dozens of nuclei is visible. Two secondary central cells are unaffected. (G) Expression of *IG1* in wild type (wt) and three ZmEAL1-RNAi lines. Ovules from three plants were dissected for each line and *IG1* expression levels determined after normalization with *GAPDH*. (H) Model showing micropylar and chalazal gene regulatory networks (GRN) at both poles of the uncellularized immature embryo sac. At the syncytical eight-nucleate stage (stage FG5) *ZmEAL1* is expressed exclusively at the micropylar pole. After cellularization *ZmEAL1* expression during stages FG6 and FG7 is maintained exclusively in the egg cell, which becomes the major organizer of cell fate in the embryo sac. By lateral inhibition it regulates precocious central cell proliferation and antipodal mis-specification. Abbreviations: AP: antipodal cells, CC: central cell, EC: egg cell, EN: endosperm, hap: hours after pollination, II: inner integument, NC: nucellar cap, NU: nucellus, OI: outer integument, SY: synergid cell, ZY: zygote. Scale bars: 50 µm.

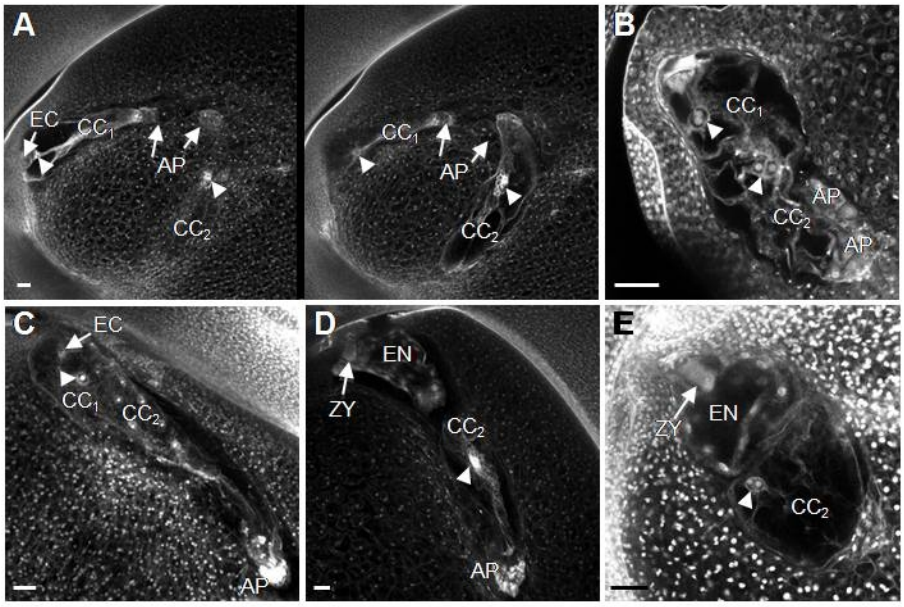

Figure 4.6 Additional examples of secondary central cells forming in the position of antipodal cells in ZmEAL1-RNAi lines. Polar nuclei are indicated in all images by arrowheads. The primary central cell is named as CC_1 and additional or secondary central cells as CC_2. (A) Two focus planes of one ovule showing a secondary central cell deeply embedded in ovular tissue. Note that a couple of antipodal cells space both central cells from each other. (B) Enlargement of two central cells showing polar nuclei in both cells. (C) Example showing precocious proliferation of the secondary central cell. (D and E) Two examples showing that fertilization of the primary central is successful and the secondary central cells remain unaffected. Abbreviations: AP: antipodal cells, CC: central cell, EC: egg cell, EN: endosperm, ZY: zygote. Scale bars: 50 µm.

Table 4.1 eal1-RNAi phenotypes. Mature female gametophytes at stage FG7 of three independent *ZmEAL1*-RNAi lines contain multiple central cells. One line (14-3) showed autonomous proliferation of central cells. Line 14-9 had a higher percentage of degenerated embryo sacs. Note that abnormal phenotypes were not observed at stage FG6 or early stage FG7.

Line	n	normal ES (%)	degenerated ES (%)	multiple CCs (%)	autonomous CC proliferation (%)
14-3	493	464 (94.1)	15 (3.1)	10 (2.0)*	4 (0,8)
14-7	1125	1008 (89.6)*	89 (7.9)	28 (2.5)*	- (0)
14-9	477	362 (75.9)*	103 (21.6)*	12 (2.5)*	- (0)
wt	455	433 (95.1)	22 (4.9)	- (0)	- (0)

n=total number of CLSM scanned embryo sacs per line (represent 100%); CC=central cell; ES=embryo sac; wt=wild type; *=p < 0,05 (*t*-test) when compared with wild type.

4.3.4 ZmEAL1 activity is required for *IG1* expression

To investigate whether egg cell generated ZmEAL1 acts in a non-cell autonomous manner, we analyzed transcript levels of the gene *IG1* that has been reported to be predominately expressed in antipodal cells of mature maize embryo sacs (Evans 2007). Ovules of three T2 plants per line were manually excised to collect ovule material for quantitative gene expression studies. As shown in Figure 4.5G transcript levels in plants of heterozygous line 14-3 were reduced to 46.4% and to 10.5% in homozygous line 14-9 plants compared to wt plants (line A188), respectively. Line 14-7 that contains multiple integrations showed a reduction of *IG1* expression to 21.6%.

4.4 Discussion

The specification and maintenance of cell fates at the eight-nucleate embryo sac stage represents a key event of plant germline development. Accessory cells are formed at both poles, enclosing the two gametic cells (egg and central cell). In Arabidopsis it was reported that patterning of the embryo sac cells depends on an intrinsic auxin gradient, probably established by its localized biosynthesis in the micropylar pole (Pagnussat *et al.* 2009). We have reported here the *ZmEAL1* gene that is expressed in the micropylar pole, but which is not significantly regulated by auxin. Another maize gene *ZmDSUL* exclusively expressed in the micropylar pole (Srilunchang *et al.* 2010) shows a similar auxin-insensitive gene expression pattern (data not shown) indicating that other/additional intrinsic factors than auxin are required to specify cell fates from the micropylar to the chalazal pole in grasses.

Moreover, it was proposed that all cells of the embryo sac possess the potential to differentiate into each other, and a non cell-autonomous lateral inhibition mechanism was proposed that prevents accessory cells from adopting gametic cell fate (Gross-Hardt, Kaegi et al. 2007). Recent genetic studies have further shown that once cell fates have been determined, the egg cell likely functions as the main organizer to maintain cell fate (Voelz, von Lyncker et al. 2012). We have reported here the first egg cell secreted small protein, ZmEAL1 that fulfills these criteria. ZmEAL1 is expressed in a polar manner and controls the fate of accessory cells (antipodal cells) that are separated from the egg cell by the large central cell by more than 150 μm in the maize embryo sac. We show that ZmEAL1 activity may also be required to control precocious proliferation of gametic cells (central cells). Due to the RNAi approach applied to down-regulate gene activity, and the low number of mutant ovules, we probably were not able to elucidate all functions of *ZmEAL1*. A full knockout would be required to investigate whether ZmEAL1 is also involved to control/maintain cell fates of egg and synergid cells. However, the direction of secretory granules indicates that ZmEAL1 activity is likely required to regulate cell behavior at the chalazal pole of the embryo sac. The finding that antipodal cells in maize are capable of adopting central cell fate is analogous to previous reports of the *lis* (*lachesis*), *clo/gfa1* and *ato* mutants (Gross-Hardt *et al.* 2007; Moll *et al.* 2008) in Arabidopsis. LIS, CLO/GFA1 and ATO encode components of the core RNA splicing machinery, and likely process transcripts that are essential for establishment and maintenance of gametic and accessory cell fate. *ZmEAL1* lacks introns, and thus does not appear to be a splicing target. Moreover, *EAL1*-like genes are absent in Arabidopsis and other eudicots genomes indicating that the molecular players required to establish and maintain cell identity are different among grasses and eudicots. Another explanation is that Arabidopsis and other eudicots may not require *EAL1* gene activity, as antipodal cells don't proliferate but instead degenerate. Nevertheless, our findings support the general model that the egg cell becomes the (major) organizer of cell specification and maintenance during the final stage of gametogenesis. It remains unclear how intrinsic location-specific mechanisms establish gametic and accessory cell fate within the uncellularized female gametophyte, and to what extent this is regulated by extrinsic positional information. Post-transcriptional mechanisms seem to play a key role, as *ZmEAL1* gene activity in all four nuclei of the micropylar pole of the female gametophyte at stage FG5 is uncoupled from translation at stage FG6, when protein appears exclusively in the egg cell. The identification of additional ZmEAL1 regulated genes as well as its own regulation may not only help to elucidate additional functions of

the gene, but may also help to explain how micropylar and chalazal gene regulatory networks (GRNs; Figure 4.5H) and egg cell identity is established. Identification of the ZmEAL1 receptor(s) and signaling pathway(s) is now necessary to understand the molecular basis of lateral inhibition of gametic cell identity in accessory cells (here prevention of central cell fate in antipodal cells).

4.5 Summary

Unlike in animals female gametes of flowering plants are not the direct products of meiosis, but develop from a functional megaspore after three rounds of free mitotic divisions. After nuclei migration and positioning the eight-nucleate syncytium differentiates into the embryo sac containing two female gametes as well as accessory cells at the micropylar and chalazal pole, respectively. We report here about the egg cell-specific peptide gene *ZmEAL1* that is activated at the micropylar pole of the eight-nucleate syncytium. Translation of *ZmEAL1* transcript is restricted to the egg cell resulting in the generation of peptide containing vesicles directed towards its chalazal pole. RNAi knock-down studies show that ZmEAL1 is required to regulate the proliferation factor gene *IG1* that is predominately expressed at the chalazal pole of the mature embryo sac in antipodal cells. We further show that ZmEAL1 is required to prevent antipodal cells from adopting central cell fate. These findings support the model that the egg cell orchestrates cell differentiation of embryo sac cells.

Chapter 5 - Characterisation of the signalling peptide ZmEAL1 in embryo development and maize cell suspension culture

5.1 Introduction

Plants are multicellular organisms and therefore require a constant flow of internal and external information in order to guarantee reliable development and proper responses to their environment. To a large extent, this task is taken over by phytohormones like auxins, cytokinins, gibberellins, abscisic acid, jasmonte, brassinosteroids, ethylene (for review see (Neumann *et al.* 2009) or strigolactones (Gomez-Roldan *et al.* 2008; Umehara *et al.* 2008). Additionally secreted peptides play a central role in cellular cross-talk. Compared to classical phytohormones like auxin or cytokinin, which are subject of intensive studies for about a century, the study of signalling peptides in plants is a quite recent research field (for review see (Bahyrycz and Konopinska 2007) and (Wheeler and Irving 2010). The first signalling peptide described in plants is called SYSTEMIN and was isolated from wounded tomato leaves. It has been shown to induce protease inhibitors (Pearce *et al.* 1991). SYSTEMIN has been shown later to be required for herbivore defence in tomato (Ryan and Pearce 2001). In another Solanaceae species tobacco a different signalling peptide named RAPID ALKALINIZATION FACTOR (RALF) was identified (Pearce *et al.* 2001). This peptide was later shown to be involved in root hair development (Wu *et al.* 2007). RALF belongs to the cysteine-rich peptides (CRP) discussed below. Yet, not only Solanaceae use signalling peptides. The *EARLY NODULIN 40* (*ENOD40*) gene was initially thought to be a long non-coding RNA expressed in Fabaceae nodules after infection by symbiotic rhizobia (Crespi *et al.* 1994). The mode of action of a short peptide encoded by the *ENOD40* gene is not completely resolved (Schell *et al.* 1999), but an ENOD40 peptide of 24 amino acids binding to sucrose synthase was detected in nodules (Rohrig *et al.* 2002). A peptide called PHYTOSULFOKINE (PSK) isolated for *Asparagus officinalis* L. (Matsubayashi and Sakagami 1996) is known to stimulate cell proliferation in low density cultures and to affect differentiation of vessel elements (Matsubayashi *et al.* 1999). The active PSK peptide comprises only five amino acids and the tyrosine residues at position one and three are sulfonated (Matsubayashi and Sakagami 1996).

The most extensively studied signalling peptide in plant development is CLAVATA 3 (CLV3, (Clark *et al.* 1995). As part of the WUSCHEL/CLAVATA-signalling pathway it is an essential player in regulation of the shoot apical meristem (SAM) size. Together with the receptor-like serine/threonine kinase CLAVATA 1 and the co-receptor-like protein CLAVATA 2 it represses WUSCHEL and restricts thereby the size of the SAM (for review see (Clark 2001). Peptides similar to CLV3 named GOLVEN have recently been shown to regulate PINFORMED turnover in gravitrophic responses (Whitford *et al.* 2012). Another *Arabidopsis* homologue of CLV3 called CLAVATA 3/EMBRYO SURROUNDING REGION-RELATED 8 (CLE8) has recently been shown to influence embryo and endosperm development. *CLE8* is expressed in early endosperm and embryo until late the globular stage (Figure 1.3) and regulates the development of endosperm and suspensor as well as seed size (Fiume and Fletcher 2012).

Another large class of plant signalling peptides are the already mentioned cysteine-rich peptides (CRPs). In general they are small in size (< 160 amino acids), contain a conserved N-terminus including a signal peptide for secretion and 4 – 16 cysteine residues in the predicted C-terminal mature part of the protein (for review see Marshall *et al.* 2011). This class of small proteins or peptides is shown to be involved in many developmental aspects of plant live. Some are antimicrobial peptides called *DEFENSINS* (Zhu *et al.* 2005). This group of peptides is highly abundant in vegetative tissues. For example more than 300 *DEFENSIN-LIKE* (*DEFL*) are found in *Medicago* (Graham *et al.* 2004) and *Arabidopsis* (Silverstein *et al.* 2007), respectively. Some CRPs are shown to be involved in stomatal development. Recessive mutants of the *EPIDERMAL PATTERNING FACTOR 1* (*epf1*) show aberrant patterning of stomata leading to irregular clustering of stomata instead of regular patterns following a one-cell spacing rule (Hara *et al.* 2007). The CRP STOMAGEN has an antagonistic function to EPF1 and EPF2 (Kondo *et al.* 2010; Sugano *et al.* 2010).

CRPs are even enriched in reproductive tissues and a number of functions have been elucidated recently. The DEFENSIN-LIKE (DEFL) protein gene *ZmES4* is expressed in the synergid cells and is shown to be required for pollen tube burst (Amien, Kliwer et al. 2010). Other synergid cell expressed CRPs are the LURE peptides, responsible for micropylar pollen tube guidance in *Torenia fournieri* and *T. concolor* (Okuda *et al.* 2009; Kanaoka *et al.* 2011). The pollen tube is not only target but also a source of CRPs. The tomato CRP LAT52 is required for pollen germination (Muschietti *et al.* 1994). The *Brassica* gene *SCR* is the determinant of sporophytic self-incompatibility (SSI, Schopfer *et*

al. 1999). CRPs have a role in seed development as well. The endosperm transfer cell specific CRP *MATERNALLY EXPRESSED GENE 1* regulates nutrient flow in the developing seed and is maternally imprinted (Gutierrez-Marcos *et al.* 2004). Recently, an egg cell-specific gene family encoding CRPs *EGG CELL1* (*EC1*) of *Arabidopsis* has been shown to be involved in sperm cell activation (Sprunck *et al. s*ubmitted).

A novel group of signalling peptides different from all above mentioned families is named after EGG APPARATUS 1 (ZmEA1), which is responsible for pollen tube guidance in maize (Márton *et al.* 2005). Recently it had been shown, that EA1 represents the attractant itself in maize (Márton *et al.* 2005). Proteins sharing the EA1-box, an area of homology to ZmEA1 can be found all over the plant kingdom (Gray-Mitsumune and Matton 2006). In maize, two genes with close homology are termed *EA1-LIKE 1* (*EAL1*) and *EA1-LIKE 2* (*EAL2*) (Krohn *et al.* submitted). The first gene has already been partially characterised (Krohn 2010; Denninger 2010; Kolb 2011) and will be explained in more detail below. For the latter EA1-homologe (ZmEAL2) molecular and genetic characterisation is still in progress (S. Übler, M.L. Márton and T. Dresselhaus, unpublished).

The main subject of this chapter, *ZmEAL1*, encodes a peptide precursor of 74 amino acids. It has a predicted signal peptide at the amino-terminus leading to a predicted mature peptide (trEAL1) of 48 amino acids. The transcript was first isolated from egg cell cDNA libraries (Dresselhaus, Lorz et al. 1994). The expression of the *ZmEAL1* is high in egg cells in mature embryo sacs and significantly decreases after double fertilisation. Expression of an EAL1-GFP fusion protein can be detected during embryo development until the transition stage (7 dap). Analysis of *eal1*-RNAi plant lines revealed a function of *ZmEAL1* during embryo sac development (***Chapter 4***; Krohn *et al.* submitted). Nevertheless, many questions regarding EAL1-signalling remain unanswered. An urgent problem is the identification of a receptor protein, probably located in the plasma membrane as it would be predicted for a secreted signal peptide. For this purpose, a yeast-2-hybrid-screen (Y2H) was conducted. A cDNA-library of embryos and endosperm 6 dap was made and screened with trEAL1 as a bait. The yielded clones were sequenced, sorted, tested on autoactivation and verified. Full length clones were generated and analysed for subcellular localisation, Y2H-interaction and Co-immune precipitation with EAL1. After these analysis, a candidate gene encoding a Sec18-homologue (Table 5.6) was selected as the most promising candidate. Further Y2H-experiments to characterise EAL1 and Sec18-homologue interaction and characterisation of the Sec18-homologue were carried out. In addition to searching for a receptor of ZmEAL1 the following questions were addressed in

this work: (i) first it was tried to purify recombinant EAL1 from different sources in order to yield material for downstream applications. Furthermore, (ii) the role of EAL1 in early embryo development was studied using *eal1*-RNAi-lines generated by N. Krohn (Krohn, Lausser et al. submitted). Additionally, (iii) the expression pattern of *EAL1-GFP* in the transition stage embryo was put in relation to marker lines expressing the auxin-efflux carrier *PIN1a-YFP* (Gallavotti *et al.* 2008) and the shoot apical meristem marker *ABPHYL1-mRFP* (Lee *et al.* 2009) under their endogenous promoters. Additionally the synthetic auxin response marker *DR5*-promoter fused to ERmRFP was studied during early seed development (Gallavotti *et al.* 2008). The last question addressed in this work (iv) relates to the identification of downstream targets of EAL1. As a screening method for targets for transcriptional regulation be EAL1, microarrays were made from samples of BMS-suspension cells treated with synthetic EAL1 peptide. One candidate gene coding for a pentatricopeptide repeat protein was verified by qRT-PCR.

5.2 Experimental procedures

5.2.1 *Zea mays* L. material preparation

5.2.1.1 Preparation of genomic DNA from maize

Maize inbred and transgenic lines were grown as described (2.2.1). Genomic DNA was prepared from maize tissue according to the following protocol. Approximately 500 mg tissue were frozen on liquid nitrogen and ground to powder using a mill (MM200, Retsch) and metal balls or mortar and pistil. 1 ml Waite-gDNA-extraction-buffer (1% N-lauryl sarcosine, 100 mM Tris/HCl pH 8.5, 10 mM EDTA, 100 mM NaCl) was added to the powder. The sample was thoroughly mixed and the metal balls were removed if necessary. 1 ml phenol:chloroform:isoamyl alcohol (25:24:1) was added and the sample was mixed for 2 min by intensive shaking. Phases were separated by centrifugation for 1 min at 20,800 rcf and the aqueous phase was transferred to a new tube. The aqueous phase was extracted with 1 ml chloroform as described above and the aqueous phase was again transferred to a fresh tube. Nucleic acids were precipitated by adding 1/10 volume 3 M sodium acetate and 1 volume isopropanol. The reaction was mixed by inverting and incubated for 30 min at 4 °C. Nucleic acids were collected by centrifugation at 20,800 rcf for 10 min at 4 °C. The supernatant was discarded and the pellet was washed with 1 ml

70% ethanol. The pellet was collected by centrifugation as described above and dried. The dried pellet was reconstituted in R40-buffer (10 mM Tris/HCl pH 7, 1 mM EDTA, 2 mg/ml RNAse-A) at 4 °C overnight (Pallotta, Graham et al. 2000). For quantification and quality control, the gDNA solution was analysed on 0.8% agaros gel stained with 0.003% ethidium bromide (Roth) and photometrically analysed using the Nanodrop ND 1000 (Peqlab).

5.2.1.2 Preparation of total RNA from maize material and DNAse treatment

Total RNA from plant material and BMS cells was isolated as described (4.2.8). Preparation and handling of RNA was done under RNAse-free conditions. Glass equipment was backed at 180 °C overnight, aqueous solutions were prepared with RNase-free BioPak water (Millipore) and plastic material was handled with gloves. Total RNA from plant tissue was used for different downstream applications. When used for preparing cDNA for RT-PCR, qRT-PCR or cloning, total RNA was isolated using the reagent Trifast® (Peqlab) as described (4.2.7). Before reverse transcription (RT) total RNA was treated with DNaseI (MBI Fermentas). 1µg was treated according to supplier's protocol and the complete reaction was used for cDNA synthesis. DNaseI-treatment was omitted for RT-PCR with primers on different exons.

For microarray analysis, total RNA was extracted according to the following protocol. Approximately 100 mg frozen BMS cells were ground to powder on liquid nitrogen and homogenised with 1 ml Z6 buffer (8 M Guanidinium-HCl, 20 mM MES, 20 mM EDTA, pH 7.0; 7 µl/ml β-mercaptoethanol was added immediately before usage). 500 µl of phenol:chloroform:isoamyl alcohol (25:24:1) was added, thoroughly mixed and stored on ice. Phases were separated by centrifugation at 20,800 rcf for 10 min. The supernatant was transferred to a new reaction tube and mixed with 1/20 volume 1 N acetic acid and 0.7 volume ethanol. The sample was mixed by inverting and centrifuged at 20,800 rcf for 10 min. The supernatant was discarded and the pellet washed intensively with 500 µl 3 M sodium acetate pH 5.2 and collected by centrifugation at 20,800 rcf for 10 min. Again the supernatant was discarded and the pellet washed intensively with 500 µl 80% ethanol. The pellet was collected by centrifugation at 20,800 rcf for 10 min. Ethanol was removed and the pellet was dried. The pellet was reconstituted in 30 µl water by 10 min incubation at 60 °C and transferred into a new reaction tube.

5.2.1.3 Preparation of proteins from maize

Crude total protein extracts were prepared from different plant tissues as follows Plant material was frozen in liquid nitrogen and ground to powder. 100 mg powder was mixed with 300 µl protein-extraction buffer PBS containing 1% Tween and protease inhibitor cocktail (Sigma). Cell debris were collected by centrifugation (5 min; 10,000 rcf; 4 °C) and 5 µl of the supernatant were each used for western analysis (5.2.11). Microsomal protein fractions were prepared according to the following protocol. Plant material was ground to powder on liquid nitrogen in a mortar with a pistil. Approximately 100 mg of the powder was thoroughly mixed with 300 µl homogenisation-buffer (330 mM sucrose; 100 mM KCl; 1 mM EDTA; 50 mM Tris/0.05% MES pH 7.5, 5 mM DTT; plant protease inhibitor cocktail, Sigma). Cell debris and nuclei were collected by centrifugation at 1,000 rcf for 15 min. The supernatant was transferred to a new tube and the pellet (P1K) was stored at -20 °C until later use. The supernatant was centrifuged at 10,000 rcf for 15 min. The supernatant was transferred to a tube suitable for ultracentrifugation (Beckman) and the pellet (P10K) was treated as described above. The supernatant was centrifuged at 100,000 rcf for 1 h. The supernatant (S100K) was transferred to a new tube and the pellet (P100K) was reconstituted in 100 µl membrane-buffer (330 mM sucrose; 20 mM DTT; 25 mM Tris/0.05% MES pH 8.5). The pellets P1K and P10K were reconstituted in 50 µl 1x SDS-PAGE sample buffer. 50 µl of P100K and S100K were supplemented with 10 µl 6x SDS-PAGE sample buffer and all samples were incubated at 65 °C for 15 min. Afterwards, samples were loaded on 10-15% SDS gels (Tris-Glycine or Tris-Tricine for <10 kDa proteins) for western blotting and Coomassie staining as described (5.2.11), respectively. Protein quantification was done photometrically according to (Bradford 1976).

5.2.2 *Nicotiana benthamiana* transient transgene expression, material preparation and protein purification.

Nicotiana benthamiana was transiently transformed and material handled as described (3.2.2) with the following exceptions. When more than one bacterial strain was used for infiltration, equal volumes of the bacterial suspensions were mixed prior to infiltration. When the 35S-promotor was used to drive transgene expression, leaves were analysed 2 days after infiltration (dai). If TMV-constructs (Lindbo 2007) were used, leaves were analysed 5 dai. For preparative protein extraction for column purification from tobacco leaves the extraction buffer was supplemented with 4 mM DIECA and 5% PVP

(Polyvinylpyrrolidone). Instead of 1% Tween, 0.1% IGEPAL was used. No reducing agent was added. For resolubilisation and batch purification, protein lysates were prepared as described below. The lysate was centrifuged at 100,000 rcf for 1 h in a preparative (L8-70M; Beckman) or an analytic (Optima™ TL; Beckman) ultracentrifuge. 3xFlag-tagged ZmEA1 and ZmEAL1 was purified using ANTI-FLAG® M2 Affinity Gel (Sigma) according to the manufacturer's protocol. Elution was done by pH-shift. Lysates and eluates were analysed as described above.

Resolubilisation of recombinant proteins was performed as follows. Microsomal fractions were prepared as described above. 50 µg total protein were resolubilised by intense mixing in 200 µl resuspension buffer (30 mM Tris pH 7.5, 3 mM $MgCl_2$ 35% glycerol) supplemented with NaCl and detergent of the desired concentration. The sample was centrifuged at 100,000 rcf at 4 °C for 60 min. The supernatant was mixed with 2x sample buffer. The pellet was reconstituted in 2x sample buffer.

Success of the transgene expression, resolubilisation and purification was monitored by Coomassie staining (PAGE-blue; MBI-Fermentas), silver staining (Chevallet *et al.* 2006) and western blot analysis (5.2.11) of samples separated on 16.5% Tris-Tricine gels (Schagger and Vonjagow 1987).

5.2.3 Bacteria culture and protein purification from *E. coli*

Bacteria were handled as described (3.2.3). The *E. coli* and *A. tumefaciens* strains used are listed in Table 5.1. DH5α (Table 3.2) and TOP10 (Invitrogen) were used for molecular cloning. Rossetta™ (Merk) was used for heterologous protein expression. GV3101 (Table 3.2) was transformed with a binary vectors (pJL3:P19; Lindbo 2007) coding for the silencing suppresser p19 from tomato bushy stunt virus (Voinnet *et al.* 2003) and the pJL TRBO-derived expression vectors. All other expression vectors were transformed into the *Agrobacteria* strain C58.

Table 5.1 Bacterial strains.

Species	Strain	Genotype	Supplier
E. coli	Rosetta™	*F^- ompT $hsdS_B(R_B^- m_B^-)$ gal dcm λ(DE3 [lacI lacUV5-T7 gene 1 ind1 sam7 nin5]) pLysSRARE (Cam^R)*	Merk
E. coli	TOP10	*F- mcrA Δ(mrr-hsdRMS-mcrBC) φ80lacZΔM15 ΔlacX74 nupG recA1 araD139 Δ(ara-leu)7697 galE15 galK16 rpsL(Str^R) endA1 $λ^-$*	Invitrogen
A. tumefaciens	C58	No information available	

For heterologous protein expression in *E. coli* 5 ml precultures of Rosetta™ clones harbouring the desired plasmid were grown overnight. 50 ml prewarmed LB-medium was inoculated with 2.5 ml overnight culture and grown until OD_{600} = 0.6. At the desired OD_{600}, 1 ml of the culture was harvested by centrifugation (20,800 rcf; 1 min). Cells (before induction) were resuspended in 50 µl 6x SDS-PAGE sample buffer and stored at –20 °C until later analysis. The rest of the culture was induced with IPTG (1 mM final concentration) and incubated at 37 °C for 4 h for heterologous protein expression. After that the culture was harvested by centrifugation (4,000 rcf; 20 min; 4 °C) and stored at –20 °C until use. 1 ml of the induced culture was harvested separately as described above but resuspended in 100 µl 6x sample buffer. For lysis the cell pellet was thawn on ice and resuspended in 5 ml/g_{cells} freshly made ice cold lysis buffer (140 mM NaCl; 2.7 mM KCl; 10 mM Na_2HPO_4; 1.8 mM KH_2PO_4; pH 7.3; 1 mM DTT; 1 mM EDTA; 1 mg/ml lysozyme, complete protease inhibitor cocktail (Roche Cat. Nr. 11 836 170 001)). The cell suspension was incubated on ice for 30 min. Afterwards the cells were lysed by sonication (6x; 10 sec burst; 10 sec rest on ice). The lysate was cleared by centrifugation (20,800 rcf; 30 min; 4 °C). The supernatant was purifed by GSTrap™ 4B colums (GE Healthcare) using a peristaltic pump according to manufacturer's protocol. Thrombin (GE Healthcare) cleavage was carried out according to supplier's instructions. Expression, purification and digest were analysed by SDS-PAGE and western analysis as described (5.2.11).

5.2.4 Yeast culture, material preparation and yeast-2-hybrid experiments

5.2.4.1 Yeast culture and strains

Saccharomyces cerivisiae was handled sterile as described for bacteria (3.2.3). Yeast strains without plasmid were grown in YPD-medium (10 g/l yeast extract; 20 g/l peptone; 20 g/l glucose) under continuous shaking (200 rpm) or on plates containing 2% agar at 30 °C. The temperature sensitive strain Sey5188 (Emr *et al.* 1983) was grown at 25 °C (permissive temperature). For selection on plasmids, yeast strains were grown on SD-minimal medium (6.7 g/l yeast nitrogen base w/o amino acids; 20 g/l glucose; dropout supplement of desired composition purchased from Clontech) lacking the corresponding amino acid/base to the heterotrophy marker encoded by the given plasmid. SD plates contained 2.2% agar. Strains used in this work are listed in Table 5.2.

Table 5.2 *Saccharomyces cervisiae* strains used in this work.

Strain	Genotype	Reference
AH109	*MATa, trp1-901, leu2-3, 112, ura3-52, his3-200, gal4*Δ, *gal80*Δ, *LYS2::GAL1UAS-GAL1TATA-HIS3, MEL1, GAL2UAS-GAL2TATA-ADE2, URA3::MEL1UAS-MEL1TATA-lacZ*	James *et al.,* 1996;
Y187	*MAT*α, *ura3-52*, *his*3-*200, ade 2-101*, *trp 1-901, leu 2-3*, *112*, *gal4*Δ, *met*–, *gal80*Δ, *URA3::GAL1*UAS-*GAL1*TATA-*lacZ, MEL1*	Harper *et al*., 1993
Sey2101	*MATα, usa3-52, leu2-3, 112, his4-519, surc2Δ-9, gal2*	Emr *et al.* 1983
Sey5188	*MATα, usa3-52, leu2-3, 112, surc2Δ-9, sec18-1 ts*	Emr *et al.* 1983

5.2.4.2 Yeast transformation

Transformation of yeast was performed as follows. One colony of the given strain was inoculated in 50 ml YPD-medium overnight at 30 °C. Cells were reinoculated in 25 ml YPD to OD_{600} = 0.5 and grown until the culture reached OD_{600} = 2. Yeast cells were harvested by centrifugation for 5 min at 5,000 rcf. The pellet was resuspended in 5 ml sterile water and centrifuged as described above. The washed pellet was resuspended in 1 ml 100 mM lithium acetate (LiAc; freshly diluted from a 1 M stock solution) and transferred to a fresh tube. The yeast cells were centrifuged for 15 sec at 20,000 rcf. The supernatant was removed and the pellet resuspended in 400 µl 100 mM LiAc. The culture was split into 50 µl aliquots. For further processing, each aliquot was centrifuged as

described above and the supernatant was removed. For each transformation reagents were added to the yeast cells in the following order:

240 µl 50% PEG
36 µl 1 M LiAc
50 µl carrier DNA (2 mg/ml; boiled for 2 min and chilled on ice prior use)
34 µl plasmid DNA, in aqueous solution (100 ng - 5 µg DNA)

Cells were resuspended by mixing and incubated at 30 °C for 30 min. Subsequently, cells were shifted to 42 °C for 20 min, centrifuged for 1 min at 3,800 rcf and resuspended in 200 µl sterile water. 20 µl of the cell suspension was plated on appropriate SD medium plates and grown for 1-2 d at 30 °C. Temperature sensitive yeast cells were transformed according to the same protocol except that all steps at 30 °C were done at 25 °C. Instead of incubation at 42 °C, cells were shifted to 30 °C. Additionally, 45 µL of DMSO were added prior shifting cells from 25 °C to 30 °C.

5.2.4.3 Plasmid preparation from yeast

Plasmids were prepared from yeast as follows. Yeast cells were grown in 3 ml of appropriate SD-medium overnight at 30 °C until stationary phase. Cells were harvested by centrifugation at 3,800 rcf for 1 min in a 1.5 mL Safelock-reaction tube. The supernatant was removed and 100 mL STET-buffer (8% Saccharose; 50 mM Tris, pH 8; 50 mM EDTA; 5% Triton-X-100) was added. Glass beads corresponding to a volume of 200 µl (diameter 0.5 mm) were added and the cells were broken up in a mill (Ribolyser). Another 100 µl of STET-buffer was added, mixed and the reaction was incubated for 3 min at 95 °C. The reaction was chilled on ice and centrifuged for 10 min at 20,000 rcf. For separation of proteins, 100 µl supernatant was mixed with 50 µl of 7.5 M ammonium acetate and incubated for 1 h at –20 °C. The precipitate was separated by centrifugation for 10 min at 20,000 rcf at 4 °C. 100 µl of the supernatant was mixed with 100 µl ethanol to precipitate DNA. The reaction was centrifuged for 10 min at 20,000 rcf at 4 °C. The supernatant was discarded and the pellet was washed with 70% ethanol. The pellet was harvested by centrifugation as described above and dried. The pellet was reconstituted in 20 µl sterile water. 5 µl were used to transform *E. coli* as described (3.2.3)

5.2.4.4 Preparation of genomic DNA from yeast

Preparation of genomic DNA form yeast was done according to (Hoffman and Winston 1987). Yeast cells were grown in 5 ml YPD medium overnight until they reached the stationary phase. The culture was harvested by centrifugation at 4,000 rcf for 5 min. The supernatant was discarded and the pellet was resuspended in 500 µl sterile water and transferred to a 1.5 ml reaction tube. The cells were centrifuged again for 5 sec at maximum speed and the supernatant discarded. The pellet was resuspended in the residual water and 200 µl DNA-cracking-buffer (2% Trition-X-100; 1% SDS; 100 mM NaCl; 10 mM Tris/HCl; pH 8; 1 mM EDTA) was added. Thereafter, 200 µl of phenol:chloroform:isoamylalcohole (25:24:1) and 0.3 g glass beads (diameter 0.5mm) were added and the reaction was mixed thoroughly for 3-4 min at ambient temperature. 200 µl of TE-buffer were added and the reaction was centrifuged for 5 min at 20,000 rcf. 200 µl of the supernatant were mixed with 1 ml ethanol in a fresh reaction tube by inverting. Precipitate nucleic acids were pelleted by centrifugation for 2 min at 20,800 rcf. The supernatant was discarded and the wet pellet was resuspended in 400 µl TE-butter containing 100 µg/ml RNaseA and incubated for 5 min at 65 °C. The DNA was precipitated by adding 1 ml ethanol and 10 µl of 4 M ammonium acetate. The reaction was mixed by inverting and the precipitated DNA collected by centrifugation at 20,800 rcf for 2 min. The supernatant was discarded and the pellet was dried. The dried pellet was reconstituted in 50 µl TE-Buffer and stored at 4 °C for later use.

5.2.4.5 Yeast-2-hybrid experiments

All strains and plasmids used in the Y2H-experiments were purchased from Clontech. Individual clones from a yeast-2-hybrid screen (Denninger 2010) and corresponding full-length clones (Kolb 2011), this work) have been transformed into the yeast strains Y187 and AH109 as described above. The strain Y187 was used as host for the bait-plasmid derived from the pGBKT7-backbone. On the other hand, AH109 was used to carry the prey-plasmids derived from the pGADT7-backbone. Both strains were mated by overnight incubation of a single colony of bait- and prey-strain at 30 °C under continuous shaking in 500 µL YPD-medium. On the next day 50 µl of the mating culture was plated on SD/-Leu/-Trp (Double drop out = DDO) and grown for 2 d at 30 °C. For testing the constructs for Y2H interaction a single colony of each mating plus positive and negative control were

suspended in sterile water and diluted 3 times 1:10. 10 µl of each dilution was spotted on a DDO plate and one plate SD/-Leu/-Trp/-His/-Ade (Quadruple drop out = QDO) and grown for 2 d at 30 °C. The DDO-plate serves as control for viability of the yeast cells and was used for the X-Gal-assay in tests with full-length clones. Growth on QDO-medium indicates activation of the *HIS2* and *ADE2* reporter system for protein-protein interaction and was used for the X-Gal-assay with the original fragments from the screen. For the X-Gal-assay, yeast spots on plates were covered with X-Gal-buffer in 0.5% agar. The X-Gal-agar was prepared by boiling a 1%-agar-solution in a test glass. After the agar was dissolved, it was mixed with the X-Gal-buffer (5 ml 1 M sodium-phosphate buffer, pH 7; 600 µl dimethylformamid (DMFA); 100 µl 10% SDS; 100 µl X-Gal (20 mg/ml in DMFA, freshly dissolved) 1:1 and poured slowly over the agar-plate with the yeast on it. For one plate a total volume of 10 ml is required. After the X-Gal-agar became solid, the plate was incubated for 1 d at 30 °C. If the blue staining was faint, the plate was re-examined after two weeks at 4 °C.

5.4.2.6 Complementation of *sec18*^{ts} growth phenotype by Y2H-candidate *#33*

For the yeast complementation test of candidate #33 the temperature sensitive strain Sey5188 (Emr *et al.* 1983) was used. The corresponding wild type strain was Sey2101 (Emr *et al.* 1983). The yeast wild type version of *SEC18* and the maize homologue #33 were expressed under the control of the *pPMA1*-promoter from the 2µ-plasmid pDR196 (Rentsch *et al.* 1995). After transformation (see above) in both strains, colonies of each transformed strain and the original strain were spotted on two YPD- and two SD/-Ura plates as described for the Y2H experiment. One YPD and one SD plate was incubated at 25 °C (permissive temperature), the other ones at 30 °C (restrictive temperature). Complementation of the *sec18*^{ts}-phenotype was monitored after 2 days incubation.

5.2.5 BMS cell culture and transient expression of fluorescence protein fusions

BMS (black Mexican sweet) suspension cells were grown as suspension culture as described (4.2.8). For further experiments, cells were used 2d after re-inoculation. Aliquots were treated with trEAL1 (synthetically produced by Centic). Cells treated with trEAL1 peptide were grown as 3 ml aliquots in 20 ml flask for sampling. In growth tests, the packed cell volume was determined by pipetting 10 ml of freshly shacked culture into a

sterile 10 ml measure cylinder. Cells were allowed to settle for 15 min by gravity and the volume of the cells was determined. Cells for RNA extraction and subsequent microarray analysis were collected with a 1 ml pipette with a cut tip into a 2 ml micro centrifuge cup. The cells were briefly centrifuged and the medium was removed with a 1 ml pipette. All cell samples were frozen on liquid nitrogen immediately after harvesting. Transient protein expression in BMS suspension cells was carried out according as described (4.2.8).

5.2.6 Acriflavine staining and microscopy

For microscopy of fresh material from fluorescent marker lines, maize ovules and developing kernel were cut longitudinally with a razor blade and mounted immediately in tap water and examined at an inverted fluorescence microscope or a CLSM (fluorescent marker lines see Table 5.4).

Table 5.4 Stable transgenic maize plant lines used in this study. All transgenic lines used are hybrids of the inbred lines A188, H99 and B73, respectively.

Line	Transgene	Selectionmarker	Reference
eal1-RNAi	*Ubi::RNAi-EAL1*	Glufosinate	(Krohn, Lausser et al. submitted)
EAL1-GFP	*EAL1::EAL1-GFP*	Glufosinate	(Krohn, Lausser et al. submitted)
DR5	*DR5::mRFP*	Glufosinate	(Gallavotti, Barazesh et al. 2008)
PIN1a	*PIN1a::PIN1a-YFP*	Glufosinate	(Gallavotti, Barazesh et al. 2008)
ABPHYL1	*ABPHYL1::ABPHYL1-mRFP*	Glufosinate	(Lee, Yu et al. 2009)

Analysis of *eal1*-RNAi-plants in early embryogenesis was carried out using cobs 7 dap as described (2.2.3). Fluorescent fusion proteins (FP) were analysed at an inverted fluorescence microscope (Nikon Eclipse TE1500) or at the obove mentioned CLSM, respectively. At the fluorescence microscope filter cubs with band-pass emission filters for GFP, YFP and RFP were used. Settings at the CLSM are given in Table 5.5.

Table 5.5 Setting for FP-detection at the CLSM

FP	Excitation	Emission filter
eGFP	488 nm	BP 505 - 550 nm
YFP	514 nm	BP 530 - 600 nm
mRFP	543 nm	BP 560 - 615 nm

5.2.7 Molecular cloning

Primers used for molecular cloning were designed as described (3.2.4). Vector maps can be found in ***Supplementary Information***. For the expression vector pJL-TRBO complete sequence information was not available (J. Lindbo, personal communication). Primer sequences are listed in Supplement Table 1.3. Maize sequences were taken from www.maizesequence.org and yeast sequences from www.yeastgenome.org.

5.2.7.1 Transient expression of affinity tagged EA1 and EAL1 proteins in tobacco

For transient overexpression of N- and C-terminal fusion proteins in *N. benthamiana* a TMV-vector system (Lindbo 2007) was used. The N-terminal fusion consisted of a 10xHis-tag with a TEV-site between the His-tag and the polylinker. Truncated versions of *EAL1* (*trEAL1*, (Krohn, Lausser et al. submitted) and *EA1* (*trEA1*, (Márton *et al.* in press)) were cloned in frame into a modified pET28 vector (L. Lehle, personal communication) using restriction sites for *Fse*I and *Asc*I (both purchased from NEB). *trEAL1* was amplified from the vector pLNU-EC222-GFP (4.2.7, (Krohn, Lausser et al. submitted) with the primer pair P23/P24. The sequence of *trEA1* was amplified from the vector pPicB-ZmEA1 (Márton, unpublished). PCR fragments were digested, ligated and transformed into DH5α. Clones were analysed by sequencing and served as template for the following cloning step. The N-terminal fusion *10xHis-TEV-trEAL1* and *10xHis-TEV-trEA1* were amplified form the corresponding pET28-vector and cloned into the pJL-TRBO ((Lindbo 2007) overexpression vector using *Pac*I and *Not*I (both purchased from NEB). The coding sequence of *10xHis-TEV-trEAL1* was amplified using the primer pair P34/P36. The sequence of *10xHis-TEV-trEA1* was amplified using the primer pair P35/P36. PCR fragments were digested and ligated as described above and transformed into DH5α. Clones were analysed by sequencing and transformed into GV3101 as described. The *Agrobacteria* clones were later on used for transient overexpression in *N. benthamiana*.

The C-terminal fusion consisted of a 3xFlag-tag. The coding sequences of *EAL1* and *EA1* were cloned in frame into a modified pcDNA3-vector (M. Schwab, personal communication) using the restriction enzyme *Bam*HI (MBI-Fermentas). The coding sequence of EAL1 was amplified form vector pLNU-EC222-GFP (4.2.5, Krohn *et al.* submitted) using the primer pair P19/P20. The sequence of EA1 was amplified form the vector pPicB-ZmEA1 using the primer pair P17/P18. Both fragments were digested and ligated as described above. Clones were analysed by sequencing and served as template for subsequent cloning steps carried out as follows: *EAL1-3xFlag* was amplified form the corresponding pcDNA3 clone using the primer pair P41/P42. *EA1-3Flag* was amplified from the corresponding pcDNA3 clone using the primer pair P41/P42. Both PCR fragments were digested and ligated into pJL-TRBO as described above for the N-terminal fusion. Clones were analysed and used as described above.

5.2.7.2 Heterologous expression in *E. coli*

For heterologous expression of the EAL1 peptide in *E. coli* the Gateway®-destination vectors pET53-GW and pGEX-GW have been used. pET53-GW harbours a *6xHis*-Tag in 5'- and *Strep*-Tag in 3'-direction of the Gateway®-cassette under control of a T7-promoter. pGEX-GW contains a *GST*-coding sequence followed by a *Thrombin* site 5' of the Gateway®-cassette. The gene of interest is driven by the *tac* promoter. As entry clones, pENTR/D/TOPO-trEAL1±BamHI for pET53-GW and pENTR/D/TOPO-BamHI for pGEX-GW were used. Entry and destination vectors were recombined via LR-clonase (Invitrogen) reaction according to supplier's protocol. This combinations lead to three expression clones coding for the translational fusion protein 6xHis-trEAL1, 6xHis-trEAL1-Strep and GST-trEAL1. The reactions were transformed into DH5α as described and analysed by sequencing. Correct clones were transformed into Rosetta-strain for protein expression as described above.

5.2.7.3 Yeast expression vectors

The coding sequence of *trEAL1* was subcloned into bait vector pGBKT7 and prey vector pGADT7 (both Clontech) by conventional cloning. For subcloning of *trEAL1* in pGBKT7, the sequence was amplified from the vector pET28-trEAL1 using the primer pair P84/P85. The fragment was subcloned into pGBKT7 using restriction sites for *Nde*I and *Eco*RI (both NEB). For cloning into pGADT7, *trEAL1* was amplified form pET28-trEAL1 using the primer pair P109/P110. The PCR fragment was subcloned with the help of *Bam*HI and *Eco*RI sites (both NEB). The coding sequence of the Y2H candidate #33 was amplified from cDNA made from embryos/endosperm 6 dap (inbred line A188) using the primer pair P101/P102 and cloned into pGBKT7 using restriction sites for *Bam*HI (NEB/MBI-Fermentas) and *Eco*RI (NEB)/*Mun*I (MBI-Fermentas). All clones were transformed into DH5α as described and analysed by DNA sequencing. The pGBKT7 clones were later on transformed into Y187 as described above. pGADT7 clones were transformed into AH109. The complete coding sequence of *EAL1* was amplified from pcDNA3-EAL1-3Flag using the primer pair P71/P72. The coding sequence without signal peptide (*trEAL*1) was amplified from the vector pET28-trEAL1 using the primer pair P70/P71. Both fragments were purified and used in a TOPO reaction (Invitrogen) creating entry clones for LR-reactions with and without *Bam*HI sites at the 3'end leading to constructs with (*Bam*HI site not present) and without (*Bam*HI site present) stop codon. The reactions were carried out according to manufacturer's protocol, transformed into TOP10 as described and analysed by DNA sequencing. The wild type allele of *ScSEC18* was amplified from gDNA isolated from the yeast strain SEY2101 using the primer pair P183/P215, purified and used in a TOPO reaction (pENTR/D-TOPO; Invitrogen). A correct clone of pENTR/D-TOPO-SEC18 and pENTR/D-TOPO-fl#33 including a *Bam*HI-site (Kolb 2011) were used in an LR-reaction (Invitrogen) together with pDR196 in order to create clones for overexpression in bakers yeast.

5.2.8 PCR-based transcript level analysis

For PCR based transcript level analysis, two different strategies (RT-PCR and qRT-PCR) were applied. For each of them total RNA was isolated form plant material using Tri-Fast (Peqlab) as described (4.2.7). Primer information is given in Supplement Table 1.3. Standard first strand synthesis was performd using Moloney Murine Leukemia Virus Reverse Transcriptase lacking RNaseH-activity (RevertAid-H; MBI-Fermentas) according to the manufacturer's protocol. DNaseI sample treatment was performed as described above or 2-3 µg of total RNA served as a template. Oligo-dT-primer (MBI-Fermentas) served as primer. The resulting cDNA was used in a RT-PCR as template (1 µl/reaction). 1 µl of cDNA was prepared as described above and used in a standard PCR (3.2.4). For the housekeeping gene *GAPDH* the primer pair GAPnew1 and GAPnew2 (4.2.9, Krohn et al. submitted) was used (expected product: cDNA 140 bp; gDNA 243 bp). Expression of *#33* was determined using the primer pair P166/P173 (expected product: cDNA 164 bp; gDNA 449 bp).

For exhaustive measurement of steady-state mRNA levels of single genes in specific tissues, qRT-PCR was applied. The reactions were carried out using Quanti-Tec SYBR-Green Kit (Qiagen) or KAPA™ SYBR® Fast Universal qPCR-mix (Peqlab) in a Realplex2 Thermocycler (Eppendorf). Each primer pair was chosen from their performance in gradient PCRs in standard PCR reactions and under qRT-PCR equipment. qRT-PCR reactions were pipetted as triplets of three biological replicates. All calculations were done using EXCEL software (Microsoft).

For expression analysis of *ECA39* (GRMZM2G061723) the primer pair P200/P201 was used (expected product: 192bp fragment). Transcript levels of a *LOB-domain containing protein* (GRMZM2G060544) were determined with help of the primer pair P204/P205 (expected product: 160 bp). Finally, the steady state mRNA levels of the *Pentatricopeptide repeat protein* (GRMZM2G468521) were assayed using the primer pair P210/P211 (expected product: 107 bp).

5.2.9 Microarray analysis

For microarray analysis total RNA was prepared as described (5.2.1.2). Samples were analyzed using a Bioanalyser (Agilent) and further processed and analysed according to the One-Color Microarray-Based Gene Expression Analysis (Quick Amp Labeling) with Tecan HS Pro Hybridization protocol given by the manufacturer (Aglient). RNA analysis, labeling and hybridisation as well as procession of the raw data was done by Dr. Urte Schlüter (University of Erlangen). GO-term analysis was done using the online-tool Agri-GO (bioinfo.cau.edu.cn/agriGO/). Processed data were handled using EXCEL (Microsoft).

5.2.10 *In vitro* transcription/translation and Co-immune precipitation (CoIP)

In vitro transcription and translation was used to obtain S^{35}-labeled trEAL1 peptide and #33 protein with amino-terminal Myc- or HA-tags, respectively. For protein production the TNT® T7 coupled wheat germ system (Promega) was used along with ^{35}S-methionin (translational grade, Hartmann) according to manufacturer's guidelines. The Y2H vectors pGBKT7-trEAL1, pGBKT7-#fl33 (both this work), pGBKT7-Lam, pGBKT7, pGADT7-T (Clontech) and pGADT7-fl#33 (Kolb 2011) served as template for the reaction. Since both vector backbones contain a T7-terminator, linearisation was not required. In each reaction a final concentration of 0.8 µCi/µl was used. The products of the reaction were used for co-immune precipitation (CoIP). CoIP experiments were carried out using magnetic Protein-G-Beads (Dynabeads Protein-G, Invitrogen). Coupling of monoclonal antibodies against c-Myc- or HA-epitops was carried out according to the supplier's protocol. 1µg of antibody were used per 25 µl of Protein-G-beads. After coupling of the antibodies, beads were equilibrated with IP-buffer (50 mM Tris; pH 7.5; 150 mM NaCl; 10 mM ATP from MBI-Fermentas; 10 mM $MgCl_2$) by washing 3 times with 100 µl. After the last washing step, beads were reconstituted with *in vitro*-transcription/translation reactions of bait- and prey-constructs which were applied in 1:1 or 1:4 ratios and filled up to a final volume of 200 µl with IP-buffer. The IP-reactions were either directly incubated at 4 °C for 16 h or incubated at room temperature for 2 h and subsequently at 4 °C for 14 h. The following day, each IP was washed 3 times with 100 µl IP-buffer and transferred to a fresh tube after the last washing step. Bound proteins were eluted from the beads by boiling them at 95 °C for 10 min in 2x Tris/Tricine-Sample-buffer. Beads were separated and the complete reaction was loaded onto a 16.5% Tris/Tricine-SDS-gel (Schagger and Vonjagow 1987)

together with 2.5 µl of each transcription/translation-reaction. IPs without antibody and the empty bait vector as template for transcription/translation were used as negative controls. After separation, the gel was treated with a fluorometric agent (Amplify, GE-Healthcare) according to the manufacturer's protocol. Fluorescence was detected on an X-ray film by incubation at –80 °C.

5.2.11 Western blot analysis

Prior to western blot analysis proteins were separated on a SDS-PAGE using Tris/Glycine (Laemmli 1970)or Tris/Tricine buffer (Schagger and Vonjagow 1987)), respectively. Separated proteins were blotted on a nitrocellulose membrane at 360 mA for 30 min. The blot was blocked 3 times for 20 min with 5% blocking solution (5% milk powder, 50 mM Tris pH 7.5, 150 mM NaCl) and subsequently incubated with primary and secondary antibodies (for working concentrations see Supplement Table 1.2). The antibody-stocks were diluted with 1% blocking solution (1% milk powder, 50 mM Tris pH 7.5, 150 NaCl) and the membrane incubated for 1 h at room temperature or overnight at 4 °C. Before the secondary antibody was applied, the blot was washed for 10 min with 1% blocking solution. Before the ECL-reagent was applied the blot was washed 5 times with water. The standard ECL-Substrate (ECL Western blotting substrate, Pierce) was used according to the manufacturer's protocol. When weak signals were expected an enhanced ECL system was used (SuperSignal® West Femto Maximum Sensitivity Substrate, Thermo Scientific) according to supplier's instructions. Signals were detected on an X-ray film (Super RX, Fujifilm). The apparent molecular weight (AMW) of bands was estimated by blotting the AMW as a function of migration length. An exponential function was fitted based on the molecular weight and the migration length of the mass ruler. This function allowed estimation of the AMW of unknown samples. Calculations were done using EXCEL (Microsoft).

5.3 Results

5.3.1 Heterologous expression of recombinant ZmEA1 and ZmEAL1

In order to gain recombinant protein for further studies, it was aimed to express the full-length peptide of ZmEA1 (Márton, Cordts et al. 2005) and ZmEAL1 (Krohn, Lausser et al. submitted) as well as the predicted mature peptides trEA1 (Márton, Cordts et al. 2005) and trEAL1 (Krohn, Lausser et al. submitted)in heterologous systems.

5.3.1.1 Expression of ZmEA1 and ZmEAL1 in *Nicotiana benthamiana*

For overexpression of affinity tagged versions of ZmEA1 and ZmEAL1 in *N. benthamiana* a vector system pJL TRBO based on the tobacco mosaic virus (TMV) (Lindbo 2007) was applied. The vector contains a TMV genome driven by a 35S (Guilley, Dudley et al. 1982)promoter. The coding sequence of the viral coat protein (CP) which is the target for transcriptional silencing (Lindbo 2007) was replaced by a multiple cloning site. This allows expression of a gene of interest under the control of the subgenomic CP promoter, which is strongly active but activated in the late phase of virus development (Lindbo 2007). As a consequence transient TMV-driven expression in tobacco takes longer (5 days) compared to 35S promoter-driven expression (2 days). The absence of the CP leads to the situation that the TMV construct is able to infect adjacent cells but cannot move systemically through the plant (Lindbo 2007). Functionality of the system was tested using a control vector harbouring eGFP (pJL TRBO-G; Lindbo 2007). 5 dai GFP expression could be verified by illumination of infiltrated tobacco leafs with UV light at 345 nm (Figure 5.1A and B). The high expression level of eGFP is evident and almost no fluorescence is detectable upon infiltration with an empty vector control. Additionally, indication that the virus-construct moves from cell to cell can be found. Carboxy-terminal fusions of EA1 and EAL1 with 3Flag-tag (Sigma) were expressed in this system. Transgene expression was verified by western blot analysis (Figure 5.1 C). The plant cell lysates were prepared without detergent and separated by centrifugation (10,000 rcf; 10 min) into pellet and supernatant. All samples showed signals only in the pellet fraction. Since such a pellet is supposed to contain cells, cell debris and large organelles like nuclei or plastids, this is indicating insolubility of the fusion protein. As protein bands of appropriate size for the large subunit of RubisCO can be found in the Coomassie-stained

gel, resembling a replica of the blotted gel (data not shown), inefficient lysis can be ruled out as explanation for the missing bands in the supernatant. The major fraction of both fusion proteins appear to form insoluble aggregates, sedimenting at the given centrifugation conditions. The EA1-contruct shows altered expression levels depending on the presence or absence of the silencing suppresser p19. The apparent molecular weight (AMW) should allow discriminating between the pre-protein-forms and the predicted mature fusion proteins. The expected molecular weight for the trEA1-3Flag construct is 10.2 kDa and the molecular weight of EA1-3Flag is 12.3 kDa. The expected molecular weight for trEAL1-3Flag is 7.9 kDa and the one of EAL1-3Flag 10.3 kDa. The AMWs calculated from the western blot signals are bigger than the predicted mature forms. The error is estimated form the thickness of the band on the blot, which is approximately 1 mm for the thicker bands. EA1-3Flag (Figure 5.1C lanes 1 - 4) samples show an AMW of 13.3 (± 0.5) kDa. In the EA1 sample in the presence of p19 (Figure 5.1C lanes 3 and 4), an additional band at 11.4 (± 0.4) kDa was detected. In the EAL1-3Flag samples (Figure 5.1C lanes 5 - 8) only a single band of approximately the same intensity in presence and absence of p19 was detected. The AMW in absence of p19 was 12.3 (± 0.5) kDa (Figure 5.1C lanes 5 and 6). In the presence of P19 (Figure 5.1C lanes 7 and 8) a signal at 14.3 (± 0.5) kDa was detected, but the higher weight is most likely due to an aberrant running behaviour due to its position at the edge of the gel. The smaller band in this sample might represent a mature fusion-protein according to its size. Constructs coding for amino-terminal 6His-tag fusions of the predicted mature forms of EA1 and EAL1 were infiltrated into tobacco as well. Transgene expression was not detected by western blot analysis (data not shown). Therefore these constructs were not used for protein expression in further experiments.

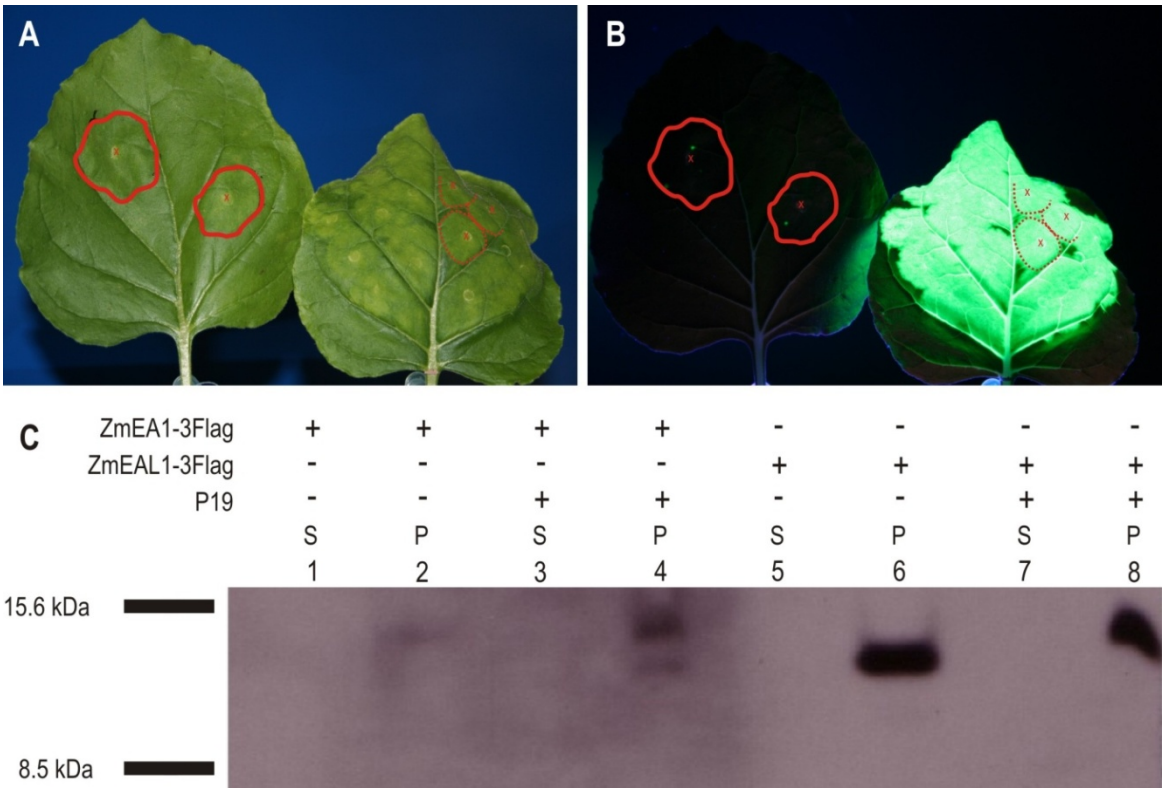

Figure 5.1 Heterologous expression of GFP, EA1- and EAL1-fusion proteins in *N. benthamiana*. (A) Leaves of *Nicotiana benthamiana* 5 dai with empty vector construct (pJL TRBO; Lindbo 2007) on the left or control vector (pJL TRBO-G(Lindbo 2007)) on the right, respectively. The empty vector construct was infiltrated in two distinct areas (red solid line). The marks of the syringe are visible (red cross). The positive control was infiltrated in approximately 2/3 of the leaf area. Three infiltration sites are marked by red crosses. The extent of spreading of the bacterial suspension in the leaf tissue is visible by a lighter green colour. The boundaries of this spreading of these three exemplary infiltration sites are highlighted by punctuated red lines). (B) After illumination with UV light (354 nm) of the same leaf as in (A) the right leaf shows an intense green fluorescence indicating high levels of eGFP. (C) Western blot analysis of crude protein lysates from tobacco leaves infiltrated with constructs for expression of C-terminal 3Flag-tag fusion proteins of ZmEA1 and ZmEAL1 detection with anti-3flag antibody. The samples were separated into pellet (P) and a supernatant (C). EA1-3Flag fusions show different signal intensities in presence or absence of p19 mainly at the predicted size of the pre-protein fusion. An additional band closer to the size of the predicted mature fusion protein band is detectable in the sample including p19. In the EAL1-samples, only one band at the predicted size of the pre-protein fusion is found. Abbreviations: P = pellet, S = supernatant.

As preliminary work for further purification steps it was investigated if microsomal fractions, containing residual soluble 3Flag-fusion proteins of both constructs can be prepared and under which conditions these proteins can be resolubilised. The downstream purification procedure via M2-Anti-3Flag affinity resins (Sigma) limited the possible

concentrations of detergent and salt. It also restricts the resolubilization conditions in terms of pH and absence of reducing agents. For ZmEA1-3Flag, resolubilization was tested in presence of 150 mM NaCl and 1% n-Octylglycosid (Figure 5.2 lane 1 and 2), 0.2% Digitonin (Figure 5.2 lane 3 and 4), 0.1% IGEPAL CA-630 (Figure 5.2 lane 5 and 6) and 5% Trition-X-100 (Figure 5.2 lane 7 and 8). In addition resolubilization in presence of 1 M NaCl (Figure 5.2 lane 9 and 10) without detergent was tested. Resolubilization was achieved with Octylglycosid, IGEPAL and Triton. No or little resolubilization was achieved using Digitonin and 1 M NaCl. High NaCl appears to influence protein stability negatively. Resolubilization of ZmEAL1-3Flag was tested using 0.1% Octylglycosid (Figure 5.2 lane 11 and 12), 5% Triton-X-100 (Figure 5.2 lane 13 and 14), 0.1% IGEPAL CA-630 (Figure 5.2 lane 15 and 16) in presence of 150 mM NaCl and in presence of 1 M NaCl without detergent (Figure 5.2 lane 17 and 18). Resolubilization was achieved using Triton and IGEPAL. Resolubilization was not found in samples treated with Octylglycosid and high salt. Resolubilization was not complete for EAL1 compared to EA1. Yet, the overall expression level of EA1 was much lower compared to EAL1. At exposure times that yielded sufficient signal intensities with EAL1 samples, almost signals were not detectable with EA1 samples (data not shown). For EA1 samples, X-ray film exposure had to be prolonged to 30 min compared to 5 min for EAL1 samples. Even after longer exposure signals were not found in the empty vector control (Figure 5.2 lane 19 and 20).

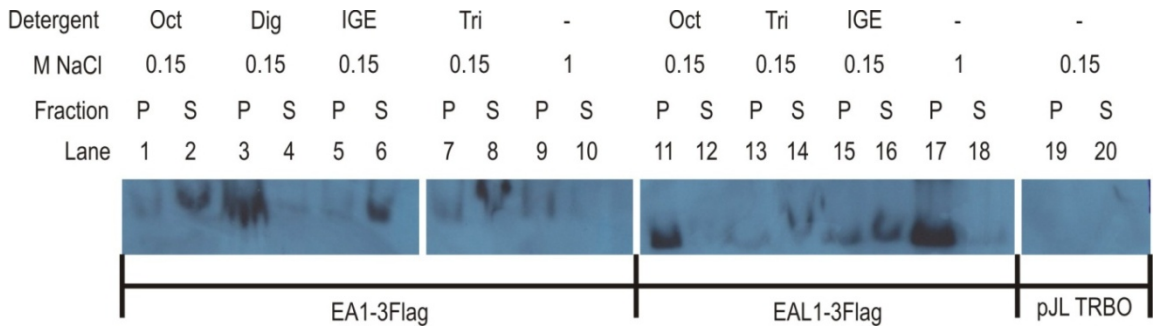

Figure 5.2 Western blot for analysis of resolubilization of ZmEA1-3Flag and ZmEAL1-3Flag with different detergents and salt concentrations. The lanes 1 – 10 show tests for resolubilization after preparation of microsomal fractions from *N. benthamiana* leaves expressing the EA1-3Flag fusion protein. 50 µg of total protein per sample were resolubilized with given concentrations of NaCl and detergent. Octylglycosid, IGEPAL-CA-630 and Trition-X-100 showed good resolubilization results. Digitonin and high salt did not yield in high rates of resolubilization. Lanes 11 – 18: resolubilization of EAL1-3Flag as described above. Triton-X-100 and IGEPAL-CA-630 led to partial resolubilization, Octylglycosid and high salt did not resolubilize EAL1-3Flag. Lanes 19-20: Empty vector control pJL TRBO; no signals were found. Abbreviations: Dig = 0.1% Digitonin, IGE = 0.1% IGEPAL-CA-630, Oct = 0.1% Octylglycosid, P = pellet, S = supernatant, Tri = 5% Trition-X-100

Form the tested conditions, 0.1% IGEPAL CA-630 and 150 mM NaCl were chosen for attempting small scale batch purification using antibody coupled resins (Sigma). After purification, proteins were separated on a gel and blotted. The amount of protein blotted represents the yield of approximately 1 g leaf material (Figure 5.3). In the empty vector control, no signals were detectable. Signals of EA1-3Flag were barely detectable; no further attempts were made to purify EA1-3Flag from tobacco. EAL1-3Flag was eluted from the affinity resins and an up scaled column purification was tried.

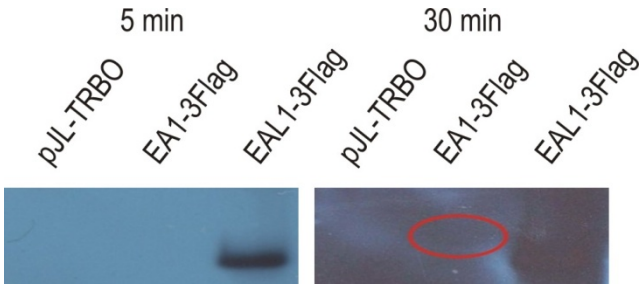

Figure 5.3 Western blot showing small-scale batch-purification of ZmEA1-3Flag and ZmEAL1-3Flag. Both pictures show the same membrane exposed for different time periods. From the EAL1-3Flag lysate, recombinant protein was isolated. EA1-Flag (encircled) was isolated only in

lower amounts compared to EAL1-Flag. In the empty vector control (pJL TRBO) no signals were found at the range of recombinant proteins. Each what contains a protein amount originating from approximately 1 g leaf material.

It was found, that EAL1-3Flag binds specifically to the affinity resins and can be eluted with low pH (Figure 5.4A). Yet, the western analysis was not suitable to estimate the yield of the purification since Flag-tagged protein of known concentration was not available. Therefore, the column purification was further up-scaled and analysed by Tris-Tricine-PAGE and subsequent silver staining. A band of the appropriate size was detectable in sample representing 1.5% of the total protein containing eluate (Figure 5.4B). 60 g of leaf material were used for the purification. Given a detection limit for silver staining of 10 ng/band and under the theoretical assumption of 100% purification yield, the maximum EAL1-3Flag content of the raw leaf material is ~ 10 ng/g. This is five orders of magnitude lower than the content of GFP achievable by this system (Lindbo 2007). 1 mg EAL1-3Flag would require under most favourable circumstances 100 kg tobacco leafs. Therefore this purification method is of no use on laboratory scale to provide material for downstream applications. For further attempts to purify recombinant EAL1, *E. coli* was applie

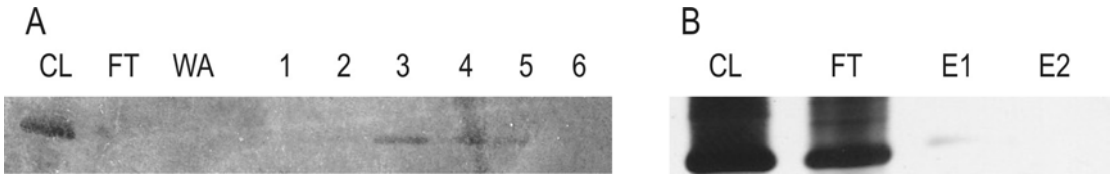

Figure 5.4 Column-purification of ZmEAL1-3Flag. (A) Western blot analysis of a column purified EAL1-3Flag. The recombinant protein was bound to the resins effectively as a signal did not appear in the flow through fraction (FT). The fusion protein was eluted by low pH and found in the eluate fractions 2 – 5. (B) Silver stained gel after affinity purification of lysates containing EAL1-3Flag. Lysates were prepared from 60 g fresh leaf material. The first eluate fraction (E1) was collected after 10 min incubation with elution buffer. Three additional bands of higher molecular weight appear in E1 (part of gel not shown). Abbreviations: CL = crude lysate, FT = flow through, WA = wash fraction, E1-6 = eluat fraction 1-6

5.3.1.2 Expression of ZmEAL1 in *E. coli*

trEAL1 was cloned into two different bacterial expression vectors. The pET53-derivate allows constructing amino-terminal 6His-Tag alone or together with carboxy-terminal Strep-Tag by Gateway® cloning. For trEAL1, a *E. coli* clone carrying a pET53-derivative could not be found that showed an inducible band of appropriate size (data not shown).

An N-terminal, thrombin-cleavable glutathione-S-transferase-tag fused to the protein trEAL1 (expected size 32.9 kDa) was successfully expressed in *E. coli* (Figure 5.5A) from a modified pGEX-vector (L. Colombo, personal communication) and partially purified by GSTrap™ 4B columns (GE Healthcare). Coomassie staining of a SDS-PAGE containing purified fractions (Figure 5.5B) revealed the presence of the GST protein correlating with the induced band after induction and the bands in eluat fractions. Notably, the induced band in the bacterial sample (34 kDa) is of higher molecular weight than the major bands in the other lanes (30 kDa).

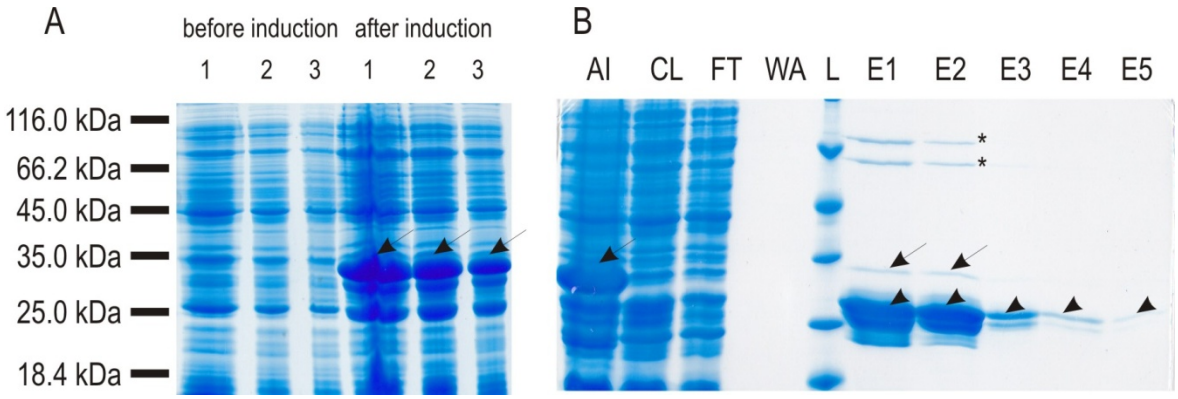

Figure 5.5 Coomassie stained gel of induced and partially purified GST-trEAL1 from *E. coli*. (A) Samples prepared from three independent *E. coli* clones (1-3) before and 4 h after induction. All clones show an induced band of appropriate size (arrow). (B) Partial purification of GST-trEAL1. The major part of the induced protein appears to be insoluble since the induced band is not present in the crude lysate. Towards the end of the washing procedure protein was no longer detected. In the eluate fractions most prominent bands (arrowheads) are found at a size lower than the induced band. At the size of the induced protein only a faint band (arrow) is visible. Additionally, two bands are found at a size around 66 kDa in eluat fractions 1 and 2 (asterisk). AI = after induction, CL = crude lysat, E1-5 = elate fractions 1-5, FT = flow through, L = ladder, WA = wash fraction. For molecular weight marker see (A).

Further analysis of the eluate fractions by thrombin digest (Figure 5.6) revealed that the complete fusion protein was present only in minor parts of the total eluted protein. A faint band (36.3 kDa; ± 1.4 kDa) above the major band (30.4 kDa; +1.1, - 1.2 kDa) before digest represented probably the full-length fusion protein. After digest a single prominent band band (28.0 kDa; ± 1.1 kDa) close to the size of free GST (~26 kDa) was found, which was already present before digest. A band at 38.7 kDa (± 1.5 kDa) originated most likely form thrombin (expected size 36 kDa). A faint band at 6.5 kDa (+0.2, -0.3 kDa) probably represented the cut fragment of the major purification product. Both samples showed a smear below the GST-bands most likely originating from protein degradation. The two bands at high molecular weight appeared to be co-purified proteins unrelated to GST-trEAL1 since they didn't show altered molecular weights upon thrombin-digestion.

Taken together the data of the GST purification suggest that GST-trEAL1 is mainly insoluble. The trEAL1 fusion gets lost during preparation of crude lysate. It has not been determined if the full-length fusion protein can be found in "inclusion bodies". Since soluble protein would be required for bioassays, no further efforts were made to generate recombinant EAL1. A peptide with the amino acid sequence of trEAL1 was therefore chemically synthesised and purchased from the company Centic.

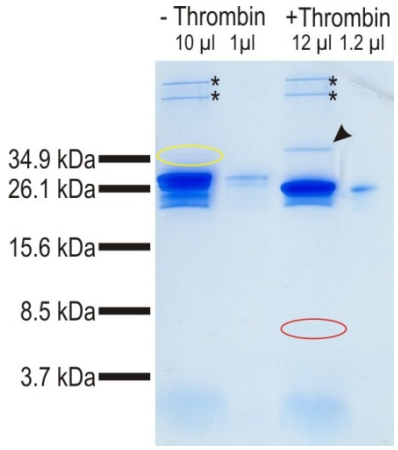

Figure 5.6 Coomassie stained gel of thrombin digest of partially purified GST-trEAL1. Eluates (Figure 5.5) were digested with thrombin in order estimate if full-length fusion protein was purified. The major bands in the gel are below the size of the fusion protein (33 kDa). A faint band (encircled in yellow) of appropriate size is visible before the digest. After digest the major band was of approximately the size of free GST. This band is already present before digest. After digestion, a band (arrowhead) of approximately the size of thrombin (36 kDa) appears. An additional very faint band (encircled in red) appears at low molecular weight. This band likely represents the cut mature EAL1 peptide. Two bands at high molecular weight (asterisk) show no size shifts and are most likely unrelated co-purified proteins.

5.3.2 Identification of interaction partners of trEAL1

In order to identify a receptor of EAL1 a yeast-2-hybrid screen was conducted. Since the current model of the mode of action of EAL1 implies that the interaction occurs in the extracellular space, a library was constructed using random hexamer primer allowing screening also of extracellular domains of prey proteins. Parts of the Y2H-experiments and experiments with interactor candidates were carried out by P. Denninger and M. Kolb in the course of their bachelor-theses (Denninger, 2010; Kolb, 2011) under my supervision. Contribution of the different authors to the entire experiment is briefly outlined in the following: the Y2H-screen for possible interaction partners of trEAL1 against a cDNA-library of maize embryos and endosperm 6 dap was conducted by P. Denninger (Denninger 2010); this work). 127 clones representing 24 different genes were identified and grouped into four categories (Table 5.6(Denninger 2010). Category 3 (protein modifying proteins) and category 4 (unknown function) proteins were tested for autoactivation and Y2H-interactions were verified (this work). Subsequently, subcellular localisation and full-length Y2H-interaction studies of candidates (Figure 5.7; Kolb 2011; this work) was conducted and further bioinformatic analysis performed. Finally detailed interaction studies were performed with candidate #33 (this work).

Table 5.6 Y2H-candidates isolated from screening of a cDNA-library of embryo/endosperm 6 dap with trEAL1 as a bait construct. 127 clones were analysed by sequencing representing 24 different genes Number in brackets indicates number of clones found in the screen. Candidates were grouped into 4 categories. Category 1 encloses "junk"-candidates like rRNA clones or frame-shift candidates. Category 2 represents known housekeeping genes. In category 3, genes coding for protein modifying proteins are summarised. Category 4 finally encloses all genes with unknown function (Denninger 2010).

Category	Gene	Σ Clones	Clone #
1	**18S rRNA**	3 [3]	
1	**COBRA-LIKE PROTEIN 4** (GRMZM2G071970)	4 [1]	
1	**INOSINE-MONOPHOSPHATE DEHYDROGENASE** (GRMZM2G100084)	2 [1]	
1	**LIPID-TRANSFER PROTEIN** (GRMZM2G071575)	1 [1]	
2	**40S RIBOSOMAL PROTEIN (S10)** (GRMZM2G067303)	7 [3]	
2	**ACTIN** (GRMZM2G067985)	1 [1]	
2	**CHAPERON t-COMPLEX PROTEIN** (GRMZM2G009871)	1 [1]	
2	**CLATHRIN HEAVY CHAIN** (GRMZM2G057576)	1 [1]	
2	**DNA/RNA HELICASE** (GRMZM2G027995)	1 [1]	
2	**ENOLASE 1** (GRMZM2G064302)	55 [12]	#3
2	**ENOLASE 2** (GRMZM2G048371)	2 [1]	
2	**ISOLEUCINE-tRNA SYNTHETASE-LIKE** (GRMZM2G348666)	2 [1]	
2	**LYSYL-tRNA SYNTHETASE** (GRMZM2G146589)	1 [1]	
2	**RNA-POLYMERASE II (ß-subunit)** (GRMZM2G023780)	1 [1]	
3	**PEPTIDYL-PROLYLI-ISOMAERASE FKBP12 (**GRMZM2G015784)	4 [1]	#5
3	**PROTEIN-DISULFIDE-ISOMERASE (PDIL1-1)** (GRMZM2G091481)	13 [3]	#75
3	**PROTEIN-PHOSPHATASE TYPE 2C (catalytic region)** (GRMZM2G015610)	1 [1]	#11
4	**Protein with AAA-ATPase/P-Loop domain** (GRMZM2G022777)	2 [1]	#54
4	**Protein with AAA-ATPase/P-Loop domain** (GRMZM2G398755)	1 [1]	#33
4	**Protein with armadillo-like helix fold** (GRMZM2G018926)	3 [1]	#44
4	**Protein with carboxypeptidase-like regulatory domain** (GRMZM2G014788)	3 [1]	#71
4	**Protein with DUF59 motive** (GRMZM2G170727)	5 [1]	#22
4	**Protein with predicted transmembrane domain** (GRMZM2G115750)	1 [1]	#109
4	**Protein with WD-40-repeat motive** (GRMZM2G096802)	2 [1]	#60

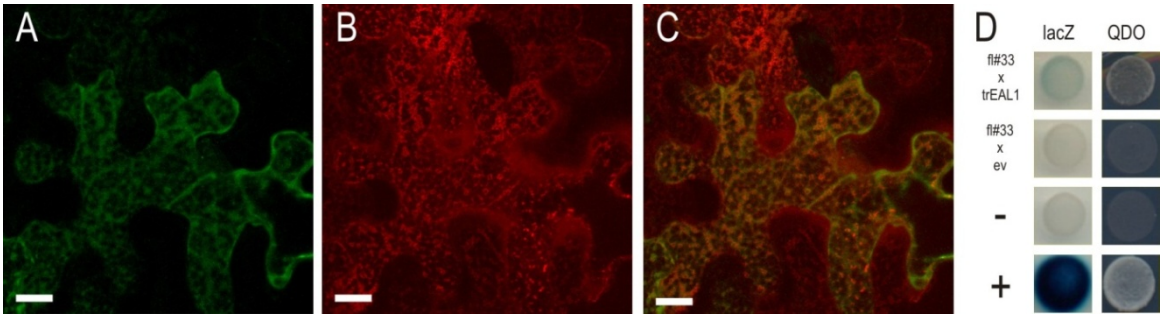

Figure 5.7 Subcellular localisation of GFP-fl#33 and its Y2H-interation with trEAL1. (A – C) Subcellular localisation of fl#33 tranlationally fused with GFP at its N-terminus (A) was co-expressed with ERmRFP (B). Both constructs show a partial overlap (C). The ER-marker showed a more distinct signal compared to more diffuse GFP-fl#33 signal. (D) The full-length construct of #33 showed Y2H-interaction with trEAL1 (Kolb 2011). Scale bar = 10 µm

5.3.2.1 Y2H-experiments on fragments and full length clones of interactor candidates

From all identified fragments of possible EAL1interactors only the ones that had been classified in group 3 (protein modifying protein) and group 4 (unknown function) were studied in more detail. Group 1 (nonsense clones) and 2 (housekeeping genes) were not further investigated. All candidates originally identified (Denninger 2010) are listed in Table 5.6. Prey plasmids were retransformed into AH109 and were mated with a yeast clone containing the empty bait vector pGBKT7 (Clontech). Diploids were plated on DDO and QDO and tested for lacZ-activity. The clones #44, #54, and #60 did not grow on QDO. #33 showed slow growth on QDO but lack of lacZ-activity unlike the other slow growing candidates #11, #71, #75 and #109 (Figure 5.8). Therefore, #33 was further analysed as well as #44, #54 and #60. Enolase (#3) was tested since it was the most abundant clone in the screen (Denninger 2010) but turned out be autoactivating.

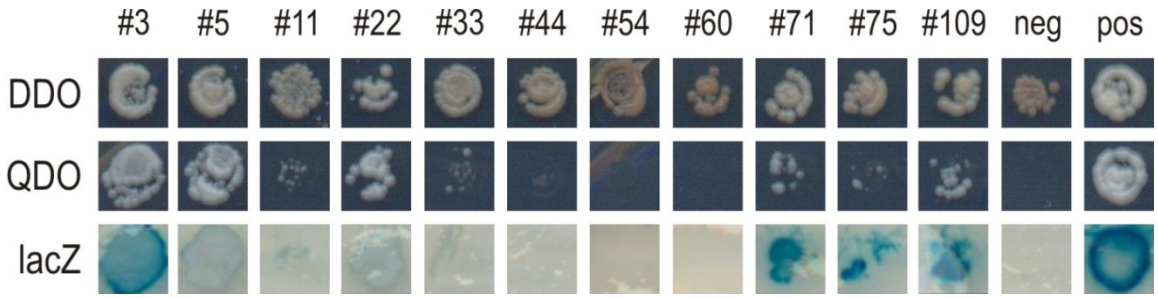

Figure 5.8 Test for autoactivation fragments of Group 3 and 4 candidates with empty bait vector. Fragments, isolated from a cDNA-libary of embryos and endosperm 6 dap (Denninger 2010) were tested for interaction with the empty bait vector pGBKT7 (Clontech) as retransformands in a Y2H-experiment. Diploid yeast cells were replica plated on DDO ($SD_{-Leu-Trp}$) and QDO ($SD_{-Leu-Trp-His-Ade}$). QDO-plates and subsequently used for tests on lacZ-activity. The fragment of the housekeeping gene *Enolase1* (#3) was included to the experiment since it was the most abundant clone in the screen. Fragments of an armadillo-like helix protein (#44), an AAA-ATPase (#54) and a WD40-repeat-protein (#60) showed no activation of the auxotrophy-marker genes and were therefore further tested. Another AAA-ATPase (#33) was also included in further studies despite weak growth on QDO because of absent lacZ-activity. The identities of all tested candidates are listed in Table 5.6.

Retransformed clones of #33, #44, #54 and #60 were mated with an independent clone of original prey vector, plated on DDO and QDO and tested for lacZ-activity (Figure 5.9). All four candidates showed reproducible Y2H-interaction with trEAL1. The differential lacZ-activity of #33 in the control and the retesting Y2H-experiment justified further analysis. The fragments of these genes originate from AAA-ATPases (#33 and #54) and a WD40-

repeat protein (#60). #44 (armadillo-repeat-protein) was not further analysed since cloning of the full-length sequence was not successful.

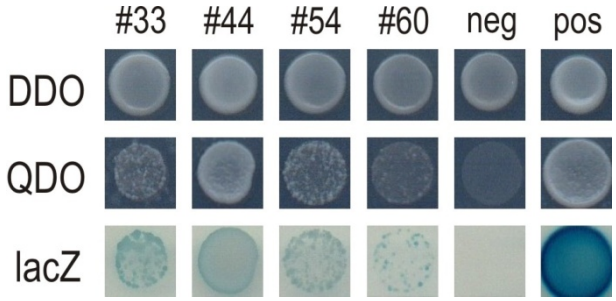

Figure 5.9 Y2H-experiment of retransformed verified fragment clones with trEAL1. The four fragments which were found to show no autoactivation were retested for interaction with trEAL1 in a Y2H-experiment. Diploid yeast cells were spotted on DDO and QDO-plates for growth assay. The QDO-plate was used for determination of lacZ-activity. All clones showed growth on QDO and lacZ-activity.

For verification of Y2H-interaction of full-length #33 (fl#33) with trEAL1 (Kolb 2011), Figure 5.7), *trEAL1* was used as prey and *fl#33* as bait construct (Figure 5.10). Diploid yeast cells were grown on DDO and QDO medium. Cells grown on DDO plates were used for test on lacZ-activity. trEAL1 did not show autoactivation in the test with the empty bait-vector. The constellation of constructs made it easy to the test trEAL1 for homodimerisation, yet with negative result. Also the full-length bait clone fl#33 did not show Y2H-interation with trEAL1 as a prey.

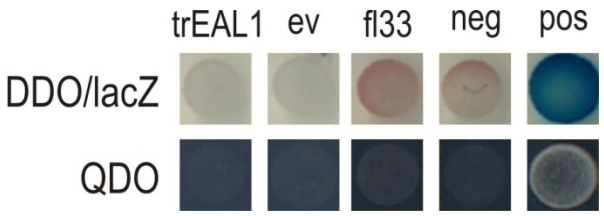

Figure 5.10 Y2H-experiment of trEAL1 and fl-#33 as bait with trEAL1 as prey. The prey construct didn't show autoactivation of the marker genes. Neither did the trEAL1 show homodimerisation, nor could the found Y2H-interaction be confirmed when bait and prey were switched.

5.3.2.2 Co-immune precipitation (CoIP) of trEAL1 and full-length interactor candidates

After fl#60 was ruled out as *bona-fide* interactor candidate by Kolb (2011) due to nuclear localisation of N- and C-terminal eGFP-fusion proteins, interaction between the ER-localised AAA-ATPases (Kolb 2011) and trEAL1 was tested by CoIP. Recombinant fusion-proteins of N-terminal epitope-tags (HA for pGADT7, c-Myc for pGBKT7) and the full-length reading frames of interactor candidates as well as the predicted mature form of EAL1 (trEAL1) were made by *in vitro* transcription/translation. *In vitro* translated proteins were radiolabelled using ^{35}S-methionine. CoIP of HA-fl#54 with c-myc-trEAL1 was never successful (Figure 5.11A). HA-fl#33 precipitated cMyc-trEAL1 in an ATP-dependent manner (Figure 5.11B), yet HA- fl#33 precipitated with cMyc-trEAL1 as well as with c-myc fused to a small nonsense peptide encoded by the multiple cloning site of the empty vector pGBKT7 (Figure 5.11C). Therefore, CoIP-experiments did not confirm the Y2H-data.

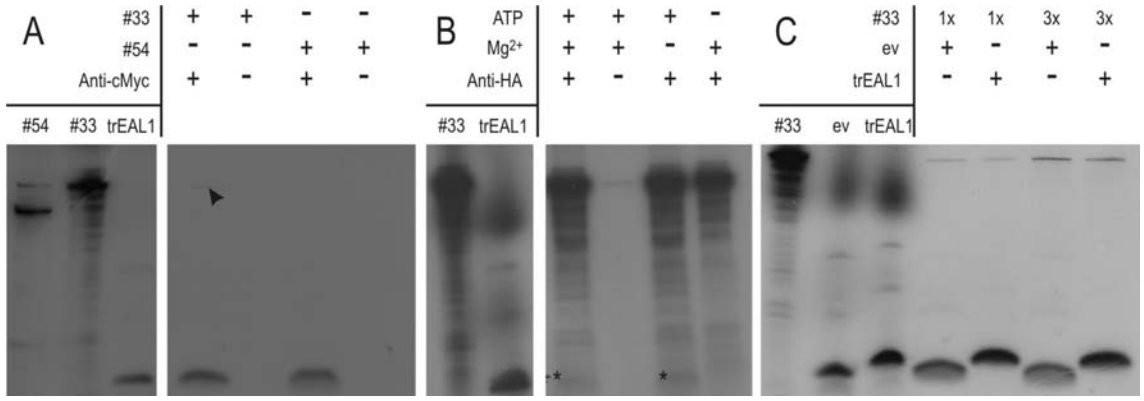

Figure 5.11 Co-immune precipitations of the interactor candidates fl#33 and fl#54 with trEAL1. (A) Co-IP of the AAA-ATPases HA-fl#33 and HA-fl#54 with cMyc-trEAL1. All samples were made by *in vitro* transcription/translation in the presence of radioactive ^{35}S-methione. 2.5 µl of each reaction was loaded as control and for orientation concerning the molecular weight of educts. fl#33-sample shows many bands of smaller size which are most likely degradation products. In the absence of an antibody against the c-myc-epitope radioactive proteins were not detected. fl#33 shows a faint band of appropriate size after Co-IP with trEAL1 (arrowhead) whereas for fl#54 a band is not visible (B) Co-IP of trEAL1 with HA-fl#33 in dependence of Mg^{2+} (10 mM $MgCl_2$) and ATP (10 mM). Signals of an appropriate size for trEAL1 (asterisk) can be found in samples containing ATP and anti-HA antibody. In the absence of antibody a faint signal at the size of fl#33 can be found indicating unspecific binding or insufficient washing. Adding Mg^{2+} appears to have no influence. (C) A translation product of the empty vector pGBKT7 (ev) was made and used to the Co-IP reaction Co-IP of #33. Co-IP can be observed together with both trEAL1 and empty vector. When three-fold volume of fl#33-reaction was put into Co-IP more fl#33-protein was found after Co-IP at similar intensities for Co-IP with trEAL1 and empty vector. Therefore, Y2H-interaction between #33 and trEAL1 was not confirmed.

5.3.2.3 Characterisation of interactor candidate #33

Since the protein-protein interaction between fl#33 and trEAL1 could not be confirmed with an independent method, the biochemical nature of #33 was characterised in order to test the plausibility of the observed Y2H-interaction (Kolb 2011), this work). For further experiments, only the complete coding sequence of #33 (fl#33) was used. In order to confirm the subcellular localization (Figure 5.7, (Kolb 2011)previously observed in the heterologous system *N. benthamiana*, the same constructs were biolistically transformed into BMS suspension cells (Figure 5.12A-C). Surprisingly, GFP-fl#33 (Figure 5.12A and C) did not show co-localization with an ER-marker (Nelson *et al.* 2007), which was co-transformed (Figure 5.12B and C). In order to confirm co-localization of fl#33 and EAL1 directly, RFP-fl#33 was expressed in tobacco (Figure 5.12D). In contrast to GFP-fl#33 (Figure 5.7A and C), RFP-fl#33 showed a cytosolic localisation similar to a *bona fide* cytosolic recombinant protein (J. Schönberger, U. Hammes and T. Dresselhaus, personal communication; Figure 5.12E) and unlike the ER-marker (Figure 5.7B). Exclusion of RFP-fl#33 from the nucleus can be explained by the size exclusion limit of the nuclear pore. Taken together, the ER-localisation of GFP-fl#33 could not be verified with independent constructs or in other expression systems than *N. benthamiana*.

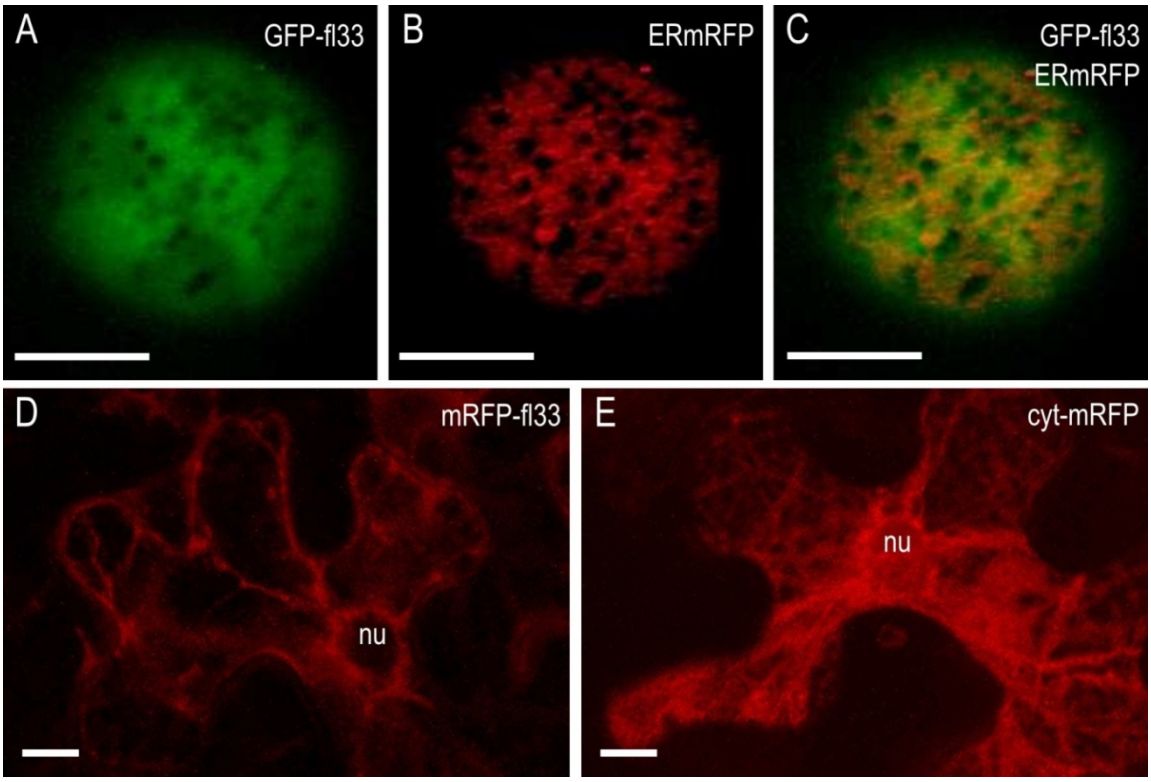

Figure 5.12 Transient expression of GFP-#fl33 in BMS cells and of RFP-fl#33 in tobacco. (A-C) Transient expression of GFP-fl33 and an ER-marker (Nelson et al 2007) in BMS suspension cells. The pictures give a view on a segment of the cell boundary. (A) Whereas GFP-fl#33 appears to be localized to the cytosol, the ER-marker (B) shows a network-like distribution. The merge image is given in C. (D) Transient expression of RFP-fl33 in tobacco leaves didn't resemble the ER-like localisation of GFP-fl#33 (Figure 5.7). Compared to the GFP-fusion protein, localization of the RFP-fl#33 fusion is weaker and more diffuse. The construct is excluded from the nucleus. (E) Cytosolic mRFP. Abbreviation: nu = nucleus, scale bars = 10 µm.

In order to identify characterised homologues of #33, BLAST searches were performed to identify homologous sequences across all organisms at the NCBI-database (blast.ncbi.nlm.nih.gov/Blast.cgi) and at the yeast genomic database SGD (www.yeastgenome.org). 66 homologous sequences across all kingdoms of eukaryotes were identified. Additionally, three sequences from the *Saccharomyces cerevisiae* genome were included in the dataset. *ScSEC18* (*YBR080C*) was found to be the closest yeast homologue. *ScCDC48* (*YDL126C*) is the closest paralogue of *SEC18* in yeast. The more distantly related AAA-ATPase gene *ScVPS4* (*YPR173C*) was chosen as an outgroup to generate the phylogram shown in Figure 5.13. Alignment of the amino acid sequence and tree calculation according to Maximum Likelihood algorithm using DNA-sequences was done using SeaView-software (Gouy et al. 2010. The resulting dendrogram (Figure 5.13) resembles the phylogenetic relationship of eukaryotes as it is widely accepted today. A

second maize gene (LOC100982066 = GRMZM2G58327) was identified as a paralogue. All homologous sequences group together with *SEC18* in a monophyletic group with *CDC48* and *VPS4* as an outgroup. Therefore #33 can be considered as maize homologues of *ScSEC18* based on its protein sequence. The biochemical activity corresponding to Sec18 was experimentally also shown for N-ethylmaleide sensitive factor-(NSF) of *Homo sapiens* (Wilson *et al.* 1992). For many other species homologues found by BLAST search are annotated as “NSF”, “NSF-like”, “vesicle fusion ATPase”, “vesicle fusion ATPase-like” or “Sec18” describing the same estimated activity. Some of the sequences are termed as hypothetical or predicted protein. In this case, they seem to be a SEC18/NSF-homologue for the given organism.

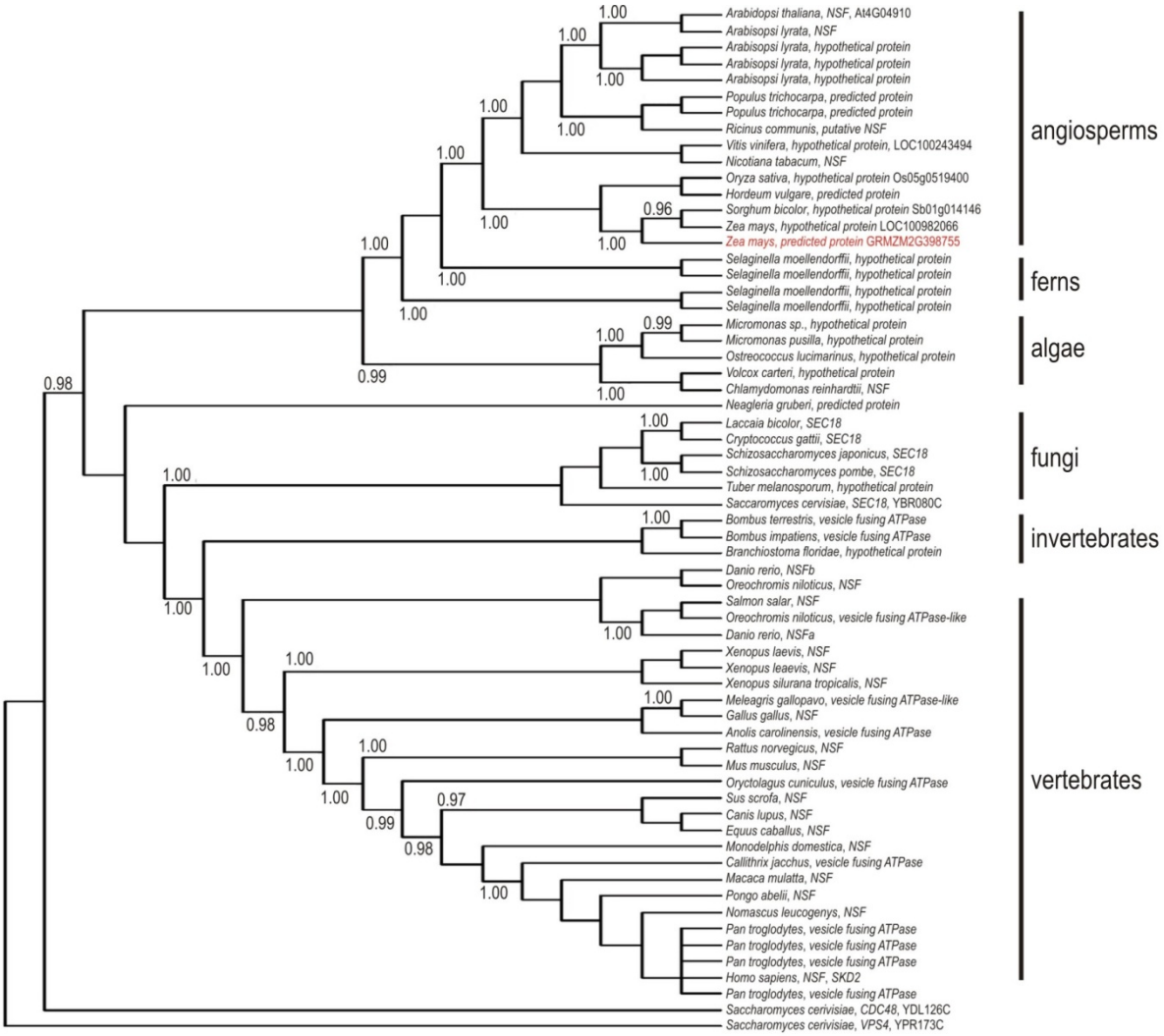

Figure 5.13 Maximum Likelihood dendrogram based on sequences homologous to #33. All branches with p-values >0.95 have their value at the base. #33 is highlighted in red. All well supported branches resemble the tree of live as it is widely accepted today. Homologues of #33 have been characterised as *NSF*-homologues, *vesicle fusing ATPase*-homologs or *SEC18*-homologues referring to the same biochemical activity.

The biochemical role of Sec18/NSF, which is the formation and ATP-dependent disassembly of 20S "fusion particles" with SNAP receptor proteins (Wilson, Whiteheart et al. 1992), is difficult to address. Nevertheless, some predicted properties of a *bona fide SEC18/NSF*-homologue like ATP-dependence (Wilson, Whiteheart et al. 1992) and formation of homo-multimers (Peters *et al.* 1990) can be tested more easily. ATP-dependent binding of peptides by #33 was already mentioned (Figure 5.11B). Formation of homo-multimers was tested here in a Y2H-experiment. fl#33 in both the bait and the prey vector showed robust growth on QDO-medium and lacZ-activity (Figure 5.14) indicating dimerization. This result would be expected from a *SEC18/NSF*-homologue.

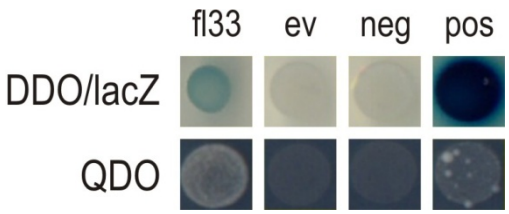

Figure 5.14 Test for dimerisation of #33 in a Y2H-experiment. Diploid yeast cells were spotted on DDO- and QDO-medium. DDO-plates were used subsequently for a lacZ-activity assay. The AAA-ATPase #33 was tested for homodimersiation and for autoactivation as bait-construct. Yeast cells show robust growth on QDO-medium and are positive for lacZ-activity.

Complementation of a yeast mutant offers an easy way for proving that the maize gene candidate #33 can take over the function of yeast *SEC18*. The yeast strain Sey5188 (Emr, Schekman et al. 1983) carries the temperature sensitive allele *sec18-1*. The strain was transformed with a shuttle vector for protein overexpression of *fl#33* and *SEC18* (cloned from the corresponding wild type strain Sey2101, (Emr, Schekman et al. 1983). Sey5188 transformed with the empty vector served as negative control. Transformed mutant as well as untransformed mutant and wild type strains were spotted on rich and selection medium and grown at permissive and restrictive temperature for 2 days (Figure 5.15). All strains showed robust growth on rich medium at permissive temperature. The same was true for all transformed strains at permissive temperature in selective media. Under these conditions, growth of the untransformed strains was not found as expected. At restrictive temperature, only the wild type strain Sey2101 and the mutant stain overexpressing *SEC18* were growing on full media. On selective media, only complementation with the yeast *SEC18* restored growth. In conclusion this data do not support the hypothesis that #33 is a functional homologue of *SEC18* from baker's yeast, since overexpression is not sufficient to rescue the temperature sensitive strain Sey5188 in contrast to *SEC18* from the corresponding wild type stain.

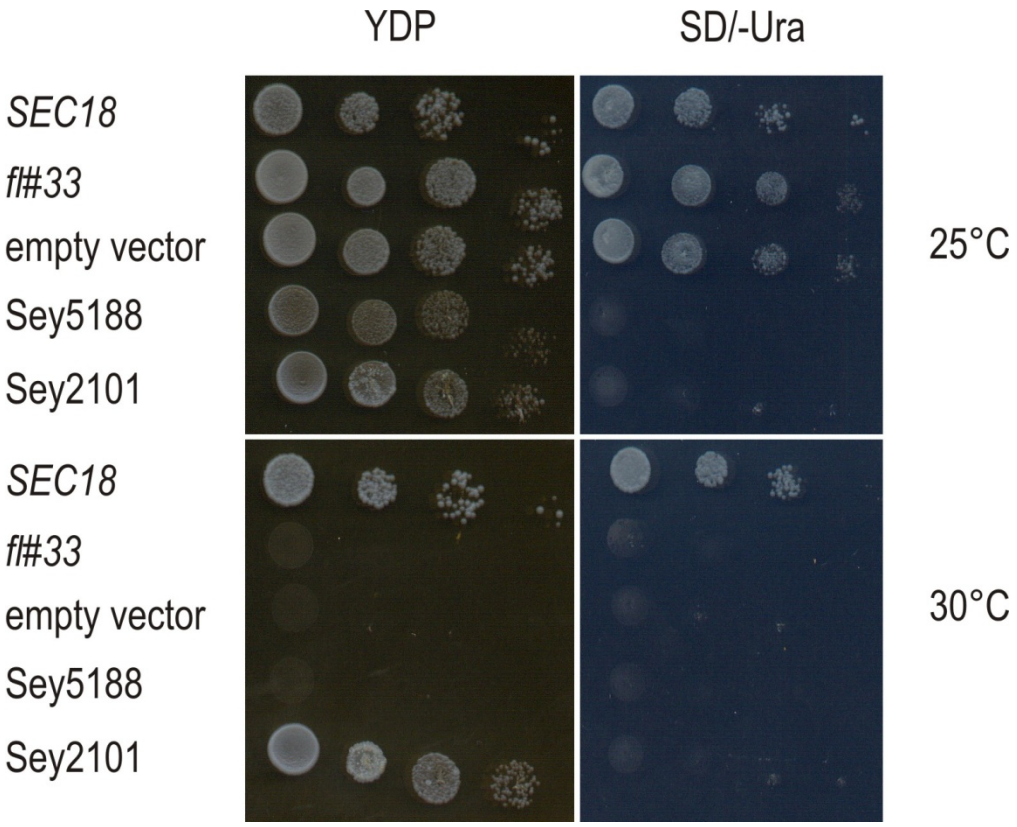

Figure 5.15 Complementation of *sec18*^{ts}-phenotype in yeast. The temperature sensitive mutant strain Sey5188 (Emr, Schekman et al. 1983) carries a mutant allele of *sec18*^{ts}. It grows normally at 25 °C (permissive temperature) but not at 30 °C (restrictive temperature). The temperature sensitive phenotype can be rescued with wild type *SEC18* cloned from the corresponding wild type strain Sey5188. Neither the empty expression vector nor the #33 clone was able to rescue the growth phenotype.

Next the expression pattern of #33 was investigated. A ubiquitous expression profile for a gene with important housekeeping function(s) was expected. Database analysis (Figure 5.16A) and experimental data (Figure 5.16B) support this hypothesis. Maize-eFP-brower (bar.utoronto.ca/efp_maiz/; Sekhon *et al.* 2011) suggests high levels of transcript in sixty different tissues (Figure 5.16A). RT-PCR analysis of nine tissues from A188 and BMS-suspension cells (Figure 5.16B) indicates presence of transcript in all samples tested. Expression was verified in adult and juvenile leaves, internodes, nods, roots, anthers, silks, ovules, seeds 6 dap and BMS suspension cells.

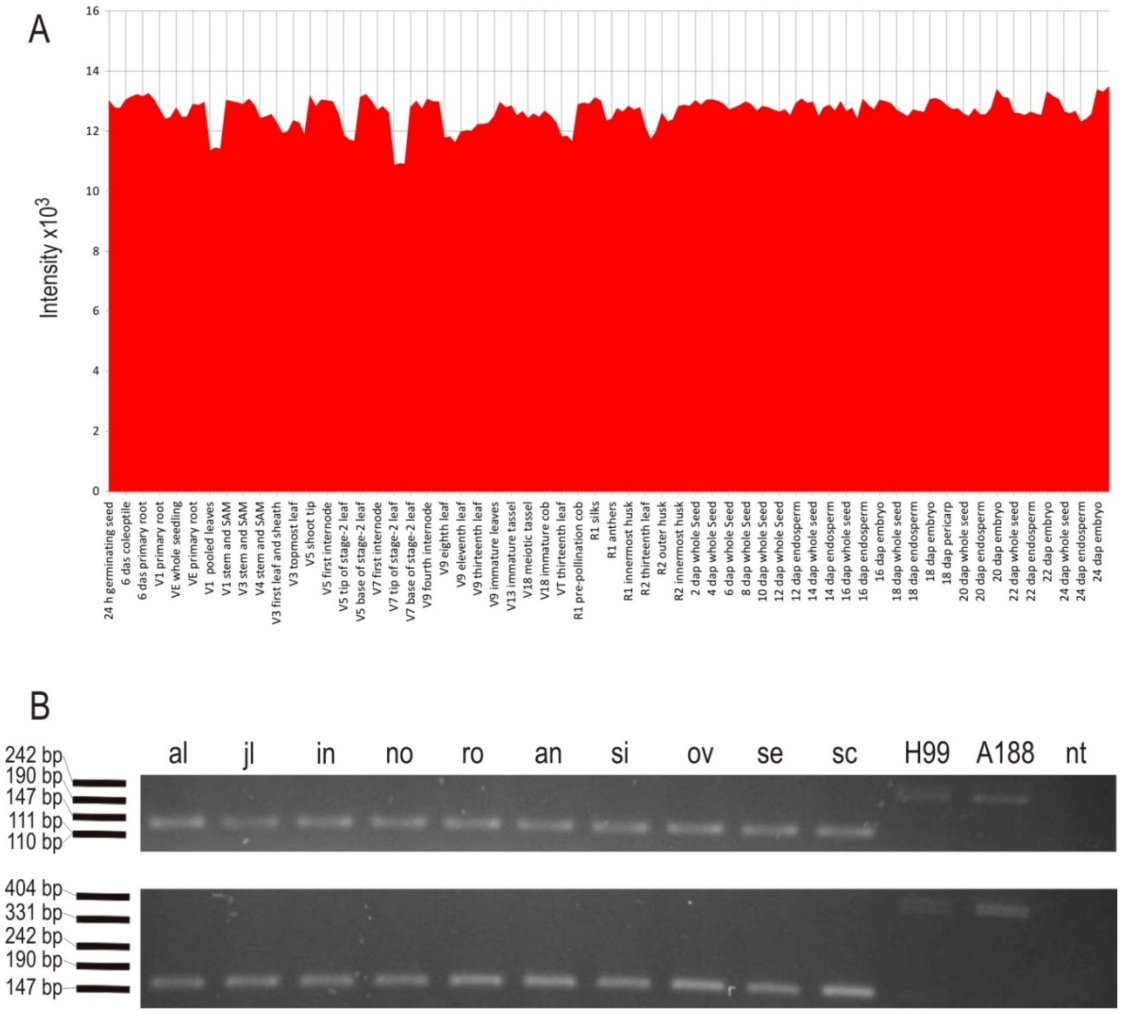

Figure 5.16 Expression of *#33* in various maize tissues according to maize-eFP-browser and experimental data. (A) Expression profile for *#33* according to publicly available data (eFP-browser: bar.utoronto.ca/efp_maiz/; Sekhon *et al.* 2011). The gene appears to be ubiquitously expressed at constant high levels in 60 tissues of the maize inbred line B73. (B) The upper gel shows RT-PCRs with *GAPDH*-Primer. The lower gel shows RT-PCR results for #33. The data found in (A) was confirmed in nine tissues investigated of the inbred line A188. The transcript of *#33* is additionally found in BMS-suspension cells (sc). Abbreviations: al = adult leaf, an = anther, in = internode, jl = juvenile leaf, ov = ovule, no = node, nt = non template, sc = suspension cells, se = seed 6 dap, si = silk, ro = root.

5.3.3 Pattern formation and the role of *ZmEAL1* in early embryo development

In order to understand the regulation of *ZmEAL1* and how it is embedded into the regulatory networks of embryo development, pattern formation in early embryo development in maize was studied using publicly available marker lines. The influence of *ZmEAL1* in early embryo development was investigated by analysing *eal1*-RNAi lines.

5.3.3.1 Expression of marker constructs in fertilization products of *Z. mays*

ZmEAL1-eGFP expression in early maize embryo development is found until late transition stage approximately 7 dap (Krohn, Lausser et al. submitted). At this time point the signal of the ZmEAL1-eGFP fusion protein is found at the adaxial side of the embryo proper in the epidermal cell layer as well as weaker in the subepidermal layer (Krohn, Lausser et al. submitted), Figure 5.17A and B). In a maize marker line expressing ERmRFP under the control of the synthetic auxin inducible promoter *DR5* (Ulmasov *et al.* 1997)a temporal or spatial overlap with *EAL1::EAL1-eGFP* activity was not observed (Figure 5.17C – H). The first *DR5* driven signal in a fertilization product of maize was found 4 dap in the endosperm at the adaxial side in vicinity to the pericarp (Figure 5.17C and D). Activation of the DR5 construct in the endosperm appears to occur shortly after cellularisation of the endosperm. This signal continues at least until 8 dap and spreads at the adaxial side of the endosperm and around the developing embryo (Figure 5.17E – H). In the embryo, the earliest *DR5* driven RFP signal was found at the abaxial side of the tip of the developing scutellum 8 dap. At the same time, an additional signal can be found in the area where later on the embryonic root will be formed (Figure 5.17G and H). In contrast to the *DR5::ERmRFP* construct, the expression of *PIN1a::PIN1a-YFP* overlapped partially with *EAL1-eGFP*-expression (Figure 5.17I – P). Direct colocalization of both constructs was difficult to achieve, since GFP and YFP fluorescence is difficult to separate in tissue samples. *PIN1a::PIN1a-YFP* expression was found only in the embryo. The first weak and diffuse signals can be found in early transition stage embryos 5 dap in the embryo proper at the adaxial side (Figure 5.17I and J). Later during embryo development expression becomes more focused on the outer cell layer at the tip of developing transition stage embryos (Figure 5.17K and L). The fusion protein is found in lateral and basal sides of the outermost cell layer and adjacent cells (Figure 5.17K and L), which becomes more and more pronounced until late transition stage (Figure 5.17M and N). At coleoptylar stage

around 8 dap *PIN1a* expression (Figure 5.17O and P) is found in a band starting at the tip of the evolving scutellum, approximately at the site of the first *DR5* signals (Figure 4.17G and H) stretching through the embryo along its longitudinal axis. In addition to the auxin related marker constructs *DR5::ERmRFP* and *PIN1a::PIN1a-YFP* a marker line expressing the construct *ABPHYL1::ABPHYL1-mRFP* was analysed. *ABPHYL1* is expressed amongst other genes in the SAM in a cytokinin-dependent manner (Giulini, Wang et al. 2004). The first expression detected in the lines was at late transition stage 7 dap. At this time point, *ABPHYL1* and *EAL1* expression partially overlap (Figures 5.17Q – T).

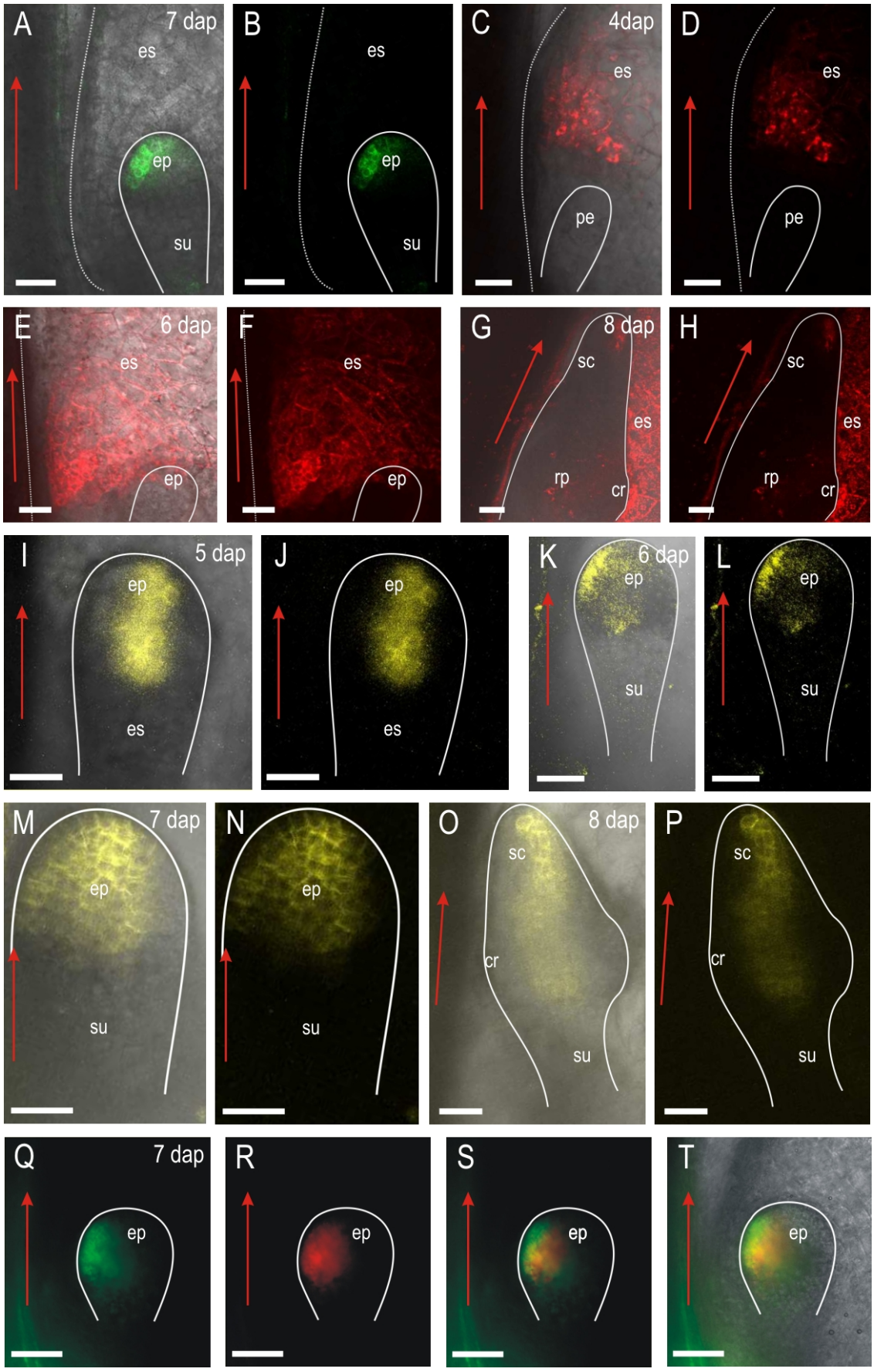
A
7 dap
es
ep
su
B
es
ep
su
C
4dap
es
pe
D
es
pe
E
6 dap
es
ep
F
es
ep
G
8 dap
sc
es
rp
cr
H
sc
es
rp
cr
I
5 dap
ep
es
J
ep
es
K
6 dap
ep
su
L
ep
su
M
7 dap
ep
su
N
ep
su
O
8 dap
sc
cr
su
P
sc
cr
su
Q
7 dap
ep
R
ep
S
ep
T
ep

Figure 5.17 Expression pattern of the marker constructs *DR5::ERmRFP*, *PIN1a::PIN1a-YFP* and *ABPHYL1::ABPHYL1-mRFP* compared with that of *EAL1::EAL1-eGFP* during early embryo development in maize. (A and B) ZmEAL1-eGFP-fusion protein can be found at the adaxial side of the embryo proper until the transition stage. The fusion protein occurs mainly in the two outer cell layers of the embryo although faint GFP signals can also be found in inner cell layers. (C and D) The auxin-inducible *DR5::ERmRFP*-construct can be first detected 4 dap in the endosperm right after cellularistion at the adaxial side above the proembryo. (E and F) Later on *DR5* activity spreads in the endosperm but is not detectable in a transition stage embryo. (G and H) The earliest *DR5* activity during embryo development was detected at the coleoptylar stage at the tip of the emerging scutellum and at the site of the future embryonic root. (I and J) C-terminal YFP-fusion of the auxin-efflux carrier PIN1a is detected first in the early transition stage embryo proper. Faint signals are detected at the tip of the embryo proper. (K and L) The first signals are located at the adaxial side of the embryo most strongly in the most outer cell layer but also in cells beneath. (M and N) At late transition stage, the signals become more pronounced and show the typical membrane location in basically all cells of the embryo proper except cells at the abaxial side. (O and P) In the coleoptylar stage, PIN1a fusion protein is found in a band from the tip of the scutellum across the embryo until the suspensor. (Q – T) A C-terminal mRFP-fusion of ABPHYL1 is first detectable in the late transition stage embryo (7 dap). At that stage, ABPHYL1-mRFP expression overlaps partially with EAL1-GFP. cr = coleoptylar ring, es = endosperm, ep = embryo proper, rp = root primordia, sc = scutellum, su = suspensor, red arrow indicates orientation of and direction towards cob axis, scale bars = 50 µm.

5.3.4.2 Analysis of *eal1*-RNAi lines during early embryo development

In order to learn more about the role of *EAL1* in early embryo development, $eal1_{RNAi}$ lines (Krohn, Lausser et al. submitted) were analysed at 7 dap. The material was produced by self-pollination of transgenic plants, which were tested for transgene expression by RT-PCR. The parental inbred line A188 served as wild type control. In terms of endosperm development, the observed phenotypes in the developing seed were categorised in three different classes. (1) endosperm of approximately 2.5 mm in length was termed “wild type” (Figure 5.18A) and (2) endosperm of more than 1 mm but less than 2 mm was termed “delayed” (Figure 5.18B). (3) Endosperm smaller than 1 mm was classified as “strongly delayed” (Figure 5.18C). Analysis of embryos suggested discriminating also different classes of embryos found in the ovule. Some embryos found in ovules originating from mutant plants are obviously smaller (Figure 5.18D) compared to “wild type” embryos (Figure 5.18E).

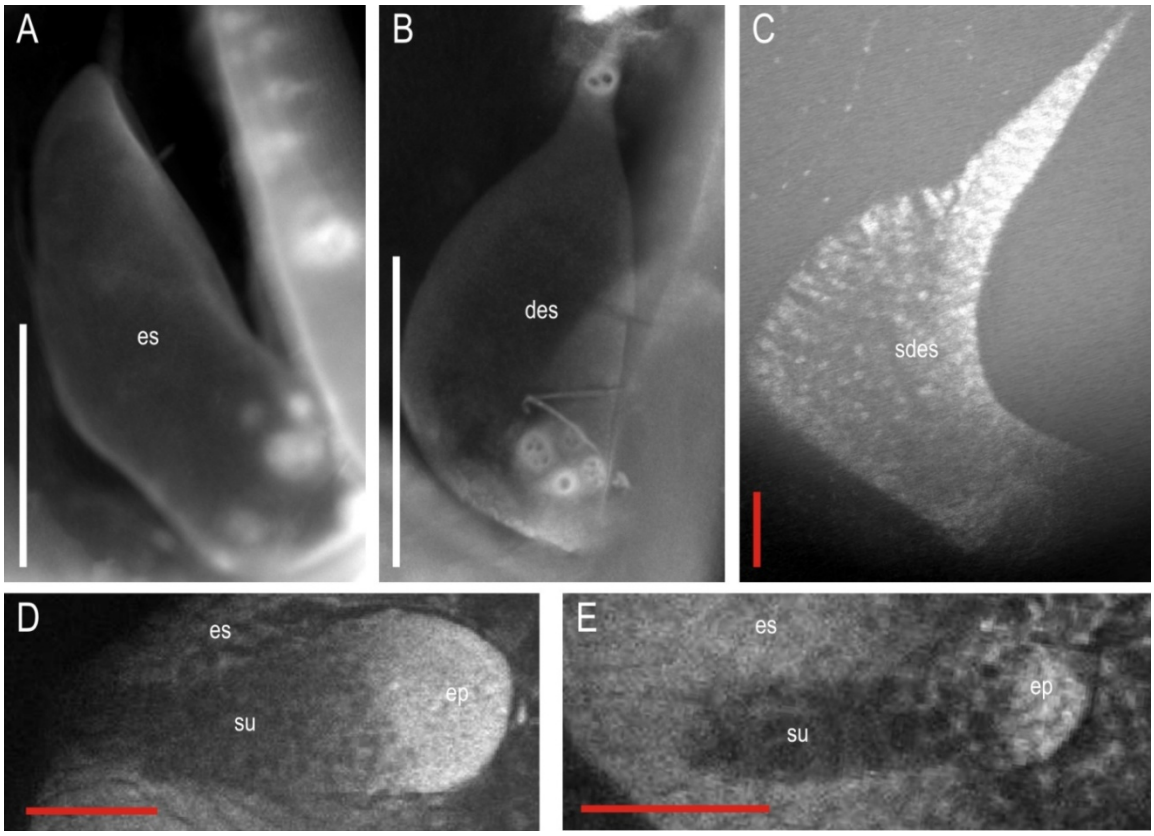

Figure 5.18 Phenotypic analysis of endosperm and embryo of *eal1*-RNAi lines 7 dap. (A) Wild type endosperm. (B and C) Endosperm, isolated from RNAi seed. Classified as "delayed endosperm" (B) or "strongly delayed endosperm" (C), respectively. (D) Wild type embryo. (E) Embryo isolated from an RNAi seed. Abbreviations: des = delayed endosperm, es = endosperm, sdes = strongly delayed endosperm, su = suspensor, white scale bar = 1 mm, red scale bar = 100 µm

Statistic analysis of endosperm length of the above mentioned categories revealed that RNAi-lines 3 and 7 show a much higher proportion of "delayed" and "strongly delayed" endosperm categories compared to the wild type. Contrarily, line 9 and wild type show similar proportions of endosperm development categories. More than 90% of the seeds in wild type and line 9 contained "wild type"-endosperm. The RNAi-line 3 showed "wild type" endosperm in approximately 2/3 of the samples. Line 7 showed less than 20% wild type endosperm and as the only line "strongly delayed" endosperm (Figure 5.19).

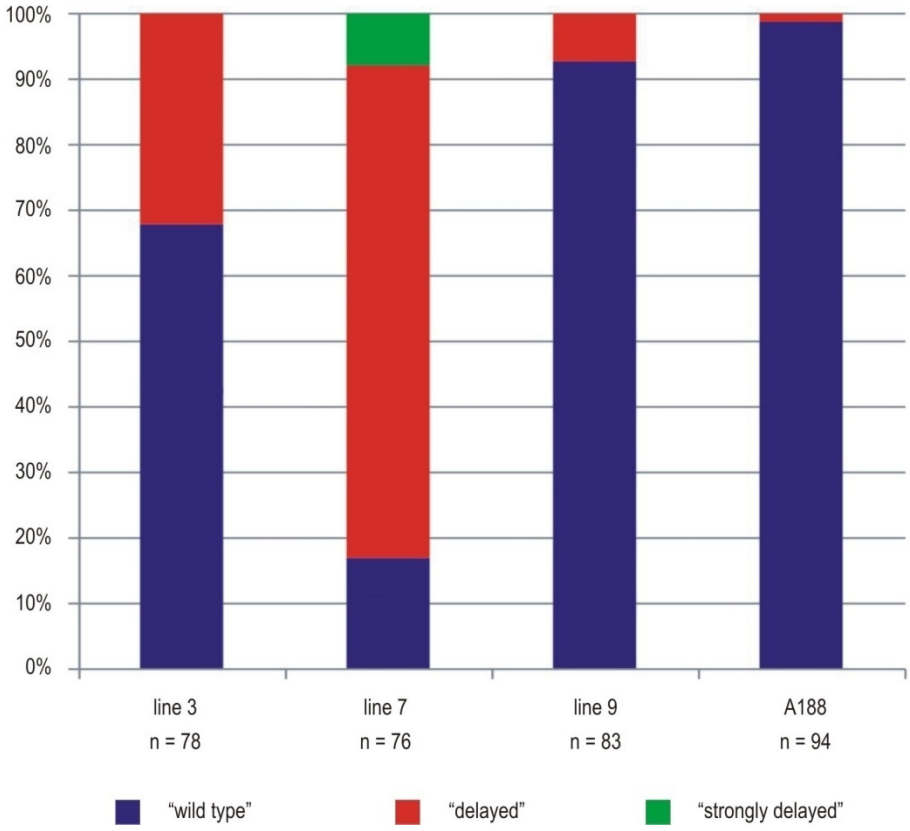

Figure 5.19 Distribution of endosperm developmental stages of endosperm in wild type and *eal1*-RNAi-lines. The endosperm of analyzed seeds was grouped into three categories by correlating its length along the longitudinal axis and after comparison to wild type endosperm. The categories were termed "wild type" (> 2 mm), "delayed" (1 – 2 mm) and "strongly delayed" (< 1 mm). The majority of endosperm tissue in the control line A188, line 3 and line 9 was termed "wild type". Line 3 and 9 contained more "delayed" endosperm compared to A188. "Strongly delayed" endosperm was found only in line 7. Statistic analysis of metric data revealed, that all differ highly significantly from each other in terms of endosperm size. The only exceptions from this are line 3 and 9, which do not differ significantly from each other.

The mean length of the endosperm in the four lines supports the impression from the classification that RNAi-line 9 (mean length = 1862 µm/mean deviation = 509 µm/ n = 30) is most similar to wild type A188 (2263 µm/352 µm/30). Line 7 (1289 µm/317 µm/31) is most different from wild type. The RNAi-line 3 (1743 µm/330 µm/30) showed an intermediate phenotype compared to line 9 and 7 but is closer to line 9. A two-sided unpaired t-test revealed that A188 and line 7 differ from all other lines with high significance ($p << 0.01$). The difference between line 3 and 9 is not significant ($p = 0.29$).
The second fertilization product, the embryo, was also analysed in terms of length along its longitudinal axis and the width at the broadest position perpendicular to the first axis. (Figure 5.20). Concerning the length of the embryos, RNAi-lines 7 and 9 differ

significantly (p-value <<0.01) form wild type whereas RNAi-line 3 resembles more or less the wild type situation in this trait (Figure 5.20A). For the width of the embryos, the situation is similar (Figure 5.20B) with the exception that also RNAi-line 3 differs significantly (p-value <0.01) from wild type in this trait.

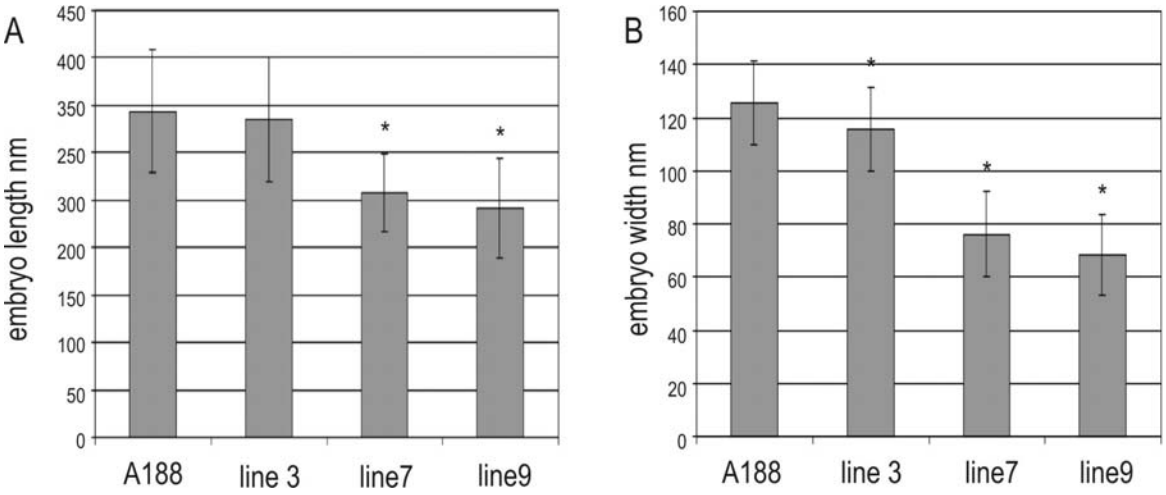

Figure 5.20 Length and width of embryos in *eal1*-RNAi and wild type lines. (A) Length of embryos measured from wild type and *eal1*-RNAi-plants. All plants were self-pollinated. (B) Width of the same embryos as in (A). Columns marked with asterisk differ significantly from wild type (p-value <0.01). Error bar indicate one mean deviation. A188: n = 34; line 3: n = 43; line 7: n = 40; line 9: n = 37.

5.3.5 Identification of downstream targets of EAL1 in BMS cells

5.3.5.1 Phenotypic analysis of BMS cells incubated with trEAL1

For further experiments BMS suspension cells were chosen as a model system. The influence of trEAL1 on cell growth was tested by adding four times synthetic peptide at a final concentration of 5 µM to growing cell cultures at the time points 0 h, 12 h, 24 h and 36 h. Growth of cultures was measured as %packed cell volume. Control cells were grown without supplement or treated with 25 µg/ml bovine serum albumin (BSA). No difference in growth behaviour could be found (Figure 5.21). In terms of cell size and shape, no obvious difference between the three treatments was found (data not shown).

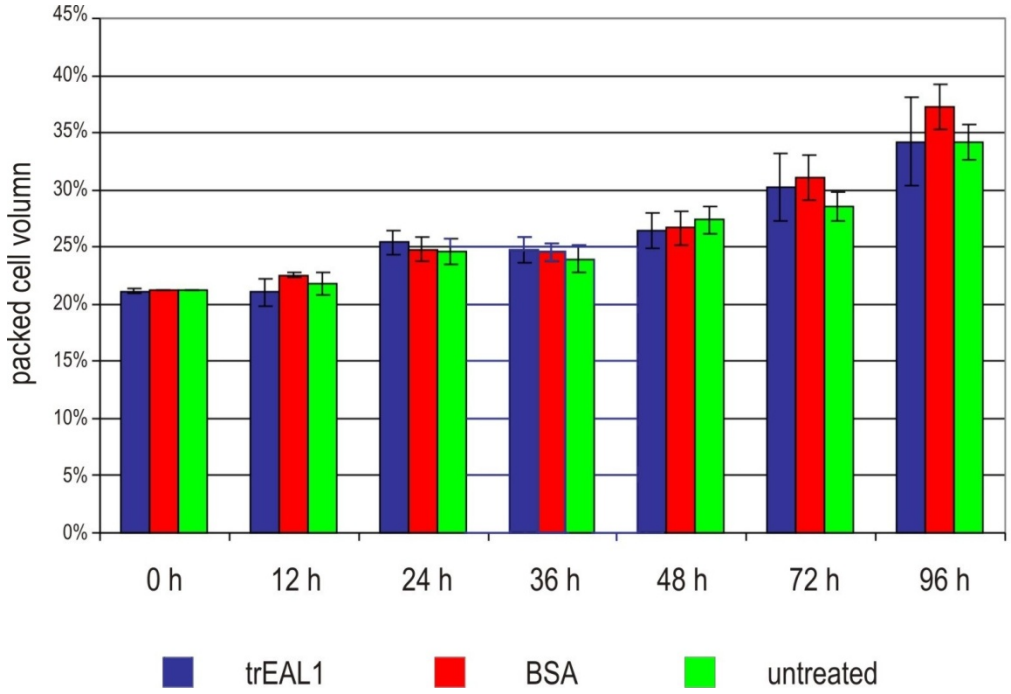

Figure 5.21 Growth of BMS cells in presence of 5 µM trEAL1. BMS cells were treated four times at time points 0 h, 12 h, 24 h and 36 h with trEAL1 and an equal mass of BSA as control. trEAL1-treated cells showed no aberrant growth behavior compared to BSA-treated and untreated cells. Error bars represent one mean deviation.

5.3.5.2 Microarray analysis of BMS cells incubated with trEAL1

Although an influence of trEAL1 on BMS cells could not be detected in terms of morphological or physiological alterations/reactions, this does not necessarily exclude a possible transient influence on the cells. In order to study whether there is such an effect, cells were treated with trEAL1 as described above. 120 min and 540 min after treatment, cells were sampled and microarray experiments were performed in collaboration with U. Schlüter and U. Sonnewald (University of Erlangen). 1047 genes were differentially expressed in the samples 120 min compared to 0 min. 168 genes differ in expression level between the samples 540 min and 0 min. 104 genes differ at both time points from time point 0 min.

A principle component analysis (PCA) revealed that the samples at time point 120 min are separated from time point 0 min and 540 min by the 1st principal component (PC). 0 min and 540 min are separated by the 2nd PC. The 1st PC is therefore describing transient events, whereas the 2nd PCA probably reflects a time dependent process (Figure 5.22). The identity of the strongest up-regulated genes in the samples is given in Table 5.7, the strongest down-regulated genes in Table 5.8.

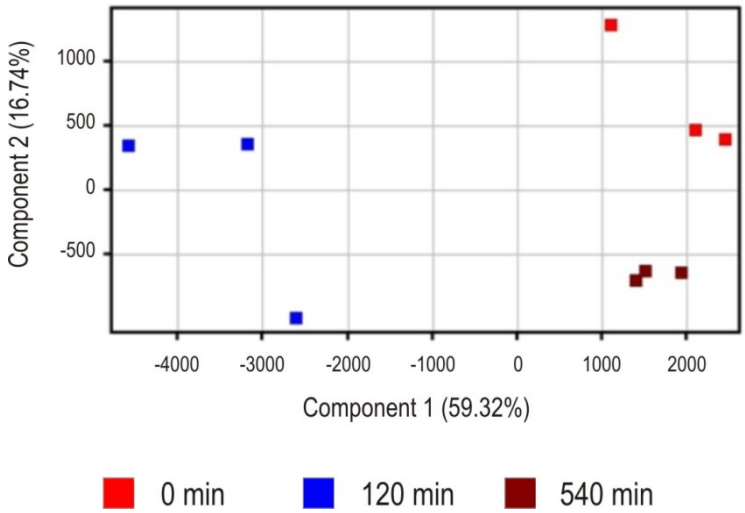

Figure 5.22 Principle component analysis of the sample data. The first principle component separates samples of time points 0 and 540 min from time point 120 min. This component might indicate a transient response of BMS-cells to trEAL1-treatment. 0 and 540 min are separated mainly by the second principle component. This component might reflect long-term effects of trEAL1 and a possible "ageing" of the cells in course of the experiment.

Table 5.7 Genes up-regulated in BMS cells after trEAL1 treatment. Genes induced by the treatment of BMS suspension cells with 5 µM trEAL1. The first 30 genes are most strongly regulated genes only in samples after 120 min. The second block of 30 genes was found to be induced after 540 min. The last 26 genes were up-regulated in both samples. Genes were considered to be unregulated when the average FC of three replicates was between 2 and 0.5. Abbreviations: FC = fold change

Locus	Description	Corrected p-value	FC Absolute
	up-regulated after 120 min		
GRMZM2G468521	Pentatricopeptide repeat (PPR) superfamily protein	0.045	12.05
GRMZM2G153404	Ca^{2+}-binding protein, EF-Hand protein superfamily	0.017	10.17
GRMZM2G053071	unknown	0.035	9.89
AC204569.3_FG002	unknown	0.022	9.44
GRMZM2G424205	unknown	0.036	8.69
GRMZM2G181415	unknown	0.043	8.45
GRMZM2G700649	unknown	0.039	8.35
AC211891.4_FG001	Zn-finger	0.024	8.26
GRMZM2G417439	unknown	0.041	7.56
GRMZM2G037284	unknown	0.044	7.49
GRMZM2G015599	unknown	0.049	7.18
GRMZM2G703656	unknown	0.032	7.15
GRMZM2G420436	Magnesium transporters: CorA family	0.04	6.98
GRMZM2G307084	DNA helicase PIF1/RRM3	0.033	6.96
GRMZM2G446999	Ubiquitin and ubiquitin-like proteins	0.047	6.81
GRMZM2G093708	unknown	0.043	6.77
GRMZM2G156376	unknown	0.046	6.7

GRMZM2G344799	Protease, Ulp1 family	0.027	6.67
GRMZM2G700049	unknown	0.039	6.64
AC185261.4_FG002	unknown	0.032	6.6
GRMZM2G120475	unknown	0.03	6.52
GRMZM2G542847	2-oxoglutarate (2OG) and Fe(II)-dependent oxygenase superfamily protein	0.048	6.47
GRMZM2G431486	unknown	0.04	6.33
AC226368.2_FG002	unknown	0.041	6.29
GRMZM2G307440	alpha/beta-Hydrolases superfamily protein	0.04	6.21
GRMZM2G099420	cinnamoyl CoA reductase	0.013	6.18
GRMZM2G020382	unknown	0.021	6.15
GRMZM2G046317	unknown	0.039	6.09
GRMZM2G704130	unknown	0.023	5.97
	up-regulated after 540 min		
GRMZM2G129954	A- type response Regulator	0.034	3.39
GRMZM2G073223	Subtilisin-related protease/Vacuolar protease B	0.006	2.89
GRMZM2G433908	RING/U-box superfamily protein	0.041	2.83
GRMZM2G121293	Subtilisin kexin isozyme-1/site 1 protease, subtilase superfamily	0.011	2.82
GRMZM2G117989	chitinase	0.009	2.8
GRMZM2G105682	uclacyanin, a protein precursor that is closely related to precursors of stellacyanins	0.011	2.77
GRMZM2G414826	Serine/threonine protein kinase, uncharacterized conserved protein	0.047	2.71
GRMZM2G431039	Glucan endo-1,3-beta-D-glucosidase	0.009	2.61
GRMZM2G419675	chitinase	0.013	2.49
GRMZM2G165919	galactinol synthase 1 (GolS1)	0.014	2.46
GRMZM2G105387	MADS box transcription factor	0.029	2.44
GRMZM2G394979	Heavy metal transport/detoxification superfamily protein	0.02	2.35
GRMZM2G154687	lipase	0.021	2.32
GRMZM2G131697	galactinol synthase 1 (GolS1)	0.02	2.32
GRMZM2G106408	Cytochrome P450 CYP4/CYP19/CYP26 subfamilies	0.023	2.3
GRMZM2G114057	Serine/threonine protein kinase, uncharacterized conserved protein	0.01	2.28
GRMZM2G113819	60s ribosomal protein L34	0.009	2.27
GRMZM2G469898	GDSL-like Lipase/Acylhydrolase superfamily protein	0.01	2.2
GRMZM2G149996	Aspartyl protease	0.021	2.18
GRMZM2G116167	unknown	0.007	2.17
GRMZM2G053493	Defense-related protein containing SCP domain	0.012	2.15
GRMZM2G156861	lipoxygenase	0.026	2.13
GRMZM2G423139	Calmodulin (EF-Hand superfamily)	0.01	2.13
GRMZM2G089982	Peroxidase superfamily protein	0.013	2.11
GRMZM2G036554	transcription factor domain containing	0.026	2.11
GRMZM2G051769	phytochrome-associated protein	0.019	2.08
GRMZM2G149700	unknown	0.031	2.08
GRMZM2G304687	unknown	0.021	2.08
GRMZM2G143352	auxin inducible gene family.	0.006	2.07
GRMZM2G068294	EID1 is an F-box protein	0.002	2.06
	up-regulated after 120min and 540min(p-value and FC given in 120/540)		
GRMZM2G161154	unknown	0.012/0.044	7.48/2.14
GRMZM2G178990	unknown	0.011/0.021	6.48/2.39

GRMZM2G153178	unknown	0.014/0.012	5.96/2.13
GRMZM2G099049	unknown	0.01/0.011	5.61/3.84
GRMZM2G366681	unknown	0.016/0.014	5.41/2.91
GRMZM2G457356	Leucine rich repeat proteins, some proteins contain F-box	0.018/0.009	3.66/2.95
GRMZM2G412986	Glycosyltransferase family 61 protein	0.011/0.006	3.51/2.01
GRMZM2G005146	unknown	0.023/0.011	3.45/3.71
GRMZM2G065088	germin-like protein (GLP5)	0.022/0.009	3.28/6.48
GRMZM2G082032	Asparaginase	0.02/0.012	3.11/3.57
GRMZM2G017671	Histidyl-tRNA synthetase	0.015/0.038	2.96/2
GRMZM2G069523	cytosolic short-chain dehydrogenase/reductase involved in the conversion of xanthoxin to ABA-aldehyde	0.02/0.026	2.65/2.52
GRMZM2G019806	bHLH transcription factor	0.018/0.002	2.64/5.07
GRMZM2G082343	bHLH transcription factor	0.012/0.002	2.47/2.82
GRMZM2G304548	unknown	0.023/0.008	2.46/2.39
GRMZM2G341658	MAC/Perforin domain-containing protein	0.019/0.003	2.4/2.2
GRMZM2G119999	homeodomain leucine zipper class I (HD-Zip I) protein	0.045/0.017	2.39/3.02
GRMZM2G022947	Cytochrome P450 CYP4/CYP19/CYP26 subfamilies	0.018/0.005	2.27/2.05
GRMZM2G414826	Serine/threonine protein kinase, uncharacterized conserved protein	0.029/0.011	2.26/3.15
GRMZM2G456997	Defense-related protein containing SCP domain	0.026/0.02	2.1/2.2
GRMZM2G025182	Plant invertase/pectin methylesterase inhibitor	0.015/0.008	2.09/2.35
GRMZM2G008406	Defense-related protein containing SCP domain	0.02/0.021	2.08/2.03
GRMZM2G465226	Defense-related protein containing SCP domain	0.015/0.011	2.05/2.05
GRMZM2G150059	Aspartyl protease	0.01/0.008	2.04/2.3
GRMZM2G121333	hydrolase/acyltransferase (alpha/beta hydrolase superfamily)	0.02/0.028	2.02/2

Table 5.8 Genes down-regulated in BMS cells after trEAL1 treatment. Genes downregulated by the treatment of BMS suspension cells with 5 µM trEAL1. The first 30 genes are most strongly regulated genes only in samples after 120 min. The second block of 30 genes was found to be induced after 540 min. The last 26 genes were down-regulated in both samples. Genes were considered to be unregulated when the average FC of the three replicates was between 2 and 0.5. Abbreviations: FC = fold change

Locus	Description	Corrected p-value	FC Absolute
	down-regulated after 120 min		
GRMZM2G101409	unknown	0.028	6.32
GRMZM2G338037	unknown	0.023	5.71
GRMZM2G131611	RING/U-box superfamily protein	0.026	4.58
GRMZM2G066291	unknown	0.023	3.83
GRMZM2G056014	Ca2+ transporting ATPase	0.031	3.57
GRMZM2G032376	GDSL-like Lipase/Acylhydrolase superfamily protein	0.020	3.53
GRMZM2G009779	Inorganic phosphate transporter	0.022	3.39
GRMZM2G041595	Inorganic phosphate transporter	0.021	3.35
GRMZM2G061723	embryo sac development arrest 39 (EDA39)	0.031	3.03
GRMZM2G177340	mRNA deadenylase subunit	0.025	2.92
GRMZM2G449681	WRKY transcription factor family	0.023	2.88
GRMZM2G115499	Nucleolar GTPase/ATPase p130	0.029	2.87
GRMZM2G141679	DREB subfamily A-6 of ERF/AP2 transcription factor family	0.033	2.82
GRMZM2G054900	calmodulin-binding family protein	0.019	2.71

GRMZM2G124037	DREB subfamily A-1 of ERF/AP2 transcription factor family	0.031	2.70
AC152495.1_FG010	Apoptotic ATPase	0.029	2.70
AC185642.4_FG001	Conserved alpha-helical protein	0.024	2.70
GRMZM2G110192	9-cis-epoxycarotenoid dioxygenase, a key enzyme in the biosynthesis of abscisic acid	0.015	2.65
GRMZM2G111711	Pathogen-induced transcription factor	0.023	2.64
GRMZM2G069082	DREB subfamily A-1 of ERF/AP2 transcription factor family	0.011	2.63
GRMZM2G149935	Galactosyltransferases	0.025	2.63
GRMZM2G057509	Core-2/I-branching beta-1,6-N-acetylglucosaminyltransferase family protein	0.023	2.57
GRMZM2G312521	Trehalose-6-phosphate synthase component TPS1 and related subunits	0.029	2.56
GRMZM2G047456	Peroxidase superfamily protein	0.027	2.54
GRMZM2G091119	Karyopherin (importin) alpha	0.038	2.52
GRMZM2G134545	Dof-type zinc finger DNA-binding family protein	0.036	2.50
GRMZM2G142712	ubiquitin regulatory protein	0.047	2.49
GRMZM2G173387	potassium transporter	0.040	2.48
GRMZM2G141214	Glucose dehydrogenase/choline dehydrogenase/mandelonitrile lyase (GMC oxidoreductase family)	0.019	2.46
GRMZM2G150363	9-cis-epoxycarotenoid dioxygenase, a key enzyme in the biosynthesis of abscisic acid	0.018	2.46
	down-regulated after 540 min		
GRMZM2G027673	stearoyl-ACP desaturase, involved in fatty acid desaturation	0.004	16.73
GRMZM2G316362	stearoyl-acyl-carrier-protein desaturase family protein	0.004	16.34
GRMZM2G123212	E3 ubiquitin ligase	0.013	5.21
GRMZM2G117164	Transcription factor HEX, contains HOX and HALZ domains	0.002	5.11
GRMZM2G404603	unknown	0.013	4.85
GRMZM2G085964	ERF (ethylene response factor) subfamily B-2 of ERF/AP2 transcription factor family	0.005	4.8
GRMZM2G013448	1-aminocyclopropane-1-carboxylate oxidase	0.002	4.59
GRMZM2G137964	unknown	0.037	4.4
GRMZM2G404608	unknown	0.011	4.32
GRMZM2G002805	C2H2 type zinc finger transcription factor family	0.01	4.15
GRMZM2G011006	Nuclear localization sequence binding protein	0.005	4.08
GRMZM2G419994	unknown	0.004	4.06
GRMZM2G023436	GTPase Rab1/YPT1, small G protein superfamily,	0.013	4.03
GRMZM2G103647	unknown	0.022	4.01
GRMZM2G049790	unknown	0.01	3.84
AC206951.3_FG017	ERF (ethylene response factor) subfamily B-2 of ERF/AP2 transcription factor family	0.013	3.78
GRMZM2G076683	Nuclear localization sequence binding protein	0.01	3.66
GRMZM2G131087	Rhodanese-related sulfurtransferase	0.018	3.53
GRMZM2G024517	unknown	0.007	3.5
GRMZM2G098346	Alcohol dehydrogenase, class III	0.01	3.5
GRMZM2G061487	DREB subfamily A-6 of ERF/AP2 transcription factor family	0.008	3.46
GRMZM2G354338	unknown	0.014	3.38
GRMZM2G449681	WRKY transcription factor family	0.009	3.29
GRMZM2G073548	unknown	0.038	3.28
GRMZM2G042639	Glutathione S-transferase	0.028	3.25
GRMZM2G444819	unknown	0.022	3.24
GRMZM2G081949	Remorin family protein	0.045	3.22
GRMZM2G162659	Collagens (type IV and type XIII), and related proteins	0.007	3.2

GRMZM2G172214	5'-AMP-activated protein kinase, gamma subunit	0.036	3.18
GRMZM2G148355	NAD(P)-binding Rossmann-fold superfamily protein	0.009	3.17
down-regulated after 120 min and 540 min (p-value and FC given as 120 min/540 min)			
GRMZM2G442658	Alcohol dehydrogenase, class III	0.012/0.009	12.52/17.51
GRMZM2G060544	LOB domain-containing protein	0.012/0.002	11.33/22.99
GRMZM2G305362	Halotolerance protein HAL3 (contains flavoprotein domain)	0.01/0.001	9.42/17.46
GRMZM2G386674	LOB domain-containing protein	0.01/0.001	6.45/14.14
GRMZM2G442658	Alcohol dehydrogenase, class III	0.034/0.014	6.22/6.29
GRMZM2G026780	unknown	0.016/0.008	5.82/8.64
GRMZM2G073044	LOB domain-containing protein	0.01/0.002	5.49/12.01
GRMZM2G069146	Transcriptional activator that binds to the DRE/CRT regulatory element	0.01/0.004	5.48/5.25
GRMZM2G305267	unknown	0.011/0.007	5.45/6.98
GRMZM2G334165	Serine/threonine protein kinase	0.031/0.047	4.57/4.57
GRMZM2G470422	nuclear Cys(2)His(2)-type zinc finger protein	0.01/0.047	4.52/4.33
GRMZM2G459614	C2H2 and C2HC zinc fingers superfamily protein	0.037/0.017	4.46/8.08
GRMZM2G124011	DREB subfamily A-1 of ERF/AP2 transcription factor family	0.013/0.028	4.26/3.85
AC203989.4_FG001	unknown	0.01/0.001	4.2/9.91
GRMZM2G106413	Wound-responsive family protein	0.034/0.011	3.89/5.75
GRMZM2G400714	Zn-finger, C2H2 transcription factor	0.015/0.002	3.85/4.37
GRMZM2G300965	Ferric reductase, NADH/NADPH oxidase and related proteins	0.011/0	3.75/7.5
GRMZM2G120320	Pathogen-induced transcription factor	0.037/0.037	3.67/2.91
GRMZM2G007939	Beta-amylase.	0.041/0.025	3.34/7.39
GRMZM2G007729	Molecular chaperone (small heat-shock protein Hsp26/Hsp42)	0.04/0.02	3.31/10.5
GRMZM2G075461	Cytochrome P450 CYP4/CYP19/CYP26 subfamilies	0.025/0.008	3.29/3.31
GRMZM2G123667	splicing factor PWI domain-containing protein	0.025/0.026	3.26/2.22
GRMZM2G041714	unknown	0.015/0.001	3.15/5.13
GRMZM2G324999	WRKY Transcription Factor Group III	0.012/0.009	3.09/2.42
AC205562.3_FG002	WRKY Transcription Factor Group III	0.019/0.008	3.03/2.51
GRMZM2G018336	regulator of the (H+)-ATPase of the vacuolar and endosomal membranes	0.028/0.012	2.91/2.47
GRMZM2G097135	Nucleolar GTPase/ATPase p130	0.01/0.003	2.89/8.67
AC225718.2_FG009	unknown	0.045/0.008	2.75/3.53
GRMZM2G123667	transcriptional activators with NAC domain	0.035/0.003	2.68/2.35
GRMZM2G003937	unknown	0.047/0.039	2.66/5.71

A gene ontology (GO) analysis of differentially expressed genes based on the publicly available database AgriGO revealed that several GO-terms were enriched in the dataset for genes differentially expressed either at the time point 540 min (Figure 5.23A) or at the time points 120 min and 540 min (Figure 5.23B). From the genes differentially expressed at 120 min a GO-term enrichment was not detected. Among others, the especially interesting transcription factors appear to be enriched in both groups. The most strongly regulated transcription factors over all groups of time points are given in Table 5.9.

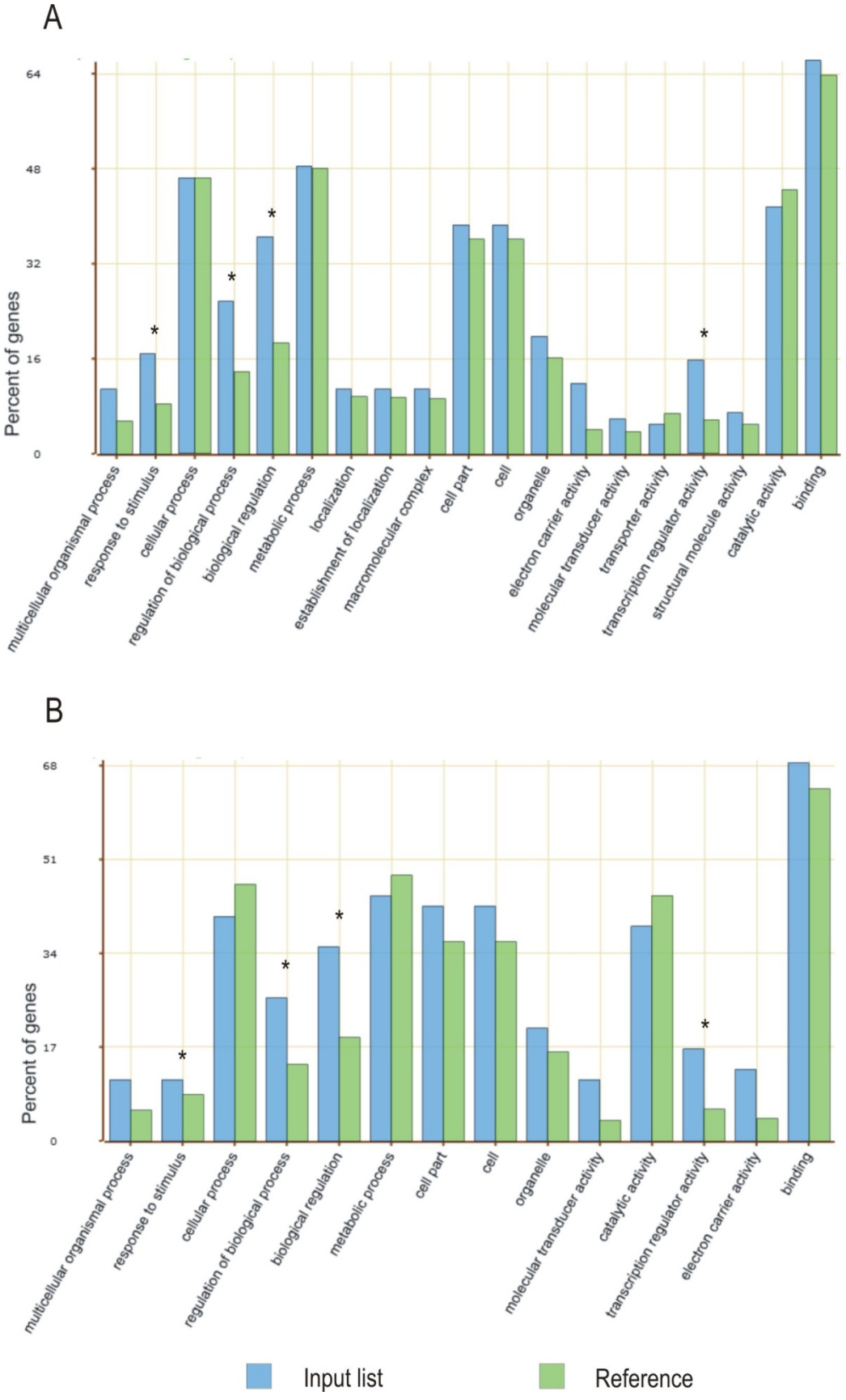
A
Percent of genes
64
48
32
16
0
multicellular organismal process
response to stimulus
cellular process
regulation of biological process
biological regulation
metabolic process
localization
establishment of localization
macromolecular complex
cell part
cell
organelle
electron carrier activity
molecular transducer activity
transporter activity
transcription regulator activity
structural molecule activity
catalytic activity
binding
B
Percent of genes
68
51
34
17
0
multicellular organismal process
response to stimulus
cellular process
regulation of biological process
biological regulation
metabolic process
cell part
cell
organelle
molecular transducer activity
catalytic activity
transcription regulator activity
electron carrier activity
binding
Input list
Reference

Figure 5.23 Gene ontology analysis of differentially expressed candidates. (A) GO terms enriched in differentially expressed genes 540 min after EAL1 treatment. Interestingly, the GO terms (asterisk) “response to stimulus”, “transcription regulator activity”, “regulation of biological process” and “biological regulation” are found. (B) GO terms enriched after 120 min and 540 min treatment. Less GO terms, compared to A were identified. Yet, the GO terms connected to transcription regulation, biological regulation and response to stimulus are enriched as well.

Table 5.9 Most strongly regulated transcription factor genes after trEAL1 treatment. Trancription factors regulated by the treatment of BMS suspension cells with 5 µM trEAL1. The first two blocks two are transcription factores regulated only in samples after 120 min. The following two blocks are transcription factores regulated only in samples after 540 min. The last two blocks are transcription factores regulated in both samples. Genes were considered to be unregulated when the average FC of the three replicates was between 2 and 0.5. Abbreviations: FC = fold change

Locus	Description	Corrected p-value	FC Absolute
	up-regulated after 120 min		
GRMZM2G119693	Transcription factor, Myb superfamily	0.042	4.44
GRMZM2G060050	Transcription factor MEIS1 and related HOX domain proteins	0.02	4.33
GRMZM2G426154	Mitochondrial transcription termination factor, mTERF	0.039	3.8
GRMZM2G048131	phytochrome-associated protein	0.014	3.17
GRMZM2G305124	transcription factor ASH1/LIN-59	0.012	3.17
GRMZM2G055257	ovate family protein	0.024	2.78
GRMZM2G137046	Basic leucine zipper (bZIP) transcription factor	0.015	2.65
GRMZM2G143274	Transcription factor, Myb superfamily	0.023	2.52
GRMZM2G086835	zinc finger protein containing only a single zinc finger.	0.034	2.51
GRMZM2G088443	bHLH transcription factor	0.03	2.46
	down-regulated after 120 min		
GRMZM2G449681	WRKY transcription factor family	0.023	2.88
GRMZM2G141679	DREB subfamily A-6 of ERF/AP2 transcription factor family	0.033	2.82
GRMZM2G124037	DREB subfamily A-1 of ERF/AP2 transcription factor family	0.031	2.7
GRMZM2G111711	Pathogen-induced transcription factor	0.023	2.64
GRMZM2G069082	DREB subfamily A-1 of ERF/AP2 transcription factor family	0.011	2.63
GRMZM2G134545	Dof-type zinc finger DNA-binding family protein	0.036	2.5
GRMZM2G087955	R2R3 factor gene family, Myb superfamily	0.025	2,43
AC209858.4_FG003	SET domain group	0.032	2.42
GRMZM2G027298	CCCH-type Zn-finger protein	0.016	2.38
GRMZM2G159592	regulator of the (H+)-ATPase of the vacuolar and endosomal membranes	0.025	2.28
	up-regulated after 540 min		
GRMZM2G129954	A- type response Regulator	0.034	3.39
GRMZM2G105387	MADS box transcription factor	0.029	2.44
GRMZM2G036554	transcription factor domain containing	0.026	2.11
GRMZM2G051769	phytochrome-associated protein	0.019	2.08
	down-regulated after 540 min		
GRMZM2G117164	Transcription factor HEX, contains HOX and HALZ domains	0.002	5.11

GRMZM2G085964	ERF (ethylene response factor) subfamily B-2 of ERF/AP2 transcription factor family	0.005	4.8
GRMZM2G002805	C2H2 type zinc finger transcription factor family	0.01	4.15
AC206951.3_FG017	ERF (ethylene response factor) subfamily B-2 of ERF/AP2 transcription factor family	0.013	3.78
GRMZM2G076683	Nuclear localization sequence binding protein	0.01	3.66
GRMZM2G061487	DREB subfamily A-6 of ERF/AP2 transcription factor family	0.008	3.46
GRMZM2G449681	WRKY transcription factor family	0.009	3.29
GRMZM2G361210	C2H2 type zinc finger transcription factor family	0.01	3.04
GRMZM2G089995	ERF (ethylene response factor) subfamily B-1 of ERF/AP2 transcription factor family	0.009	3.01
GRMZM2G025062	ERF (ethylene response factor) subfamily B-2 of ERF/AP2 transcription factor family	0.005	2.85
up-regulated after 120 min and 540 min (p-value and FC given as 120 min/540 min)			
GRMZM2G065088	bHLH transcription factor	0.018/0.002	2.64/5.07
GRMZM2G099049	bHLH transcription factor	0.012/0.002	2.47/2.82
GRMZM2G082032	homeodomain leucine zipper class I (HD-Zip I) protein	0.045/0.017	2.39/3.02
down-regulated after 120 min and 540 min (p-value and FC given as 120 min/540 min)			
GRMZM2G060544	LOB domain-containing protein	0.012/0.002	11.33/22.99
GRMZM2G386674	LOB domain-containing protein	0.01/0.001	6.45/14.14
GRMZM2G073044	LOB domain-containing protein	0.01/0.002	5.49/12.01
GRMZM2G069146	Transcriptional activator that binds to the DRE/CRT regulatory element	0.01/0.004	5.48/5.25
GRMZM2G470422	nuclear Cys(2)His(2)-type zinc finger protein	0.01/0.007	4.52/4.33
GRMZM2G459614	C2H2 and C2HC zinc fingers superfamily protein	0.037/0.017	4.46/8.08
GRMZM2G124011	DREB subfamily A-1 of ERF/AP2 transcription factor family	0.013/0.028	4.26/3.85
GRMZM2G400714	Zn-finger, C2H2 transcription factor	0.015/0.002	3.85/4.37
GRMZM2G120320	Pathogen-induced transcription factor	0.037/0.037	3.67/2.91
GRMZM2G324999	WRKY Transcription Factor Group III	0.012/0.009	3.09/2.42

Three genes chosen from the microarray data were tested by qRT-PCR in order to verify the observed regulation by an independent method. Additionally, the genes were tested on samples with solvent-treated cells for the same time points as the trEAL1-treated samples. The genes chosen were *LOB-domain containing protein* (GRMZM2G060544), *Embryo sac development arrest 39* (*EDA39*, GRMZM2G061723) and *Pentatricopeptide repeat (PPR) superfamily protein* (GRMZM2G468521). In the array analysis, the *LOB-domain containing protein* was down-regulated by 11fold at time point 120 min and by 23fold at time point 540 min. *EDA39* was also downregulated by 3fold at time point 120 min. Finally, the *Pentatricopeptid repeat superfamily protein* was found to be 12fold upregulated 120 min after treatment. Analysis of the RNA-samples used for microarray and comparison with control samples revealed that two of the three investigated genes, *EDA39* (GRMZM2G061723) and *LOB domain containing protein* (GRMZM2G060544), appear to be affected rather by the handling than by action of trEAL1 (Table 5.9). All three candidate genes show the same tendency of expression level alteration in the qRT-PCR

experiment and the array experiment. Only *Pentatricopeptid superfamily protein* does not show regulation in the control experiment in the same way as upon trEAL1 treatment.

Table 5.9 Verification of chosen array-candidates by qRT-PCR. Expression was tested in samples from cells treated with 5 µM trEAL1 and solvent (control), respectively. Data comprise the mean of three biological replicates. FC = fold change

		FC qRT-PCR EAL1		FC qRT-PCR control		FC array	
Locus	**Description**	**120 min**	**540 min**	**120 min**	**540 min**	**120 min**	**540 min**
GRMZM2G468521	Pentatricopeptid superfamily protein	4.28	1.84	0.53	0.24	12.05	2>FC>0.5
GRMZM2G061723	EDA39	0.42	0.55	0.49	0.61	0.33	2>FC>0.5
GRMZM2G060544	Lob domain containing protein	0.07	0.03	0.02	0.01	0.22	0.04

5.4 Discussion

5.4.1 Interaction partner of trEAL1

In order to identify an interaction partner of trEAL1, a Yeast Two-Hybrid-screen (Y2H) was carried out (Denninger 2010). Further analysis of the candidate genes isolated left no *bona fide* candidate for interaction with trEAL1, which could explain phenotypes observed in embryo sac (Krohn *et al.* submitted) and embryo development (this chapter). An AAA-ATPase, a homologue of *SEC18* from baker's yeast (Novick and Scheckman 1979) or N-ethylmaleimide-sensitive factor (NSF) from human (Wilson *et al.* 1992) showed robust Y2H-interaction with its full-length version (Kolb 2011), but the interaction could not be verified by an independent method. Co-immune precipitation was applied but failed to prove specific interaction. FRET-assays in tobacco leaf-epidermis cells were not promising since a RFP-tagged version of fl#33 was not localised equally to EAL1-GFP. Expression level of EAL1-RFP was thus too low to be detected with the settings applied. It may be that fl#33 requires multimerisation in order to be targeted to the ER as shown by Kolb (2011). In this case, multimerisation of RFP-fl#33 would be disturbed by RFP as observed for some viral proteins (M. Heinlein, personal communication). Regardless of possible properties of fl#33, it appears to be a cytosolic protein associated under certain condition with the ER. Under normal conditions it cannot get in contact with EAL1, which is most likely secreted via the secretory pathway (Krohn, Lausser et al. submitted). Nevertheless, EAL1 is a very small peptide. This allows speculations about missorting or a transient

cytoplasmatic localization. Protein synthesis could be too fast for ER import (Shao and Hegde 2011) and the peptide would end up in the cytosol. This situation would allow interaction between #33 and EAL1. Speculative function of this interaction could be modulation of #33-activity by EAL1 and thereby modulation of secretion of postulated signal, which would then be responsible for *eal1*-phenotypes. Alternatively on could speculate about the role of #33 as a "sensor" for small secretory peptides in the cytosol, which would go along with unspecific peptide binding in the Co-IP-experiment. Yet, both hypotheses lack any proof or supporting evidence other than the Y2H-interaction and further experiments are awaited.

5.4.3 Pattern formation and regulation of ZmEAL1 by auxin

In order to learn more about the role of ZmEAL1 in early embryo development and the regulation of *ZmEAL1* several transgenic maize lines were analyzed during 1 – 8 dap. The expression domain of ZmEAL1 in the transition stage overlaps partially with *PIN1a::PIN1a-YFP* and *ABPHYL1::ABPHYL1-mRFP* (Figure 5.25). Since presence of an auxin-efflux carrier allows speculating about the presence of auxin as well, *ZmEAL1* might be regulated by auxin. Earlier studies using immunolocalisation of auxin (Forestan, Meda et al. 2010) indicate the presence of auxin in the domain of *ZmEAL1*-expression. However, auxin signaling could not be confirmed by analysis of DR5::ERmRFP plant lines. The *bona fide* auxin-regulated synthetic promoter-construct *DR5* shows no activity in the transition stage embryo (Figure 5.25). Yet, this doesn't exclude auxin dependent gene expression to occur. The observed patterns of *DR5::ERmRFP* and *PIN1a::PIN1a-YFP* are furthermore opposing data published recently (Forestan, Meda et al. 2010). Expression of *PIN1a* in the endosperm during 1 - 8 dap was not observed. This indicates that *PIN1*-expression in the basal endosperm transfer layer (BETL) and the embryo surrounding region (ESR, Forestan *et al.* 2010) is either due to *PIN1b*/*PIN1c* expression or *PIN1a-YFP* expression in this area is below the detection limit for YFP by the CLSM used in this study. In the endosperm 6 dap *DR5* expression is not found in the ESR, which is surprising considering the finding of high levels of auxin in this area (Forestan, Meda et al. 2010). The *DR5* expression pattern found in coleoptylar stage embryos fits with the known auxin distribution as well (Forestan, Meda et al. 2010). Nevertheless, *DR5* activity was not observed in earlier developmental stages of the embryos or in BETL or aleurone cell which are supposed to have high auxin levels (Forestan, Meda et al. 2010).

The missing overlap of *DR5* driven marker gene expression and *EAL1* expression could be explained by either different modes of auxin-dependent gene regulation for *DR5* and *EAL1* or by the low expression dose of *DR5* in transition stage embryos which is not detected by the CLSM used in this study. Recently it had been shown, that the marker system *DII-Venus*, which is degraded in response to auxin, detects temporal and spatial auxin signaling pattern, which only partially overlap with *DR5* expression (Brunoud *et al.* 2012). Alternatively one could postulate that auxin-dependent gene expression does not occur in early stages of maize embryo development. Yet, this seems to be unlikely since *PIN1* expression in NPA-treated kernels is altered and developmental phenotypes occur (Forestan, Meda et al. 2010). At least in BMS-suspension cells, the expression of *ZmEAL1* is not dependent on auxin. This was also found by using a promoter-reporter construct (*pEAL1::GFP*) in the same cell type (Krohn 2010). Still, it is possible that *ZmEAL1*-expression could be auxin-dependent in another context than BMS-cells. Tissue-specific sensitivity of gene expression to phytohormones is shown for example for *ABPHYL1*, the third marker line applied in this work. *ABPHYL1-mRFP* and *EAL1-GFP* show partial overlap of expression domains in the transition stage embryo. For cytokinin-dependent expression of A-type response regulators it was shown that all but *ZmRR3* (= *ABPHYL1*) could be induced by trans-zeatin infiltration in maize leaves (Asakura *et al.* 2003). Later it was shown for *ABPHYL1* that its expression domain expands upon kinetin treatment and is therefore cytokinin-dependent (Giulini, Wang et al. 2004). Cytokinin-dependent alterations of gene-expression levels were not detectable in BMS-cells neither upon treatment with trans-zeatin, kinetin or the cytokinin-signalling inhibitor PI-55 (Nisler *et al.* 2010). Detailed RT-PCR-experiments with different control genes remained unsuccessful (data not shown). Therefore, the question if *ZmEAL1*-expression is possibly cytokinin-dependent as suggested by the partial overlap of *ZmEAL1-GFP*- and *ABPHYL1-mRFP* expression remains unanswered so far. The overlap of *ABPHYL1* and *EAL1* further indicates that the expression domain of *EAL1* includes the area of the emerging SAM. If this is true, *EAL1*-expression should overlap with the maize homologue of *SHOOT MERISTEMLESS* called *KNOTTED 1* (Smith, Jackson et al. 1995) and at its expression in the protoderm with *OUTER CELL LAYER 4* (Ingram, Boisnard-Lorig et al. 2000). A maize line carrying a *KNOTTED1::GFP-KNOTTED1* construct might soon be available for colocalization studies (maize.jcvi.org). Further hints on the role of EAL1 could be found in the analysis of *eal1*-RNAi lines in early embryo development.

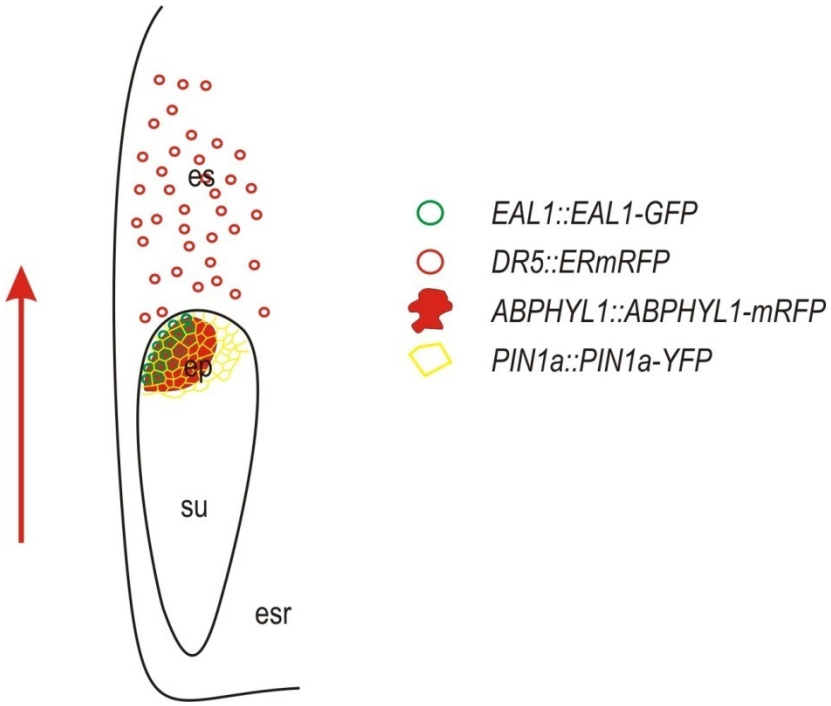

Figure 5.25 Cartoon of marker gene expression in transition stage maize embryos. EAL1-GFP, PIN1a-YFP and ABPHYL1-mRFP partially overlap in transition stage embryos of maize. The auxin-dependent *DR5*-promoter is not expressed in the embryo at this stage. The red arrow indicates position and orientation of the cob axis. ep = embryo proper, esr = embryo surrounding region, su = suspensor.

The role of ZmEAL1 in early embryo development remains unclear, although embryo and endosperm development might be affected in the analyzed RNAi-lines. Up to now it cannot be excluded that the observed variations are within the physiological range of maize embryo development. The used wild type samples were collected from an inbred line (A188), which is one of the two parental lines of the RNAi-lines analysed. Since hybrid genotypes are usually more robust and faster in their development than inbred lines (Meyer *et al.* 2007) it seems to be unlikely that the observation of delayed embryo development is due to normal genetic variation between the lines. A dramatic effect with obvious changes in cell identities as it is observed in the ovules of the same RNAi-lines (***Chapter 4***) was at least not detectable.

In order to form a hypothesis how EAL1 can influence embryo sac, embryo and endosperm development one has to consider the possible interplay between these structures. Recently the mutant *stunter1* (*stt1*; Phillips and Evans 2011), which is affected in male and female gametophyte development, was shown to have also defects in embryo and endosperm development, respectively. Considering the data currently published, it cannot be decided if *stt1* defects in embryo development are due to defective endosperm or

due to *stt1*-dependent effects in the embryo itself. Similarly, it can currently not be decided, if the endosperm defects observed in *eal1*-RNAi are due to *eal1* effects in the embryo (maybe even the central cell) or due to non-cell autonomous functions of embryo expressed *EAL1* in the endosperm itself.

5.4.5 Downstream targets of ZmEAL1 signalling

Understanding ZmEAL1 signalling requires identification of downstream elements. The microarray experiment delivered a list of candidates for EAL1-dependent genes. In a first selection of this list, two genes have been shown to be false positives and seem to be rather regulated by the handling of the cells than by action of the peptide trEAL1. Yet, one of the tested genes, a pentatricopeptide-repeat (PPR) protein (GRMZM2G468521) seems to be induced by trEAL1. PPR protein expression is absent at timepoint 0 and 540. This type of protein thought to be involved in organelle gene expression (for review see Saha *et al.* 2007). For *Arabidopsis* it has been shown that this type of protein is also involved in embryo development. Interestingly, the embryos of homozygous T-DNA-insertion lines arrest in early developmental phases (Cushing *et al.* 2005). Although no significant number of arrested embryos was found in *eal1*-RNAi-plants, the hampered embryo development found in the RNAi-lines could therefore be due to action of a PPR-protein.

Interesting candidate genes that can be deduced from the array data so far are the large number of transcription factors which are found to be strongly regulated at both time points. Also proteins involved in signaling are found to be probably regulated upon trEAL1-treatment. A calcium binding EF-hand protein (GRMZM2G153404) is found to be strongly up-regulated after 2 h (see 3.1 for calcium signaling). Also signal transduction proteins like a so far uncharacterized putative serine/threonin-kinase (GRMZM2G114057) is up-regulated after 9 h. Also links to phytohormone signaling can be found. The strongest up-regulated gene after 9 h is an A-type response regulator (GRMZM2G129954) which is a protein involved in cytokinin signaling (Perilli *et al.* 2011). A gene annotated as being auxin inducible (GRMZM2G143352) is up-regulated at the same timepoint.

In microarray analysis expression of the putative target *INDETERMINDE GAMETOPHYTE* 1 (*IG1*, ***Chapter 4***) was not detectable in BMS-suspension cell (data not shown). The trEAL1-treated suspension cells mimic an overexpression situation and could be equal to a second allele in maize, showing EAL1 dependent *IG1* expression. Since absence of signals in the microarray experiments is no proof of absence for gene

expression, qRT-PCR on BMS-samples could be applied for determining EAL1-dependent *IG1* expression. Alternatively, samples of ovule or embryo tissue could be treated with EAL1-peptide and be analyzed for regulation of *ZmIG1* or other potential targets of EAL1-signalling.

5.4.6 Outlook

Major questions of the biology of ZmEAL1 remain still open. On the technical side, there is a urgent need for better genetic support of the data obtained so far. Because it was not possible to show down-regulation of *EAL1* in the RNAi-lines, final proof of relevance of all observed phenotypes, the dramatic ones in embryo sac development and the discrete ones in embryo development, is missing. Even if down-regulation would be shown in embryo tissue, which would be easier on the technical level compared to ovules, additional independent *EAL1*-RNAi-lines have to be studied. Hitherto, a transposon insertion or TILLING line affecting the locus of ZmEAL1 is not available. Therefore, construction of misexpression-lines would to be the only choice for improving support of the genetic data. In parallel, treatment of tissues and explants with synthetic trEAL1 mimicking EAL1-overexpression can be a valuable tool for studying EAL1-dependent transient effects on steady-state-mRNA levels of single genes like *ZmIG1* or the EAL1-dependent PPR-protein. A similar strategy could be applied to revisit regulation of *ZmEAL1* itself be phytohormones. Synthetic hormones and inhibitors (PCIB for auxin or PI-55 for cytokinin) are at hand and could be used in tissues combined with *in situ* hybridisation or qRT-PCR in order to address phytohormone dependent gene expression-regulation of EAL1. With the help of the fusion protein plant line, these studies could be expanded from the transcriptional to the translational level.

The findings about trEAL1-regulated genes in BMS-cells have three implications for future experiments: First, the dataset of downstream targets might contain a number of false positives that need to be removed by a control array experiment with untreated cells sampled after 120 min or 540 min, respectively. Second, the remaining candidates, at least the PPR-protein need to be verified during embryogenesis in wild type and *eal1*-RNAi-background. Finally, the EAL1-dependent gene expression change of the PPR-protein indicates that BMS-suspension cells react on trEAL1 treatment. In other words they must express a receptor protein, which was initially aimed to be identified during a Y2H-

experiment. BMS cells now provide a tool to identify the receptor using biochemical methods and labeled synthetic EAL1.

5.5 Summary

For gaining new insights into the function and signaling pathway of the novel secreted peptide ZmEAL1 several experiments were performed: in order to get recombinat peptide for downstream applications, ZmEAL1 and its homolog ZmEA1 were expressed in various systems. Expression of recombinant fusion proteins of ZmEA1 and ZmEAL1 in *Nicotiana benthamiana* and *Escherichia coli* did not yield sufficient soluable peptide amounts for downstream applications. Therefore, chemically synthesised peptide of the predicted mature form of ZmEAL1 (trEAL1) was purchased and used for bioassays.

A yeast-2-hybrid (Y2H) screen was carried out in collaboration with two bachelor students (Denninger 2010; Kolb 2011) to identify putative interaction partners of ZmEAL1. A homologue of the yeast SEC18 protein as found be the best candidate (the protein was named as #33 after the clone from the screen, (Denninger 2010). The yeast Sec18 protein, homologous to human N-ethylmaleide-sensitive factor (NSF), is required for dissasembly of the 20S "fusion particle" after vesicle fusion (Wilson, Whiteheart et al. 1992). Specific interaction between #33 and EAL1 could not be confirmed by a method independent of the Y2H-system. #33 could not rescue yeast cells carrying the temperature sensitive allele *sec18*^{ts}. Yet, #33 exhibits some features of SEC18/NSF proteins. It could be shown to form homodimers in Y2H-experiments. Furthermore binding to small peptides (cMyc-trEAL1 and cMyc) was ATP-dependent. Nevertheless, subcellular localization experiments indicated that #33 is a cytosolic protein, which under certain conditions is attached to the ER from the cytosolic side. It is unlikely that #33 is an *in vivo* interaction partner of ZmEAL1.

It was previously described, that *ZmEAL1* is expressed during embryogenesis until the transition stage. The expression pattern of *EAL1-GFP* in the transition stage embryo partially overlapps with *PIN1a-YFP* and *ABPHYL1-mRFP* protein localization but not with the activity of the *DR5*-promoter construct. Although probably not regulated by auxin in the same AuxRE-dependent pathway as *DR5*, *EAL1* expression could still be downstream of auxin. It can be speculated, that the partial overlap of expression domains of *EAL1-GFP* and *PIN1a-YFP* points at presence of auxin in this area.

The influence of EAL1 on development of fertilisation products of maize is probably marginal compared to the striking developmental defects during embryo sac development. Endosperm and embryo 7 dap appeared to be smaller in two of three *eal1*-RNAi-lines compared to wild type. Treatment of BMS-cells with trEAL1 did not have obvious phenotypic effects. Nevertheless, microarray analysis identified a number of candidate targets of EAL1-signalling. Among those are LOB-domain transcriptional regulators (GRMZM2G073044 and GRMZM2G386674). A pentatricopeptide repeat protein (PPR) was found to be induced two hours after treatment of suspension cells with synthetic EAL1. This expression pattern could be validated by qRT-PCR. Validation of other candidates is awaited.

Chapter 6 - Comprehensive discussion and outlook

Sexual reproduction of angiosperms is a multistage process involving two sporophytic generations (parents and embryo) and one gamteophytic generation (male and female gametophyte). The central hallmark of this process is double fertilization (Nawaschin 1898; Guignard 1899). In order to achieve the unification of male (sperm cells) and female gametes (egg cell and central cell) sperm cells have to be delivered to the female gametophyte. The structure which delivers the sperm cells is the pollen tube (cell). Pollen tube development is also summarised as progamic development of the male gametophyte (Bedinger and Fowler 2009). In ***Chapter 2*** it is shown that progamic pollen tube development in maize is mainly governed by the sporophyte. Five phases of progamic pollen tube development were defined in homology to *Arabidopsis* (Johnson and Preuss 2002). The influence of the female gametophyte appears to be restricted to the micropylar region, similar to the area controlled by EGG APPARATUS 1 (EA1) dependent micropylar pollen tube guidance (Márton *et al.* 2005). This is in contrast to *Arabidopsis* where the female gametophyte is requiered for micropylare (short range) and funicular (long range) pollen tube guidance (Johnson and Preuss 2002). Intra-specific hybridisation barriers related to *GAMTOPHYTE FACTOR 1* (*Ga1*, Nelson 1952) and inter-specific barriers between maize and *Tripsacum dactyloides* (Mangelsdorf and Reeves 1931) point at a specific interaction between pollen tubes and transmitting tracts. From that we conclude, that targeting of the transmitting tracts by the pollen tubes is an actively regulated process and not exclusively governed by the tissue architecture as formerly assumed (Heslop-Harrison *et al.* 1985).

The most interesting future research field in this context is transmitting tract targeting by the pollen tube. Cloning of the *Ga1*-gene would be a step forward in understanding the communication between pollen tube and transmitting tract. It would allow achieving a deeper understanding of this interaction by employing molecular tools in addition to the genetic ones available. So far, it is unclear whether pollen tube attraction by the transmitting tracts is constitutive or induced upon pollination. No other genes are known to be involved in this process. Candidates for such genes would be *TEOSINTHE CROSSING BARRIER 1* (Kermicle and Evans 2005) or *GAMEOPHYTE FACTOR 2* (Kermicle and Evans 2010). The puzzling finding, that for the silk expressed allele of the recessive null allele *ga1* allows genotype independent fertilization whereas the dominate allele *Ga1s* confers a fertilization barrier promises an interesting molecular basis of this pathway.

Not only cell-cell communication, also intracellular signalling is an important aspect of fertilization. Calcium is a major signalling compound which has already been shown to be involved in double fertilization of plants. Pollen tube growth has been shown to depend on calcium *in vitro* and *in vivo* (Iwano, Shiba et al. 2004). Gamete fusion requires calcium *in vitro* (Kranz, Bautor et al. 1991). In ***Chapter 3*** the construction of marker lines, comprising tools for studying calcium signaling during double fertilization is discussed. A plasma membrane marker for gametophytic cells was supposed to highlight gametophyte cell boundaries during fertilization. The recombinant calcium probe CerTN-L15 (Heim and Griesbeck 2003) was expressed in vegetative tissues and gametophytic cell types (egg cell, synergids and pollen). Initial trails to proof functionality of the probe in pollen tubes failed. Meanwhile two lines were shown to detect reliably calcium signals *in vivo* in roots and synergids (P. Denninger and G. Grossmann in collaboration).

Future experiments applying the calcium sensor lines established within the course of this thesis will help to address many open questions on calcium signaling during double fertilisation. Calcium spiking in the synergids upon pollen tube arrival has been reported (P. Denninger and G. Grossmann personal communication), but its biological meaning remains unclear. Several mutants like *feronia* (Escobar-Restrepo, Huck et al. 2007), *nortia* (Kessler *et al.* 2010) *lorelei* (Capron *et al.* 2008) or even *myb98* (Kasahara *et al.* 2005)) could be tested for occurrence of such calcium spiking. On the other hand, calcium signaling components (pumps, channels, calmodulines, etc.) which are expressed in pollen, synergids and egg cells could be identified already from microarray experiments (L. Šolijć and S. Sprunck, unpublished). Characterization of mutants of such genes in terms of fertilization defects and aberrant calcium signalling would allow modeling the calcium signaling network during fertilization. Further characterization of the wild type situation of calcium signaling is still required. An open question is whether calcium waves or spikes occur in pollen tubes upon arrival at the micropyle at the same time as the synergid spikes occur. Do calcium levels rise in pollen tubes prior to sperm cell release? Furthermore, it has to be shown if the calcium waves observed during *in vitro* fertilization of the egg cell (Antoine *et al.* 2001) can also be found *in vivo*. The constructed calcium sensor lines comprise the basic tool to address these questions.

A different type of signaling molecules are peptides. A class of peptides which is only partially characterized is the EA1-box family, named after ZmEA1 from maize (Márton *et al*. 2005). As shown in ***Chapter 4***, EA1-LIKE 1 (EAL1) is expressed in egg cells and after fertilisation until the transition stage. *eal1*-RNAi-ovules exhibit developmental defects including degenerated embryo sacs, supernumerary polar nuclei and central cell like structures as well as autonomous endosperm development. The *LATERAL ORGAN BOUNDARY* transcription factor gene *INDETERMINED GAMETOPHYTE 1* (Evans 2007) was shown to be down-regulated in *eal1*-RNAi ovules. *EAL1* expression itself was found to be independent of auxin. The peptide appears to accumulate at the chalazal pole of the egg cell. In ***Chapter 5*** the additional role of EAL1 during early embryogenesis is discussed. The expression domain partially overlaps with expression of *PINFORMED 1a* (*PIN1a*) and *ABERRANT PHYLOTAXY 1* (*ABPHYL1*) but not with *DR5*. In BMS cells, an additional potential target, a pentatricopeptide repeat protein, was identified. In *eal1*-RNAi-lines early development of endosperm and embryo seem to be delayed. Finally, a yeast-2-hybrid screen delivered a homologe of yeast *SEC18* as putative interaction partner of EAL1.

The findings of ***Chapter 4*** and ***5*** characterize ZmEAL1 as a novel signaling peptide required for cell identity control in embryo sac development and regulation of embryo and endosperm development after fertilization. Although some advances have been made to study this novel signaling peptide many points need to be verified. First, the genetic data on *eal1* mutants after fertilization rely on a single mutant allele (RNAi) which doesn't allow to discriminate between true *eal1* phenotypes and off-target effects as observed frequently in other systems (Ma *et al.* 2006). Therefore at least one additional knock-out line would be required to verify the observed phenotypes. Unfortunately such a line (Ac/Ds insertion, Mu-stocks, TILLING) could not be found yet in public databases (http://popcorn.maizegdb.org) until now, but might be available in the future. An overexpression line could also be used for validation of the RNAi data. This situation can be mimicked by the use of synthetic EAL1 peptide on suspension cells and tissue samples. Therefore, microarray data discussed in ***Chapter 5*** can be validated analyzing mRNA-levels of candidate genes in RNAi-line samples and *vice versa*. Additionally, wildtype and RNAi tissue samples can be treated with EAL1 and be used for transcription analysis or be tested for complementation of the RNAi-phenotypes. It will be difficult to verify the developmental RNAi-effects, since EAL1 cannot be applied to its gametophytic or embryonic expression domain *in planta. In vitro* cultures of immature embryos (Mol *et al.*

1993) and ovule (Lobanova and Enaleeva 1998) are difficult but possible. The discrete phenotypes of *eal1*-RNAi-embryos on the other hand might be difficult to be reproduced in an *in vitro* system. A protocol for *in vitro* of ovules faces the problem of low abundance of RNAi-phenotypes.

The regulation of *EAL1* itself is unclear as well. It seems to be independent of auxin in suspension cells, but this doesn't necessarily apply to its usual expression domain. Similar observations were made for *ABPHYL1* which is inducible by cytokinin in shoots and SAM (Giulini, Wang et al. 2004) but not in leaves (Asakura *et al.* 2003). On the other hand, it is possible that *EAL1* expression is dependent on cytokinin since the expression domain partially overlaps with *ABPHYL1*. Expression studies in maize using tissue samples treated with cytokinin or the cytokinin signaling inhibitor PI-55 (Nisler *et al.* 2010) could help to address this question. Cytokinin dependent chances of *bona fide* cytokinin regulated genes in BMS cells were not detectable so far.

Finally, the search for a receptor of EAL1 still goes on. The *SEC18*-homologe, isolated from the Y2H-screen is a puzzling candidate. A cytosolic protein, such as SEC18-protein (Novick and Schekman 1979), can interact with a secreted peptide only if the peptide is missorted into the cytosol. This is not unlikely for small peptides (Shao and Hegde, 2011) like EAL1, but the putative function of a SNARE-recycling *SEC18*-homologe is difficult to integrate with the observed non-cellautonomous phenotypes of *eal1*-RNAi lines. It would be required to postulate the regulation of secretion of another signal by EAL1 in a *SEC18*-homologe-dependend manner. If the cytological data in ***Chapter 4*** are taken into account, this scenario appears to be less likely than EAL1 being the secreted signal itself.

Furthermore, the extracellular EAL1-similar signalling peptide EA1 was recently shown to be sufficient for short range pollen tube guidance (Márton *et al.* 2005). Biochemical approaches of identifying an interaction partner of EAL1 could not been made, since affinity tagged versions of EAL1 could not be produced and purified in large amounts within the course of this thesis. BMS suspension cell could be valuable tool in this context. Up to now it is still to be shown that the observed trEAL1-related transcription changes are really EAL1-dependent and not due to a putative "factor X". A powerful tool to rule out such effects would be verification of complementary transcriptional changes in *eal1*-RNAi-lines relative to wild type. This independent method would proof the EAL1-specific effect on transcription of target genes isolated from the microarray data. Once BMS suspension culture is verified to respond to the EAL1 peptide, this material could be a good starting point for purification of an EAL1-receptor.

References

Abbe, E. C. and O. L. Stein (1954). "The growth of the shoot apex in maize: Embryogeny." Amer Jour Bot **41**((4)): 285-293.

Ali, R., W. Ma, F. Lemtiri-Chlieh, D. Tsaltas, Q. Leng, S. von Bodman and G. A. Berkowitz (2007). "Death don't have no mercy and neither does calcium: Arabidopsis CYCLIC NUCLEOTIDE GATED CHANNEL2 and innate immunity." Plant Cell **19**(3): 1081-1095.

Amien, S., I. Kliwer, M. L. Marton, T. Debener, D. Geiger, D. Becker and T. Dresselhaus (2010). "Defensin-Like ZmES4 Mediates Pollen Tube Burst in Maize via Opening of the Potassium Channel KZM1." Plos Biology **8**(6).

Antoine, A. F., C. Dumas, J. E. Faure, J. A. Feijo and M. Rougier (2001). "Egg activation in flowering plants." Sexual Plant Reproduction **14**(1-2): 21-26.

Arnold, M. L. and S. A. Hodges (1995). "Are Natural Hybrids Fit or Unfit Relative to Their Parents." Trends in Ecology & Evolution **10**(2): 67-71.

Asakura, Y., T. Hagino, Y. Ohta, K. Aoki, K. Yonekura-Sakakibara, A. Deji, T. Yamaya, T. Sugiyama and H. Sakakibara (2003). "Molecular characterization of His-Asp phosphorelay signaling factors in maize leaves: Implications of the signal divergence by cytokinin-inducible response regulators in the cytosol and the nuclei." Plant Molecular Biology **52**(2): 331-341.

Bahyrycz, A. and D. Konopinska (2007). "Plant signalling peptides: some recent developments." Journal of Peptide Science **13**(12): 787-797.

Bass, H. W., W. F. Marshall, J. W. Sedat, D. A. Agard and W. Z. Cande (1997). "Telomeres cluster de novo before the initiation of synapsis: A three-dimensional spatial analysis of telomere positions before and during meiotic prophase." Journal of Cell Biology **137**(1): 5-18.

Batistic, O., N. Sorek, S. Schueltke, S. Yalovsky and J. Kudla (2008). "Dual fatty acyl modification determines the localization and plasma membrane targeting of CBL/CIPK Ca2+ signaling complexes in Arabidopsis." Plant Cell **20**(5): 1346-1362.

Becker, B. and B. Marin (2009). "Streptophyte algae and the origin of embryophytes." Annals of Botany **103**(7): 999-1004.

Becker, D., R. Brettschneider and H. Lorz (1994). "Fertile Transgenic Wheat from Microprojectile Bombardment of Scutellar Tissue." Plant Journal **5**(2): 299-307.

Bedinger, P. A. and J. E. Fowler (2009). The Maize Male Gametophyte. J. L. Bennetzen and S. C. Hake, Springer-Verlag New York, Inc.; Springer-Verlag**:** 57-77.

Berridge, M. J., M. D. Bootman and H. L. Roderick (2003). "Calcium signalling: Dynamics, homeostasis and remodelling." Nature Reviews Molecular Cell Biology **4**(7): 517-529.

Bertani, G. (1951). "Studies on lysogenesis. I. The mode of phage liberation by lysogenic Escherichia coli." Jour Bact **62**((3)): 293-300.

Beyhl, D., S. Hoertensteiner, E. Martinoia, E. E. Farmer, J. Fromm, I. Marten and R. Hedrich (2009). "The fou2 mutation in the major vacuolar cation channel TPC1 confers tolerance to inhibitory luminal calcium." Plant Journal **58**(5): 715-723.

Boisson-Dernier, A., S. Frietsch, T.-H. Kim, M. B. Dizon and J. I. Schroeder (2008). "The peroxin loss-of-function mutation abstinence by mutual consent disrupts male-female gametophyte recognition." Current Biology **18**(1): 63-68.

Bommert, P. and W. Werr (2001). "Gene expression patterns in the maize caryopsis: clues to decisions in embryo and endosperm development." Gene **271**(2): 131-142.

Booy, G., F. A. Krens and R. J. Bino (1992). "Analysis of Pollen-Tube Growth in Cultured Maize Silks." Sexual Plant Reproduction **5**(3): 227-231.

Bradford, M. M. (1976). "Rapid and Sensitive Method for Quantitation of Microgram Quantities of Protein Utilizing Principle of Protein-Dye Binding." Analytical Biochemistry **72**(1-2): 248-254.

Brettschneider, R., D. Becker and H. Lorz (1997). "Efficient transformation of scutellar tissue of immature maize embryos." Theoretical and Applied Genetics **94**(6-7): 737-748.

Brunoud, G., D. M. Wells, M. Oliva, A. Larrieu, V. Mirabet, A. H. Burrow, T. Beeckman, S. Kepinski, J. Traas, M. J. Bennett and T. Vernoux (2012). "A novel sensor to map auxin response and distribution at high spatio-temporal resolution." Nature **482**(7383): 103-U132.

Capron, A., M. Gourgues, L. S. Neiva, J.-E. Faure, F. Berger, G. Pagnussat, A. Krishnan, C. Alvarez-Mejia, J.-P. Vielle-Calzada, Y.-R. Lee, B. Liu and V. Sundaresan (2008). "Maternal Control of Male-Gamete Delivery in Arabidopsis Involves a Putative GPI-Anchored Protein Encoded by the LORELEI Gene." Plant Cell **20**(11): 3038-3049.

Chen, H., R. S. Nelson and J. L. Sherwood (1994). "Enhanced Recovery of Transformants of Agrobacterium-Tumefaciens after Freeze-Thaw Transformation and Drug Selection." Biotechniques **16**(4): 664-&.

Cheong, Y. H., K. N. Kim, G. K. Pandey, R. Gupta, J. J. Grant and S. Luan (2003). "CBL1, a calcium sensor that differentially regulates salt, drought, and cold responses in Arabidopsis." Plant Cell **15**(8): 1833-1845.

Cheong, Y. H., G. K. Pandey, J. J. Grant, O. Batistic, L. Li, B.-G. Kim, S.-C. Lee, J. Kudla and S. Luan (2007). "Two calcineurin B-like calcium sensors, interacting with protein kinase CIPK23, regulate leaf transpiration and root potassium uptake in Arabidopsis." Plant Journal **52**(2): 223-239.

Chevallet, M., S. Luche and T. Rabilloud (2006). "Silver staining of proteins in polyacrylamide gels." Nature Protocols **1**(4): 1852-1858.

Christensen, C. A., E. J. King, J. R. Jordan and G. N. Drews (1997). "Megagametogenesis in Arabidopsis wild type and the Gf mutant." Sexual Plant Reproduction **10**(1): 49-64.

Clapham, D. E. (1995). "Calcium Signaling." Cell **80**(2): 259-268.

Clapham, D. E. (2007). "Calcium signaling." Cell **131**(6): 1047-1058.

Clark, S. E. (2001). "Cell signalling at the shoot meristem." Nature Reviews Molecular Cell Biology **2**(4): 276-284.

Clark, S. E., M. P. Running and E. M. Meyerowitz (1995). "Clavata3 Is a Specific Regulator of Shoot and Floral Meristem Development Affecting the Same Processes as Clavata1." Development **121**(7): 2057-2067.

Clough, S. J. and A. F. Bent (1998). "Floral dip: a simplified method for Agrobacterium-mediated transformation of Arabidopsis thaliana." Plant Journal **16**(6): 735-743.

Crespi, M. D., E. Jurkevitch, M. Poiret, Y. Daubentoncarafa, G. Petrovics, E. Kondorosi and A. Kondorosi (1994). "Enod40, a Gene Expressed During Nodule Organogenesis, Codes for a Nontranslatable Rna Involved in Plant-Growth." Embo Journal **13**(21): 5099-5112.

Cushing, D. A., N. R. Forsthoefel, D. R. Gestaut and D. M. Vernon (2005). "Arabidopsis emb175 and other ppr knockout mutants reveal essential roles for pentatricopeptide repeat (PPR) proteins in plant embryogenesis." Planta **221**(3): 424-436.

De Smet, I., S. Lau, U. Mayer and G. Juergens (2010). "Embryogenesis - the humble beginnings of plant life." Plant Journal **61**(6): 959-970.

Denninger, P. (2010). Untersuchungen zur Rolle des Signalpeptids ZmEAL1 und des Pflanzenhormons Auxin
in der Embryogenese von Mais. Department for cell biology and plant biochemistry. Regensburg, University of Regensburg.
Dhalluin, K., E. Bonne, M. Bossut, M. Debeuckeleer and J. Leemans (1992). "Transgenic Maize Plants by Tissue Electroporation." Plant Cell **4**(12): 1495-1505.
Diboll, A. G. and D. A. Larson (1966). "An Electron Microscopic Study of Mature Megagametophyte in Zea Mays." American Journal of Botany **53**(4): 391-&.
Digonnet, C., D. Aldon, N. Leduc, C. Dumas and M. Rougier (1997). "First evidence of a calcium transient in flowering plants at fertilization." Development **124**(15): 2867-2874.
Dodd, A. N., J. Kudla and D. Sanders (2010). The Language of Calcium Signaling. Annual Review of Plant Biology, Vol 61. **61:** 593-620.
Dresselhaus, T., S. Amien, M. Marton, A. Strecke, R. Brettschneider and S. Cordts (2005). "TRANSPARENT LEAF AREA1 encodes a secreted proteolipid required for anther maturation, morphogenesis, and differentiation during leaf development in maize." Plant Cell **17**(3): 730-745.
Dresselhaus, T., C. Hagel, H. Lorz and E. Kranz (1996). "Isolation of a full-length cDNA encoding calreticulin from a PCR library of in vitro zygotes of maize." Plant Molecular Biology **31**(1): 23-34.
Dresselhaus, T., A. Lausser and M. L. Marton (2011). "Using maize as a model to study pollen tube growth and guidance, cross-incompatibility and sperm delivery in grasses." Annals of Botany **108**(4): 727-737.
Dresselhaus, T., H. Lorz and E. Kranz (1994). "Representative Cdna Libraries from Few Plant-Cells." Plant Journal **5**(4): 605-610.
Dresselhaus, T. and S. Sprunck (in press). "Plant fertilization: maximizing reproductive success." Current Biology **22**.
Drobak, B. K. and P. A. C. Watkins (2000). "Inositol(1,4,5)trisphosphate production in plant cells: an early response to salinity and hyperosmotic stress." Febs Letters **481**(3): 240-244.
Dumas, C. and T. Gaude (2006). "Fertilization in plants: Is calcium a key player?" Seminars in Cell & Developmental Biology **17**(2): 244-253.
Ebel, C., L. Mariconti and W. Gruissem (2004). "Plant retinoblastoma homologues control nuclear proliferation in the female gametophyte." Nature **429**(6993): 776-780.
Emr, S. D., R. Schekman, M. C. Flessel and J. Thorner (1983). "An Mf Alpha-1-Suc2 (Alpha-Factor-Invertase) Gene Fusion for Study of Protein Localization and Gene-Expression in Yeast." Proceedings of the National Academy of Sciences of the United States of America-Biological Sciences **80**(23): 7080-7084.
Endo, M. (2009). "Calcium-Induced Calcium Release in Skeletal Muscle." Physiological Reviews **89**(4): 1153-1176.
Escobar-Restrepo, J.-M., N. Huck, S. Kessler, V. Gagliardini, J. Gheyselinck, W.-C. Yang and U. Grossniklaus (2007). "The FERONIA receptor-like kinase mediates male-female interactions during pollen tube reception." Science **317**(5838): 656-660.
Evans, M. M. S. (2007). "The indeterminate gametophyte1 gene of maize encodes a LOB domain protein required for embryo sac and leaf development." Plant Cell **19**(1): 46-62.
Evans, M. M. S. and U. Grossniklaus (2009). The Maize Megagametophyte. Handbook of Maize: Its Biology**:** 79-104.
Finkler, A., R. Ashery-Padan and H. Fromm (2007). "CAMTAs: Calmodulin-binding transcription activators from plants to human." Febs Letters **581**(21): 3893-3898.

Fiume, E. and J. C. Fletcher (2012). "Regulation of Arabidopsis Embryo and Endosperm Development by the Polypeptide Signaling Molecule CLE8." The Plant cell **24**(3): 1000-12.

Forestan, C., S. Meda and S. Varotto (2010). "ZmPIN1-Mediated Auxin Transport Is Related to Cellular Differentiation during Maize Embryogenesis and Endosperm Development." Plant Physiology **152**(3): 1373-1390.

Franklin-Tong, V. E., T. L. Holdaway-Clarke, K. R. Straatman, J. G. Kunke and P. K. Hepler (2002). "Involvement of extracellular calcium influx in the self-incompatibility response of Papaver rhoeas." Plant Journal **29**(3): 333-345.

Frietsch, S., Y.-F. Wang, C. Sladek, L. R. Poulsen, S. M. Romanowsky, J. I. Schroeder and J. F. Harper (2007). "A cyclic nucleotide-gated channel is essential for polarized tip growth of pollen." Proceedings of the National Academy of Sciences of the United States of America **104**(36): 14531-14536.

Gallavotti, A., S. Barazesh, S. Malcomber, D. Hall, D. Jackson, R. J. Schmidt and P. McSteen (2008). "sparse inflorescence1 encodes a monocot-specific YUCCA-like gene required for vegetative and reproductive development in maize." Proceedings of the National Academy of Sciences of the United States of America **105**(39): 15196-15201.

Ge, L. L., H. Q. Tian and S. D. Russell (2007). "Calcium function and distribution during fertilization in angiosperms." American Journal of Botany **94**(6): 1046-1060.

Gebert, M., T. Dresselhaus and S. Sprunck (2008). "F-Actin Organization and Pollen Tube Tip Growth in Arabidopsis Are Dependent on the Gametophyte-Specific Armadillo Repeat Protein ARO1." Plant Cell **20**(10): 2798-2814.

George, L., S. M. Romanowsky, J. F. Harper and R. A. Sharrock (2008). "The ACA10 Ca2+-ATPase regulates adult vegetative development and inflorescence architecture in Arabidopsis." Plant Physiology **146**(2): 716-728.

Giulini, A., J. Wang and D. Jackson (2004). "Control of phyllotaxy by the cytokinin-inducible response regulator homologue ABPHYL1." Nature **430**(7003): 1031-1034.

Gomez-Roldan, V., S. Fermas, P. B. Brewer, V. Puech-Pages, E. A. Dun, J.-P. Pillot, F. Letisse, R. Matusova, S. Danoun, J.-C. Portais, H. Bouwmeester, G. Becard, C. A. Beveridge, C. Rameau and S. F. Rochange (2008). "Strigolactone inhibition of shoot branching." Nature **455**(7210): 189-U22.

Graham, M. A., K. A. T. Silverstein, S. B. Cannon and K. A. VandenBosch (2004). "Computational identification and characterization of novel genes from legumes." Plant Physiology **135**(3): 1179-1197.

Gray-Mitsumune, M. and D. P. Matton (2006). "The Egg apparatus 1 gene from maize is a member of a large gene family found in both monocots and dicots." Planta **223**(3): 618-625.

Gross-Hardt, R., C. Kaegi, N. Baumann, J. M. Moore, R. Baskar, W. B. Gagliano, G. Juergens and U. Grossniklaus (2007). "LACHESIS restricts gametic cell fate in the female gametophyte of Arabidopsis." Plos Biology **5**(3): 494-500.

Grossniklaus, U. (2011). "Plant germline development: a tale of cross-talk, signaling, and cellular interactions." Sexual Plant Reproduction **24**(2): 91-95.

Guignard, L. (1899). "Sur les anthérozoïdes et la double copulation sexuelle chez les végétaux angiospermes." Rev Gén Bot **11** 129–135.

Guilley, H., R. K. Dudley, G. Jonard, E. Balazs and K. E. Richards (1982). "Transcription of Cauliflower Mosaic-Virus DNA - Detection of Promoter Sequences, and Characterization of Transcripts." Cell **30**(3): 763-773.

Guitton, A. E. and F. Berger (2005). "Loss of function of MULTICOPY SUPPRESSOR OF IRA 1 produces nonviable parthenogenetic embryos in Arabidopsis." Current Biology **15**(8): 750-754.

Guo, F. L., B. Q. Huang, Y. Z. Han and S. Y. Zee (2004). "Fertilization in maize indeterminate gametophyte1 mutant." Protoplasma **223**(2-4): 111-120.

Gutierrez-Marcos, J. F., L. M. Costa, C. Biderre-Petit, B. Khbaya, D. M. O'Sullivan, M. Wormald, P. Perez and H. G. Dickinson (2004). "maternally expressed gene1 is a novel maize endosperm transfer cell-specific gene with a maternal parent-of-origin pattern of expression." Plant Cell **16**(5): 1288-1301.

Hamamura, Y., C. Saito, C. Awai, D. Kurihara, A. Miyawaki, T. Nakagawa, M. M. Kanaoka, N. Sasaki, A. Nakano, F. Berger and T. Higashiyama (2011). "Live-Cell Imaging Reveals the Dynamics of Two Sperm Cells during Double Fertilization in Arabidopsis thaliana." Current Biology **21**(6): 497-502.

Hamilton, R. H. and M. Z. Fall (1971). "Loss of Tumor-Initiating Ability in Agrobacterium-Tumefaciens by Incubation at High Temperature." Experientia **27**(2): 229-&.

Hara, K., R. Kajita, K. U. Torii, D. C. Bergmann and T. Kakimoto (2007). "The secretory peptide gene EPF1 enforces the stomatal one-cell-spacing rule." Genes & Development **21**(14): 1720-1725.

Haswell, E. S., R. Peyronnet, H. Barbier-Brygoo, E. M. Meyerowitz and J.-M. Frachisse (2008). "Two MscS homologs provide mechanosensitive channel activities in the Arabidopsis root." Current Biology **18**(10): 730-734.

Heim, N. and O. Griesbeck (2003). "Genetically encoded indicators of cellular calcium dynamics based on troponin C and GFP." Society for Neuroscience Abstract Viewer and Itinerary Planner **2003**.

Heslop-Harrison, J. (1982). "Pollen-Stigma Interaction and Cross-Incompatibility in the Grasses." Science **215**(4538): 1358-1364.

Heslop-Harrison, Y., J. Heslop-Harrison and B. J. Reger (1985). "The Pollen-Stigma Interaction in the Grasses .7. Pollen-Tube Guidance and the Regulation of Tube Number in Zea-Mays-L." Acta Botanica Neerlandica **34**(2): 193-211.

Heslop-Harrison, Y., B. J. Reger and J. Heslop-Harrison (1984). "The Pollen-Stigma Interaction in the Grasses .6. the Stigma (Silk) of Zea-Mays-L as Host to the Pollens of Sorghum-Bicolor (L) Moench and Pennisetum-Americanum (L) Leeke." Acta Botanica Neerlandica **33**(2): 205-227.

Heslop-Harrison, Y. and K. R. Shivanna (1977). "Receptive Surface of Angiosperm Stigma." Annals of Botany **41**(176): 1233-&.

Higashiyama, T. and Y. Hamamura (2008). "Gametophytic pollen tube guidance." Sexual Plant Reproduction **21**(1): 17-26.

Higashiyama, T., S. Yabe, N. Sasaki, Y. Nishimura, S. Miyagishima, H. Kuroiwa and T. Kuroiwa (2001). "Pollen tube attraction by the synergid cell." Science **293**(5534): 1480-1483.

Hiscock, S. J. and S. M. McInnis (2003). "Pollen recognition and rejection during the sporophytic self-incompatibility response: Brassica and beyond." Trends in Plant Science **8**(12): 606-613.

Hoffman, C. S. and F. Winston (1987). "A 10-Minute DNA Preparation from Yeast Efficiently Releases Autonomous Plasmids for Transformation of Escherichia-Coli." Gene **57**(2-3): 267-272.

House, L. R. and O. E. Nelson (1958). "Tracer study of pollen-tube growth in cross-sterile maize." Jour Heredity **49**((1)): 18-21.

Hrabak, E. M., C. W. M. Chan, M. Gribskov, J. F. Harper, J. H. Choi, N. Halford, J. Kudla, S. Luan, H. G. Nimmo, M. R. Sussman, M. Thomas, K. Walker-Simmons, J. K.

Zhu and A. C. Harmon (2003). "The Arabidopsis CDPK-SnRK superfamily of protein kinases." Plant Physiology **132**(2): 666-680.
Huang, B. Q. and S. D. Russell (1992). "Female Germ Unit - Organization, Isolation, and Function." International Review of Cytology-a Survey of Cell Biology **140**: 233-293.
Huang, B. Q. and W. F. Sheridan (1994). "Female Gametophyte Development in Maize - Microtubular Organization and Embryo Sac Polarity." Plant Cell **6**(6): 845-861.
Huang, S. R., Y. Q. An, J. M. McDowell, E. C. McKinney and R. B. Meagher (1997). "The Arabidopsis ACT11 actin gene is strongly expressed in tissues of the emerging inflorescence, pollen, and developing ovules." Plant Molecular Biology **33**(1): 125-139.
Ingouff, M., Y. Hamamura, M. GourgueS, T. Higashiyama and F. Berger (2007). "Distinct dynamics of HISTONE3 variants between the two fertilization products in plants." Current Biology **17**(12): 1032-1037.
Ingouff, M., P. E. Jullien and F. Berger (2006). "The female gametophyte and the endosperm control cell proliferation and differentiation of the seed coat in Arabidopsis." Plant Cell **18**(12): 3491-3501.
Ingouff, M., T. Sakata, J. Li, S. Sprunck, T. Dresselhaus and F. Berger (2009). "The two male gametes share equal ability to fertilize the egg cell in Arabidopsis thaliana." Current Biology **19**(1): R19-R20.
Ingram, G. C., C. Boisnard-Lorig, C. Dumas and P. M. Rogowsky (2000). "Expression patterns of genes encoding HD-ZipIV homeo domain proteins define specific domains in maize embryos and meristems." Plant Journal **22**(5): 401-414.
Inoue, H., H. Nojima and H. Okayama (1990). "High-Efficiency Transformation of Escherichia-Coli with Plasmids." Gene **96**(1): 23-28.
Iwano, M., H. Shiba, T. Miwa, F. S. Che, S. Takayama, T. Nagai, A. Miyawaki and A. Isogai (2004). "Ca2+ dynamics in a pollen grain and papilla cell during pollination of Arabidopsis." Plant Physiology **136**(3): 3562-3571.
Jaffe, L. F. (1983). "Sources of Calcium in Egg Activation - a Review and Hypothesis." Developmental Biology **99**(2): 265-276.
Jensen, W. A. (1965). "Ultrastructure and Histochemistry of Synergids of Cotton." American Journal of Botany **52**(3): 238-&.
Johnson, M. A. and D. Preuss (2002). "Plotting a course: Multiple signals guide pollen tubes to their targets." Developmental Cell **2**(3): 273-281.
Kaegi, C., N. Baumann, N. Nielsen, Y.-D. Stierhof and R. Gross-Hardt (2010). "The gametic central cell of Arabidopsis determines the lifespan of adjacent accessory cells." Proceedings of the National Academy of Sciences of the United States of America **107**(51): 22350-22355.
Kanaoka, M. M., N. Kawano, Y. Matsubara, D. Susaki, S. Okuda, N. Sasaki and T. Higashiyama "Identification and characterization of TcCRP1, a pollen tube attractant from Torenia concolor." Annals of Botany **108**(4): 739-747.
Kanaoka, M. M., N. Kawano, Y. Matsubara, D. Susaki, S. Okuda, N. Sasaki and T. Higashiyama (2011). "Identification and characterization of TcCRP1, a pollen tube attractant from Torenia concolor." Annals of Botany **108**(4): 739-747.
Kapil, R. N. and A. K. Bhatnagar (1981). "Perspectives in Experimental Embryology." Proceedings of the International Botanical Congress **13**: 51.
Karimi, M., A. Depicker and P. Hilson (2007). "Recombinational cloning with plant gateway vectors." Plant Physiology **145**(4): 1144-1154.
Kasahara, R. D., M. F. Portereiko, L. Sandaklie-Nikolova, D. S. Rabiger and G. N. Drews (2005). "MYB98 is required for pollen tube guidance and synergid cell differentiation in Arabidopsis." Plant Cell **17**(11): 2981-2992.

Kermicle, J. L. and M. M. S. Evans (2005). "Pollen-pistil barriers to crossing in maize and teosinte result from incongruity rather than active rejection." Sexual Plant Reproduction **18**(4): 187-194.

Kermicle, J. L. and M. M. S. Evans (2010). "The Zea mays Sexual Compatibility Gene ga2: Naturally Occurring Alleles, Their Distribution, and Role in Reproductive Isolation." Journal of Heredity **101**(6): 737-749.

Kessler, S. A., H. Shimosato-Asano, N. F. Keinath, S. E. Wuest, G. Ingram, R. Panstruga and U. Grossniklaus (2010). "Conserved Molecular Components for Pollen Tube Reception and Fungal Invasion." Science **330**(6006): 968-971.

Kikuchi, S., H. Kino, H. Tanaka and H. Tsujimoto (2007). "Pollen tube growth in cross combinations between Torenia fournieri and fourteen related species." Breeding Science **57**(2): 117-122.

Kim, B.-G., R. Waadt, Y. H. Cheong, G. K. Pandey, J. R. Dominguez-Solis, S. Schueltke, S. C. Lee, J. Kudla and S. Luan (2007). "The calcium sensor CBL10 mediates salt tolerance by regulating ion homeostasis in Arabidopsis." Plant Journal **52**(3): 473-484.

Klepek, Y. S., D. Geiger, R. Stadler, F. Klebl, L. Landouar-Arsivaud, R. Lemoine, R. Hedrich and N. Sauer (2005). "Arabidopsis POLYOL TRANSPORTER5, a new member of the monosaccharide transporter-like superfamily, mediates H+-symport of numerous substrates, including myo-inositol, glycerol, and ribosele." Plant Cell **17**(1): 204-218.

Kolb, M. (2011). Charakterisierung putativer Interaktionspartner des Signalpeptids ZmEAL1. Department of cellbiology and plant biochemistry. Regensburg, University of Regensburg.

Kondo, T., R. Kajita, A. Miyazaki, M. Hokoyama, T. Nakamura-Miura, S. Mizuno, Y. Masuda, K. Irie, Y. Tanaka, S. Takada, T. Kakimoto and Y. Sakagami (2010). "Stomatal Density is Controlled by a Mesophyll-Derived Signaling Molecule." Plant and Cell Physiology **51**(1): 1-8.

Kranz, E., J. Bautor and H. Lorz (1991). "Invitro Fertilization of Single, Isolated Gametes of Maize Mediated by Electrofusion." Sexual Plant Reproduction **4**(1): 12-16.

Krohn, N. (2010). Analysis of polarity establishment during megagametogenesis and early zygotic embryogenesis in Zea mays. Cellbiology and plant biochemistry. Regensburg, University of Regensburg. **PhD**.

Krohn, N., A. Lausser, M. Juranić and T. Dresselhaus (submitted). "Egg cell signaling by ZmEAL1 controls antipodal cell fate."

Kudla, J., Q. Xu, K. Harter, W. Gruissem and S. Luan (1999). "Genes for calcineurin B-like proteins in Arabidopsis are differentially regulated by stress signals." Proceedings of the National Academy of Sciences of the United States of America **96**(8): 4718-4723.

Laemmli, U. K. (1970). "Cleavage of Structural Proteins During Assembly of Head of Bacteriophage-T4." Nature **227**(5259): 680-&.

Laohavisit, A., J. C. Mortimer, V. Demidchik, K. M. Coxon, M. A. Stancombe, N. Macpherson, C. Brownlee, A. Hofmann, A. A. R. Webb, H. Miedema, N. H. Battey and J. M. Davies (2009). "Zea mays Annexins Modulate Cytosolic Free Ca2+ and Generate a Ca2+-Permeable Conductance." Plant Cell **21**(2): 479-493.

Lausser, A. (2007). Untersuchungen zur Kreuzungsinkompatibilität bei Z. mays L. und T. dactyloides L. Cellbiology and plant biochemistry. Regensburg, University of Regensburg. **Diploma**.

Lausser, A. and T. Dresselhaus (2010). "Sporophytic control of pollen tube growth and guidance in grasses." Biochemical Society Transactions **38**: 631-634.

Lausser, A., I. Kliwer, K.-o. Srilunchang and T. Dresselhaus (2010). "Sporophytic control of pollen tube growth and guidance in maize." Journal of Experimental Botany **61**(3): 673-682.

Lee, B.-h., S.-i. Yu and D. Jackson (2009). "Control of Plant Architecture: The Role of Phyllotaxy and Plastochron." Journal of Plant Biology **52**(4): 277-282.

Lewis, D. and L. K. Crowe (1958). "Unilateral Interspecific incompatibility in flowering plants." Heredity **12**((2)): 233-256.

Li, H., Y. K. Lin, R. M. Heath, M. X. Zhu and Z. B. Yang (1999). "Control of pollen tube tip growth by a pop GTPase-dependent pathway that leads to tip-localized calcium influx." Plant Cell **11**(9): 1731-1742.

Lindbo, J. A. (2007). "TRBO: A high-efficiency tobacco mosaic virus RNA-Based overexpression vector." Plant Physiology **145**(4): 1232-1240.

Lobanova, L. and N. Enaleeva (1998). "The development of embryo sacs in in vitro ovaries of Nicotiana tabacum L." Plant Science **132**(2): 191-202.

Long, J. A., E. I. Moan, J. I. Medford and M. K. Barton (1996). "A member of the KNOTTED class of homeodomain proteins encoded by the STM gene of Arabidopsis." Nature **379**(6560): 66-69.

Luan, S., J. Kudla, M. Rodriguez-Concepcion, S. Yalovsky and W. Gruissem (2002). "Calmodulins and calcineurin B-like proteins: Calcium sensors for specific signal response coupling in plants." Plant Cell **14**: S389-S400.

Ma, H. and V. Sundaresan (2010). Development of Flowering Plant Gametophytes. Plant Development. **91:** 379-412.

Ma, Y., A. Creanga, L. Lum and P. A. Beachy (2006). "Prevalence of off-target effects in Drosophila RNA interference screens." Nature **443**(7109): 359-363.

Malho, R., A. Moutinho, A. van der Luit and A. J. Trewavas (1998). "Spatial characteristics of calcium signalling: the calcium wave as a basic unit in plant cell calcium signalling." Philosophical Transactions of the Royal Society of London Series B-Biological Sciences **353**(1374): 1463-1473.

Mangelsdorf, P. C. and R. G. Reeves (1931). "Hybridization of maize, Tripsacum and Euchlaena." Journal of Heredity **22**(11): 329-343.

Marshall, E., L. M. Costa and J. Gutierrez-Marcos (2011). "Cysteine-Rich Peptides (CRPs) mediate diverse aspects of cell-cell communication in plant reproduction and development." Journal of Experimental Botany **62**(5): 1677-1686.

Martin, F. W. (1959). "Staining and Observing Pollen Tubes in the Style by Means of Fluorescence." Stain Technology **34**(3): 125-128.

Márton, M. L., S. Cordts, J. Broadhvest and T. Dresselhaus (2005). "Micropylar pollen tube guidance by egg apparatus 1 of maize." Science **307**(5709): 573-576.

Márton, M. L., A. Fastner, S. Uebler and T. Dresselhaus (in press). "Overcoming Hybridizations Barriers by Secreting the Maize Pollen Tube Attractant ZmEA1 from Arabidopsis Ovules. ." Current Biology **22**.

Matsubayashi, Y. and Y. Sakagami (1996). "Phytosulfokine, sulfated peptides that induce the proliferation of single mesophyll cells of Asparagus officinalis L." Proceedings of the National Academy of Sciences of the United States of America **93**(15): 7623-7627.

Matsubayashi, Y., L. Takagi, N. Omura, A. Morita and Y. Sakagami (1999). "The endogenous sulfated pentapeptide phytosulfokine-alpha stimulates tracheary element differentiation of isolated mesophyll cells of zinnia." Plant Physiology **120**(4): 1043-1048.

McAinsh, M. R., C. Brownlee and A. M. Hetherington (1992). "Visualizing Changes in Cytosolic-Free Ca2+ During the Response of Stomatal Guard-Cells to Abscisic-Acid." Plant Cell **4**(9): 1113-1122.

McClure, B. A. and V. Franklin-Tong (2006). "Gametophytic self-incompatibility: understanding the cellular mechanisms involved in "self" pollen tube inhibition." Planta **224**(2): 233-245.

Meyer, S., H. Pospisil and S. Scholten (2007). "Heterosis associated gene expression in maize embryos 6 days after fertilization exhibits additive, dominant and overdominant pattern." Plant Molecular Biology **63**(3): 381-391.

Meyerhoff, O., K. Muller, M. R. Roelfsema, A. Latz, B. Lacombe, R. Hedrich, P. Dietrich and D. Becker (2005). "AtGLR3.4, a glutamate receptor channel-like gene is sensitive to touch and cold." Planta **222**(3): 418-427.

Michard, E., P. T. Lima, F. Borges, A. C. Silva, M. T. Portes, J. E. Carvalho, M. Gilliham, L.-H. Liu, G. Obermeyer and J. A. Feijo (2011). "Glutamate Receptor-Like Genes Form Ca2+ Channels in Pollen Tubes and Are Regulated by Pistil D-Serine." Science **332**(6028): 434-437.

Mo, Y. Y., C. Nagel and L. P. Taylor (1992). "Biochemical Complementation of Chalcone Synthase Mutants Defines a Role for Flavonols in Functional Pollen." Proceedings of the National Academy of Sciences of the United States of America **89**(15): 7213-7217.

Mol, R., E. Matthysrochon and C. Dumas (1993). "Invitro Culture of Fertilized Embryo Sacs of Maize - Zygotes and 2-Celled Proembryos Can Develop into Plants." Planta **189**(2): 213-217.

Moll, C., L. von Lyncker, S. Zimmermann, C. Kaegi, N. Baumann, D. Twell, U. Grossniklaus and R. Gross-Hardt (2008). "CLO/GFA1 and ATO are novel regulators of gametic cell fate in plants." Plant Journal **56**(6): 913-921.

Mori, I. C., Y. Murata, Y. Yang, S. Munemasa, Y.-F. Wang, S. Andreoli, H. Tiriac, J. M. Alonso, J. F. Harper, J. R. Ecker, J. M. Kwak and J. I. Schroeder (2006). "CDPKs CPK6 and CPK3 function in ABA regulation of guard cell S-type anion- and Ca2+-permeable channels and stomatal closure." Plos Biology **4**(10): 1749-1762.

Muehlbauer, G. J., J. E. Fowler, L. Girard, R. Tyers, L. Harper and M. Freeling (1999). "Ectopic expression of the maize homeobox gene Liguleless3 alters cell fates in the leaf." Plant Physiology **119**(2): 651-662.

Muschietti, J., L. Dircks, G. Vancanneyt and S. McCormick (1994). "Lat52 Protein Is Essential for Tomato Pollen Development - Pollen Expressing Antisense Lat52 Rna Hydrates and Germinates Abnormally and Cannot Achieve Fertilization." Plant Journal **6**(3): 321-338.

Nakayama, S. and R. H. Kretsinger (1994). "Evolution of the Ef-Hand Family of Proteins." Annual Review of Biophysics and Biomolecular Structure **23**: 473-507.

Nardmann, J. and W. Werr (2009). Patterning of the Maize Embryo and the Perspective of Evolutionary Developmental Biology. Handbook of Maize: Its Biology**:** 105-119.

Nardmann, J., R. Zimmermann, D. Durantini, E. Kranz and W. Werr (2007). "WOX gene phylogeny in Poaceae: A comparative approach addressing leaf and embryo development." Molecular Biology and Evolution **24**(11): 2474-2484.

Nawaschin, S. (1898). "Resultate einer Revision der Befruchtungsvorgange bei Lilium martagon und Fritillaria tenella " Bull Acad Imp Sci St Pétersbourg **9** pp. 377–382.

Nelson, B. K., X. Cai and A. Nebenfuehr (2007). "A multicolored set of in vivo organelle markers for co-localization studies in Arabidopsis and other plants." Plant Journal **51**(6): 1126-1136.

Nelson, O. E. (1952). "Non-Reciprocal Cross-Sterility in Maize." Genetics **37**(2): 101-124.

Nelson, O. E. (1994). The gametophyte factors of maize. The maize handbook, Springer-Verlag New York, Inc.; Springer-Verlag**:** 496-503.

Neumann, K., A. Kumar and J. Imani (2009). Phytohormones and Growth Regulators. Plant Cell and Tissue Culture-A Tool in Biotechnology: Basics and Application**:** 227-233.

Niggli, E. (1999). "Localized intracellular calcium signaling in muscle: Calcium sparks and calcium quarks." Annual Review of Physiology **61**: 311-335.

Nisler, J., M. Zatloukal, I. Popa, K. Dolezal, M. Strnad and L. Spichal (2010). "Cytokinin receptor antagonists derived from 6-benzylaminopurine." Phytochemistry **71**(7): 823-830.

Nobiling, R. and H. D. Reiss (1987). "Quantitative-Analysis of Calcium Activity and Measurements of Calcium Gradients in Growing Pollen Tubes of Lilium-Longiflorum." European Journal of Cell Biology **43**: 39-39.

Novick, P. and R. Schekman (1979). "Secretion and Cell-Surface Growth Are Blocked in a Temperature-Sensitive Mutant of Saccharomyces-Cerevisiae." Proceedings of the National Academy of Sciences of the United States of America **76**(4): 1858-1862.

Okuda, S., H. Tsutsui, K. Shiina, S. Sprunck, H. Takeuchi, R. Yui, R. D. Kasahara, Y. Hamamura, A. Mizukami, D. Susaki, N. Kawano, T. Sakakibara, S. Namiki, K. Itoh, K. Otsuka, M. Matsuzaki, H. Nozaki, T. Kuroiwa, A. Nakano, M. M. Kanaoka, T. Dresselhaus, N. Sasaki and T. Higashiyama (2009). "Defensin-like polypeptide LUREs are pollen tube attractants secreted from synergid cells." Nature **458**(7236): 357-U122.

Oono, Y., C. Ooura, A. Rahman, E. T. Aspuria, K. Hayashi, A. Tanaka and H. Uchimiya (2003). "p-chlorophenoxyisobutyric acid impairs auxin response in Arabidopsis root." Plant Physiology **133**(3): 1135-1147.

Pagnussat, G. C., M. Alandete-Saez, J. L. Bowman and V. Sundaresan (2009). "Auxin-Dependent Patterning and Gamete Specification in the Arabidopsis Female Gametophyte." Science **324**(5935): 1684-1689.

Pagnussat, G. C., H.-J. Yu and V. Sundaresana (2007). "Cell-fate switch of synergid to egg cell in Arabidopsis eostre mutant embryo sacs arises from misexpression of the BEL1-like homeodomain gene BLH1." Plant Cell **19**(11): 3578-3592.

Pallotta, M. A., R. D. Graham, P. Langridge, D. H. B. Sparrow and S. J. Barker (2000). "RFLP mapping of manganese efficiency in barley." Theoretical and Applied Genetics **101**(7): 1100-1108.

Pandey, G. K., Y. H. Cheong, K. N. Kim, J. J. Grant, L. G. Li, W. Hung, C. D'Angelo, S. Weinl, J. Kudla and S. Luan (2004). "The calcium sensor calcineurin B-Like 9 modulates abscisic acid sensitivity and biosynthesis in Arabidopsis." Plant Cell **16**(7): 1912-1924.

Pang, S. Z., D. L. DeBoer, Y. Wan, G. B. Ye, J. G. Layton, M. K. Neher, C. L. Armstrong, J. E. Fry, M. A. W. Hinchee and M. E. Fromm (1996). "An improved green fluorescent protein gene as a vital marker in plants." Plant Physiology **112**(3): 893-900.

Parmacek, M. S. and J. M. Leiden (1991). "Structure, Function, and Regulation of Troponin-C." Circulation **84**(3): 991-1003.

Paroutis, P., N. Touret and S. Grinstein (2004). "The pH of the secretory pathway: Measurement, determinants, and regulation." Physiology **19**: 207-215.

Pearce, G., D. S. Moura, J. Stratmann and C. A. Ryan (2001). "Production of multiple plant hormones from a single polyprotein precursor." Nature **411**(6839): 817-820.

Pearce, G., D. Strydom, S. Johnson and C. A. Ryan (1991). "A Polypeptide from Tomato Leaves Induces Wound-Inducible Proteinase-Inhibitor Proteins." Science **253**(5022): 895-898.

Peiter, E., F. J. M. Maathuis, L. N. Mills, H. Knight, J. Pelloux, A. M. Hetherington and D. Sanders (2005). "The vacuolar Ca(2+)-activated channel TPC1 regulates germination and stomatal movement." Nature **434**(7031): 404-408.

Peng, X.-B., M.-X. Sun and H.-Y. Yang (2009). "Comparative Detection of Calcium Fluctuations in Single Female Sex Cells of Tobacco to Distinguish Calcium Signals Triggered by in vitro Fertilization." Journal of Integrative Plant Biology **51**(8): 782-791.

Perilli, S., L. Moubayidin and S. Sabatini (2011). "The molecular basis of cytokinin function." Current Opinion in Plant Biology **13**(1): 21-26.

Peters, J. M., M. J. Walsh and W. W. Franke (1990). "An Abundant and Ubiquitous Homooligomeric Ring-Shaped Atpase Particle Related to the Putative Vesicle Fusion Proteins Sec18p and Nsf." Embo Journal **9**(6): 1757-1767.

Phillips, A. R. and M. M. S. Evans (2011). "Analysis of stunter1, a Maize Mutant with Reduced Gametophyte Size and Maternal Effects on Seed Development." Genetics **187**(4): 1085-U189.

Pollak, P. E., K. Hansen, J. D. Astwood and L. P. Taylor (1995). "Conditional Male-Fertility in Maize." Sexual Plant Reproduction **8**(4): 231-241.

Poole, R. J. (1978). "Energy Coupling for Membrane-Transport." Annual Review of Plant Physiology and Plant Molecular Biology **29**: 437-460.

Ram, S. G., V. Thiruvengadam, S. H. Ramakrishnan and J. R. K. Bapu (2008). "Investigation on pre-zygotic barriers in the interspecific crosses involving Gossypium barbadense and four diploid wild species." Euphytica **159**(1-2): 241-248.

Randolph, L. F. (1936). "Developmental morphology of the caryopsis in maize." Jour Agric Res **53**((1)): 881-916.

Reiser, L. and R. L. Fischer (1993). "The Ovule and the Embryo Sac." Plant Cell **5**(10): 1291-1301.

Rentsch, D., M. Laloi, I. Rouhara, E. Schmelzer, S. Delrot and W. B. Frommer (1995). "Ntr1 Encodes a High-Affinity Oligopeptide Transporter in Arabidopsis." Febs Letters **370**(3): 264-268.

Rieseberg, L. H. and J. H. Willis (2007). "Plant speciation." Science **317**(5840): 910-914.

Rijavec, T. and M. Dermastia (2010). "Cytokinins and their Function in Developing Seeds." Acta Chimica Slovenica **57**(3): 617-629.

Ritchie, S. M., S. J. Swanson and S. Gilroy (2002). "From common signalling components to cell specific responses: insights from the cereal aleurone." Physiologia Plantarum **115**(3): 342-351.

Roberts, S. K., I. Gillot and C. Brownlee (1994). "Cytoplasmic Calcium and Fucus Egg Activation." Development **120**(1): 155-163.

Rohrig, H., J. Schmidt, E. Miklashevichs, J. Schell and M. John (2002). "Soybean ENOD40 encodes two peptides that bind to sucrose synthase." Proceedings of the National Academy of Sciences of the United States of America **99**(4): 1915-1920.

Roy, S. J., M. Gilliham, B. Berger, P. A. Essah, C. Cheffings, A. J. Miller, R. J. Davenport, L. H. Liu, M. J. Skynner, J. M. Davies, P. Richardson, R. A. Leigh and M. Tester (2008). "Investigating glutamate receptor-like gene co-expression in Arabidopsis thaliana." Plant Cell and Environment **31**(6): 861-871.

Ryan, C. A. and G. Pearce (2001). "Polypeptide hormones." Plant Physiology **125**(1): 65-68.

Saha, D., A. M. Prasad and R. Srinivasan (2007). "Pentatricopeptide repeat proteins and their emerging roles in plants." Plant Physiology and Biochemistry **45**(8): 521-534.

Sambrook, J. and D. W. Russell (2001). Molecular cloning: A laboratory manual. Molecular cloning: A laboratory manual.

Schagger, H. and G. Vonjagow (1987). "Tricine Sodium Dodecyl-Sulfate Polyacrylamide-Gel Electrophoresis for the Separation of Proteins in the Range from 1-Kda to 100-Kda." Analytical Biochemistry **166**(2): 368-379.

Schell, J., T. Bisseling, M. Dulz, H. Franssen, K. Fritze, M. John, T. Kleinow, A. Lessnick, E. Miklashevichs, K. Pawlowski, H. Rohrig, K. van de Sande, J. Schmidt, H. H. Steinbiss and M. Stoll (1999). "Re-evaluation of phytohormone-independent division of tobacco protoplast-derived cells." Plant Journal **17**(5): 461-466.

Schiott, M., S. M. Romanowsky, L. Baekgaard, M. K. Jakobsen, M. G. Palmgren and J. F. Harper (2004). "A plant plasma membrane Ca2+ pump is required for normal pollen tube growth and fertilization." Proceedings of the National Academy of Sciences of the United States of America **101**(25): 9502-9507.

Schopfer, C. R., M. E. Nasrallah and J. B. Nasrallah (1999). "The male determinant of self-incompatibility in Brassica." Science **286**(5445): 1697-1700.

Scott, R. J., S. J. Armstrong, J. Doughty and M. Spielman (2008). "Double fertilization in Arabidopsis thaliana involves a polyspermy block on the egg but not the central cell." Molecular Plant **1**(4): 611-619.

Sekhon, R. S., H. Lin, K. L. Childs, C. N. Hansey, C. R. Buell, N. de Leon and S. M. Kaeppler (2011). "Genome-wide atlas of transcription during maize development." Plant Journal **66**(4): 553-563.

Shao, S. and R. S. Hegde (2011). "A Calmodulin-Dependent Translocation Pathway for Small Secretory Proteins." Cell **147**(7): 1576-1588.

Shigaki, T. and K. D. Hirschi (2006). "Diverse functions and molecular properties emerging for CAX cation/H+ exchangers in plants." Plant Biology **8**(4): 419-429.

Shimizu, K. K. and K. Okada (2000). "Attractive and repulsive interactions between female and male gametophytes in Arabidopsis pollen tube guidance." Development **127**(20): 4511-4518.

Silverstein, K. A. T., W. A. Moskal, Jr., H. C. Wu, B. A. Underwood, M. A. Graham, C. D. Town and K. A. VandenBosch (2007). "Small cysteine-rich peptides resembling antimicrobial peptides have been under-predicted in plants." Plant Journal **51**(2): 262-280.

Singh, M., S. Goel, R. B. Meeley, C. Dantec, H. Parrinello, C. Michaud, O. Leblanc and D. Grimanelli (2010). "Production of Viable Gametes without Meiosis in Maize Deficient for an ARGONAUTE Protein." Plant Cell **23**(2): 443-458.

Smith, L. G., D. Jackson and S. Hake (1995). "Expression of Knotted1 Marks Shoot Meristem Formation During Maize Embryogenesis." Developmental Genetics **16**(4): 344-348.

Smyth, D. R., J. L. Bowman and E. M. Meyerowitz (1990). "Early Flower Development in Arabidopsis." Plant Cell **2**(8): 755-767.

Sossountzov, L., L. Ruizavila, F. Vignols, A. Jolliot, V. Arondel, F. Tchang, M. Grosbois, F. Guerbette, E. Miginiac, M. Delseny, P. Puigdomenech and J. C. Kader (1991). "Spatial and Temporal Expression of a Maize Lipid Transfer Protein Gene." Plant Cell **3**(9): 923-933.

Sparkes, I. A., J. Runions, A. Kearns and C. Hawes (2006). "Rapid, transient expression of fluorescent fusion proteins in tobacco plants and generation of stably transformed plants." Nature Protocols **1**(4): 2019-2025.

Sprunck, S. and R. Gross-Hardt (2011). "Nuclear behavior, cell polarity, and cell specification in the female gametophyte." Sexual Plant Reproduction **24**(2): 123-136.

Sprunck, S., S. Rademacher, F. Vogler, U. Grossniklaus and T. Dresselhaus (submitted). "Egg cell-secreted EC1 triggers sperm cell activation during double fertilization."

Srilunchang, K.-o., N. G. Krohn and T. Dresselhaus (2010). "DiSUMO-like DSUL is required for nuclei positioning, cell specification and viability during female gametophyte maturation in maize." Development **137**(2): 333-345.

Stael, S., B. Wurzinger, A. Mair, N. Mehlmer, U. C. Vothknecht and M. Teige (2012). "Plant organellar calcium signalling: an emerging field." Journal of Experimental Botany **63**(4): 1525-1542.

Sugano, S. S., T. Shimada, Y. Imai, K. Okawa, A. Tamai, M. Mori and I. Hara-Nishimura (2010). "Stomagen positively regulates stomatal density in Arabidopsis." Nature **463**(7278): 241-U130.

Swanson, R., A. F. Edlund and D. Preuss (2004). "Species specificity in pollen-pistil interactions." Annual Review of Genetics **38**: 793-818.

Tapken, D. and M. Hollmann (2008). "Arabidopsis thaliana Glutamate Receptor Ion Channel Function Demonstrated by Ion Pore Transplantation." Journal of Molecular Biology **383**(1): 36-48.

Thomas, D., P. Lipp, S. C. Tovey, M. J. Berridge, W. H. Li, R. Y. Tsien and M. D. Bootman (2000). "Microscopic properties of elementary Ca2+ release sites in nonexcitable cells." Current Biology **10**(1): 8-15.

Tian, H. Q. and S. D. Russell (1997). "Calcium distribution in fertilized and unfertilized ovules and embryo sacs of Nicotiana tabacum L." Planta **202**(1): 93-105.

Trewavas, A. (1999). "Le calcium, c'est la vie: Calcium makes waves." Plant Physiology **120**(1): 1-6.

Ulmasov, T., J. Murfett, G. Hagen and T. J. Guilfoyle (1997). "Aux/IAA proteins repress expression of reporter genes containing natural and highly active synthetic auxin response elements." Plant Cell **9**(11): 1963-1971.

Umehara, M., A. Hanada, S. Yoshida, K. Akiyama, T. Arite, N. Takeda-Kamiya, H. Magome, Y. Kamiya, K. Shirasu, K. Yoneyama, J. Kyozuka and S. Yamaguchi (2008). "Inhibition of shoot branching by new terpenoid plant hormones." Nature **455**(7210): 195-U29.

Valero, M., S. Richerd, V. Perrot and C. Destombe (1992). "Evolution of Alternation of Haploid and Diploid Phases in Life-Cycles." Trends in Ecology & Evolution **7**(1): 25-29.

Van Der Pluijm, J. E. (1964). "An electron microscopic investigation of the filiform apparatus in the embryo sac of Torenia founieri." H. F. Linskens, Editor. Pollen Physiology and Fertilization. A Symposium, 1963: p. 8-16.

Vandesompele, J., K. De Preter, F. Pattyn, B. Poppe, N. Van Roy, A. De Paepe and F. Speleman (2002). "Accurate normalization of real-time quantitative RT-PCR data by geometric averaging of multiple internal control genes." Genome Biology **3**(7).

Vernoud, V., M. Hajduch, A. S. Khaled, N. Depege and P. M. Rogowsky (2005). "Maize Embryogenesis." Maydica **50**(3-4): 469-483.

Verret, F., G. Wheeler, A. R. Taylor, G. Farnham and C. Brownlee (2010). "Calcium channels in photosynthetic eukaryotes: implications for evolution of calcium-based signalling." New Phytologist **187**(1): 23-43.

Voelz, R., L. von Lyncker, N. Baumann, T. Dresselhaus, S. Sprunck and R. Gross-Hardt (2012). "LACHESIS-dependent egg-cell signaling regulates the development of female gametophytic cells." Development **139**(3): 498-502.

Voinnet, O., S. Rivas, P. Mestre and D. Baulcombe (2003). "An enhanced transient expression system in plants based on suppression of gene silencing by the p19 protein of tomato bushy stunt virus." Plant Journal **33**(5): 949-956.

Vollbrecht, E. and S. Hake (1995). "Deficiency Analysis of Female Gametogenesis in Maize." Developmental Genetics **16**(1): 44-63.

Wang, X. M. (2001). "Plant phospholipases." Annual Review of Plant Physiology and Plant Molecular Biology **52**: 211-+.

Ward, W. W., H. J. Prentice, A. F. Roth, C. W. Cody and S. C. Reeves (1982). "Spectral Perturbations of the Aequorea Green-Fluorescent Protein." Photochemistry and Photobiology **35**(6): 803-808.

Wheeler, G. L. and C. Brownlee (2008). "Ca2+ signalling in plants and green algae - changing channels." Trends in Plant Science **13**(9): 506-514.

Wheeler, J. I. and H. R. Irving (2010). "Evolutionary advantages of secreted peptide signalling molecules in plants." Functional Plant Biology **37**(5): 382-394.

White, P. J. and M. R. Broadley (2003). "Calcium in plants." Annals of Botany **92**(4): 487-511.

Whitford, R., A. Fernandez, R. Tejos, A. C. Perez, J. Kleine-Vehn, S. Vanneste, A. Drozdzecki, J. Leitner, L. Abas, M. Aerts, K. Hoogewijs, P. Baster, R. De Groodt, Y.-C. Lin, V. Storme, Y. Van de Peer, T. Beeckman, A. Madder, B. Devreese, C. Luschnig, J. Friml and P. Hilson (2012). "GOLVEN Secretory Peptides Regulate Auxin Carrier Turnover during Plant Gravitropic Responses." Developmental Cell **22**(3): 678-685.

Whittemore, A. T. and B. A. Schaal (1991). "Interspecific Gene Flow in Sympatric Oaks." Proceedings of the National Academy of Sciences of the United States of America **88**(6): 2540-2544.

Widmer, A., C. Lexer and S. Cozzolino (2009). "Evolution of reproductive isolation in plants." Heredity **102**(1): 31-38.

Wilson, D. W., S. W. Whiteheart, M. Wiedmann, M. Brunner and J. E. Rothman (1992). "A Multisubunit Particle Implicated in Membrane-Fusion." Journal of Cell Biology **117**(3): 531-538.

Wilson, Z. A. and D.-B. Zhang (2009). "From Arabidopsis to rice: pathways in pollen development." Journal of Experimental Botany **60**(5): 1479-1492.

Wu, J., E. L. Kurten, G. Monshausen, G. M. Hummel, S. Gilroy and I. T. Baldwin (2007). "NaRALF, a peptide signal essential for the regulation of root hair tip apoplastic pH in Nicotiana attenuata, is required for root hair development and plant growth in native soils." Plant Journal **52**(5): 877-890.

Yadegari, R. and G. N. Drews (2004). "Female gametophyte development." Plant Cell **16**: S133-S141.

Yang, B., D. Thorogood, I. Armstead and S. Barth (2008). "How far are we from unravelling self-incompatibility in grasses?" New Phytologist **178**(4): 740-753.

Yang, T. B. and B. W. Poovaiah (2002). "A calmodulin-binding/CGCG box DNA-binding protein family involved in multiple signaling pathways in plants." Journal of Biological Chemistry **277**(47): 45049-45058.

Yang, W.-C., D.-Q. Shi and Y.-H. Chen (2011). Female Gametophyte Development in Flowering Plants. Annual Review of Plant Biology, Vol 61. **61:** 89-108.

Young, B. A., R. T. Sherwood and E. C. Bashaw (1979). "Cleared-Pistil and Thick-Sectioning Techniques for Detecting Aposporous Apomixis in Grasses." Canadian Journal of Botany-Revue Canadienne De Botanique **57**(15): 1668-1672.

Zhu, S.-Y., X.-C. Yu, X.-J. Wang, R. Zhao, Y. Li, R.-C. Fan, Y. Shang, S.-Y. Du, X.-F. Wang, F.-Q. Wu, Y.-H. Xu, X.-Y. Zhang and D.-P. Zhang (2007). "Two calcium-dependent protein kinases, CPK4 and CPK11, regulate abscisic acid signal transduction in Arabidopsis." Plant Cell **19**(10): 3019-3036.

Zhu, S., B. Gao and J. Tytgat (2005). "Phylogenetic distribution, functional epitopes and evolution of the CS alpha beta superfamily." Cellular and Molecular Life Sciences **62**(19-20): 2257-2269.

Zimmermann, R. and W. Werr (2005). "Pattern formation in the monocot embryo as revealed by NAM and CUC3 orthologues from Zea mays L." Plant Molecular Biology **58**(5): 669-685.

Supplementary information

Antibiotics, antibodies and primer

Supplement table 1.1. Antibiotic concentrations for stock solutions and *E. coli* and *A. tumefaciens* media. Working concentrations for *E. coli* and *A. tumefaciens* are given in [µg/mL]. Stock solution were prepared with autoclaved water under sterile conditions, filter sterilised and stored at -20°C until use.

Antibiotic	**Stock [mg/mL]**	***E.coli* [µg/mL]**	***A. tumefacies* [µg/mL]**
Ampicillin	100	100	-
Kanamycin	50	50	100
Spectinomycin	100	100	250
Gentamycin	40	10	40
Tetracyclin[1]	10	10	-
Rifampecin[2]	10	-	10

[1]Stock solution was prepared with p.a. ethanol. [2]Stock solution was prepared with p.a. methanol.

Supplement table 1.2. Antibody stocks and working concentration. Catalogue numbers are given in brackets. Abbreviations WB = western blot, IP = immune precipitation, HRP = horse reddish peroxidase

Epitop	**Host**	**Conjugate**	**Stock**	**Working concentrations**	**Reference**
c-Myc	mouse	non	2 µg/µl	1 : 5.000 WB; 1 : 100 IP	Sigma Aldrich (M 4439)
HA	mouse	non	1 µg/µl	1 : 5.000 WB; 1 : 100 IP	Sigma Aldrich (H 3663)
GFP	mouse	non	0.4 µg/µl	1 : 5.000 WB	Roche (11 814 460 001)
3xFlag	mouse	non	5 µg/µl	1 : 1.000 – 1 : 5000 WB	Sigma Aldrich (F 3165)
Ig-G (mouse)	goat	HRP		1 : 5.000 WB	Sigma Aldrich (M6150)

Supplement table 1.3. Primer sequences

Number	*Name*	Sequence (5´- 3´)
P7	pMyb98-for	ATGGAGCTCGCGTCGACAGTTG
P8	pMyb98-rev	AGGGACTGACTAGTGGATC
P9	pEC1-for	CAAAAGCTGGAGCTCTCTAGAG
P10	pEC1-rev	GGCCGACTAGTATCCTTCTCAAC
P11	CerTN-forward-I	AAAAAAGCAGGCTGCCACCATGGTGAGCAAGGGCGAG
P12	attB1-CerTN	GGGGACAAGTTTGTACAAAAAAGCAGGCTGCCACCATG
P13	CerTN-reverse-I	TCTGGCGCACCATCATCA
P14	CerTN-forward-II	TCGAGGAGTTCCTGGTGAT
P15	CerTN-reverse-II	AGAAAGCTGGGTTCAGCGTTACTTGTACAGCTCGTCCATG
P16	attB2-CerTN	GGGGACCACTTTGTACAAGAAAGCTGGGTTCA
P17	ZmEA1-Flag forward I	GGGGAGATCtATGTCATCCTGCCCGG
P18	ZmEA1-Flag reversed I	GGGGAGATCtTATATATATCAAAGGTAGAAGCAGAAAC
P19	ZmEC222-Flag forward I	GGGGGGATCCATGGGAGCAGTGTTCTCACTAC
P20	ZmEC222-Flag reversed I	GGGGGGATCCGCGAGCAAACATACGAAC
P21	ZmEA1-His-TEV forward I	GGGGGGCCGGCCAGGGATGATGATGAAGGCG
P23	ZmEC222-His-TEV forward I	GGGGGGCCGGCCATCTGTTTGTCCCTTGGTG
P24	ZmEC222-His-TEV reversed I	GGGGGGCGCGCCTTAGCGAGCAAACATACGAAC
P25	CerTN-Eco52I-rev	CGAAGTCAATGCGGCCGTCA
P26	CerTN-Eco52I-for	AACAATGACGGCCGCATTGA
P30	pAro1-II-for	TCGGGTACCGAGCTCAGATCTAAGCTG
P31	pAro1-II-rev	TGTCGACGCGGCCGCACTAGTCAGATC
P34	HisTEV-EC222-Not	GGGGGGGCGGCCGCTTAGCGAGCAAACATACGAAC
P35	HisTEV-EA1-Not	GGGGGGGCGGCCGCTTAGCTAGCGATCGAACAG
P36	HisTEV-Pac	GGGGGGTTAATTAAGCCACCATGGTGCACCACCACCATCATC
P41	Flag-Not	TCTAGATGCATGCTCGAGCGG
P42	EC222-Flag-Pac	GGGGGGTTAATTAAGCCACCATGGGAGCAGTGTTCTCACTAC
P43	EA1-Flag-Pac	GGGGGGTTAATTAAGCCACCATGTCATCCTGCCCGGCC
P48	ZmEA1-His-rev-II	GGGGGGGGCGCGCCCTAGCTAGCGATCGAACAGGCA
P51	ACT11 forward	GGGGGAGCTCTTTCTTCTTTGATCTTAAAGTTCC
P52	ACT11 reversed	GGGGACTAGTTTTCTATATCCTGTCAAAATTGAT
P53	PLT5 forward	CACCATGACAGGTGCCACACCG
P54	PLT5 reversed	CGAACTTTGTGTGTCTCCTTC
P71	tr-EBP1-rev	GGATCMGCGAGCAAACATACGAACAG
P72	fl-EBP1 for	CACCATGGGAGCAGTGTTCTCACTAC
P84	EBP1-bait-for	GGGGCATATGTCTGTTTGTCCCTTGGTG
P85	EBP1-bait-rev	GGGAATTCTTAGCGAGCAAACATACGAAC
P97	SAUR1-fw	GTTCGGGTTCCGGCACGAGG
P98	SAUR1-rev	AGACGACGAGAGCGAGGCCT
P99	qEAL1-1-for	ACAATGGTTGCACCGGGCGTC
P100	qEAL1-1-rev	AAAGCTGCGGGTTCGCAAGGA
P101	Y2H-33-fw	GGGGCAATTGATGACCTCAGGGCAAAGGG
P102	Y2H-33-rev	GGGGGGATCCTTAGTAACGGATAATATCACTCAAG
P109	Y2H-EAL1-EcoRI-fw	GGGGGAATTCTCTGTTTGTCCCTTGGTG
P110	Y2H-EAL1-BamHI-rev	GGGGGGATCCTTAGCGAGCAAACATACGAAC

P123	qEAL1-2-for	GTCCAGCTGTGGCATCTGTT
P124	qEAL1-2-rev	TGTGGAGGACTGCGAAGTAA
P133	GAPnew1[1]	AGGGTCCACTCAAGGGTATCAT
P134	GAPnew2[1]	ACAAGCTTGACGAAGTGGTC
P141	ubi3[2]	TAAGCTGCCGATGTGCCTGCGTCG
P142	ubi4[2]	CTGAAAGACAGAACATAATGAGCACAGGC
P166	33-Exp-an-f1	CGTGTTCTCTGTGACCTACC
P173	33-Exp-an-r2	GAGCAGCCATCTCAACAAGTGTG
P183	Sec18-rev-XhoI	GGCTCGAGTTATGCGGATTGGGTCATCA
P188	LA-IG-for-II	TACGAGTTCGGCTACTCGAC
P189	LA-IG-rev-II	ATCGATCCGCCTACTGACCG
P200	ESAR-array-forI	CAGCAGCAGCAGCAGCACTT
P201	ESAR-array-revI	TGGTAGCCGATCAGAGAACG
P204	LOBd-array-forI	CCTGCTGCCTGTGTCAAGAT
P205	LOBd-array-revI	CTACGGTACATGGCGCAAGA
P210	PPR-array-forII	CTATGCTACGCCGTAGCCAC
P211	PPR-array-revII	TTCCAGGTAGTGCCTCCAAG
P215	sec18-426-for-II	CACCGGATCCATGTTCAAGATACCTGGTTTTGG
	222-Mlu[1]	CAGTACGCGTCCACGTGCA
	222-Eco[1]	CCGGGAATTCATCACTCTCCTTC
	222-Bam[1]	CTGAGGATCCACGTGCACC
	A188-EC222-GFP-fwd[1]	TCGAGCGGCCGCCCGGGCAGGTATCGCGTACGGG
	EC222-GFP-control-rev[1]	TGTGTCGGATCCGATCTTGAAGGAGAGTGATGAA
	B73-EC222-GFP-fwd[1]	GACACAGCGGCCGCAATGAACAAGCTCAAGCGTAG
	B73-EC222-GFP-rev[1]	TGTGTCACTAGTGCCAGCAAACATACGAACAGC
	ZmGap1[1]	AGGGTGGTGCCAAGAAGGTTG
	ZmGap2[1]	GTAGCCCCACTCGTTGTCGTA
	UbiD-fwd[1]	CACACACACAACCAGATCTC
	ZmEC222-1-fwd[1]	CACTCTCCTTCAAGATCATGG
	ZmEC222-500-rev[1]	ATAGGCATTATATTGCAAGCGACG
	ZmEC222-RT-fwd[1]	CGCGGTGTCTATCAATAGTACC
	222-Mlu[1]	CAGTACGCGTCCACGTGCA

[1]Sequence taken from (Krohn *et al*. submitted). [2]Sequence taken from (Muehlbauer *et al.* 1999)

Vector maps

Vector maps are listed in alphabetical order. For TMV-based vectors, no sequence information is available (Lindbo 2007). Vector maps were drawn using Vectro NTI.

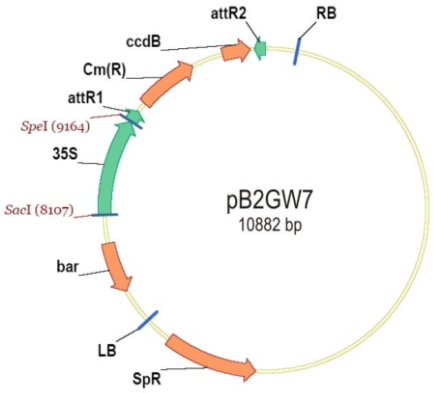

Spectinomycin resistance (SpR): 5543 - 6650 (C)
Glufosinate resistance (bar): 7245 -7796 (C)
Chloramphenicol resistance (CmR): 9408 - 10067
ccdB-toxin (ccdB): 10409 - 10714
Right border (RB): 320 - 343
Left border (LB): 6855 - 6877
35S promoter (35S): 8110 - 9182
Attachment site R1 (attR1): 9172 - 9295
Attachment site R2 (attR2): 10755-10879

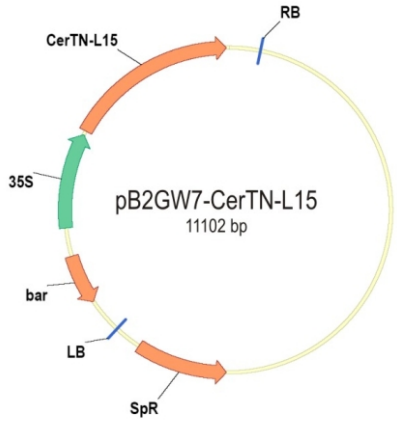

Spectinomycin resistance (SpR): 5560 - 6567 (C)
Glufosinate resistance (bar): 7262 -7813 (C)
CerTN-L15 CDS (CerTN-L15): 9223 - 11086
Right border (RB): 337 - 360
Left border (LB): 6872 - 6894
35S promoter (35S): 8127 - 9179

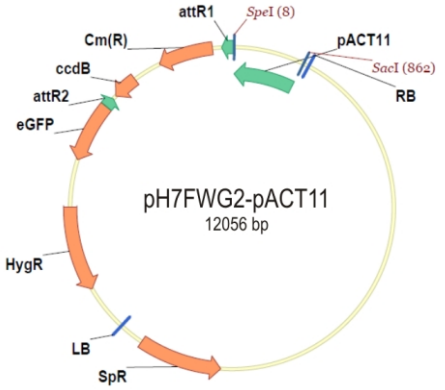

Spectinomycin resistance (SpR): 6152 - 7159 (C)
Hygromycin resistance (HygR): 8027 - 9050 (C)
Chloramphenicol resistance (CmR): 11164 - 11827 (C)
ccdB-toxin (ccdB): 10517 - 10822 (C)
eGFP CDS (eGFP): 9625 - 10346(C)
Right border (RB): 928 - 959
Left border (LB): 7464 - 7486
ACT11 promoter (pACT11): 9 - 856
Attachment site R1 (attR1): 10352 - 10476
Attachment site R2 (attR2): 11932 - 12050

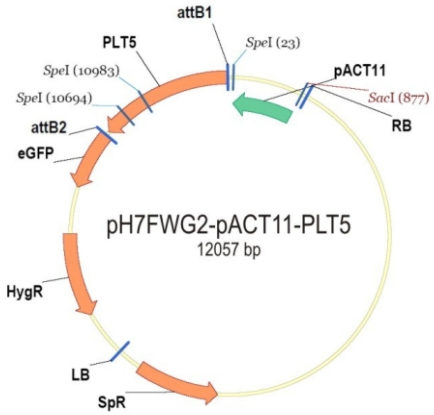

Spectinomycin resistance (SpR): 6167 -7174 (C)
Hygromycin resistance (HygR): 8042 - 9065 (C)
eGFP CDS (eGFP): 9640 - 10360 (C)
AtPLT5 CDS (PLT5): 10408 - 12028 (C)
Right border (RB): 943 - 967
Left border (LB): 7479 - 7501
ACT11 promoter (pACT11): 22 - 876
Attachment site B1 (attB1): 12047 - 15
Attachment site B2 (attB2): 10368 - 10388

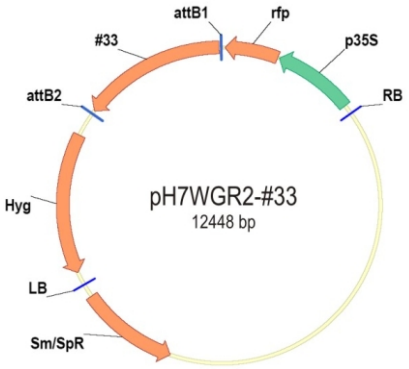

Spectinomycin resistance (SpR): 22 - 696 (C)
Hygromycin resistance (Hyg): 8459 - 10245 (C)
mRFP CDS (rfp): 22 - 696 (C)
#33 CDS (#33): 10604 - 12418 (C)
Right border (RB): 1765 - 1964
Left border (LB): 8123 - 8455
35S promoter (p35S): 718 - 1745
Attachment site B1 (attB1): 10561 - 10581
Attachment site B2 (attB2): 8123 - 8455

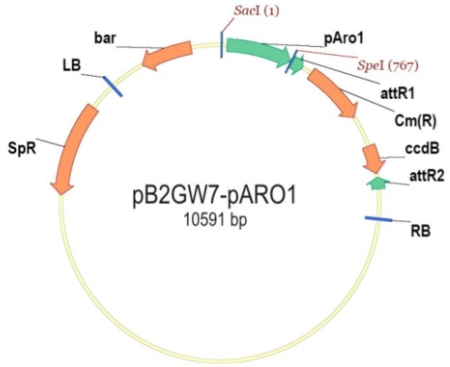

Spectinomycin resistance (SpR): 8028 - 9035 (C)
Glufosinate resistance (bar): 9730 -10281 (C)
Chloramphenicol resistance (CmR): 1011 - 1670
ccdB-toxin (ccdB): 2012 - 2317
Right border (RB): 2805 - 2828
Left border (LB): 9340 - 9362
ARO1 promoter (pARO1): 58 - 759
Attachment site R1 (attR1): 778 - 902
Attachment site R2 (attR2): 2358 - 2458

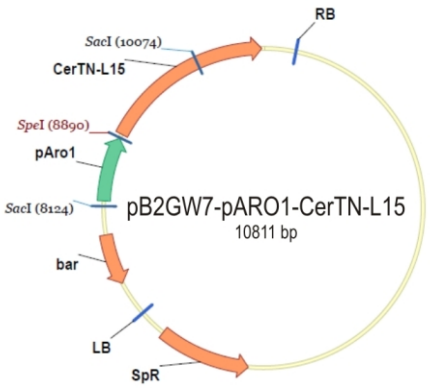

Spectinomycin resistance (SpR): 5560 - 6567 (C)
Glufosinate resistance (bar): 7262 -7813 (C)
CerTN-L15 CDS (CerTN-L15): 8932 - 10795
Right border (RB): 337 - 360
Left border (LB): 6872 - 6894
ARO1 promoter (pARO1): 8181 - 8882

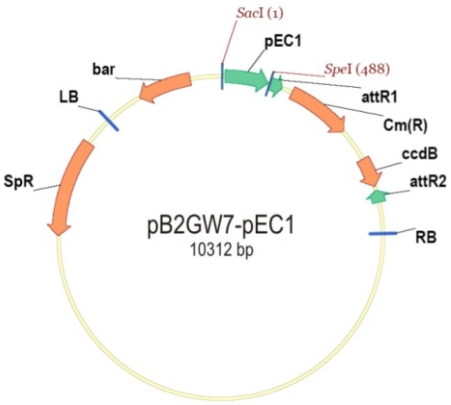

Spectinomycin resistance (SpR): 7749 - 8750 (C)
Glufosinate resistance (bar): 9451 - 10002 (C)
Chloramphenicol resistance (CmR): 732 - 1391
ccdB-toxin (ccdB): 1733 - 2038
Right border (RB): 2526 - 2543
Left border (LB): 9061 - 9083
EC1 promoter (pEC1): 28 - 473
Attachment site R1 (attR1): 499 - 623
Attachment site R2 (attR2): 2079 - 2203

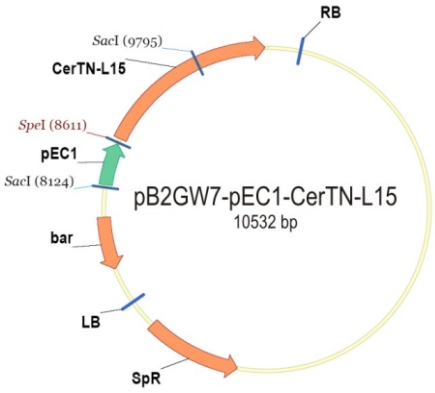

Spectinomycin resistance (SpR): 5560 - 6567 (C)
Glufosinate resistance (bar): 7262 -7813 (C)
CerTN-L15 CDS (CerTN-L15): 8653 - 10516
Right border (RB): 337 - 360
Left border (LB): 6872 - 6894
EC1 promoter (pEC1): 8151 - 8596

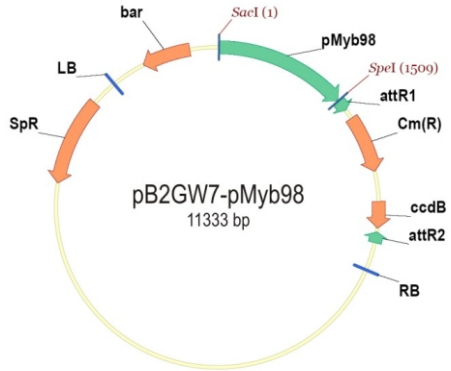

Spectinomycin resistance (SpR): 8770 - 9777 (C)
Glufosinate resistance (bar): 10472 - 11023 (C)
Chloramphenicol resistance (CmR): 1753 - 2412
ccdB-toxin (ccdB): 2754 - 3059
Right border (RB): 3507 - 3570
Left border (LB): 10082 -10104
MYB98 promoter (pMyb98): 7 - 1501
Attachment site R1 (attR1): 1520 - 1644
Attachment site R2 (attR2): 3100 - 3224

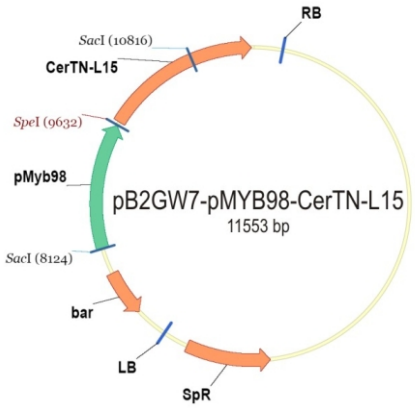

Spectinomycin resistance (SpR): 5560 - 6567 (C)
Glufosinate resistance (bar): 7262 -7813 (C)
CerTN-L15 CDS (CerTN-L15): 9408 - 10067
Right border (RB): 337 - 360
Left border (LB): 6872 - 6894
MYB98 promoter (pMYB98): 8110 - 9182

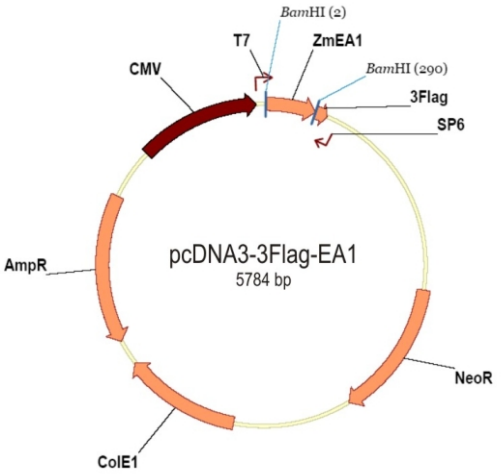

Neomycin resistance (NeoR): 1583 -2378
Ampicillin restistance (AmpR): 3882 - 4743 (C)
Origin of replication (ColE1): 3064 - 3738
CMV promoter (CMV): 5038 -5702
T7 promoter (T7): 5743 - 5761
SP6 promoter (SP6): 431 - 440 (C)
3Flag-tag (3Flag): 295 - 360
ZmEA1 CDS (ZmEA1): 6 - 288

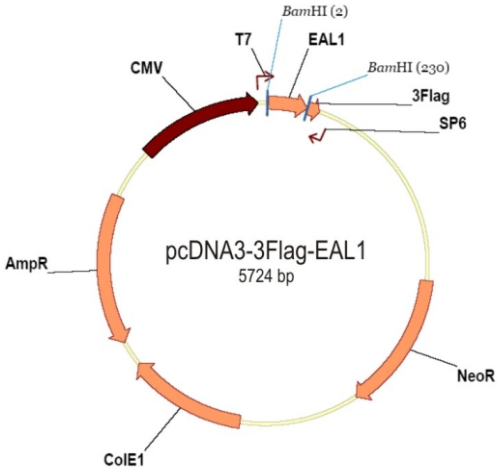

Neomycin resistance (NeoR): 1523 - 2318
Ampicillin restistance (AmpR): 3822 - 4683 (C)
Origin of replication (ColE1): 3004 - 3687
CMV promoter (CMV): 4978- 5682
T7 promoter (T7): 5683 - 5701
SP6 promoter (SP6): 371 - 389 (C)
3Flag-tag (3Flag): 235 - 300
ZmEAL1 CDS (ZmEAL1): 6 - 228

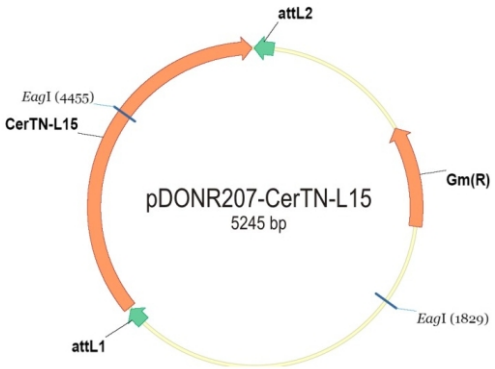

Gentamycin resistance (GmR): 872 - 1405 (C)
CerTN-L15 CDS (CerTN-L15): 3366 - 5229
Attachment site L1 (attL1): 4361 - 3356
Attachment site L2 (attL2): 5238 - 88

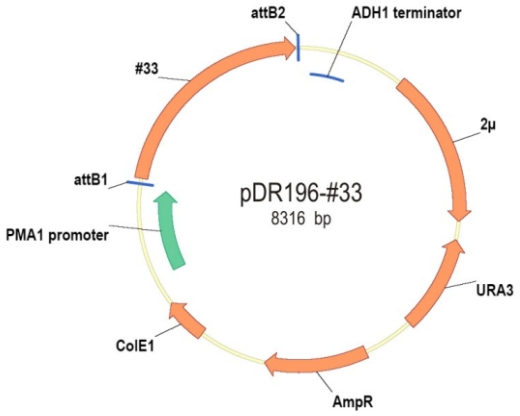

Ampicillin resistance (AmpR): 3581 - 4441
URA3 CDS (URA3): 2346 - 3149 (C)
#33 CDS (#33): 6473 - 8287
Origin of replication (ColE1): 5013 - 5374
Origin of replication (2µ): 889 - 2189
PMA1 promoter: 5615 - 6387
ADH1 terminator: 107 -430
Attachment site B1 (attB1): 6429 - 6449
Attachment site B2 (attB2): 8310 - 14

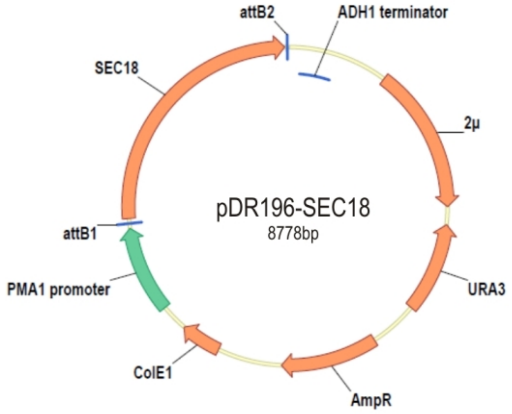

Ampicillin resistance (AmpR): 3581 - 4441
URA3 CDS (URA3): 2346 - 3149 (C)
ScSEC18 CDS (SEC18): 6473 - 8749
Origin of replication (ColE1): 5013 - 5374
Origin of replication (2µ): 889 - 2189
PMA1 promoter: 5615 - 6387
ADH1 terminator: 107 -430
Attachment site B1 (attB1): 6429 - 6449
Attachment site B2 (attB2): 8310 - 14

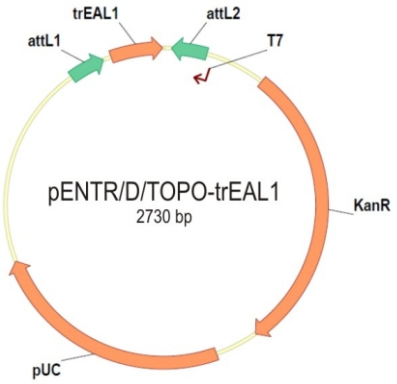

Kanamycin resistance (KanR): 286 - 1095
Origin of replication (pUC): 1216 - 1889
T7 promoter (T7): 136 - 152 (C)
ZmEAL1 predicted mature peptide (trEAL1):2583 - 2727
Attachment site L1 (attL1): 2461 - 2560
Attachment site L2 (attL2): 17- 116

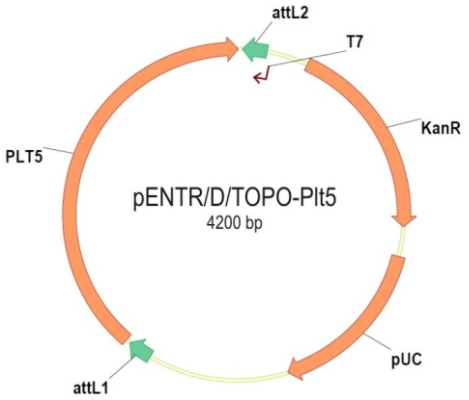

Kanamycin resistance (KanR): 286 - 1095
Origin of replication (pUC): 1216 - 1889
T7 promoter (T7): 136 - 152 (C)
AtPLT5 CDS (Plt5): 2577 - 4200
Attachment site L1 (attL1): 2461 - 2560
Attachment site L2 (attL2): 17- 116

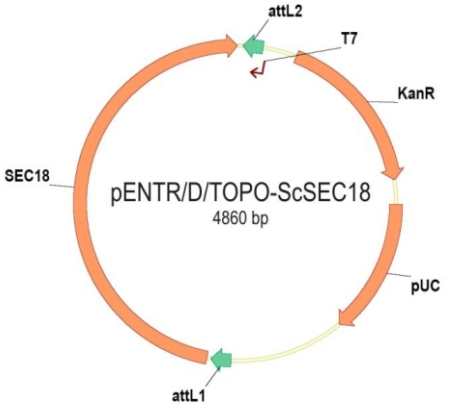

Kanamycin resistance (KanR): 286 - 1095
ScSEC18 CDS (SEC18): 2581 - 4857
Origin of replication (pUC): 1216 - 1889
T7 promoter (T7): 136 - 152
Attachment site L1 (attL1): 2461 - 2560
Attachment site L2 (attL2): 17 - 116

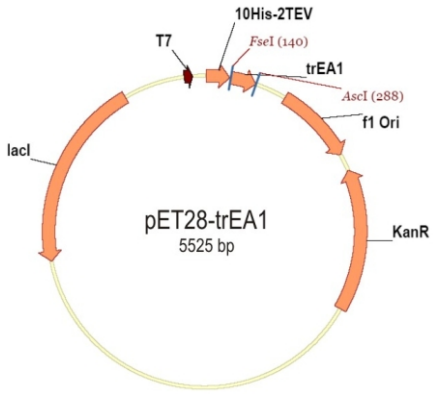

Kanamycin resistance (KanR): 1021 - 1834 (C)
lac repressor (lacI): 3976 - 5058 (C)
10His-2TEV-tag (10His-2TEV): 1 - 134
Origin of replication (f1 Ori): 471 - 932
T7 promoter (T7): 5413 - 5459
Predicted mature ZmEA1 (trEA1): 142 - 285

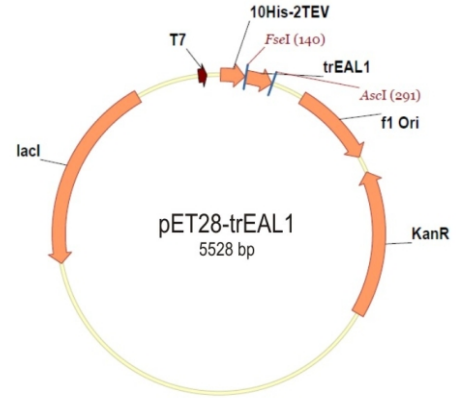

Kanamycin resistance (KanR): 1024 - 1837 (C)
lac repressor (lacI): 3979 - 5061 (C)
10His-2TEV-tag (10His-2TEV): 1 - 134
Origin of replication (f1Ori): 473 - 933
T7 promoter (T7): 5416 - 5462
Predicted mature ZmEAL1 (trEAL1): 142 - 288

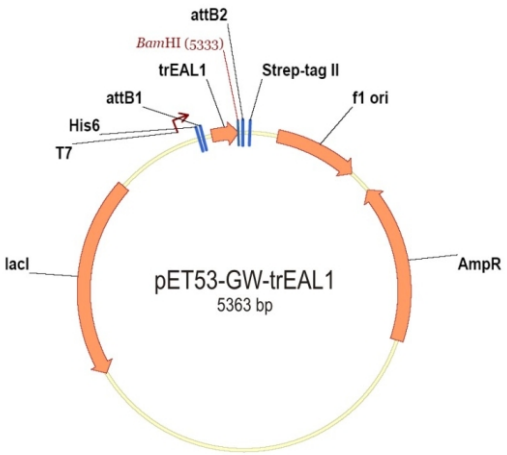

Ampicillin resistance (AmpR): 741 - 1601 (C)
lac repressor (lacI): 3359 - 4638 (C)
Predicted mature ZmEAL1 (trEAL1): 5190 - 5334
Strep-tag II (Strep-tag II): 23 - 46
6xHis-tag (His6): 5122 - 5139
Origin of replication (f1 ori): 5029 - 5045
T7 promoter (T7): 172 - 619
Attachment site B1 (attB1): 5144 - 5164
Attachment site B2 (attB2): 5357- 14

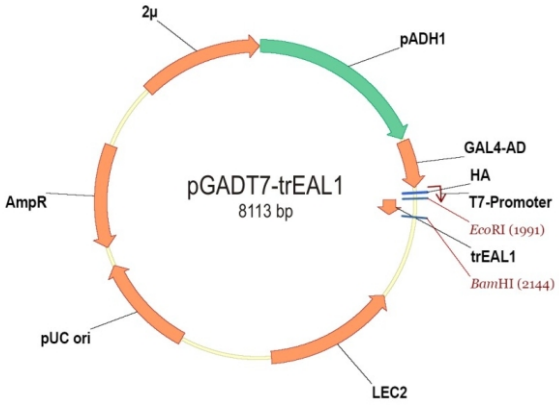

Ampicillin resistance (AmpR): 5699 - 9559 (C)
ZmEAL1 predicted mature peptide (trEAL1): 1996 - 2143
GAL4-AD CDS (GAL4-AD): 1501 - 1899
HA-tag (HA): 1942 - 1968
LEU2 CDS (LEU2): 2848 - 3939 (C)
GAL4 DNA-BD CDS (GAL4 DNA-BD): 255 695 (C)
Origin of replication (2μ): 7113 - 8113
Origin of replication (pUC ori): 4706 - 5543
ADH1 promoter (pADH1): 7 - 1479

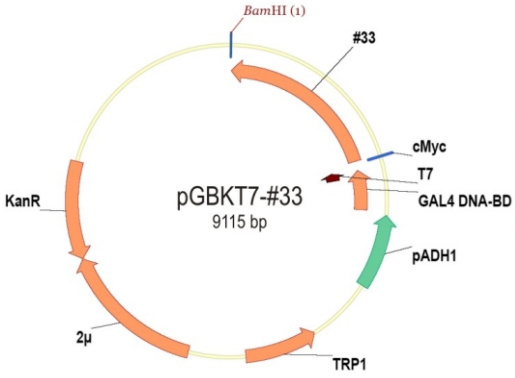

Kanamycin resistance (KanR): 6285 - 7207 (C)
#33 CDS (#33): 6 - 1820 (C)
cMyc-tag (cMyc): 1845 - 1877 (C)
TRP1 CDS (TRP1): 3724 - 4398 (C)
GAL4 DNA-BD CDS (GAL4 DNA-BD): 255 - 695 (C)
Origin of replication (2μ): 4936 - 6281
ADH1 promoter (pADH1): 2401 - 3095 (C)
T7 promoter (T7): 1890 - 1994 (C)

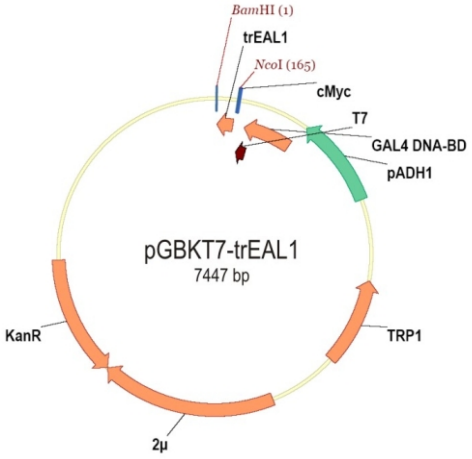

Kanamycin resistance (KanR): 4617 - 5539 (C)
ZmEAL1 predicted mature peptide (trEAL1): 6 - 152 (C)
cMyc-tag (cMyc): 177 - 209 (C)
TRP1 CDS (TRP1): 2059 - 2730 (C)
GAL4 DNA-BD CDS (GAL4 DNA-BD): 255 695 (C)
Origin of replication (2μ): 3268 - 4613
ADH1 promoter (pADH1): 136 - 152 (C)

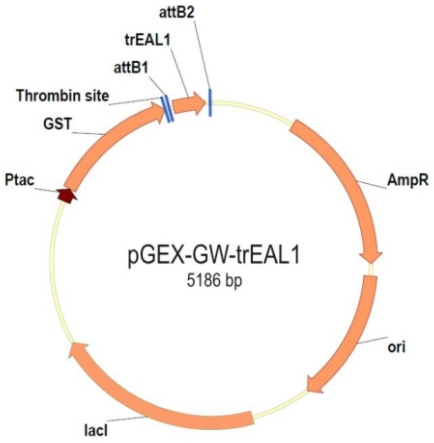

Ampicillin resistance (AmpR): 435 - 1296
Mature peptide of ZmEAL1 CDS (trEAL1): 4989 - 5157
Glutathion-S-Transferase (GST): 4285 - 4944
Lac repressor (lacI): 2376 - 3456
Origin of replication (ori): 1360 - 2056
tac-promoter (Ptac): 4215 - 4228
Thrombin site (Thrombin site): 4945 - 4962
Attachment site B1 (attB1): 4967 - 4987
Attachment site B2 (attB2): 5180 - 14

Abbreviations

AMW	apparent molecular weight
AZ	abscission zone
BETL	basal endosperm transfer layer
BMS	Black Mexican Sweet (maize line)
BSA	bovine serum albumin
CaM	calmodulin
CC	central cell
CDS	coding sequence
cDNA	complementary DNA
CFP	cyan fluorescent protein
CLSM	confocal laser scanning microscop
CoIP	co-immune precipitation
CP	coat protein
dai	days after infiltration
dap	days after pollination
DDO	double drop out (minimal yeast medium)
DIC	differential interference contrast
eGFP	enhanced green fluorescent protein
ER	endoplasmatic reticulum
ESR	embryo surrounding region
FG	female gametophyte
FP	fluorescenct protein
gDNA	genomic DNA
NSF	N-ethylmaleimide-sensitive factor

MG	male gametophyte
MMC	megaspore mother cell
mRFP	monomeric red fluorescent protein
pcv	packed cell volume
PMC	pollen mother cell
PT	pollen tube
QDO	quadruple drop out (minimal yeast medium)
rcf	radial centrifugal force
RNAi	RNA-interference
RyR	ryanodine receptor
SR	sarcoplasmatic reticulum
TILLING	targeting induced local lesions in genomes
TMV	tobacco mosaic virus
TT	transmitting tract
YFP	yellow fluorescent protein

Acknowledgements

First of all, thanks to Prof. Dr. Thomas Dresselhaus for the opportunity to work in his group and for material and non-material support. Special thanks is needed for his support of attending international meetings and visits of the groups of Prof. Jörg Kudla (Universiy of Münster) and Prof. Oliver Griesbeck (MPI Neurobiology, Martinsried).

I'd like to thank also Dr. Stefanie Sprunck, Dr. Ulrich Hammes, Dr. Mihaela Màrton and Dr. Manfred Gartz for their help on technical questions, experimental design and critical remarks. Special thank goes to Dr. Mariana Mondragon-Palomino for teaching me her qRT-PCR protocol and her critical remarks on this manuscript. Thanks to Prof. Dr. Klaus Grasser and Dr. Marion Grasser for allowing the use of equipment. Thanks to the former department members Dr. Guido Grossmann for teaching me confokal microscopy, Dr. Svenja Rademacher for her critical remarks on this manuscript and PD Dr. Jürgen Stolz for his advise. It was a special honour and pleasure to have the (officially) retired Prof. Dr. Widmar Tanner and Prof. Ludwig Lehle around. Thanks to Prof. Lehle for his advice on *in-vitro* translation and Co-IP and providing the Sey5188-strain and to Prof. Tanner for advice and encouragement in difficult times.

Thanks to my PhD-colleagues and all current other and former members of the department of cell biology and plant biochemistry for their help, advice, input and the good working atmosphere. Special thanks go to the technicians of the "maize lab" Angelika Rechenmacher and Ingrid Fuchs keeping the lab together, Veronica Mrosek for help in administrative questions and to Günther Peissig for plant care. Special thanks goes also to Philipp Denninger and Martina Kolb for collaboration during their bachelor thesis and to Josef Simmel and Mari-Theresa Weickert for working with me as undergraduate students for some time.

Thanks to our collaborators Dr. Urte Schlüter (University of Erlangen) for microarray hybridisation and statistic analysis, Prof. David Jackson (Cold Spring Harbour laboratories) and Prof. Anne Sylvester (Universtiy of Wyoming) for seeds of fluorescence marker lines, Prof. Lukas Spíchal (Palackỳ University, Olomounc) for providing the cytokinin inhibitor PI-55 and Prof. John Lindbo (University of California, San Francisco) for providing the TMV-constructs.

Last but not least, I acknowledge the *Univerität Bayern e.V.* for financial support during the first 2½ years of this thesis.